High-resolution mapping of heteroduplex DNA formed during UV-induced and spontaneous mitotic recombination events in yeast

Yi Yin[1,2], Margaret Dominska[1], Eunice Yim[1] and Thomas D. Petes[1,3]

[1]Department of Molecular Genetics and Microbiology and University Program in Genetics and Genomics, Duke University Medical Center, Durham, NC 27710, USA.

[2]Current address: Department of Genome Sciences, University of Washington, Seattle, WA 98195, USA

[3]Corresponding author

Running head: Mapping of heteroduplex DNA

Key words/phrases: mitotic recombination, mismatch repair, heteroduplex DNA, gene conversion, ultraviolet light

Corresponding author:

Thomas D. Petes

Department of Molecular Genetics and Microbiology

Box 3054, Duke University Medical Center

Durham, NC 27710

Telephone: (919) 684-4986

Fax: (919) 684-6033

Email: tom.petes@duke.edu

Abstract

In yeast, DNA breaks are usually repaired by homologous recombination (HR). An early step for HR pathways is formation of a heteroduplex, in which a single-strand from the broken DNA molecule pairs with a strand derived from an intact DNA molecule. If the two strands of DNA are not identical, there will be mismatches within the heteroduplex DNA (hetDNA). In wild-type strains, these mismatches are repaired by the mismatch repair (MMR) system, producing a gene conversion event. In strains lacking MMR, the mismatches persist. Most previous studies involving hetDNA formed during mitotic recombination were restricted to one locus. Below, we present a global mapping of hetDNA formed in the MMR-defective *mlh1* strain. We find that many recombination events are associated with repair of double-stranded DNA gaps and/or involve Mlh1-independent mismatch repair. Many of our events are not explicable by the simplest form of the double-strand break repair model of recombination.

Introduction

Homologous recombination (HR) is important for repairing double-stranded DNA breaks (DSBs) in diploid yeast. Although several different HR pathways have been described (Symington *et al*., 2014), the earliest steps of all pathways have a common intermediate in which a single DNA strand from one duplex invades the homologous template (green boxed region of Fig. 1). In Fig. 1, chromosomes are shown as double-stranded DNA structures with the two homologs drawn in different colors. Following the DSB, the broken ends are processed by 5' to 3' degradation in a two-step process with limited resection (about 100 bases) performed by Sae2 and the Mre11-Rad50-Xrs2 proteins, followed by more extensive resection (>1 kb) utilizing the redundant pathways of Exo1 or Dna2 with the Sgs1-Top3-Rmi1 complex (Symington, 2014). The 3' single strand derived from the broken end then invades the unbroken template chromosome forming a heteroduplex, a region of duplex DNA derived from the different DNA molecules. In Fig. 1, heteroduplexes are shown as paired strands of different colors.

For all pathways, the invading 3' end is used as a primer to catalyze DNA synthesis (shown as red dotted lines). The subsequent steps differ for each pathway. In the synthesis-dependent strand-annealing (SDSA) pathway (Fig. 1A), following DNA synthesis, the invading strand is displaced and reanneals to the other processed broken end. Repair of the single-stranded gap (dotted blue line) completes the event. In this pathway, a region of heteroduplex occurs on only one of the two homologs, and SDSA events are not associated with crossovers.

In the two-ended SDSA pathway (Fig. 1B), DNA synthesis is primed from both broken ends. Before ligation of the DNA strands to form a double Holliday junction, the invading end dissociates from the template and re-pairs with the other broken end. The net result of this event is a NCO in which one chromatid has a heteroduplex with a strand switch at the DSB site. The other chromatid has no heteroduplex. The same product can be formed by a double SDSA event in which the two broken ends invade different sister chromatids, synthesize DNA using

these templates, and then disassociate from the sister chromatids and reanneal with each other (Martini *et al.*, 2011).

In the double-strand-break-repair (DSBR) pathway, the strand displaced by DNA synthesis from the invading strand pairs with the other broken end (Fig. 1C). Repair synthesis results in formation of a double Holliday junction (dHJ) intermediate. There are several mechanisms to resolve dHJs. First, the two junctions could be migrated toward each other, and decatenated by the Sgs1p-Top3p-Rmi1p complex (dissolution). By this mechanism, there are two regions of hetDNA flanking the DSB, both located on the molecule that was originally broken.

Alternatively, the dHJ could be resolved by HJ resolvases such as Mus81p and Yen1p to form either crossover (CO) or non-crossover (NCO) products. Resolution of both HJs in the same orientation (for example, cleavage of both junctions as shown by the horizontal arrows terminated by circles) results in NCO products, whereas cleavage in different orientations (one HJ cleaved as shown with vertical arrows terminated by diamonds, and the other cleaved as shown with horizontal arrows) results in CO products (Fig. 1). For both types of resolution, the hetDNA is on both sides of the DSB, and both the donor and recipient DNA molecule have hetDNA.

In the last pathway of HR (Fig. 1D), break-induced replication (BIR), the invading strand results in a migrating D-loop replication structure that duplicates chromosomal sequences conservatively from the point of strand invasion to the end of the chromosome (Donnianni and Symington, 2013; Saini *et al.*, 2013). In this pathway, the second part of the broken DNA is lost, and no heteroduplex is associated with either the donor or recombinant DNA molecule.

If the two strands of DNA that compose the heteroduplex have non-identical sequences, the heteroduplex will contain mismatches (Fig. 2). Correction of these mismatches by the mismatch enzymes results in gene conversion, the non-reciprocal transfer of information between the two chromosomes (Symington *et al.*, 2014). In Fig. 2A, the heteroduplex has four mismatches, if these mismatches are excised from the “blue” strand, and the resulting gap is filled in using the

"red" strand as a template, a conversion event is observed. Alternatively, if the mismatches are removed from the red strand, no conversion would be observed; such events are termed "restorations". A third possibility is that the mismatches would be excised from both strands resulting in "patchy" repair. In strains that lack MMR, mismatches are not repaired and two non-identical daughter cells are produced (Fig. 2B). In MMR-proficient strain, the patterns of heteroduplex formation may be obscured. For example, resolution of the dHJ can result in one or two chromatids that have heteroduplexes (Fig. 1C). Following MMR, these two types of intermediates are indistinguishable because both yield the same type of conversion tracts (Fig. 2C and 2D).

Mitchel *et al*. (2010) examined patterns of heteroduplex formation in recombination events between a linearized plasmid and a chromosome in an MMR-deficient strain. There were multiple sequence differences spaced about 50 bp apart within an 800 bp region of homology. By sequencing the single-colony transformants, they could detect the unrepaired mismatches that defined the length of the heteroduplex. From their analysis, they concluded: 1) most of the heteroduplexes unassociated with crossovers (NCO) were restricted to one side of the DSB site, consistent with their formation by the SDSA pathway rather than the DSBR pathway, 2) most of the heteroduplexes associated with crossovers (CO) had the patterns consistent with the DSBR pathway, and 3) most of the heteroduplexes extended less than 500 bp from the DSB site on the plasmid. In general, the observations of Mitchel *et al*. were consistent with the predictions of the model described in Fig. 1.

In previous studies, we developed methods of detecting and mapping spontaneous and UV-induced crossovers and associated gene conversion events throughout the genome (St. Charles *et al*., 2012; St. Charles and Petes, 2013; Yin and Petes, 2013). Our analysis utilized diploids that were heterozygous for about 55,000 single-nucleotide polymorphisms (SNPs) and microarrays capable of distinguishing heterozygous SNPs and homozygous SNPs. One important conclusion from this analysis was that mitotic gene conversion tracts (median length

of 11 kb, St. Charles and Petes, 2013) were generally much longer than meiotic conversion tracts (median length of about 2 kb; Mancera *et al*., 2008). This observation suggests that either heteroduplexes are much longer in mitosis than in meiosis or that long mitotic gene conversion tracts involve a different intermediate such as a large double-stranded DNA gap. Our previous experiments were done in MMR-proficient strains. In the current study, using *mlh1* (MMR-deficient) diploids, we show that some mitotic recombination events involve long heteroduplexes, although other events are consistent with gap repair. In addition, however, we find that recombination events initiated at a previously-described spontaneous mitotic recombination hotspot caused by an inverted pair of retrotransposons (St. Charles and Petes, 2013; Yim *et al*., 2014) often involve long (> 20 kb) double-stranded gaps rather than very long heteroduplexes. We previously showed that most spontaneous crossovers between homologs had patterns of gene conversion that indicate that recombinogenic DSBs occur in unreplicated DNA (Lee *et al*., 2009; Lee and Petes, 2010). Our current study is consistent with this conclusion.

In our previous mapping of gene conversion tracts in MMR-proficient strains, we found that about 20% of the UV-induced and spontaneous events (St. Charles and Petes, 2013; Yin and Petes, 2013) were “patchy” in which markers exhibiting gene conversion flanked markers that were not converted. One simple explanation of this observation is that mismatches within one heteroduplex are sometimes repaired in a non-concerted manner by conversion-type repair and restoration-type repair. If this explanation is correct then, in the absence of repair, mismatches within a heteroduplex should be continuous (Reyes *et al*., 2015). However, in the *mlh1* strain used in this study, we find that about one-third of heteroduplexes contain mismatches flanking regions without mismatches (discontinuous heteroduplexes). Such patterns can be explained by Mlh1- independent MMR, and/or template-switching during repair synthesis. We also find recombination events that are inconsistent with the canonical DSBR models, and require additional steps such as branch migration of the Holliday junctions and/or sequential invasion of broken DNA ends.

The model of recombination shown in Fig. 1 is based primarily on studies of meiotic and mitotic recombination in yeast. Such studies often involve single meiotic recombination hotspots or mitotic recombination events induced by site-specific endonucleases. In addition, the distribution of markers (SNPs) used to analyze the events are usually sparsely distributed, and clustered near the initiating DNA lesion. Lastly, most of these studies utilized wild-type yeast strains in which some patterns of heteroduplex formation were obscured by mismatch repair. The patterns of recombination observed in our study are likely to reflect a more realistic assessment of the complex events that occur during recombination. Similar conclusions have been reached by global analyses of meiotic recombination in yeast using methods similar to those employed in our study (Mancera *et al.*, 2008; Martini *et al.*, 2011).

Results

Experimental system

The system that we previously used to analyze mitotic recombination in MMR-proficient strains is illustrated in Fig. 3. The experimental diploids were homozygous for the *ade2-1* ochre mutation located on chromosome XV. In the absence of a nonsense suppressor, such strains form red colonies. The chromosome arm to be assayed for recombination had a heterozygous insertion of the *SUP4-o* gene encoding an ochre suppressor located near the telomere. Diploids with zero, one, and two copies of *SUP4-o* form red, pink, and white colonies, respectively. Therefore, prior to the recombination event, cells have one copy of *SUP4-o* and form pink colonies. A cell that has a reciprocal crossover between the centromere and the *SUP4-o* marker will form a red/white sectored colony, assuming that both daughter cells have one recombinant and one non-recombinant chromosome (Fig. 3A). In addition to the heterozygous *SUP4-o* marker, the diploids were heterozygous for about 55,000 single-nucleotide polymorphisms (SNPs) because they were constructed by mating two sequence-diverged haploids, W303-1A and YJM789 (Lee *et al*., 2009; St. Charles *et al*., 2012). To determine the position of the crossover and to detect conversion events associated with the crossover, we used microarrays in which loss of heterozygosity (LOH) could be detected for about 13,000 SNPs. Each SNP was represented by four 25-base oligonucleotides, two containing the Watson and Crick strands of the W303-1A allele and two containing the Watson and Crick strands of the YJM789 allele. By hybridizing genomic DNA derived from the red and white sectors, we could map the position of the crossover and associated gene conversion tract (St. Charles *et al*., 2012). Details of this analysis are provided in Materials and Methods.

In our previous analysis, we examined spontaneous recombination events in two types of MMR-proficient strains: those with the *SUP4-o* marker located about 100 kb from *CEN5* and those with the *SUP4-o* marker located about 1 Mb from *CEN4*. Most of the crossovers were associated with gene conversion events (solid-line boxes in Fig. 3). Although some of the

sectored colonies had the expected pattern of conversion in which one daughter cell is homozygous for SNPs located near the crossover event and the daughter is heterozygous (Fig. 3A), more than half of the crossovers were associated with conversion events in which both daughter cells were homozygous for SNPs derived from one homolog (region marked 4:0 in Fig. 3B). This pattern indicates that two sister chromatids were broken at the same position, consistent with a model in which the recombinogenic DSB occurs in G_1, and the broken chromosome is replicated to produce two broken sister chromatids. The 4:0 tracts are often adjacent to 3:1 tracts as in Fig. 3B. We interpret such hybrid tracts as reflecting the repair of two sister chromatids in which the extent of heteroduplex formation is different for the repair of each DSB (Lee *et al*., 2009; St. Charles *et al*., 2012).

To examine mismatch-containing heteroduplexes, we constructed two diploids in the hybrid genetic background that lacked the mismatch repair protein Mlh1p (details in Supplementary file 1 - Table S1). Both the Msh2 and Mlh1 proteins have central roles in the repair of mismatches resulting from bases misincorporated during DNA replication or formed within heteroduplexes during recombination. Elimination of these proteins elevates global mutation rates and the frequency of post-meiotic segregation to approximately the same extent (Huang *et al.*, 2003; Stone and Petes, 2006). Both the Msh2p and Mlh1p are involved in the rejection of heteroduplexes that have closely-spaced mismatches with Msh2p having a stronger effect in most assays of this activity (Chakraborty and Alani, 2016). Msh2, but not Mlh1, has a role in processing branched DNA structures such as the intermediates associated with the single-strand annealing recombination pathway (Symington *et al.*, 2014). We chose to examine heteroduplexes in the *mlh1* strain to avoid the possibility of losing recombination intermediates that might require Msh2p for processing. Although it is possible that some recombination intermediates could be lost in the *mlh1* strain by Msh2-dependent heteroduplex rejection, our analysis described below demonstrated that the level of mitotic recombination was not substantially affected by the *mlh1* mutation.

To detect crossovers, we used a colony-sectoring assay similar to that employed previously (Lee *et al*., 2009; St. Charles and Petes, 2013). The heterozygous insertion of *SUP4-o* required for the sectoring assay was located near the right end of chromosome IV in diploid YYy311, and near the left end of chromosome V in diploid YYy310. In wild-type strains in which mismatches within the heteroduplex are corrected by the MMR enzymes, each sector will contain cells of only one genotype (Fig. 3). In contrast, in the MMR-deficient strains, there may be two different genotypes in one or both sectors. In Fig. 4A, we show the patterns of heteroduplex formation expected by the DSBR pathway in a MMR-deficient cell in which recombination initiates as a consequence of a single broken chromatid in G_2 of the cell cycle. Both the D1 and D2 daughter cells retain heteroduplexes with mismatches. In Fig. 4A, the cells derived from D1 are in the white sector, and those derived from D2 are in the red sector. When the chromosomes in D1 are replicated, two different genotypes will be observed in the granddaughter cells, GD1-1 and GD 1-2. In addition, if the heteroduplexes are on different chromatid as expected for the DSBR pathway, there will also be two different genotypes in cells derived from D2.

On the left side of Fig. 4B, we show the pattern of heteroduplexes expected for an event initiated by a DSB in an unreplicated blue chromosome (producing two sister chromatids broken at the same position as the result of DNA replication) that was repaired in G_2 of the cell cycle. Such cells can also produce two genotypes in each sector (Fig. 4B). In the white sector, two types of granddaughter cells with different genotypes are shown. In the region shown in the black rectangle, GD1-1 is homozygous for the blue-derived SNPs and GD1-2 is heterozygous. In addition, in the regions defined by the green rectangles for GD1-1 and GD1-2, although both genotypes are heterozygous, the coupling of the heterozygous regions is different. In GD1-1, the blue and red SNPs within the green rectangle are on the same chromosome as the centromere-proximal blue and red SNPs, whereas in GD1-2, the blue and red SNPs within the rectangle are coupled to the centromere-proximal red and blue SNPs, respectively. As described below, for our analysis, we looked for different genotypes within sectors by methods

that allowed us to examine the locations of heterozygous and homozygous SNPs, and to determine the coupling of heterozygous regions. It is important to emphasize that there is a one-to-one correspondence between the chromosomes within the sectors (labeled 1-8 on the right side of the figure) and the DNA strands in the mother cell in which the recombination event occurred (strands labeled 1-8 on the left side of the figure).

Most of our data were obtained from G_1-synchronized YYy310 cells treated with 15 J/m^2 of UV. This treatment stimulates mitotic recombination on chromosome V >10^3-fold and results in about ten unselected events on other chromosomes (Yin and Petes, 2013). To detect cells of different genotypes within each sector of red/white sectored colonies (reflecting a crossover on chromosome V), we first purified 10-20 white and red colonies from each sector. Initially, we performed a SNP-specific microarray array of genomic DNA isolated from one of the white colonies to locate the approximate position of the recombination event. For example, we analyzed one white colony (YYy310.9-5W1) derived from a sectored red/white colony number 5 derived from UV-treated YYy310.9 cells. In Fig. 5, the red and blue circles represent hybridization to W303-1A- and YJM789- derived-oligonucleotides, respectively. Hybridization values (Y-axis) are normalized such that a value of about 1 indicates that the experimental DNA sample is heterozygous for the W303-1A- and YJM789-derived-alleles (additional details in Materials and Methods); the X-axis shows Saccharomyces Genome Database (SGD) coordinates on chromosome V. LOH events that duplicate the sequences from one allele and remove sequences from the other are associated with hybridization values of about 1.5 and 0.3, respectively. Thus, by microarray analysis (Fig. 5A), the strain (a granddaughter derived from a white sector) shown in Fig. 5A was homozygous for YJM789-derived SNPs from the left end of chromosome V to SGD coordinate 51915. The strain was heterozygous for SNPs between 53612 to 54198, and then homozygous for W303-1A-derived SNPs from coordinates 56117 to 57170. Lastly, the strain was heterozygous for SNPs between coordinates 60701 and *CEN5*. As will be discussed below, this strain represents one of the two granddaughter genotypes

observed in the white sector.

Based on this information, we examined genomic DNA from eight white colonies and eight red colonies by PCR analysis to look for different genotypes within one sector. We chose to examine SNPs that were near the transitions of heterozygous and LOH regions. For example, at position 51707, there is a polymorphism that distinguishes the YJM789- and W303-1A-derived SNPs (Lee *et al*., 2009). In the W303-1A genome, this polymorphism is part of a restriction enzyme recognition site for *Dra*I that is absent in YJM789. Consequently, we PCR-amplified the region containing this site from the individual white and red colonies, treated the resulting fragments with *Dra*I, and examined the resulting products by gel electrophoresis. Five of the white colonies were homozygous for the YJM789-form of the SNP, and three were heterozygous, demonstrating that this SNP was included as an unrepaired mismatch in one of the daughter cells. By a similar approach, we showed that SNPs heterozygous in the starting strain at coordinates 54915, 56166, and 57448 were homozygous for the W303-1A-form of the SNP in three red colonies, and heterozygous in the remaining five. Thus, this analysis allowed us to unambiguously define two different granddaughter genotypes in both the white (GD1-1, name shortened to W1 in Supplementary Figures (Supplementary file 2); GD1-2, name shortened to W2) and red (GD2-1, name shortened to R1; GD2-2, name shortened to R2).

The complete analysis of the granddaughter genotypes required two additional steps. First, we mapped one representative of each granddaughter genotype using whole-genome SNP arrays. This analysis allows us to map heterozygous and homozygous SNPs on chromosome V and unselected events throughout the genome. The coordinates for transitions between heterozygous and homozygous SNPs for the UV-treated YYy310 samples are in Supplementary file 1 - Table S2. An example of the SNP microarray analysis for one granddaughter diploid strain derived from the white sector (YYy310.9-5W1) is shown in Fig. 5A.

Many of the granddaughter isolates, such as that shown in Fig. 5A, had two or more heterozygous regions. To examine the coupling relationships of the heterozygous regions, we

sporulated the four granddaughter diploids derived from each sectored colony, and dissected tetrads. One spore derived from each strain was then examined by microarrays. The pattern shown in Fig. 5B represents the analysis of one haploid spore derived from granddaughter W1. This pattern shows the arrangement of SNPs on the top chromosome of Fig. 5C, and the arrangement of SNPs on the other homolog (bottom chromosome of Fig. 5C) can be directly inferred.

This analysis allowed a complete determination of the arrangement of SNPs in W1, W2, R1, and R2, and was performed for all sectored colonies. An example of how the patterns of LOH in the granddaughter cells can be used to figure out the pattern of heteroduplexes in the mother cell is shown in Fig. 6. Each chromosome in the granddaughter cells has the same pattern of SNPs as one of the DNA strands in the daughter cell. The source of the centromeres determines which of the chromosomes in the granddaughter cells was derived from which chromosome in the daughter cell. For example, in Fig. 6, the chromosomes labeled 1 and 2 have red centromeres, and were derived from the daughter chromosome with the red centromere. Chromosomes 5 and 6 were derived from the daughter chromosome with the blue centromere. Similarly, both the daughter chromosomes labeled 1 and 2 from the white sector and the daughter chromosomes labeled 3 and 4 from the red sector have red centromeres, and were connected as a pair of sister chromatids to the red centromere in the original mother cell.

The transitions between regions of homozygous and heterozygous SNPs for all events are given in Supplementary file 1 - Table S2, and Supplementary file 1 - Table S3 summarizes the classes of these events as crossovers (CO) and non-crossovers (NCO). An important feature of our analysis is that once we have defined daughter and granddaughter cells based on the crossover on the selected chromosome, this lineage information also can be applied to unselected CO and NCO events on other chromosomes. For example, although the NCO event shown in Fig. 4C does not generate a sector, our whole-genome microarray analysis of granddaughter cells defined by the selected crossover allows us to detect and to fully describe

the unselected event.

Our analysis of hetDNA included three types of experiments. First, we examined seven sectored colonies derived from the UV-treated YYy310 strain in which the *SUP4-o* marker was inserted near the left end of chromosome V. In addition to the selected crossover on chromosome V, these strains had about ten unselected events (both crossovers and conversions unassociated with crossovers) per strain because of the recombinogenic effects of UV (Yin and Petes, 2013). Second, we analyzed five spontaneous crossovers on chromosome V in YYy310. Lastly, we characterized six spontaneous crossovers on chromosome IV in strain YYy311 (heterozygous for the *SUP4-o* marker on the right end of chromosome IV) that were associated with the HS4 recombination hotspot.

Analysis of selected crossovers on chromosome V and unselected recombination events induced by UV in YYy310.

We found previously (Yin and Petes, 2013) that more than half of the recombination events detected in G_1-synchronized diploids treated with high doses of UV had the pattern of recombination indicative of the repair of a G_1-associated DSB (Fig. 3B). In addition, DSBs induced by UV were detected by gel electrophoresis (Covo *et al.*, 2012). Such DSBs could be formed as a consequence of nucleotide-excision-repair (NER) enzymes acting on two very closely-spaced lesions on opposite strands or as the result of expansion of short single-stranded NER-generated gaps on opposite strands by the action of Exo1p. Cells treated with low doses of UV (1 J/m^2) primarily had patterns of gene conversion (3:1 events) indicative of a single broken chromatid (Fig. 3A). Based on our analysis of UV-induced LOH events in wild-type and *rad14* (NER-defective) cells (Yin and Petes, 2015), single-broken chromatids are likely generated two different ways: by replication of a chromosome with an NER-generated gap, and by Mus81-dependent processing of DNA structures formed when a replication fork is blocked by an unprocessed UV-generated lesion.

We examined seven sectored colonies derived from two isogenic independently-constructed

YYy310 diploids (YYy310-9 and YYy310-10). By the methods described above, we identified two different genotypes within each sector in all seven sectored colonies; these genotypes are designated W1 and W2, and R1 and R2 for the white and red sectors, respectively. Our diagnosis of granddaughter genotypes was initially based on PCR analysis of SNPs associated with the selected crossover on chromosome V. For five of the seven sectored colonies, this analysis was sufficient to detect W1, W2, R1, and R2. For the two sectored colonies in which we could not identify two genotypes in the sectors using markers on V, we used unselected events on other chromosomes to identify the granddaughters.

In addition to the seven selected crossovers, there were 71 unselected crossover or gene conversion events among the sectored colonies. Interpretations of eight classes of relatively simple recombination events (described in detail below) are shown in Supplementary file 2 - Figs. S1 and S2. In Supplementary file 2 - Figs. S3-S80, all of the selected and unselected events are shown, with the upper part of the figure depicting the pattern of heterozygous and homozygous SNPs on the two chromosomes of the granddaughter of the white (W1 and W2) and red (R1 and R2) sectors. The bottom part of each figure shows the inferred patterns of heterozygous and homozygous SNPs in the mother cells, prior to the segregation of chromosomes into the daughters. Each chromatid is depicted as double- stranded DNA and circles of different colors at the same positions on the two strands indicate unrepaired mismatches in heteroduplexes. In the discussion below, SNPs from the W303- 1A-derived homolog will be called “red SNPs” and those from the YJM789-derived homolog will be called “blue SNPs”, consistent with the figures. Below, we summarize some of our findings based on this complex dataset.

SCB and DSCB events are approximately equally frequent

First, we can divide the events into two major classes, those in which the event was initiated by a single broken chromatid in S or G_2 (SCB, single chromatid break) and those initiated by two broken chromatids (DSCB, double-sister-chromatid break), likely reflecting replication of a

chromosome broken in G_1. The heteroduplex patterns inferred from our analysis of granddaughter cells for two events are shown in Figure 7. In the event shown in Fig. 7A, only chromatid 2 has a heteroduplex, suggesting that the initiating event was a SCB. In contrast, in Fig. 7B, chromatids 1 and 3 have the CO configuration of markers, whereas chromatid 4 has a NCO configuration. This observation suggests that this event was initiated by a DSCB. Of 77 events that could be unambiguously classified (Supplementary file 1 - Table S3), there were 39 SCB and 38 DSCB events. In previous studies of events in wild-type strains treated with the same dose of UV (Yin and Petes, 2013), we also found approximately equal frequencies of these two classes (Supplementary file 1 - Table S6).

Our conclusion that many of the observed recombination events, both spontaneous and UV-induced, reflect a G_1-initiated DSB is surprising, but consistent with our previous studies (Lee *et al*., 2009; St. Charles and Petes, 2012; Yin and Petes, 2013). In considering this conclusion, a number of points need to be emphasized. First, we propose that DSCB events result from replication of a broken chromosome. This DSB cannot be efficiently repaired in G_1 because the enzymes involved in end resection and resolution of recombination intermediates are not active in G_1 (Symington *et al.*, 2014). An alternative pathway to DSB repair in G_1 cells is non-homologous end-joining (NHEJ). In yeast, however, this pathway is inefficient (Siede *et al.*, 1996). In addition, when we previously compared the frequency of mitotic crossovers in diploids that were heterozygous at the mating type locus (a condition that represses NHEJ, Kegel *et al.*, 2001) or hemizygous (active NHEJ), there was no consistent difference in the frequency of mitotic crossovers and the ratios of G_1/G_2 events in the two types of strains (Barbera and Petes, 2006; Lee *et al*., 2009; Yin and Petes, 2013).

Since the repair of the broken chromosome in G_1 is inefficient, we suggest that the broken chromosome is replicated to produce two chromatids that are broken at the same positions. Since the equivalent location of the breaks precludes repair by sister-chromatid recombination, they are repaired by interaction with the chromatids of the intact homolog, resulting in the

observed LOH events. It is important to emphasize that DSCBs may actually represent a less common DNA lesion than SCBs. Our system, however, detects only those events that lead to LOH. Repair of DSBs by recombination between sister chromatids is undetectable by our system. Using a different genetic system, Kadyk and Hartwell (1992) concluded that >90% of the DSBs generated in G_2-synchronized yeast were a consequence of sister-chromatid recombination rather than inter-homolog exchange; we observed a similar ratio for spontaneous events (Zhao *et al*., 2017). Although the current analysis is restricted to examining those events that lead to LOH, LOH events are critical for the development of some classes of tumors (Cavanee *et al.*, 1985).

In addition to the DSCB events, we observed a substantial number of SCBs in UV-treated cells. Such events likely have two sources. Although most small single-stranded gaps resulting from NER are likely repaired in G_1, some may persist into S. Replication of a nicked template would result in an SCB. An alternative source of SCBs may be unexcised dimers that stall the replication fork, resulting in an S-phase-associated DSB (Yin and Petes, 2015).

Excluding the selected CO events on chromosome V, of the 33 DSCB events, 22 had two NCOs, 9 had one NCO and one CO, and two had two COs. For our mechanistic interpretation of these events (to be described in detail below), we consider the two repair events resulting from the DSCB separately. The chromatids involved in a CO are almost always clear since the terminal SNPs at each end of the chromatid are altered in their coupling relative to the centromere as described above for chromatids 1 and 3 of Fig. 7B. For NCO events that have a single recombinant chromatid, we cannot determine which of the two non-recombinant chromatids was the donor of sequence information. For example, in Fig. 7A, the donor chromatid could be either chromatid 3 or 4 since these chromatids are identical. For such events, in Supplementary file 1 - Table S3, we arbitrarily assigned one chromatid as the donor.

It should be emphasized that in our experiments, as in prior studies (Lee *et al*., 2009; St. Charles and Petes, 2013; Yin and Petes, 2013), the DSCB events are far too frequent to

represent two independent SCB events. The frequency of red/white sectored colonies (reflecting a crossover on chromosome V) in the UV-treated YYy310 strain was about 1.5%. About half of these events are a consequence of SCB. The likelihood of two independent SCB events resulting in an apparent DSCB is about $(0.75\%)^2$ or 5.6×10^{-4}; we observed two orders of magnitude more DSCB events than this calculated frequency. In addition, the calculated frequency was based on double events occurring anywhere within the 120 kb between the *SUP4- o* insertion and *CEN5*. Most of the DSCB events involve DSBs that occur within a few kb of each other. Lastly, half of the time, two independent events would have donor chromatids derived from different homologs; only three of the DSCB events involved different homologs. Lastly, we point out that our measurement of the frequency of observed SCBs is an underestimate of the formation of SCBs, since many of the SCBs are likely to be repaired by sister-chromatid recombination (Kadyk and Hartwell, 1992).

Many previous studies of recombination in yeast show that the chromosome with the initiating DNA lesion acts a recipient of sequence information transferred from the intact donor chromosome (Symington *et al*., 2014). From our analysis, we can determine whether the homologs derived from the haploid parents YJM789 and W303-1A were equally susceptible to the initiating DNA lesion. As shown in Supplementary file 1 - Table S3, of the 38 DSCB events, 18 were initiated on the YJM789-derived homolog and 20 were initiated on the W303-1A-derived homolog. Of 40 SCBs (the event shown in Supplementary file 2 - Fig. S60 had two SCBs), the numbers initiated on the YJM789 and W303-1A homologs were 15 and 25, respectively; by chi-square analysis, these numbers are not significantly different from a 1:1 ratio (p=0.16). As expected, therefore, both homologs are equally susceptible to recombinogenic UV-induced DNA lesions.

Location of the DNA lesion that initiates recombination

For some events, the pattern of SNPs in recombinant chromatids allowed us to predict locations of the initiating DNA lesion, although most of these predictions had a degree of

uncertainty. For single SCB events, the predicted position on the chromatid with the recombinogenic DNA lesion (likely a DSB) is shown as an arrow labeled DSB1 in Supplementary file 2 - Figs. S3-S80. For example, in Supplementary file 2 - Fig. S4, we show an arrow to the left of the conversion tract in chromatid 3. With equal validity, the arrow could have been placed to the right side or in the middle of the conversion tract. For DSCB events that are explicable by a single DSB on an unreplicated chromosome (Supplementary file 2 - Fig. S15), we show the DNA lesions by labeled arrows at the same positions on the replicated chromatids. In events that appear to require two independent DNA lesions (for example, Supplementary file 2 - Fig. S3), DSBs are labeled DSB1 and DSB2. For some DSCB events, we used information for all the recombinant chromatids to infer the position of the initiating DSB. For example, in Supplementary file 2 - Fig. S9, the initiating lesion for the NCO event on chromatid 3 could be placed at either end or in the middle of the conversion/heteroduplex tract. The pattern of the heteroduplex tract in chromatid 4, however, suggested the location of the initiating DSB shown by the arrow in Supplementary file 2 - Fig. S9.

Simple classes of CO and NCO chromatids

The 116 UV-induced CO and NCO events in YYy310 were classified into nine groups (Supplementary file 1 - Table S3), Classes 1-8 representing events with relatively straightforward interpretations (71 events) and a "Complex" class requiring more complicated mechanisms (45 events). In our discussion of mechanisms, we will assume that the recombinogenic lesion is a DSB, although there is evidence that DNA nicks are also recombinogenic (Fabre *et al*., 2002; Lettier *et al*., 2006; Davis and Maizels, 2014). As described above, the DSCB events are most easily explained as reflecting a DSB in G_1; the SCB events could be initiated by either a DSB in S/G_2 or a DNA molecule that is nicked in G_1 and replicated to generate the DSB in S/G_2.

In the discussion of classes below, we use the term “heteroduplex” to refer to duplex regions with mismatches, indicating DNA strands derived from different homologs. Conversion tracts are

regions in which both of the interacting chromatids have homoduplexes derived from the donor chromatid (Fig. 2), and restoration tracts are regions in which the mismatches in heteroduplexes were inferred to be corrected to restore the original sequence of the recipient chromatid. The eight classes of events (Fig. 8, Classes 1-4 in Supplementary file 2 - Fig. S1 and Classes 5-8 in Supplementary file 2 - Fig. S2) are: Class 1 (NCO, single continuous heteroduplex tract on one side of putative DSB site), Class 2 (NCO, single continuous conversion tract on one side of putative DSB site), Class 3 (NCO, hybrid heteroduplex/conversion tract located on one side of putative DSBs site), Class 4 (CO, heteroduplex on only one side of putative DSB site), Class 5 (NCO, heteroduplex on one side of putative DSB site, and conversion tract on the other), Class 6 (CO, uni-directional heteroduplexes on both chromatids propagated in opposite directions), Class 7 (CO, no observable heteroduplex or conversion tract on either recombinant chromatid), Class 8 (NCO; two recombinant chromosomes, one containing a conversion tract, and the second with a heteroduplex involving SNPs at the same position). The number of events in each of these classes are shown in Table 1.

Before discussing these classes in detail, we point out that heteroduplexes can be detected only if the heteroduplex includes a SNP. The diploid used in our study is heterozygous for about 55,000 SNPs, but only 13,000 of these SNPs are included on the microarrays (St. Charles *et al*., 2012). Since the average distance between SNPs, as assayed by the microarray, is about 1 kb, a fraction of short heteroduplex/conversion tracts will be undetectable (St. Charles *et al*., 2012; Zheng *et al*, 2016). We estimated the fraction of undetected events using the same procedure as Mancera *et al.* (2008) and Martini *et al.* (2011). Assuming that all crossovers are associated with heteroduplexes on both interacting chromatids, we determined what fraction of such chromatids had an observable heteroduplex or conversion (Table S3). Of 33 crossovers, 23 had regions of heteroduplex on both recombined chromatids, 8 had only one region of heteroduplex on the two chromatids, and 2 had no detectable heteroduplex on either chromatid. Thus, we estimate that our methods detect about 80% (54/66) of the conversion events that are

unassociated with crossovers. This calculation is dependent on the assumption that the lengths of the crossover-associated conversions are similar to those of the conversions that are unassociated with crossovers.

The largest class, Class 1, has the pattern of SNPs expected for events initiated by the SDSA pathway (Fig. 1A, Fig. 8A). Class 2 events could also reflect SDSA events, however, the observed conversion tracts are not consistent with the simplest form of the DSBR model. One possibility is that, following disengagement of the invading end, the mismatches in the heteroduplex are repaired by an Mlh1-independent pathway (Fig. 8B). Coïc *et al*. (2000) reported the existence of a short-patch (<12 bp) Msh2-independent repair pathway in yeast. This pathway was hypothesized to explain a small number of recombination events in *msh2* strains in which regions of unrepaired mismatches were interspersed with repaired mismatches. No genes in this pathway have been identified, although Coïc *et al.* (2000) argued that the nucleotide excision repair proteins were not involved. Alternatively, short-patch mismatches close to the DSB could be removed by the proofreading activity of polymerase δ (Anand *et al*., 2017). Although such pathways could explain conversion tracts limited to one or a few closely-spaced SNPs (Supplementary file 2 - Fig. S4, for example), it seems unlikely to explain conversion tracts extending over several kb (Supplementary file 2 - Fig. S23: for example).

An alternative model is that the Class 2 NCO events are a consequence of the repair of a double-stranded DNA gap (Fig. 8C). In experiments in which gapped plasmids are transformed into yeast, gap-repair occurs readily (Orr-Weaver *et al*.,1981), and such gap repair was an intrinsic part of the original DSBR model (Szostak *et al*., 1983). Since in most meiotic recombination events in yeast, DSBs are processed by degradation of only one strand of the duplex (De Massy *et al*., 1995), gap repair is usually not considered part of the standard DSBR model. Giannattasio *et al.* (2010), however, reported that the Exo1p could cause expansions of nucleotide excision repair tracts from 30 bases to several kb. Based on our previous observations that showed a two-fold reduction in UV-induced mitotic recombination in the *exo1*

mutants, we previously suggested that Exo1-mediated tract expansion has a role in generating recombinogenic lesions in UV-treated cells (Yin and Petes 2014); the Exo1p could be involved in the long-tract Class 2 events. In summary, we suggest that events with long conversion tracts may reflect the repair of a double-stranded DNA gap, and short regions of conversion may represent Mlh1-independent MMR. Another possible mechanism for Class 2 events is that the broken end invades the homolog, and copies sequences by a BIR-like mechanism before disengaging from the homolog and re-engaging with the other broken end.

Class 3 NCO events are similar to Class 2, and have a similar mechanistic explanation. For Class 3 events, however, mismatches in one segment of the heteroduplex are repaired and those in the adjacent segment are not (Fig. 8D). Alternatively, the conversion tract could be generated by repair of a double-stranded DNA gap with a region of heteroduplex adjacent to the repair tract (Fig. 8E). The Class 4 CO events resemble the classic DSBR pathway except heteroduplexes are observed on only one site of the putative DSB site. One possibility is that the event occurs by the DSBR pathway but one heteroduplex does not include a heterozygous SNP and, therefore, is not observable (Fig. 8F). Studies of meiotic recombination suggest that heteroduplexes flanking the recombination-initiating DNA lesion are often of different lengths (Merker *et al*., 2003; Jessop *et al*., 2005).

Class 5 NCO events are explicable as reflecting the repair of one broken end with a double-stranded DNA gap and one broken end with the canonical processing of one strand (Fig. 8G) Following SDSA, a recombinant chromatid in which the putative DSB site is flanked by a heteroduplex on one side and a conversion tract on the other will be produced. The Class 6 CO events have the structure predicted for a CO in the DSBR pathway (Fig. 1, Fig. 8H). There were only two such events in our dataset. Class 7 events resemble Class 4 and Class 6 events except there are no observed heteroduplexes on either side of the putative DSB site. Class 7 COs might reflect intermediates with short heteroduplexes or heteroduplexes that are in regions that do not include SNPs (Fig. 8I).

In the Class 8 NCO events, both interacting chromatids have recombinant SNPs, and the conversion tract on one chromatid overlaps with the heteroduplex tract on the other (Fig. 8J and 8K). In Fig. 8J, this class is generated by formation of a dHJ with one region of short/undetectable heteroduplex, followed by resolution of the dHJ as a NCO. An alternative possibility is that branch migration occurs to generate regions of heteroduplex on both chromatids (Fig. 8K). Mlh1-independent repair of mismatches in one, but not both, of the heteroduplexes could produce the observed pattern.

If we assume that not all heteroduplexes are detectable, Classes 1, 4, 6, and 7 are consistent with the DSBR model of Fig. 1. For CO classes with uni-directional heteroduplexes on both chromatids (propagated in opposite directions), all events had the pattern expected for nick-directed resolution of Holliday junctions. As shown in Fig. 1, nick-directed cleavage of the junctions (sites marked as 1, 2, 7 and 8) result in a different pattern of heteroduplexes than cleavage of unnicked junctions (sites marked as 2, 4, 5, and 6). Previously, a bias of the same type was detected for recombination events involving plasmid integration (Mitchel *et al.*, 2010). This observation is also consistent with previous studies that showed that *mus81* strains, but not *yen1* strains, had reduced frequencies of crossovers without an effect on gene conversions (Ho *et al.*, 2010; Yin and Petes, 2015); Mus81, but not Yen1, has a substrate preference for nicked junctions (Schwartz and Heyer, 2011).

Most of the other events require Mlh1-independent mismatch correction or the repair of a double-stranded DNA gap. These classes, however, represent only half of the total “simple” events. As discussed below, the complex classes require even more radical departures from the canonical recombination model.

Complex classes of CO and NCO chromatids

Those events that were classified as complex are shown in Supplementary file 1 - Table S3. A more detailed description of the complex classes is in Supplementary file 1 - Table S4, and possible interpretations of these events are shown schematically in Supplementary file 2. Of the

SCB events, 35 of 40 were “simple” (Classes 1-8) and only 5 were complex. Assuming the same distribution for the 38 DSCB events, the expected frequencies of DSCBs with two simple events, one simple and one complex event, and two complex events are 29, 8, and 1, respectively. We observed (Supplementary file 1 - Table S2) 12, 11, and 15 of these classes, respectively, a very significant ($p<0.0001$ by chi-square test) departure from this expectation. This observation suggests that the timing of the recombinogenic DSB (G_1 versus G_2) may influence the complexity of its repair. Below, we will discuss two of these complex events in detail. We note that many of these events can be explained by more than one mechanistic pathway, and we have tried to describe the simplest one.

The event depicted in Supplementary file 2 - Fig. S8 (re-drawn in Fig. 9A) is a DSCB event initiated on the red chromosome. The CO occurred between chromatids 1 and 4. One feature of the CO that is not consistent with the canonical DSBR model is that heteroduplexes are observed at the same position on both crossover chromatids. This pattern is consistent with the possibility of branch migration of one of the Holiday junctions in the rightward direction, resulting in a region of symmetric heteroduplexes (Fig. 9B). Since the heteroduplex tract is longer on chromatid 4 than on chromatid 1, there was likely a region of Mlh1-independent conversion-type repair of mismatches on chromatid 4. In the NCO event (involving chromatids 2 and 3), chromatid 2 had two regions of heteroduplex in which there was a strand switch at the junction of the putative DSB site. This pattern can be explained by formation of a dHJ that was resolved by dissolution (Fig. 9C). As for the CO event, we also need to postulate a region of Mlh1-independent MMR at one end of the heteroduplex tract.

The event shown in Supplementary file 2 - Fig. S16 (re-drawn in Fig. 10A) is also a DSCB event with the CO involving chromatids 1 and 3, and the NCO involving chromatid 4. The CO event is consistent with the classic DSBR model (Fig. 10B). If we assume that the NCO event was initiated by a DSB at the same position, the heteroduplex spanning the DSB site is inconsistent with the DSBR model. One mechanism to explain the observed NCO pattern is that

the right broken end undergoes degradation of both strands, and the left end is extended by invasion of the sister chromatid (Fig. 10C). This invading end is then unpaired from the sister chromatid and pairs with the right end. After processing the dHJ in the NCO mode, the net result of these steps is a recombinant chromatid with a region of heteroduplex that spans the initiating DSB site.

Of the 46 complex events described in Supplementary file 1 - Tables S3 and S4, about 40% (18 of 46) can be explained by mechanisms involving template switching, branch migration, or independent invasion of two broken ends. In addition, this relatively large fraction of complex events is not solely a characteristic of UV-induced events in *mlh1* strains. About one-third of the spontaneous events in a wild-type strain (St. Charles and Petes, 2013), and 15% of the UV-induced events in a wild-type strain (Yin and Petes, 2013) appear associated with "patchy" repair of mismatches and/or branch migration.

Lengths of conversion/heteroduplex tracts in UV-treated YYy310

The median lengths of conversion/heteroduplex tracts in NCO and CO events in UV-treated YYy310 were 5.4 kb (95% confidence limits [CL] of 3.6-7.2 kb) and 10 kb (CL 5.7-17 kb), respectively; the median length of all tracts was 6.1 kb (CL 4.8-8.5 kb). For the CO events, we summed the lengths of the tracts on the two CO chromatids, since these events reflect the repair of a single DSB. These lengths are similar to those previously determined for the UV-treated isogenic wild-type strain (Yin and Petes, 2013): 5.7 kb (CL 4.5-6.6) for NCO events; 8.2 kb (CL 6.6-10.3) for CO events; 6.4 kb (CL 5.8-7.3) for all tracts. Thus, the Mlh1p does not have a significant role in determining the length of conversion tracts (Supplementary file 1 - Table S7).

Analysis of spontaneous crossovers on chromosome V in YYy310.

Although most of the conclusions from our study are based on UV-induced events in YYy310, we also examined five spontaneous crossovers on chromosome V by similar procedures. No unselected crossover or BIR events were observed among these sectors. The coordinates for LOH transitions in the granddaughter cells of each colony, and the classification

of these events as Classes 1-8 or complex events are shown in Supplementary file 1 - Tables S2 and S3, respectively. The events are depicted in Supplementary file 2 - Figs. S81-S85, and the mechanisms that explain these events are in Supplementary file 2 - Figs. S125-S129.

All five sectored colonies reflected DSCBs with one CO and one NCO event. Nine of the ten COs and NCOs were complex with similar features to the UV-induced complex events (Mlh1-independent repair, gap repair, branch migration, and independent invasion of two broken ends) (Supplementary file 1 - Table S4). Thus, the complexity of the patterns of recombination observed in the UV-induced events is not likely to be a consequence of the multiple DNA lesions introduced by UV. The higher proportion of complex events relative to the UV-induced exchanges may be a consequence of the nature of the recombinogenic lesion or differences in the mechanism of DNA repair in cells that have a single DNA lesion versus those with high levels of DNA damage."

Analysis of spontaneous crossovers at the HS4 hotspot on chromosome IV in YYy311.

Previously, we showed that an inverted pair of Ty elements resulted in a spontaneous mitotic recombination hotspot (termed "HS4") on the right arm of chromosome IV (St. Charles and Petes, 2013). We subsequently showed that HS4-associated conversion events were associated with very long (>25 kb) conversion tracts (Yim *et al*., 2014); conversion tracts associated with a similar pair of inverted Ty elements on chromosome III also have very long conversion tracts (median length of 41 kb; Chumki *et al*., 2016). To monitor the activity of this hotspot in an *mlh1* strain, we inserted the *hphMX4* and *URA3* markers centromere-proximal and centromere-distal to HS4 on one of the two homologs in the *mlh1* diploid YYy311. In addition, the YJM789-derived copy of IV has an insertion of *SUP4-o* near the right telomere. A crossover between the two markers results in a red/white sectored colony in which the white sector is resistant to hygromycin (Hyg^R) and 5-fluoro-orotate ($5\text{-}FOA^R$), and the red sector is Hyg^R $5\text{-}FOA^S$ (Fig. 11). In an isogenic wild-type strain, 17% of sectored red/white colonies result from a crossover in the *hphMX4-URA3* interval (St. Charles and Petes, 2013). 17% (101/593) of the

spontaneous sectoring events in the isogenic *mlh1* strain YYy311 occurred in this same interval, indicating that loss of Mlh1 does not reduce the activity of HS4. We examined six of the sectored colonies by SNP microarrays (Supplementary file 1 - Tables S2-S4), and five had patterns of recombination indicating an HS4-initiated event (shown in Supplementary file 2 - Figs. S87-S91). Since the recombination event in sectored colony shown in Supplementary file 2 - Fig. S86 is initiated somewhere in the interval 968-978 kb, and HS4 is located in the interval 981-993 kb, this event is not likely to be HS4-initiated. Since the 56 kb *hphMX4-URA3* interval is considerably larger than the size of the HS4 hotspot (12 kb), it is not surprising that some crossovers in the *hphMX4-URA3* region are not HS4-mediated. Mechanisms consistent with the HS4-mediated events are shown in Supplementary file 2 - Figs. S87-S90.

Based on the five HS4-initiated events, we can make several generalizations. In all events, at least three chromatids had transitions between W303-1A- and YJM789-derived sequences, indicating that all HS4-initiated events involved the repair of two sister chromatids broken at approximately the same position. Second, all events are initiated on the red (W303-1A-derived homolog), as expected since the YJM789-derived homolog lacks HS4 hotspot activity (St. Charles and Petes, 2013). Third, with the exception of the event in Supplementary file 2 - Fig. S88, gaps of at least 25 kb are observed in the HS4-initiated events; these gaps are much larger than necessary to remove the approximately 9 kb HS4-related heterology that is present in W303-1A but absent in YJM789-derived homolog (St. Charles and Petes, 2013). Fourth, many of these gaps are flanked by heteroduplexes on one or both sides. Gaps can be propagated symmetrically from HS4 (Supplementary file 2 - Fig. S89) or with a bias toward or away from the centromere. Fifth, some of the gaps (regions of 4:0 segregation without heteroduplexes) are interrupted by regions of heteroduplex (chromatid 4 of Supplementary file 2 - Fig. S91). Such a pattern can be explained by a template switch to a sister chromatid as shown in Supplementary file 2 - Fig. S91.

We also used SNP microarrays to examine twelve red/white sectored colonies with a

crossover in the *hphMX4-URA3* interval in UV-treated YYy311. Since it was clear that none of these twelve colonies had an HS4-mediated event, we did not attempt to look for two genotypes within each sector, In addition, a smaller fraction of events (10%, 10/102) were in the *hphMX4-URA3* interval in the UV-treated samples of YYy311 than in the untreated samples. Thus, HS4 is a hotspot for spontaneous, but not UV-stimulated recombination events.

Effect of the *mlh1* mutation on the frequency of mitotic crossovers

Two different assays can be used to monitor the effect of the *mlh1* mutation on crossovers: the frequencies of spontaneous and UV-induced red/white sectored colonies compared to wild-type, and the frequency of unselected crossovers in UV-treated cells. These two assays yield somewhat different results. We observed slightly more (<two-fold) spontaneous red/white sectored colonies in YYy311 than in the isogenic wild-type strain (53 sectored colonies/998395 total colonies [$5.3x10^{-5}$/division]) in the *mlh1* strain versus 55 sectors/1761664 total [$3.1x10^{-5}$/division; St. Charles and Petes, 2013]). A similar slight elevation was observed for UV-treated YYy311 cells: 378 sectors/3228 total (11.7%) in the *mlh1* strain versus 127 sectors/1420 total (8.9%) in the isogenic wild-type strain. In addition, the frequency of UV-stimulated sectored colonies in YYy310 (*SUP4-o* on chromosome V) is higher than the UV-stimulated events in the isogenic wild-type strain: 45 sectors/2980 colonies (1.5%) and 68 sectors/7194 colonies (0.9%), respectively.

An elevated frequency of crossovers could be explained by the heteroduplex-rejecting properties of Mlh1p (Harfe and Jinks-Robertson, 2000). If this mechanism was relevant to our system, we might expect a higher density of SNPs and in/dels in the heteroduplex tracts of *mlh1* strains than observed in tracts in the wild-type strain. In the UV-treated *mlh1* strain, we observed 2688 SNP+in/dels in tracts with a total length of 635041 bp, a density of 0.0042. In the UV-treated wild-type strain (Yin and Petes, 2013), we found 15387 SNP+in/dels in tracts totaling 4573874 bp, a density of 0.0034. By a Mann-Whitney comparison, the difference in density is of borderline significance (p=0.06).

In contrast to the first assay, the second assay indicates that Mlh1p positively influences the frequency of crossovers. In our previous study of unselected recombination events, in twenty UV-induced sectored colonies in the wild-type strain (Yin and Petes, 2013), we observed 141 interstitial LOH events, 50 COs, and 10 BIR events for a total of 201 LOH events (10.1/sectored colony). In seven sectored colonies of the *mlh1* YYy310 strain, we found 65 interstitial LOH events, 6 COs, and 0 BIR events for a total of 71 LOH events (10.1/sectored colony) (Supplementary file 1 - Table S8). The reduction in the number of COs is statistically significant ($p=0.003$ by Fisher exact test). Although the discrepancy in the two assays prevents a strong conclusion about the effect of Mlh1p on mitotic crossovers, the direct assay of unselected crossovers by microarrays is less prone to artifacts than the frequency of red/white sectors since colony color can be affected by a variety of different types of genetic alterations including mitochondrial mutations (Kim *et al*., 2002).

Discussion

The main conclusion from our analysis is that about one-third of mitotic recombination events are not explicable by the simplest forms of the double-strand-break repair model. More specifically, we need to invoke branch migration of Holliday junctions, template switching during repair synthesis, repair of double-stranded DNA gaps, and/or Mlh1-independent MMR. Our analysis confirms our previous conclusion that more than half of spontaneous crossovers and recombination events induced by high doses of UV reflect the repair of two sister chromatids broken at approximately the same position, likely resulting from replication of chromosome broken in G_1. We also show that mitotic recombination events involve heteroduplexes that are longer than those observed for meiotic exchanges. In a previous study, we characterized a hotspot for spontaneous mitotic recombination events (HS4) associated with an inverted pair of Ty elements (St. Charles and Petes, 2013). In the current study, we show that the very long conversion tracts associated with HS4-initiated events (Yim *et al*., 2014) are associated with the repair of long double-stranded DNA gaps. In addition, HS4 hotspot activity is independent of Mlh1p and is not induced by UV.

Complexity of recombination events

Before discussing exceptions to the recombination model shown in Fig. 1, it is important to point out that about two-thirds of the observed events do fit this model. Among the exceptional events are those in which the two interacting chromatids have heteroduplexes involving SNPs at the same positions (for example, the CO chromatids 1 and 4 in Supplementary file 2 - Fig. S8). Symmetric heteroduplexes of this type can be explained as a consequence of branch migration of a Holliday junction. We previously suggested that branch migration may explain complex patterns of SNPs in MMR-proficient strains (St. Charles *et al*., 2012; Yin and Petes, 2013). Branch migration during meiotic recombination in yeast would be detectable as two spores with post-meiotic segregation within one tetrad (aberrant 4:4). Such events are rare in yeast, although a few percent of the total aberrant segregants had this pattern in an *msh2* strain

(Martini *et al*., 2011).

In the current DSBR model, gene conversion events are a consequence of the repair of mismatches in heteroduplexes. Thus, in the absence of MMR, conversion events should be absent. In our study, we frequently observed conversion tracts, some adjacent to a heteroduplex tract (Supplementary file 2 - Fig. S5, chromatid 4) and some "solo" conversions (Supplementary file 2 - Fig. S4, chromatid 3) One possible source for such events is Mlh1-independent MMR. In cell-free extracts, MMR is only partially defective in the absence of Mlh1 if there is a 5' nick near the mismatch (Genschel and Modrich, 2009). In addition, Coïc *et al*. (2000) identified a short-patch repair system in *S. cerevisiae* that was independent of the classic MMR system. The exonuclease activity of DNA polymerase δ could also remove mismatches close to the DSB (Anand *et al.,* 2017). If these uncharacterized systems are responsible for the conversion events observed in our studies, they are most likely to be involved in those events with short conversion tracts. We suggest that long conversion tracts (chromatid 2, Supplementary file 2 - Fig. S33; Supplementary file 2 - Figs. S87-91) likely reflect the repair of a large double-stranded DNA gap. Although DSBs are usually thought to be processed by 5'-3' degradation of the broken ends, resection of the 3' "tails" has also been observed (Zierhut *et al*., 2008). It is clear that *S. cerevisiae* has the ability to repair double- stranded DNA gaps (Orr-Weaver *et al*., 1981) and, in the first version of the DSBR model, both gap repair and MMR were presented as mechanisms for generating a gene conversion event (Szostak *et al*., 1983).

We also observed both short and long tracts of restoration. For example, the long heteroduplex tract in chromatid 2 of Supplementary file 2 - Fig. S3 is interrupted by several one-SNP restoration tracts; such tracts may reflect Mlh1-independent MMR. In Supplementary file 2 - Fig. S44, a long heteroduplex tract on chromatid 1 is interrupted by a long tract of restoration. As shown in Supplementary file 2 - Fig. S44, this pattern can be explained by a template switch, followed by SDSA. In invoking template switching to explain certain patterns of SNP segregation, we point out that such switches were also proposed as intermediates in the production of

complex meiotic recombination events (Martini *et al*., 2011). In addition, template switching is commonly observed during break-induced replication (Smith *et al*., 2007). Since the sister chromatid is a preferred substrate for the repair of DSBs in mitosis (Kadyk and Hartwell, 1992; Bzymek *et al*., 2010), a template switch to the sister chromatid would not be unexpected.

In previous mitotic (Miura *et al*., 2012) and meiotic recombination studies (Martini *et al*., 2011), some events appear to reflect independent interactions of the left and right broken ends with the intact template. For example, Martini *et al*. proposed that a double SDSA event could produce a NCO chromatid in which heteroduplexes with a strand switch were separated by a region of restoration. Similarly, in our analysis, some events are likely to reflect double-ended invasions. In Supplementary file 2 - Fig. S83, the CO chromatid 4 has a heteroduplex with a strand switch that flanks the putative DSB site. This pattern, which is unexpected by the DSBR model, can be explained by invasion of the right broken end, followed by processing, and subsequent invasion of the left broken end.

The complex patterns of recombination observed in our study are also found in global analysis of meiotic recombination events in wild-type (Mancera *et al*., 2008) and *msh2* (Martini *et al*., 2011) strains. In the Mancera *et al*. study, more than 10% of the conversion tracts were described as “complex”, and, in the Martini *et al*. analysis, the majority of the CO- associated heteroduplex tracts required Msh2-independent MMR, branch migration, template switches, and/or the repair of double-stranded gaps. These observations contrast with other studies of mitotic recombination events induced with an endonuclease at a specific site; such events tend to have simpler patterns of marker segregation (Nickoloff *et al*., 1999; Mitchel *et al*., 2010). Our studies differ from most previous studies in several ways: the nature of the recombinogenic lesions, the timing of the DSBs during the cell cycle, and the diverse genetic location of the recombinogenic lesions. With regard to the third point, if DNA lesions at different regions of the genome utilize different pathways of repair, as suggested by meiotic recombination studies (Medhi *et al*., 2016), then a global analysis of recombination would reveal more heterogeneity of

recombinant products than studies based on a single locus. Lastly, we point out our analysis is performed in diploid cells whereas many of studies of HO-induced events are done in haploids with duplicated sequences. Any or all of these factors may result in the greater complexity observed in our recombination events.

Comparison of recombination events in wild-type and *mlh1* strains

In general, our observations support the main conclusions of our previous studies of spontaneous (St. Charles and Petes, 2013) and UV-induced (Yin and Petes, 2013) mitotic recombination. In wild-type and *mlh1* strains, exchanges induced by high levels of UV in G_1-synchronized cells represent DSCBs and SCBs with approximately the same frequency. All five of the spontaneous events selected on chromosome IV in the *mlh1* strain YYy311 were DSCB events as were the majority of spontaneous events in the wild-type strain (St. Charles and Petes, 2013). In contrast, recombination events induced by low levels of DNA polymerase alpha (Song *et al*., 2014) or delta (Zheng *et al*., 2016) usually reflect the break of a single chromatid.

Esposito (1978) previously proposed that mitotic recombination in yeast was initiated in G_1-associated DSB that formed a Holliday junction connecting the two unreplicated homologs. Mismatch correction occurred in the heteroduplex regions, and the resulting intermediate was replicated to produce both CO and NCO recombinant products. By this model, granddaughter cells would not be expected to be genotypically different. Our analysis rules out this model.

In addition to its role in the repair of mismatches, the Mlh1p has two other functions related to recombination. First, in conjunction of Mlh3p, Mlh1p stimulates meiotic crossovers (Hunter and Borts, 1997; Wang *et al*., 1999); this function is likely related to its single-strand nicking activity (Rogacheva *et al*., 2014). If Mlh1p had a similar role in mitotic recombination, we would expect a hypo-Rec phenotype in *mlh1* strains. Conversely, for recombination substrates with diverged sequences, Mlh1 has anti-recombination activity (Nicholson *et al*., 2000). Strains lacking *mlh1* have seven-fold more crossovers than wild-type strains for substrates with 9% sequence divergence. Although this degree of divergence is much greater than the average 0.5%

divergence existing between the homologs in YYy310 and YYy311, strains lacking the Msh2 and Msh3 repair proteins have an elevated frequency of crossovers relative to wild-type for 350 bp substrates with a single mismatched base (Datta *et al*., 1997).

Based on the data described above, it is difficult to predict the effect of the *mlh1* mutation on mitotic recombination in our system. As discussed in the Results section, we find an elevated frequency of sectored colonies in the *mlh1* strain compared to the wild-type strain, but a reduced frequency of crossovers among unselected UV-induced recombination events. Although the results indicating a several-fold reduced frequency of crossovers in the *mlh1* strain are likely to be less prone to artifacts than the sectored colony assay, further experiments are needed to substantiate them.

Analysis of the HS4 mitotic recombination hotspot

Previously, we demonstrated that an inverted pair of Ty elements on the W303-1A-derived copy of chromosome IV stimulated mitotic recombination (St. Charles and Petes, 2013); this hotspot was called “HS4”. The HS4-associated recombination events have the following properties (St. Charles and Petes, 2013; Yin and Petes, 2014; Yim *et al*., 2014): 1) they are DSCB events, 2) both of the Ty elements are required for hotspot activity, 3) the events are initiated on the W303-1A homolog presumably because the YJM789 homolog lacks the inverted pair of elements, 4) HS4 activity requires the Exo1p, and 5) conversion events associated with HS4 are extraordinarily long with a median size >50 kb. Our analysis of five HS4-related events (Supplementary file 2 - Figs. S87-91) shows that most have the properties expected for the repair of a large double-stranded gap (long conversion events) with flanking heteroduplex regions. Since the HS4 hotspot on the W303-1A-derived homolog is a pair of inverted repeats and the comparable region on the YJM789 homolog has only a partial Ty element in the same location (St. Charles and Petes, 2013), a DSB occurring within HS4 would require a region of end resection of at least 10 kb to expose sequence homologies between the two homologs. In general, the conversion/heteroduplex tracts for the HS4-induced events exceed 10 kb by a

considerable amount (Supplementary file 1 – Table S9). For example, in the NCO event on chromatid 2 of Supplementary file 2 - Fig. S91, the total length of the conversion/heteroduplex region is 39 kb, comparable to the lengths of conversion tracts observed in the wild-type strain (Yim *et al*., 2014).

Our data show that the very long conversion tracts observed in wild-type strains are not a consequence of extremely long heteroduplexes, but reflect an intermediate that does not have mismatched bases. Since we observe many other events that are explicable as gap repair, this is our preferred explanation for the HS4-associated events, which is consistent with the observation that the activity of HS4 requires Exo1p (Yin and Petes, 2014). The possible role of Exo1p is the expansion of a single-stranded nick into a large single-stranded gap before DNA replication, facilitating the formation of secondary structures involving the inverted Ty elements that could be subsequently processed by structure-specific nucleases to form the recombinogenic DSB. As described above, the broken ends would require extensive single-stranded processing because of the heterology in order to invade the homolog. These long single-stranded regions could be susceptible to endonucleolytic attack, resulting in the observed double-stranded gaps. We cannot, however, rule out the generation of these long conversion tracts by a BIR-like mechanism (Yim *et al*., 2014). We found that HS4-associated hotspot was not stimulated by UV. This result argues that the activity of HS4 is not a consequence of random DNA breaks located near in the inverted repeat, but is likely a consequence of a DSB induced in a secondary structure in the DNA that is formed independently of nearby DSBs. Lastly, we suggest that the long conversion tracts associated with HS4 might be a general property of recombination events initiated in a large heterozygous insertion.

Summary

In conclusion, our global analysis of UV-induced and spontaneous mitotic recombination events in an MMR-deficient yeast strain demonstrates that many of the events are more complex than predicted by the current DSBR model. We find that many gene conversion tracts

are generated by a mechanism that does not involve the Mlh1-dependent repair of mismatches within a heteroduplex.

Materials and Methods

Strains

Constructions of the hybrid diploid strains YYy310 (isogenic isolates YYy310.9, YYy310.10) and YYy311 (isogenic isolates YYy311.1 and YYy311.3) are described in detail in Supplementary file 1 - Table S1. In brief, the *MLH1* gene was deleted from haploid derivatives of W303-1A and YJM789; these strains have about 0.5% sequence divergence (Wei *et al*., 2007). The primary difference between YYy310 and YYy311 is the location of the tRNA suppressor gene *SUP4-o*: located near the left telomere of the YJM789-derived chromosome V homolog in YYy310, and near the right telomere of the YJM789-derived chromosome IV homolog in YYy311. As explained in the text, this heterozygous insertion allows detection of crossovers as red/white sectored colonies. In addition, in the YYy311 strain on the W303-1A-derived homolog, the previously-described HS4 hotspot (St. Charles and Petes, 2013) was flanked by *hphMX4* and *URA3* markers. In both YYy310 and YYy311, the *MATα* locus was deleted to allow G_1-synchronization with α-factor. This deletion also prevents the strains from undergoing meiosis in normal growth conditions. As noted below, however, such strains can be induced to undergo meiosis using special sporulation conditions.

Isolation of granddaughter cells derived from red/white sectors

Most of the details of this analysis are described in the main text. In brief, we purified about 10-20 individual colonies from the red and white sectors. We analyzed one purified colony by SNP-specific microarrays to determine the approximate location of the selected recombination event. We then identified SNPs within these regions that could be assayed by a combination of PCR followed by treatment of the resulting PCR fragment with a diagnostic restriction enzyme. This procedure was previously used to detect LOH events on chromosome V (Lee *et al*., 2009). We employed this type of analysis with about 10-20 individual red and white colonies derived from each sector using the PCR primers and restriction enzymes listed in Supplementary file 1 - Table S5. If two PCR samples produced different fragment sizes after treatment with the

restriction enzyme, we concluded that these strains represented the two granddaughters within the sector. We were able to detect most granddaughter cells using SNPs located on chromosomes V (YYy310) or IV (YYy311). However, for some sectored colonies, we used SNPs located on other chromosomes (Supplementary file 1 - Table S5). For some chromosomal regions, the SNPs did not result in an altered restriction enzyme recognition site. Consequently, for some events, we examined SNPs by sequencing PCR fragments from the relevant regions of the genome. The primers used in this analysis are also shown in Supplementary file 1 - Table S5.

Meiotic analysis of marker coupling

For granddaughter cells with multiple heterozygous regions interspersed with homozygous regions (for example, Fig. 6A), we determined the coupling of these regions by examining microarrays of single spore cultures derived from the four granddaughters. Although the diploidsYYy310 and YYy311 lack *MATα* locus, these strains can be sporulated in medium containing 5 mM nicotinamide (St. Charles *et al*., 2012). By examining a single spore, we could generally determine the coupling relationships of the markers in each granddaughter. For example, the pattern of hybridization to SNPs shown for the spore in Fig. 68 demonstrates that the two regions of heteroduplex in the granddaughter cell are on different homologs. For most of the granddaughter cells, the SNP patterns of one daughter spore allowed unambiguous conclusions. However, if the pattern of SNPs in the spore was inconsistent with that observed in the diploid or if additional crossovers were observed within 50 kb of the mitotic recombination event, we considered the possibility of a meiotic crossover. Consequently, for such events, we examined the segregation pattern of SNPs flanking the region of mitotic exchange in several additional spores derived from the granddaughter cells. The primer pairs and restriction enzymes used in this analysis are described in Supplementary file 1 - Table S5. Complicating meiotic recombination events were rare, as expected, because the *mlh1* mutation substantially reduces the frequency of meiotic crossovers in yeast (Hunter and Borts, 1997).

Spontaneous red/white sectors generally had no unselected events. To determine coupling relationships within heterozygous regions, we used a different procedure from that described for the UV-induced events. We screened for monosomy on the chromosome with the selected event using a marker located centromere-proximal to the exchange. In YYy310, the heterozygous *URA3* gene was on the same chromosome arm (left arm of V) as the selected crossover, but was located centromere-proximal to the mitotic exchange. We selected for loss of the copy of V that had the *URA3* gene by using medium containing 5-fluoro-orotate. We confirmed the loss using PCR analysis, and restriction enzyme digestion of the resulting PCR product. Chromosome V-specific SNP microarrays were then used to determine the coupling of markers along the remaining homolog. A similar procedure was used to examine spontaneous events on yeast chromosome IV in YYy311. In YYy311, we selected monosomic strains that lacked the heterozygous *TRP1* marker located near *CEN4* using medium containing 5-fluoroanthranilic acid (Toyn *et al*., 2000).

SNP microarrays

We used three types of SNP-Microarrays in our analysis: a whole-genome microarray (St. Charles *et al*., 2012) and microarrays to SNPs on chromosome IV (St. Charles and Petes, 2013) and chromosome V (Yin and Petes, 2013). The sequences of the oligonucleotides in the microarrays and their designs are on the Gene Expression Omnibus Website (https://www.ncbi.nlm.nih.gov/geo/) under the addresses GPL20144 (whole-genome), GPL21552 (chromosome IV), and GPL21274 (chromosome V). In brief, for each heterozygous SNP, we designed four 25-base oligonucleotides, two identical to the Watson and Crick strands of the W303-1A allele and two identical to the YJM789 allele. The heterozygous SNP was located near the middle of each oligonucleotide. Since the efficiency of hybridization is higher when genomic DNA is perfectly matched to the oligonucleotide than when there is a mismatch between the genomic DNA and the oligonucleotide, by measuring the ratio of hybridization of the experimental DNA to a control heterozygous strain for the four SNP-specific

oligonucleotides, we can determine whether the genomic DNA is heterozygous for SNP or homozygous for either allele. In our experiments, the ratios of hybridization to the different oligonucleotides were normalized by comparing these ratios to a control heterozygous diploid. Genomic DNA from the experimental strains (derived from YYy310 or YYy311) was labeled with the Cy5-dUTP fluorescent nucleotide and DNA from an isogenic wild-type strain was labeled with Cy3-dUTP. The labeled samples were mixed and hybridized to the microarray. Details concerning the hybridization conditions and determining the levels of hybridization to the oligonucleotide probes are in St. Charles *et al*. (2012) and St. Charles *et al*. (2013). The data for all of these hybridization experiments are on the GEO Website (GSE100497).

Calculation of conversion/heteroduplex tract lengths

Two types of conversion/heteroduplex events were observed in our studies: events unassociated with crossovers and events associated with crossovers. For the first class, we averaged the distance between the closest heterozygous SNPs flanking the tract (the maximum tract length) and the homozygous SNPs located at the borders of the conversion/heteroduplex tract (the minimum tract length). For crossover-associated conversion/heteroduplex tracts, we averaged the distance between the homozygous SNPs flanking the tract (the maximum tract length), and the distance between the SNPs that were within the tract closest to the borders of the crossover.

Bioinformatics and statistical analysis

The two haploid strains for W303 and YJM789 that were sequenced previously (St. Charles *et al*., 2012) were analyzed for the number of SNPs and insertions/deletions (in/dels) in gene conversion tracts. Paired-end reads were aligned to the S288c reference genome version 3 (downloaded from sad Cer3 in UCSC Genome Browser; https://genome.ucsc.edu) by BWA-MEM software (Li, 2013) and SNPs were determined using samtools (Li *et al*., 2009). Because our SNP-Microarray was based on S288c reference genome version 2 (downloaded from sacCer2 in UCSC Genome Browse), we translated the positions of the SNPs from the

microarray to the version 3 reference genome before counting the number of SNPs and indels within each of the conversion tracts. We then used BEDTools (Quinlan and Hall, 2010) to count the number of SNPs within the conversion tracts. RStudio (http://www.rstudio.com/ used for various statistical tests used in this study.

Acknowledgements

We thank members of the Petes and Jinks-Robertson labs for suggestions during the course of this work, and Sue Jinks-Robertson, Yee Fang Hum, Dao-Qiong Zheng and Ke Zhang for comments or help with the manuscript. The research was supported by NIH grants GM24110, GM52319, 1R35GM118020, and 5T32GM007754-37.

References

Anand R, Beach A, Li K, Haber J. 2017. Rad51-mediated double-strand break repair and mismatch correction of divergent substrates. *Nature* **544**:377-380.

Barbera MA, Petes TD. 2006. Selection and analysis of spontaneous reciprocal mitotic cross-overs in Saccharomyces cerevisiae. *PNAS* **103**:12819-12824.

Bzymek M, Thayer NH, Oh SD, Kleckner N, Hunter N. 2010. Double Holliday junctions are intermediates of DNA break repair. *Nature* **464**:937-942.

Cavenee WK, Hansen MF, Nordenskjold M, Kock E, Maumenee I, Squire JA, Phillips RA, Gallie BL. (1985). Genetic origin of mutations predisposing to retinoblastoma. *Science* **228**: 501-503.

Chakraborty U, Alani E 2016. Understanding how mismatch repair proteins participate in the repair/anti-recombination decision. *FEMS Yeast Research* **16**: fow071.

Chumki S, Dunn MK, Coates TF, Mishler JD, Younkin EM, Casper AM. 2016. Remarkably long-tract gene conversion induced by fragile site instability in *Saccharomyces cerevisae*. *Genetics* **204**:115-128.

Coïc E, Gluck L, Fabre F. 2000. Evidence for short-patch mismatch repair in *Saccharomyces cerevisiae*. *The EMBO Journal* **19**:3408-3417.

Covo S, Ma W, Westmoreland JW, Gordenin DA, Resnick MA. 2012. Understanding the origins of UV-induced recombination through manipulation of sister chromatid cohesion. *Cell Cycle* **11**:3927-3944.

Datta A, Hendrix M, Lipsitch M, Jinks-Robertson S.1997. Dual roles for DNA sequence identity and the mismatch repair system in the regulation of mitotic crossing-over in yeast. *PNAS* **94**:9757-9762.

Davis L, Maizels N. 2014. Homology-directed repair of DNA nicks via pathways distinct from canonical double-strand break repair. *PNAS* **111**:E924-932.

De Massy B, Rocco V, Nicolas A. 1995. The nucleotide mapping of DNA double-strand breaks

at the *CYS3* initiation site of meiotic recombination in *Saccharomyces cerevisiae*. *The EMBO Journal* **14:**4589-4598.

Donnianni RA, Symington LS. 2013. Break-induced replication occurs by conservative DNA synthesis. *PNAS* **110**:13475-13480.

Esposito MS. 1978. Evidence that spontaneous mitotic recombination occurs at the two-strand stage. *PNAS* **75**:4436-4440.

Fabre F, Chan A, Heyer, WD, Gangloff S. 2002. Alternate pathways involving Sgs1fTop3 , Mus81/Mms4, and Srs2 prevent formation of toxic recombination intermediates from single-stranded gaps created by DNA replication. *PNAS* **99**:16887- 16892.

Genschel J, Modrich P. 2009. Functions of MutLalpha, replication protein A (RPA), and HMGB1 in 5'-directed mismatch repair. *Journal of Biological Chemistry* **284**:21536-21544.

Giannattasio M, Follonier C, Tourriere H, Puddu F, Lazzaro F, Pasero P, Lopes M, Plevani P, Muzi-Falconi M. 2010. Exo1 competes with repair synthesis, converts NER intermediates to long ssDDNA gaps, and promotes checkpoint activation. *Molecular Cell* **40:**50-62.

Harfe BD, Jinks-Robertson S. 2000. DNA mismatch repair and genetic instability. *Annual Review of Genetics* **34**:359-399.

Ho CK, Maxon G, Lam AF, Symington LS. 2010. Mus81 and Yen1 promote reciprocal exchange during mitotic recombination to maintain genetic integrity in budding yeast. *Molecular Cell* **40**:988-1000.

Huang M-E, Rio AG, Nicolas A, Kolodner RD. 2003. A genomewide screen in *Saccharomyces cerevisiae* for genes that suppress the accumulation of mutations. *PNAS* **100**:11529-11534.

Hunter N, Borts RH.1997. Mlh1 is unique among mismatch repair proteins in its ability to promote crossing-over during meiosis. *Genes & Development* **11**:1573-1582.

Jessop L, Allers T, Lichten M. 2005. Infrequent co-conversion of markers flanking a meiotic recombination initiation site in *Saccharomyces cerevisiae*. *Genetics* **169**:1353-1367.

Kadyk LC, Hartwell LH.1992. Sister chromatids are preferred over homologs as substrates for

recombinational repair in *Saccharomyces cerevisiae*. *Genetics* **132**:469-487.

Kegel A, Sjostrand JO, Astrom SU. 2001. Nej1p, a cell type-specific regulator of nonhomologous end joining in yeast. *Curr. Biol.* **16:**1611-1617.

Kim G, Sikder H, Singh KK. 2002. A colony color method identifies the vulnerability of mitochondria to oxidative damage. *Mutagenesis* **17**:375-381.

Lee PS, Greenwell PW, Dominska M, Gawel M, Hamilton M, Petes TD. 2009. A fine-structure map of spontaneous mitotic crossovers in the yeast *Saccharomyces cerevisiae*. *PLoS Genetics* **5**:e1000410.

Lee PS, Petes TD. 2010. From the Cover: mitotic gene conversion events induced in G_1-synchronized yeast cells by gamma rays are similar to spontaneous conversion events. *PNAS* **107**:7383-7388.

Lettier G, Feng Q, de Mayolo AA, Erdeniz N, Reid RJ, Lisby M, Mortensen UH, Rothstein R. 2006. The role of DNA double-strand breaks in spontaneous homologous recombination in S. cerevisiae. *PLoS Genetics* **7**:e1001006.

Li H. 2013. Aligning sequence reads, clone sequences and assembly contigs with BWA-MEM, arXiv:1303.3997v1[q-bio.GN]. https://arxiv.org/abs/1303.3997

Li H, Handsaker B, Wysoker A, Fennell T, Ruan J, Homer N, Marth G, Abecasis G, Durbin R. 2009. The sequence alignment/map format and SAMtools. *Bioinformatics* **25**:2078-2079.

Mancera E, Bourgon R, Brozzi A, Huber W, Steinmetz LM. 2008. High-resolution mapping of meiotic crossovers and non-crossovers in yeast. *Nature* **454**:479-485.

Martini E, Borde V, Legendre M, Audic S, Regnault B, Soubigou G, Dujon B, Llorente B. 2011. Genome-wide analysis of heteroduplex DNA in mismatch repair-deficient yeast cells reveals novel properties of meiotic recombination pathways. *PLoS Genetics* **7**:e1002305.

Medhi D, Goldman AS, Lichten M. 2016. Local chromosome context is a major determinant of crossover pathway biochemistry during budding yeast meiosis. *Elife* **5**:e19669.

Merker JD, Dominska M, Petes TD. 2003. Patterns of heteroduplex formation associated with

the initiation of meiotic recombination in the yeast *Saccharomyces cerevisiae*. *Genetics* **165**:47-63.

Mitchel K, Zhang H, Welz-Voegele C, Jinks-Robertson S. 2010. Molecular structures of crossover and noncrossover intermediates during gap repair in yeast: implications for recombination. *Molecular Cell* **38**:211-222.

Miura T, Yamana Y, Usui T, Ogawa HI, Yamamoto MT, Kusano K. 2012. Homologous recombination via synthesis-dependent strand annealing in yeast requires Irc1 and Srs2 DNA helicases. *Genetics* **191**:65-78.

Nickoloff JA, Sweetser DB, Clikeman JA, Khalsa GJ, Wheeler SL. 1999. Multiple heterologies increase mitotic double-strand break-induced allelic gene conversion tract lengths in yeast. *Genetics* **153**:665-679.

Nicholson A, Hendrix M, Jinks-Robertson S, Crouse GF. 2000. Regulation of mitotic homeologous recombination in yeast: Functions of mismatch repair and nucleotide excision repair genes. *Genetics* **154**:133-146.

Orr-Weaver TL, Szostak JW, Rothstein RJ. 1981. Yeast transformation: a model system for the study of recombination. *PNAS* **78**:6354-6358.

Quinlan AR, Hall IM. 2010. BEDTools: a flexible suite of utilities for comparing genomic features. *Bioinformatics* **26**:841-842. https://genome.ucsc.edu

Reyes GX, Schmidt TT, Kolodner RD, Hombauer H. 2015. New insights into the mechanism of DNA mismatch repair. *Chromosoma* **124:**443-462.

Rogacheva MV, Manhart CM, Chen C, Guarne A, Surtees J, Alani E. 2014. Mlh1-Mlh3, a meiotic crossover and DNA mismatch repair factor, is a Msh2-Msh3-stimulated endonuclease. *Journal of Biological Chemistry* **289**:5664-5673.

Saini N, Ramakrishnan S, Elango R, Ayyar S, Zhang Y, Deem A, Ira G, Haber JE, Lobachev KS, Malkova A. 2013. Migrating bubble during break-induced replication drives conservative DNA synthesis. *Nature* **502**:389-392.

Schwartz EK, Heyer WD. 2011. Processing of joint molecules intermediates by structure-specific endonucleases during homologous recombination in eukaryotes. *Chromosoma* **120:** 109-127.

Siede W, Friedl AA, Dianova I, Eckardt-Schupp F, Friedberg EC. 1996. The *Saccharomyces cerevisiae* Ku autoantigen homologue affects radiosensitivity only in the absence of homologous recombination. *Genetics* **142**:91-102.

Smith CE, Llorente B, Symington LS. 2007. Template switching during break-induced replication. *Nature* **447**:102-105.

Song W, Dominska M, Greenwell PW, Petes TD. 2014. Genome-wide high-resolution mapping of chromosome fragile sites in *Saccharomyces cerevisiae*. *PNAS* **111**:E2210-2218.

St. Charles J, Hazkani-Covo E, Yin Y, Andersen SI, Dietrich FS, Greenwell PW, Malc E, Mieczkowski P, Petes TD. 2012. High-resolution genome-wide analysis of irradiated (UV and gamma-rays) diploid yeast cells reveals a high frequency of genomic loss of heterozygosity (LOH) events. *Genetics* **190**:1267-1284

St. Charles J, Petes TD. 2013. High-resolution mapping of spontaneous mitotic recombination hotspots on the 1.1 Mb arm of yeast chromosome IV. *PLoS Genet* **9**:e1003434.

Stone JE, Petes TD. (2006). Analysis of the proteins involved in the *in vivo* repair of base-base mismatches and four-base loops formed during meiotic recombination in the yeast *Saccharomyces cerevisiae*. *Genetics* **173**:1223-1239.

Symington LS, Rothstein R, Lisby M. 2014. Mechanisms and regulation of mitotic recombination in *Saccharomyces cerevisiae*. *Genetics* **198**:795-835.

Symington LS. 2014. End resection at double-strand breaks: mechanism and regulation. *Cold Spring Harbor Perspectives in Biology* **6**:1-18.

Szostak JW, Orr-Weaver TL, Rothstein R, Stahl FW. 1983. The double-strand-break-repair model for recombination. *Cell* **33**: 25-35.

Toyn JH, Gunyuzlu PL, White WH, Thompson LA, Hollis GF. 2000. A counterselection for the

tryptophan pathway in yeast: 5-fluoroanthranilic acid resistance. *Yeast* **16**:553-560.

Wang TF, Kleckner N, Hunter N. 1999. Functional specificity of MutL homologs in yeast evidence for three Mlh1-based heterocomplexes with distinct roles during meiosis in recombination and mismatch correction. *PNAS* **96**:13914-13919.

Wei W, McCusker JH, Hyman RW, Jones T, Ning Y, Cao Z, Gu Z, Bruno D, Miranda M, Nguyen M, Wilhelmy J, Komp C, Tamse R, Wang X, Jia P, Luedi P, Oefner PJ, David L, Dietrich FS, Li Y, Davis RW, Steinmetz LM. 2007. Genome sequencing and comparative analysis of *Saccharomyces cerevisiae* strain YJM789. *PNAS* **104**:12825-12830.

Yim E, O'Connell KE, St. Charles J, Petes TD. 2014. High-resolution mapping of two types of spontaneous mitotic gene conversion events in *Saccharomyces cerevisiae*. *Genetics* **198**:181-192.

Yin Y, Petes TD. 2013. Genome-wide high-resolution mapping of UV-induced mitotic recombination events in *Saccharomyces cerevisiae*. *PLoS Genet* **9**:e1003894.

Yin Y, Petes TD. 2014. The role of Exo1p exonuclease in DNA end-resection to generate gene conversion tracts in *Saccharomyces cerevisiae*. *Genetics* **197**:1097-1109.

Yin Y, Petes TD. 2015. Recombination between homologous chromosomes induced by unrepaired UV-generated DNA damage requires Mus81p and is suppressed by Mms2p. *PLoS Genetics* **11**:e1005026.

Zhao Y, Dominska M, Petrova A, Bagshaw H, Kokoska RJ, Petes TD. 2017. Properties of mitotic and meiotic recombination in the tandemly-repeated *CUP1* gene cluster in the yeast Saccharomyces cerevisiae. *Genetics* **206:**785-800.

Zheng DQ, Zhang K, Wu XC, Mieczkowski PA, Petes TD. 2016. Global analysis of genomic instability caused by DNA replication stress in *Saccharomyces cerevisiae*. *PNAS* **113**:E8114-8121.

Zierhut C, Diffley JF. 2008. Break dosage, cell cycle stage and DNA replication influence DNA double strand break response. *The EMBO Journal* **27**:1875-1885.

Figure legends

Figure 1. The DSBR repair pathways. The chromatids are shown as double-stranded molecules with arrows at the 3' ends. The broken chromatid is colored blue and the intact template chromatid is red. Dotted lines indicate newly-synthesized DNA. Regions of heteroduplex DNA (hetDNA) are outlined by black boxes. All pathways are initiated by invasion of one processed broken end into the unbroken chromatid, forming a D-loop.

A. One-ended Synthesis-dependent strand annealing (SDSA). Following DNA synthesis primed by the invading 3' end, the invading end dissociates from the intact molecule, and re-anneals with the second broken end. The net result is an NCO event with hetDNA extending uni-directionally from the break.

B. Two-ended SDSA. In this mechanism, following DNA synthesis from the invading end, the other broken end pairs with the D-loop and initiates DNA synthesis. Before ligation to generate a dHJ intermediate, the invading end disengages from the template and re-pairs with the other broken end. The net result is a single chromatid with a bi-directional heteroduplex that has a strand switch at the site of the initiating DSB.

C. Double Holliday junction (dHJ) intermediate. Following DNA synthesis from one invading end, the second broken end pairs with the D-loop (second-end capture). This intermediate can be dissolved by migrating the two junctions inwards, followed by decatenation; this pathway results in a NCO with a bi-directional heteroduplex, identical to the product of the two-ended SDSA mechanism. Alternatively, it can also be resolved by cutting the junctions symmetrically to generate NCOs (cuts at arrows marked 1, 2, 3, and 4 or 5, 6, 7, and 8), or asymmetrically (cuts at arrows marked 2, 4, 5, and 6 or 1, 3, 7 and 8) to generate COs. For both types of resolution, the heteroduplexes are located on different chromatids, flanking the DSB site, and pointing in opposite directions. Note that cuts at positions 1, 3, 7, and 8 reflect nick-directed resolution of the junctions.

D. Break-induced replication (BIR). In this pathway, one broken end invades the intact

template and copies DNA sequences by conservative replication to the end of the template. The other broken end is lost. Except for the initial strand invasion, heteroduplex intermediates are not relevant to this pathway.

Figure 2. Patterns of mismatch repair in a MMR-proficient strain. Chromatids are shown as double-stranded DNA structures with circles indicating SNPs. For all parts of the figure, the blue chromatid is broken and, consequently, is the recipient of sequence information from the red chromatid. For these examples, all intermediates were resolved as NCO events. In Figs. 2A, 2C, and 2D, the products shown on the right side of each panel are a consequence of mismatch repair in the mother cell. In Fig. 2B, the products are shown in two daughter cells following replication of the chromosomes of the mother cell.

A. Repair of mismatches within a single heteroduplex. In the top panel, the mismatches in the heteroduplex are repaired using the bottom strand as a template, resulting in a conversion event. In the middle panel, the upper strand is used as a template for MMR, resulting in a blue chromatid that is identical to an unbroken chromatid. In the bottom panel, some mismatches undergo conversion-type repair and others restoration-type repair.

B. Loss of mismatches as a consequence of DNA replication. Replication of a chromatid with a heteroduplex results in one product that appears to have undergone conversion-type repair, and a second that is the same as a chromatid without a recombination event.

C. Repair of mismatches intwo chromatids with uni-directional heteroduplexes propagated in opposite directions. If mismatches within the two heteroduplexes are repaired using the red strand as a template, a conversion event that is identical to that shown in the upper panel of Fig. 2A would be generated.

D. Repair of mismatches in a one chromatid with a bi-directional heteroduplex that has a strand switch. If all mismatches are repaired using the red strand as a template, the resulting conversion product is identical to that shown in Figs. 2A and 2C.

Figure 3. Detection and analysis of crossovers induced by DSBs in single chromatids or in

unreplicated chromosomes in an MMR-proficient diploid. The lines show the two strands of each chromosome/chromatid, and ovals indicate centromeres. The strain is homozygous for *ade2-1*, an ochre allele that, in the absence of the *SUP4-o* ochre suppressor, forms a red colony. In the strains used in our study, one copy of *SUP4-o* is inserted near the telomere of one homolog. Strains with zero, one or two copies of the suppressors form red, pink and white colonies, respectively. Black triangles indicate the positions of cleavages of the dHJ. Heteroduplex intermediates are enclosed by dotted black lines, and conversion tracts are enclosed in thin black lines. Chromosomes in daughter cells are outlined by thick black rectangles, and D1 and D2 denote the two daughter cells resulting from the crossover.

A. Crossover initiated by a single chromatid break (SCB). Following the crossover, segregation of one recombined and one parental chromatid into each cells will generate one cell homozygous for *SUP-o* and one cell lacking *SUP4-o*; subsequent divisions will lead to a red/white sectored colony. If mismatches in both heteroduplexes undergo conversion-type repair, a 3:1 conversion event would be observed; within the boxed region, three chromatids have information derived from the red chromatid and one has information derived from the blue chromatid.

B. Crossover initiated by a DSB in an unreplicated blue chromosome, resulting in double sister-chromatid breaks (DSCB). DNA replication of the broken chromosome would result in,two broken sister chromatids. We show the middle pair of chromatids repaired as a crossover, and the top chromatid repair by an SDSA event. In this example, we show the heteroduplex associated with the SDSA event as longer than those of the CO-associated hetDNAs. If all of mismatches are repaired as conversion events, we would see a hybrid 3:1/4:0/3:1 conversion tract. The 4:0 pattern is diagnostic of a DSCB event.

Figure 4. Expected recombination-associated segregation patterns of SNPs into daughter and granddaughter cells in MMR-deficient strains following a G_2- or G_1-induced DSB. We show heteroduplexes with unrepaired mismatches (outlined in dashed lines) in the daughter cells D1

and D2. Replication of unrepaired mismatches in heteroduplexes results in granddaughter cells with two different genotypes; these differences are outlined in the right side of the figure by thin black lines. The events shown in Figs. 4A and 4B were selected because the crossovers between the heterozygous *SUP4-o* marker generated daughter cells that had two copies (resulting in a white sector) or no copies (resulting in a red sector) of *SUP4-o*. The NCO event shown in Fig. 4C was on a homolog that did not contain the *SUP4-o* marker (shown in thin red and blue lines) and was unselected.

A. CO-associated SCB (selected crossover). If the crossover occurred by the DSBR pathway, we would expect that both sectors would have granddaughter cells with different SNP patterns.

B. CO-associated DSCB (selected crossover). As in Fig. 4A, both sectors would have granddaughter cells with different SNPs. One distinguishing feature of the DSCB is that both granddaughter cells of one sector (GD1-1 and GD1-2) have different coupling relationships for SNPs in the same region as outlined in the green rectangle.

C. NCO-associated SCB (unselected). Strains treated with UV have many unselected events. Since these events are induced by UV at the same time as the selected event, we can use the information identifying GD1-1, GD1-2. GD2-1, and GD2-2 from the selected event to determine the patterns of heteroduplex formation for the unselected event by using whole-genome SNP arrays. In the depicted event, only one of the sectors had granddaughters with different genotypes.

Figure 5. Microarray analysis of one granddaughter cell in a sectored colony resulting from a recombination event on chromosome V. By methods described in the text, we identified two granddaughter genotypes associated with the red and white sectors of the YYy310-9-5WR sectored colony. SNP-specific microarrays were done on genomic DNA isolated from all four granddaughter strains, and from spore derivatives of each of these granddaughters.

A. Microarray analysis of the W1 granddaughter strain. Genomic DNA was isolated, and

hybridized to SNP-specific microarrays in competition with differentially-labeled genomic DNA from a heterozygous control strain (details in Materials and Methods). The Y axis shows the hybridization ratio of the experimental samples to allele-specific SNPs normalized to the hybridization levels of the control heterozygous sample; blue and red circles indicate hybridization ratios to YJM789- and W303-1A-specific SNPs, respectively. Heterozygous samples have a ratio of about 1, samples in which the strain-specific allele is present in two copies have a ratio of about 1.7, and those in which the strain-specific allele is missing have a ratio of about 0.3. The X axis has SGD coordinates for chromosome V in the region of the recombination event. Between the left telomere (coordinate 1) and coordinate 51915, the W1 granddaughter is homozygous for the YJM789-derived SNPs, and heterozygous for SNPs between coordinates 60701 and the right telomere. In summary, chromosome V in this strain has a large terminal region that is homozygous for YJM789 SNPs, a short region of heterozygous SNPs, a short region that is homozygous for W303-1A SNPs, and a large heterozygous region that makes up the remainder of the chromosome.

B. Microarray analysis of a spore derived from the W1 granddaughter strain. The W1 diploid was sporulated, and dissected. We examined the genomic DNA of one spore by SNP microarrays. From the pattern of SNPs in the spore, we conclude that one homolog in W1 has blue SNPs for the heterozygous region located near coordinates 55000 and red SNPs for the heterozygous region located between coordinates 60000, and the right telomere. The other homolog has the reciprocal pattern.

C. Inferred arrangement of red and blue SNPs on the two homologs of W1 based on the microarray results shown in Figs. 5A and 5B. This pattern is reproduced in the top part of Supplementary file 2 - Fig. S8.

Figure 6. Correlation of SNP patterns in granddaughter cells with heteroduplex patterns in the mother cell. The example shown is the same crossover on chromosome V described in Fig. 5 (YYy310-9-5WR sectored colony). Each chromatid/chromosome is shown as a double-

stranded DNA molecule with ovals and circles showing the centromeres. As in Fig. 5, red and blue lines signify sequences derived from W303-1A and YJM789, respectively. By the methods described in the text, we identified two genotypes within each sector. The microarray analysis illustrated in Fig. 5 allowed us to determine the patterns of LOH in each granddaughter cell (top of the figure). Each chromosome in the granddaughter cell was derived by replication by chromosomes in the daughter cells (middle of the figure). Chromosomes with the same color of centromere in the granddaughter cells must derive from a daughter chromosome with a centromere of the same color. Numbers in bold represent chromatids (top part of figure) or individual DNA strands (bottom part of the figure). For example, chromatids 1 and 2 in the W1 and W2 granddaughters must represent the strands labeled 1 and 2 in the white daughter cell. A similar procedure can be used to assign the strands to the chromosomes in all of the daughter cells. The chromosomes in the daughter cells represent segregants of the G_2 chromatids in the mother cell. The daughter chromosomes with red centromeres must have been derived from the paired sister chromatids with the red oval centromere, and a similar conclusion can be drawn about the blue centromeres of the daughter chromosomes and the oval blue centromere in the mother cell. By the pattern of SNPs, we can also conclude that the chromatids in the mother cell with strands 1 and 2, and 7 and 8 were involved in a CO, whereas the other two chromatids were involved in the NCO mode of repair. Numbers that are not in bold represent transitions between W303-1A-derived SNPs and YJM789-derived SNPs; transitions with the same number have identical breakpoints with the resolution of our microarray analysis.

Figure 7. Examples of heteroduplex patterns associated with SCB- and DSCB-initiated events. Both the SCB event shown in 7A and the DSCB event shown in 7B were unselected events from the same sectored colony (YYy310-905WR; Supplementary file 1 - Table S3). The 7A event occurred on chromosome IV (labeled IV-2 in Supplementary file 1 - Table S3), and the 7B event was on chromosome XIV. The distances between SNPs (shown as red or blue circles) are to the scale shown above each set of chromatids.

A. Inferred pattern of heteroduplexes in an SCB event. The patterns of markers in the granddaughter cells that define the patterns inferred in the G_2 mother cell are in Supplementary file 2 - Fig. S6.

A. Inferred pattern of heteroduplexes in an DSCB event. The patterns of markers in the granddaughter cells that define the patterns inferred in the G_2 mother cell are in Supplementary file 2 - Fig. S16.

Figure 8. Mechanisms that generate Classes 1-8 recombination events. For all events, we show the initiating DSB on the blue chromatid. Dotted lines show sequences generated by replication or during mismatch repair. Black arrows indicate the position of the initiating DSB. The mechanisms are discussed in detail in the main text. Red and blue lines represent DNA strands of the W303-1A-derived chromatid and YJM789-derived chromatid, respectively. Arrows on these strands indicate the 3' ends.

A. Class 1. Class 1 events are NCOs formed by one-ended SDSA.

B. Class 2. These NCO events could be generated by one-ended SDSA, followed by Mlh1p-independent MMR.

C. Class 2. An alterative possibility is that Class 2 events reflect repair of a double-stranded DNA gap.

D. Class 3. In this NCO class, the heteroduplex region is adjacent to a conversion tract. Such events could reflect a heteroduplex tract in which mismatches are repaired in one part of the tract and left unrepaired in the other.

E. Class 3. An alternative model for this class is that the conversion tract is the result of repair of a double-stranded DNA gap with a heteroduplex region at one end.

F. Class 4. For this CO class, a heteroduplex is observed on one chromatid but not the other. This class could be explained by the DSBR pathway in which heteroduplex region is short relative to the other; if the short heteroduplex does not contain a mismatch, it would be undetectable.

G. Class 5. In this NCO class, the heteroduplex region is located on the opposite of the DSB site from the conversion region. This pattern is consistent with the repair of a double-stranded DNA gap that was restricted to one of the broken ends.

H. Class 6. This CO class is identical to the pattern expected for the DSBR model.

I. Class 7. In this CO class, no heteroduplexes or conversion tracts are observed adjacent to the crossover, consistent with the formation of a dHJ with short heteroduplex tracts that do not include mismatches.

J. Class 8. In this NCO class, one chromatid has a conversion tract, and the other chromatid has a heteroduplex involving SNPs at the same position. This event could reflect resolution of a dHJ intermediate in the NCO model in which one region of heteroduplex is undetectable.

K. Class 8. An alternative mechanism involves branch migration of a HJ, followed by resolution of the intermediate in a NCO mode. Mismatches in one of the two chromatids are repaired to generate a conversion tract.

Figure 9. Complex DSCB event derived from analysis shown in Supplementary file 2 - Fig. S8. We infer that the recombination-initiating DSB was on a blue chromosome that was replicated to produce two broken blue chromatids.

A. Depiction of heteroduplexes and conversion tracts present in the mother cell before chromosome segregation. The double-headed arrow indicates the position of the initiating DSB.

B. Mechanism to produce the CO chromatids 1 and 4. Following invasion of the left end of the broken chromatid, one HJ underwent branch migration resulting in a region of symmetric heteroduplexes. The dHJ intermediate was processed to yield a CO as shown by the short arrows. Mismatches in a region of the heteroduplex on the upper chromatid were repaired to yield a conversion event. We suggest that the small homoduplex region near the DSB site did not include a SNP and was, therefore, undetectable.

C. Mechanism to produce the NCO chromatids 2 and 3. Following dHJ formation, the intermediate was dissolved, resulting in bidirectional heteroduplexes on chromatid 2. In addition,

as in Fig. 8B, we hypothesize that there was a region of mismatch repair in one of the heteroduplexes.

Figure 10. Complex DSCB event derived from the analysis shown in Supplementary file 2 - Fig. S16. As in Fig. 8, the initiating DSB was on the blue chromosome.

A. Depiction of recombinant chromatids in mother cell before segregation of chromosomes into the daughters.

B. CO between chromatids 1 and 3. The pattern of heteroduplexes on these chromatids is that expected from the DSBR model.

C. NCO between chromatids 2 and 4. In this event, the heteroduplex spans the putative DSB site on chromatid 4. The right broken end underwent resection of both strands before strand invasion. The left end was extended by invasion of the sister chromatid. Following annealing of the extended end to the D-loop, the intermediate was processed as a NCO. We suggest that the small region of heteroduplex on the red chromatid did not contain a SNP and was not detectable.

Figure 11. System for detecting crossovers at the HS4 hotspot on chromosome IV (strain YYy311). The W303-1A- and YJM789-derived chromatids are shown in red and blue, respectively. On the W303-1A-derived homolog, the HS4 hotspot is flanked by the *hphMX4* and *URA3* markers; *SUP4-o* is located near the telomere of the YJM789-derived homolog. Since the recombinogenic DSB is located at HS4, HS4-initiated events usually result in loss of HS4 as shown.

Table 1. Description of classes of "simple" recombination events and number of observed events in each class.[1]

Class	Description of Class	Example	Number observed
1	NCO, unidirectional heteroduplex, no strand switch; one-ended SDSA, Fig. 1A	Chromatid 2 of Fig. 7A	26
2	NCO, single continuous conversion tract on one side of DSB site	Chromatid 3 of Fig. S4	18
3	NCO, hybrid heteroduplex/conversion tract located on one side of DSB site	Chromatid 4 of Fig. S5	12
4	CO, heteroduplex on only one chromatid on one side of DSB site	Chromatids 1 and 4 of Fig. S21	5
5	NCO involving only one chromatid with heteroduplex on one side of DSB and conversion tract on the other	Chromatid 3 of Fig. S14	4
6	CO, uni-directional heteroduplexes on both chromatids propagated in opposite directions	Chromatids 1 and 3 of Fig. S16	2
7	CO, no detected heteroduplex or conversion tract on either chromatid	Chromatids 1 and 3 of Fig. S24	2
8	NCO, one chromatid with uni-directional conversion tract and one chromatid with uni-directional heteroduplex on same side of DSB	Chromatids 2 and 3 of Fig. S67	2

[1]These classes are further described in the text and are depicted in Fig. 8.

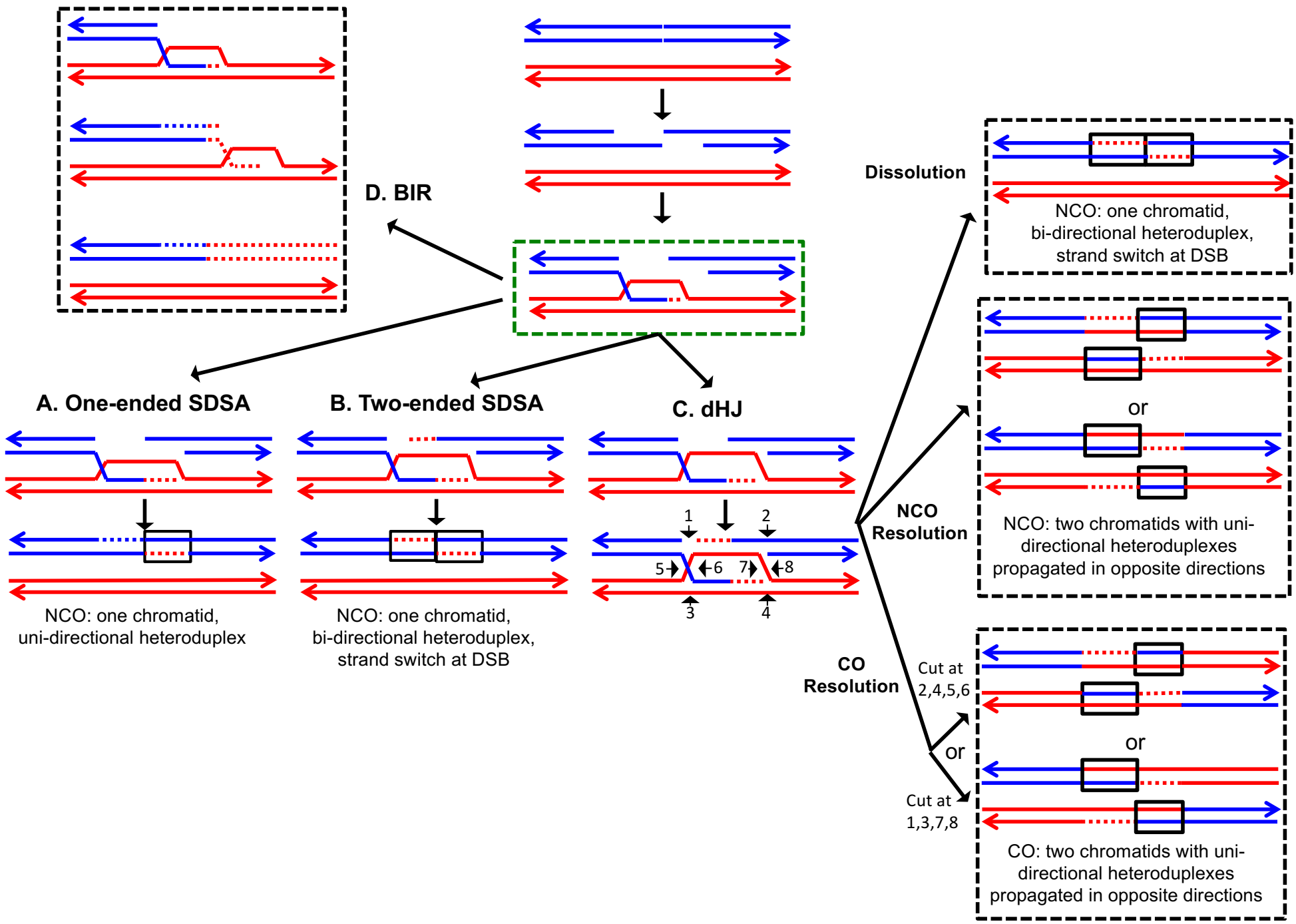
D. BIR
A. One-ended SDSA
B. Two-ended SDSA
C. dHJ
NCO: one chromatid,
uni-directional heteroduplex
NCO: one chromatid,
bi-directional heteroduplex,
strand switch at DSB
1
2
3
4
5
6
7
8
Dissolution
NCO: one chromatid,
bi-directional heteroduplex,
strand switch at DSB
NCO
Resolution
or
NCO: two chromatids with uni-
directional heteroduplexes
propagated in opposite directions
CO
Resolution
Cut at
2,4,5,6
or
Cut at
1,3,7,8
or
CO: two chromatids with uni-
directional heteroduplexes
propagated in opposite directions

A. Repaired mismatches, single heteroduplex

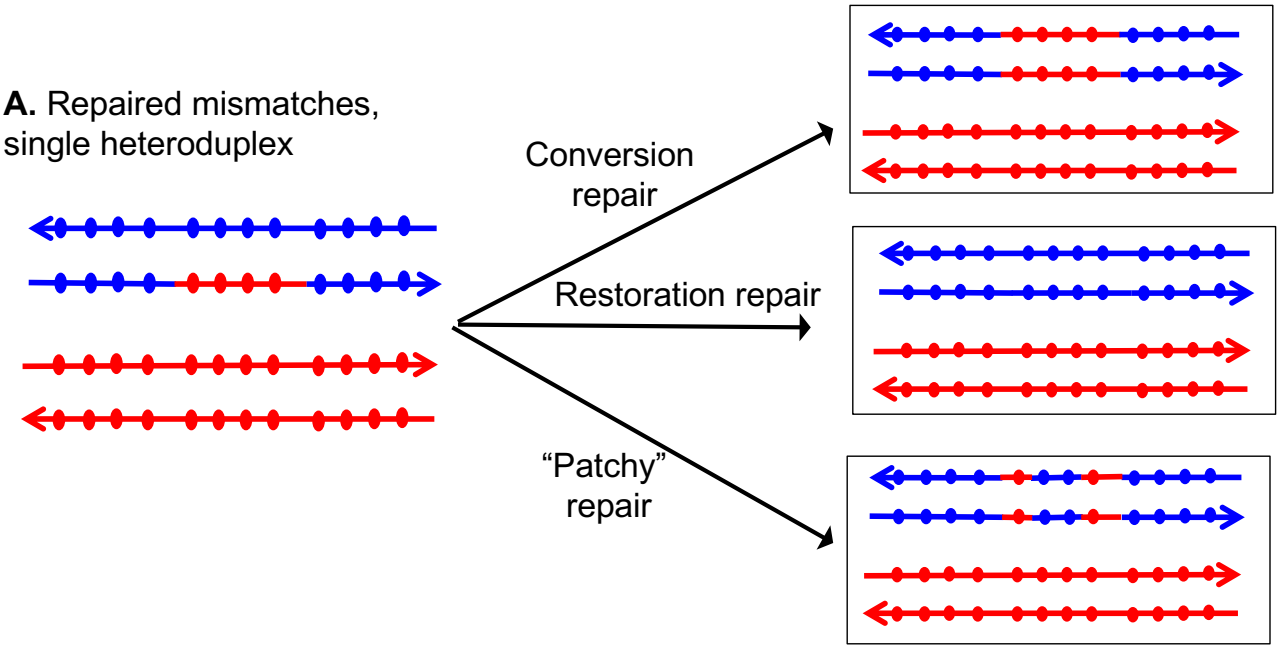

B. Unrepaired mismatches, single heteroduplex

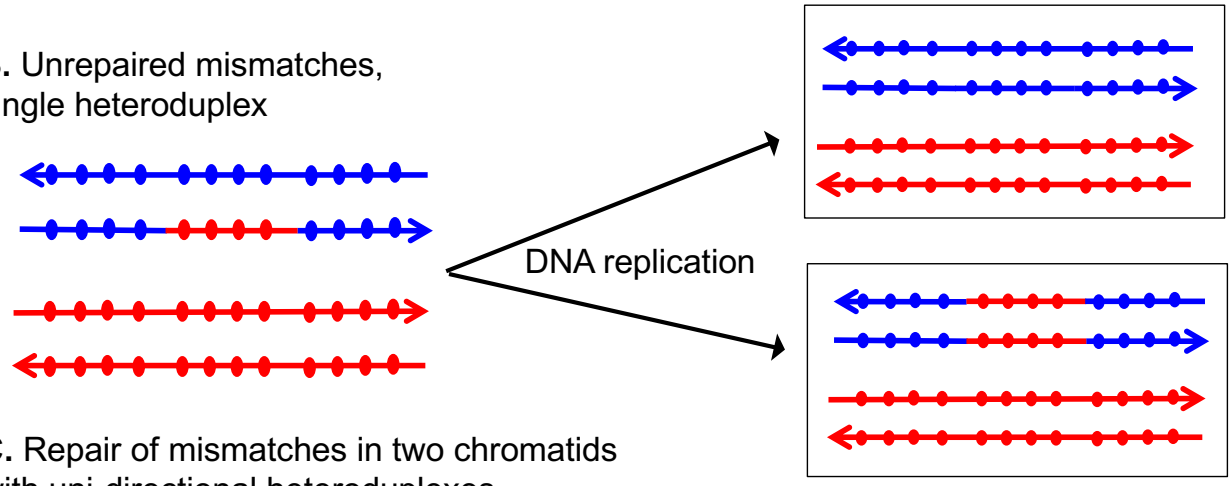

C. Repair of mismatches in two chromatids with uni-directional heteroduplexes propagated in opposite directions

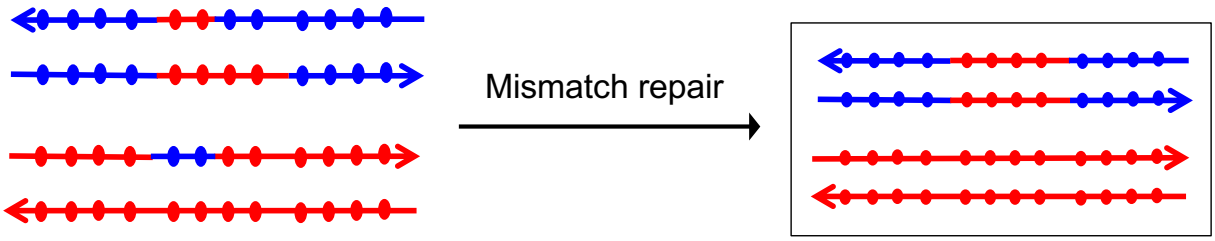

D. Repair of mismatches in one chromatid with a bi-directional heteroduplex that has a strand switch

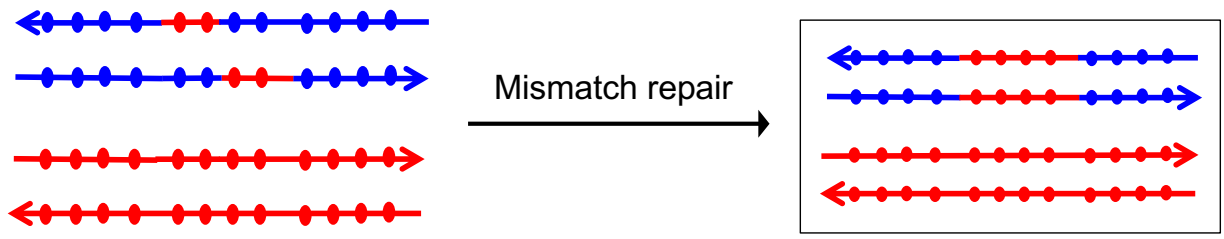

Fig.3

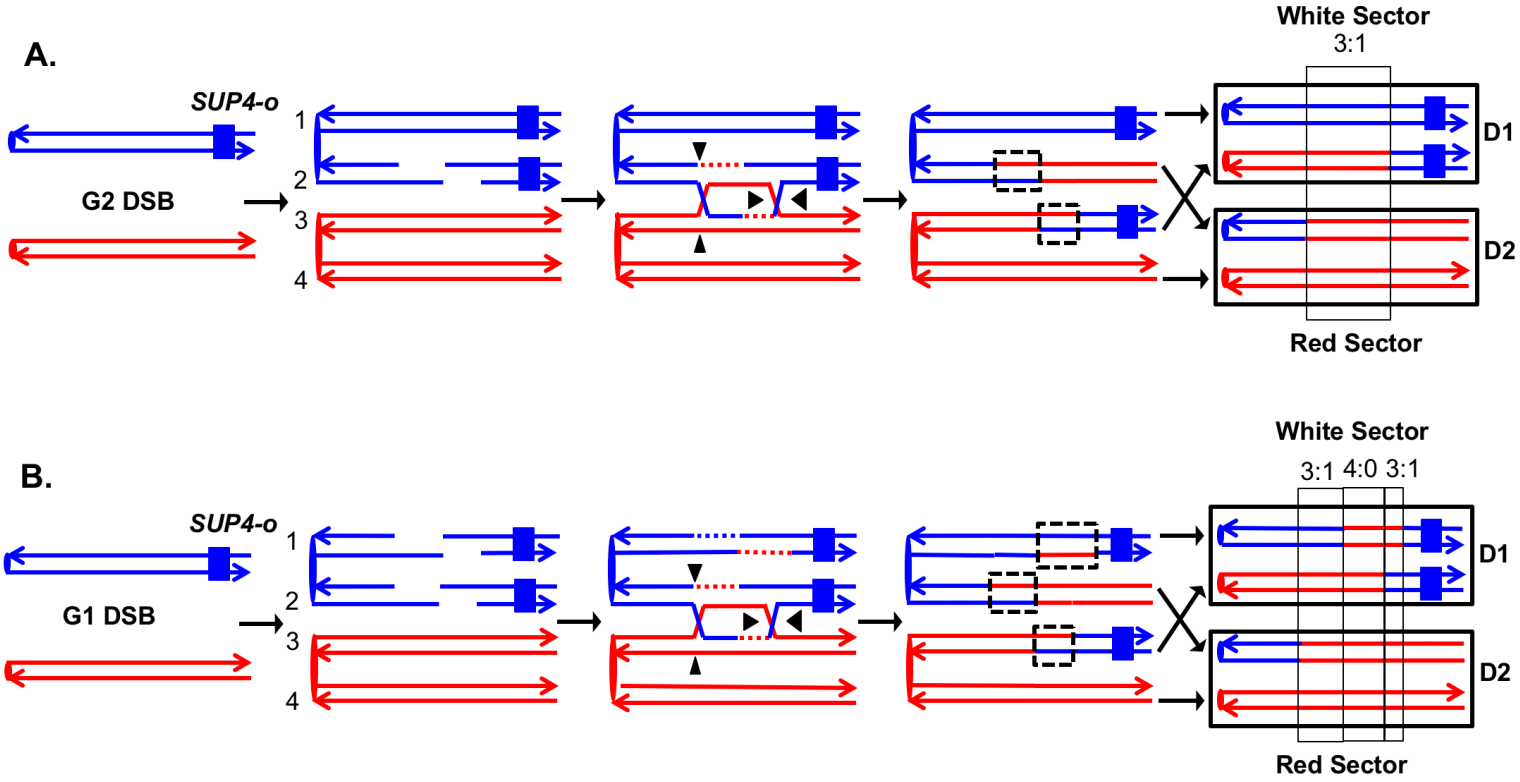
A.
SUP4-o
G2 DSB
1
2
3
4
White Sector
3:1
D1
D2
Red Sector
B.
SUP4-o
G1 DSB
1
2
3
4
White Sector
3:1 4:0 3:1
D1
D2
Red Sector

Fig.4

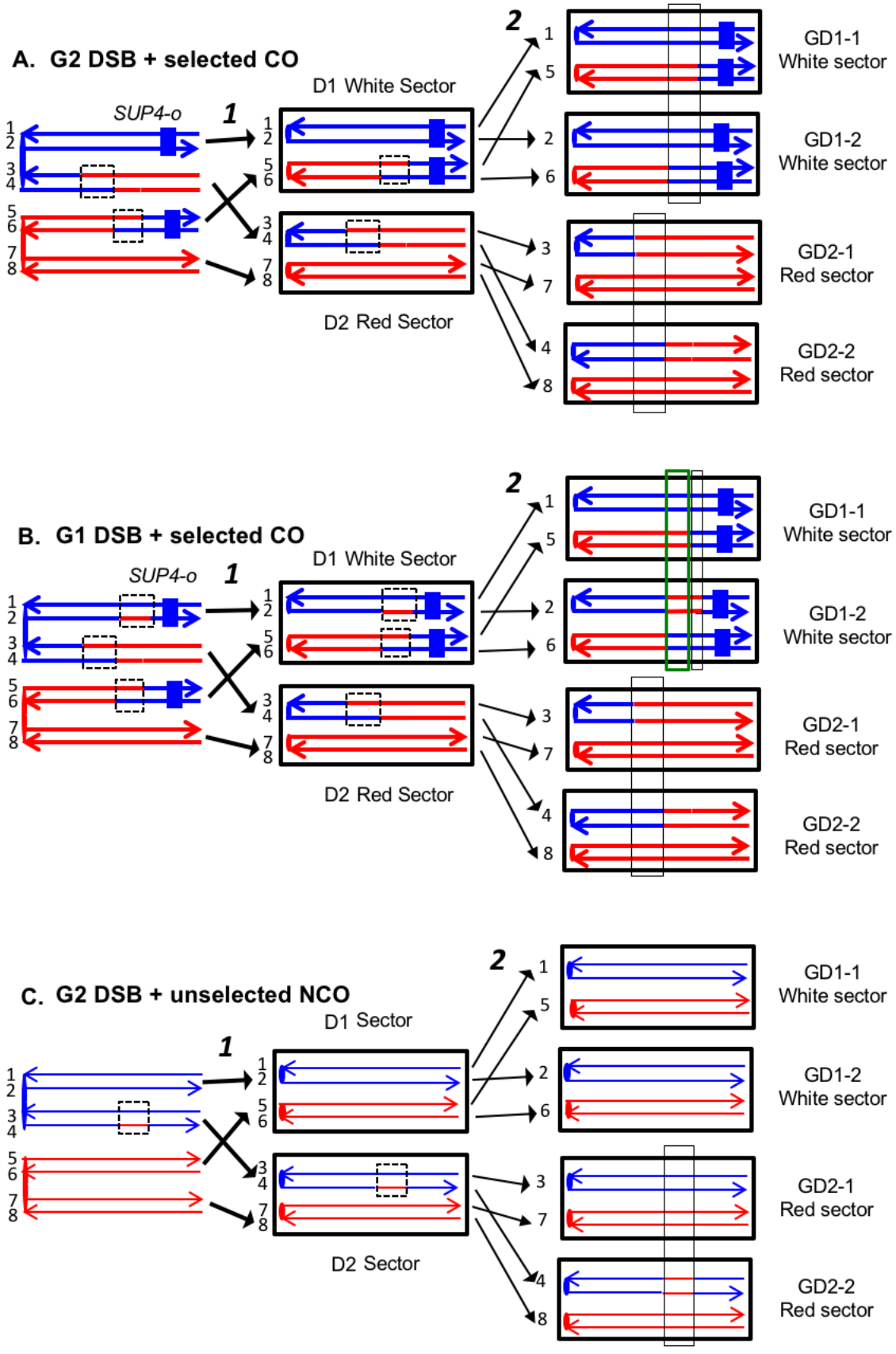
A. G2 DSB + selected CO
SUP4-o
1
2
D1 White Sector
D2 Red Sector
GD1-1
White sector
GD1-2
White sector
GD2-1
Red sector
GD2-2
Red sector
B. G1 DSB + selected CO
C. G2 DSB + unselected NCO
D1 Sector
D2 Sector

Fig.5

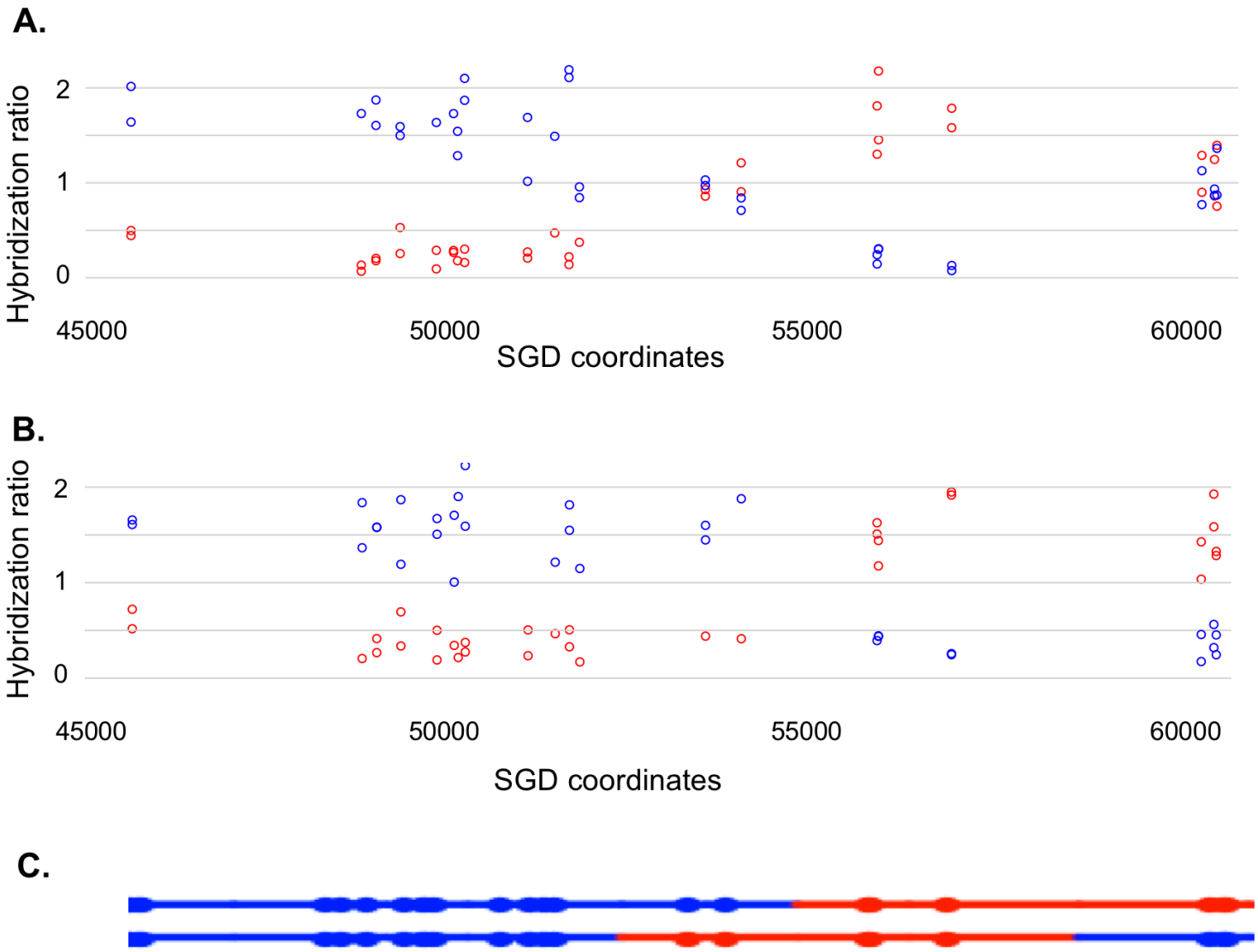
A.
Hybridization ratio
2
1
0
45000
50000
55000
60000
SGD coordinates
B.
Hybridization ratio
2
1
0
45000
50000
55000
60000
SGD coordinates
C.

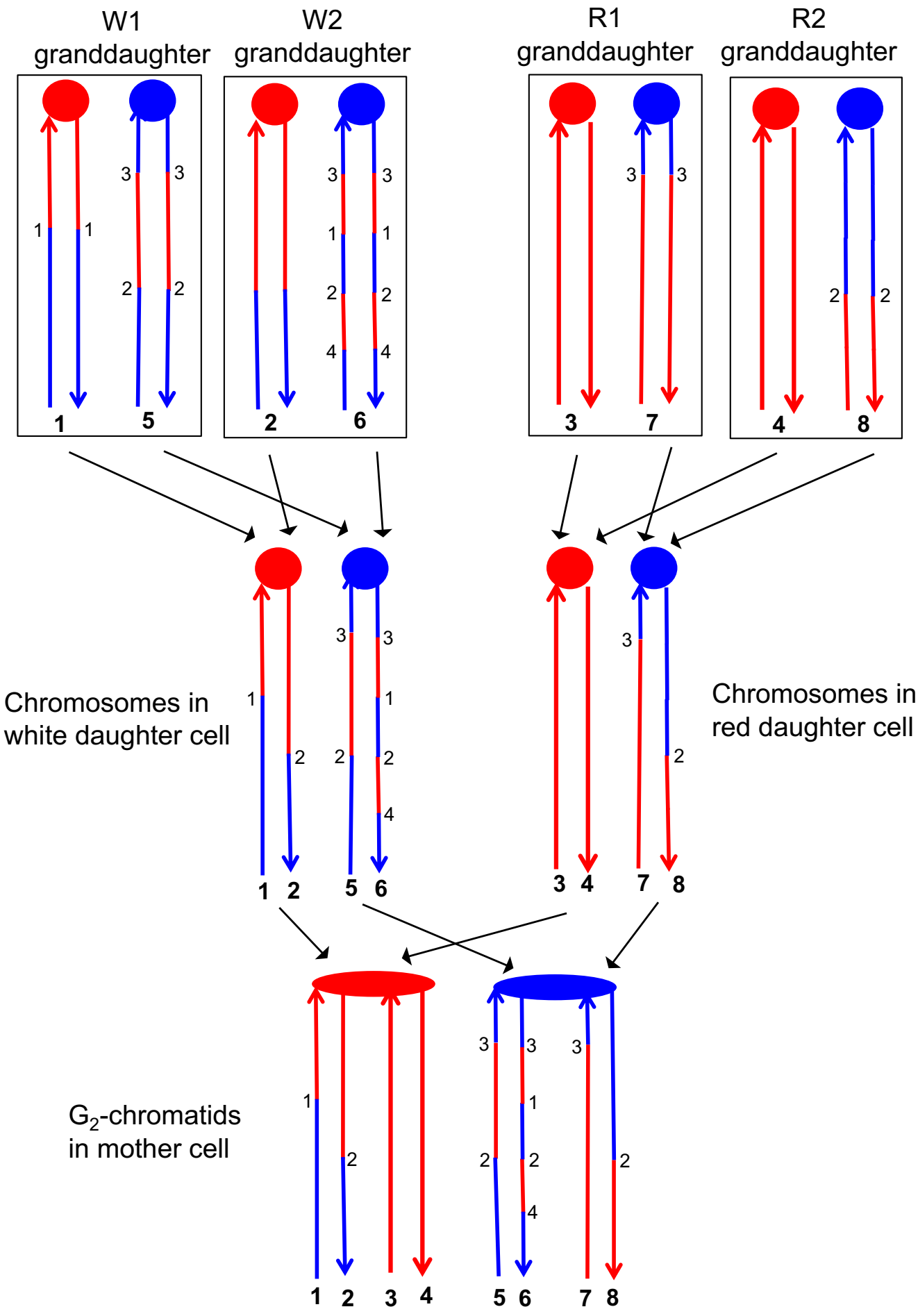
W1 granddaughter
W2 granddaughter
R1 granddaughter
R2 granddaughter
1
5
2
6
3
7
4
8
Chromosomes in white daughter cell
Chromosomes in red daughter cell
1 2
5 6
3 4
7 8
G_2-chromatids in mother cell
1 2 3 4
5 6
7 8

Fig.7

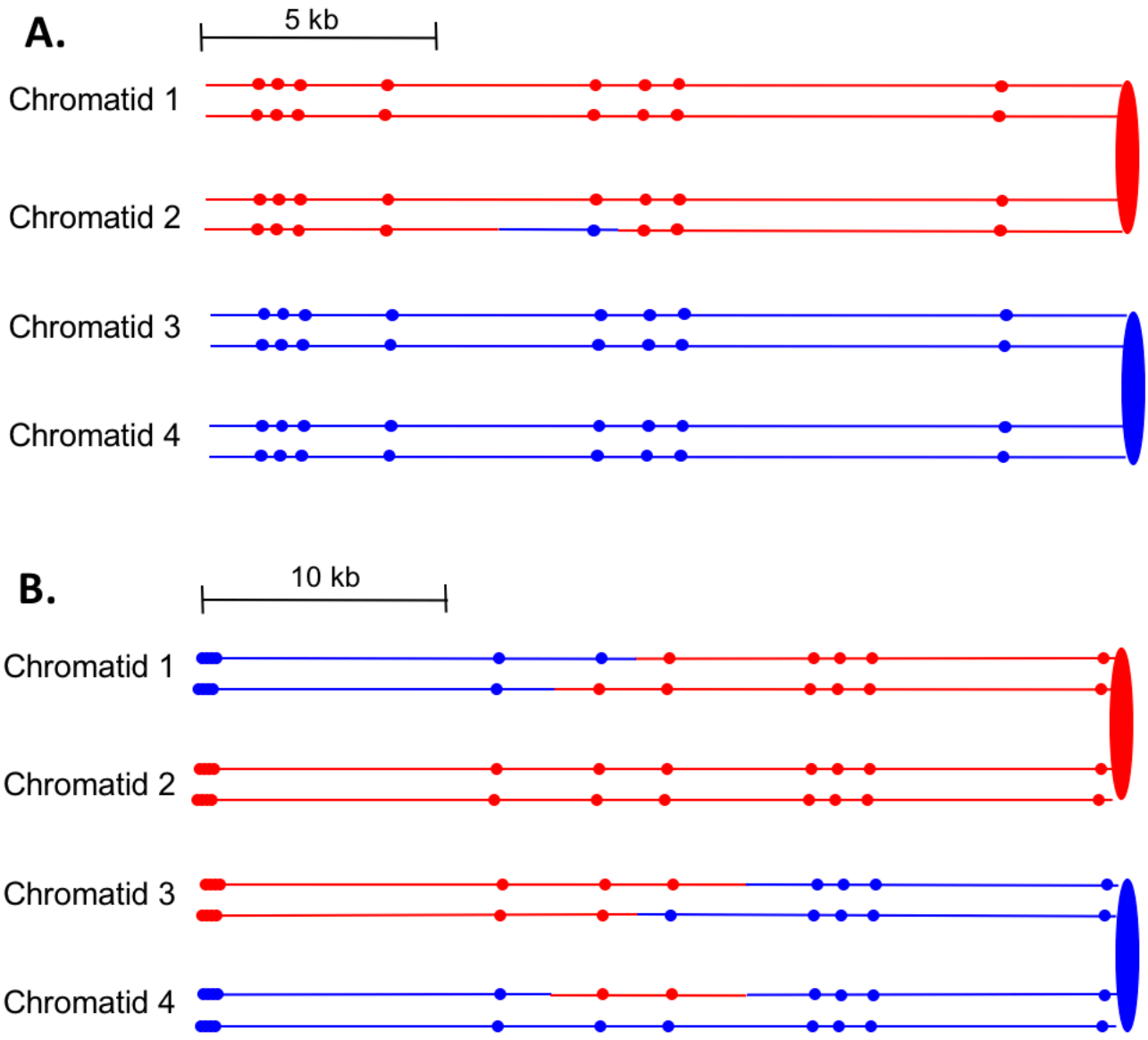
A.
5 kb
Chromatid 1
Chromatid 2
Chromatid 3
Chromatid 4
B.
10 kb
Chromatid 1
Chromatid 2
Chromatid 3
Chromatid 4

Fig.8

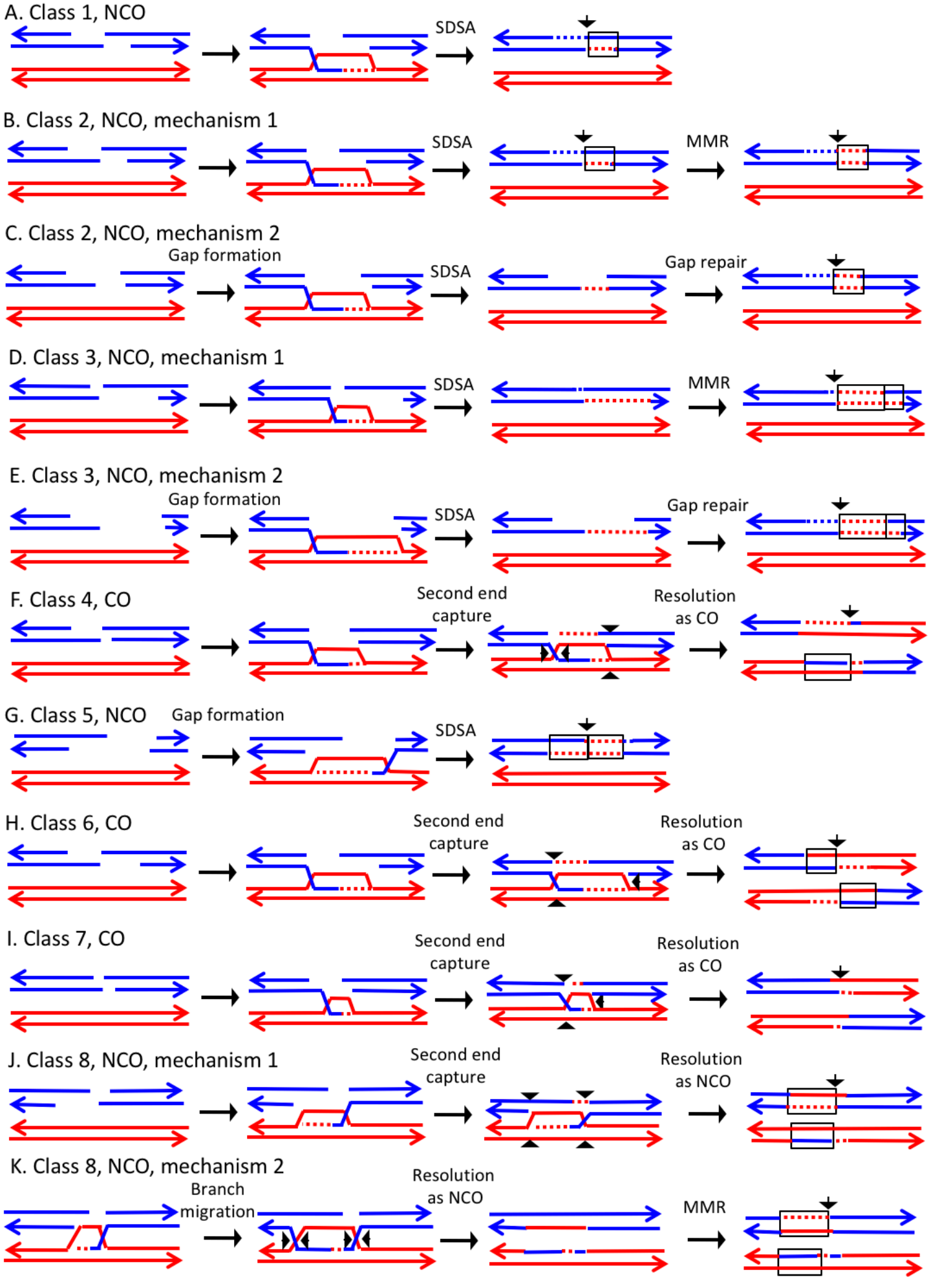
A. Class 1, NCO
SDSA
B. Class 2, NCO, mechanism 1
SDSA
MMR
C. Class 2, NCO, mechanism 2
Gap formation
SDSA
Gap repair
D. Class 3, NCO, mechanism 1
SDSA
MMR
E. Class 3, NCO, mechanism 2
Gap formation
SDSA
Gap repair
F. Class 4, CO
Second end capture
Resolution as CO
G. Class 5, NCO
Gap formation
SDSA
H. Class 6, CO
Second end capture
Resolution as CO
I. Class 7, CO
Second end capture
Resolution as CO
J. Class 8, NCO, mechanism 1
Second end capture
Resolution as NCO
K. Class 8, NCO, mechanism 2
Branch migration
Resolution as NCO
MMR

Fig.9

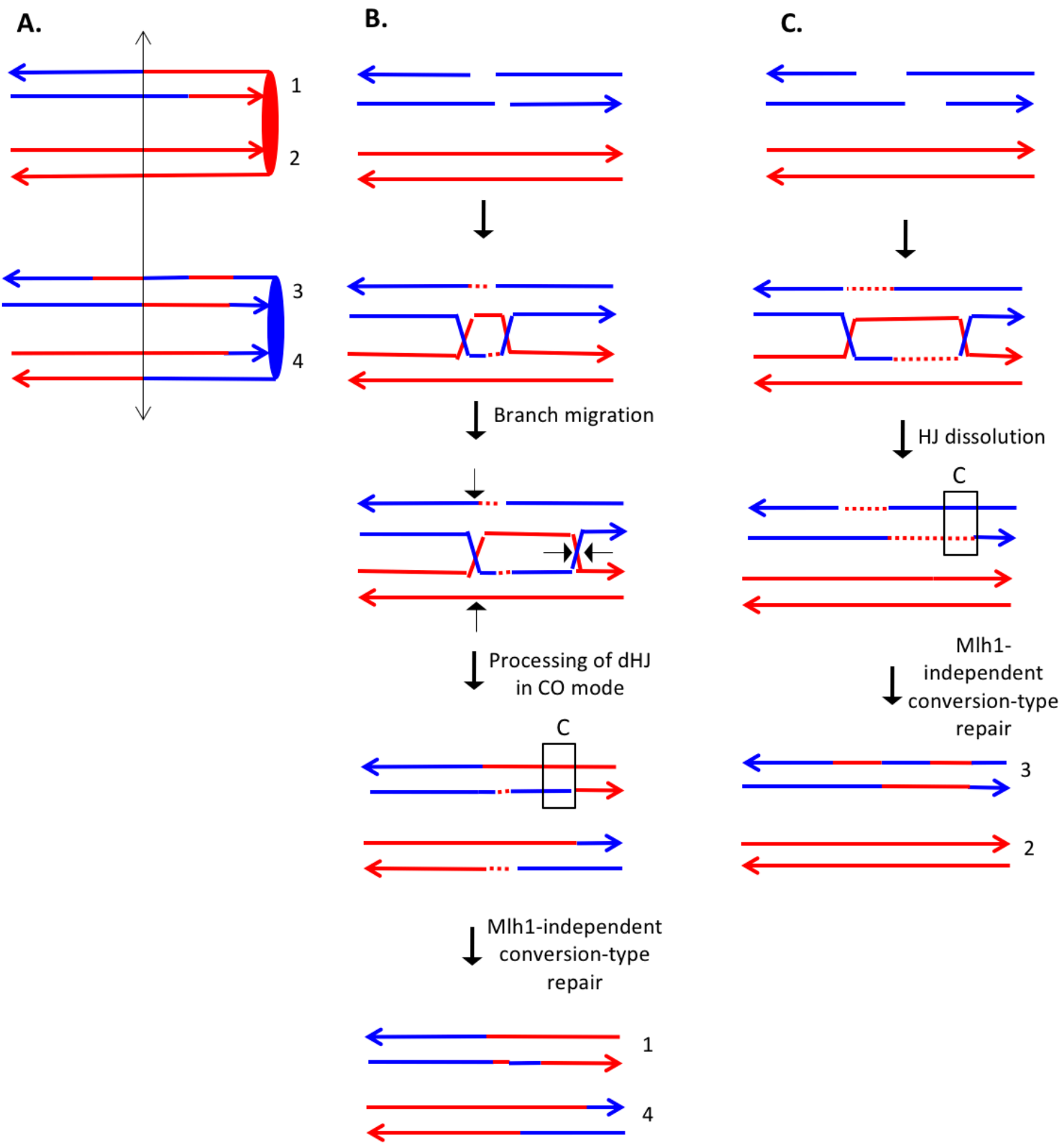
A.
1
2
3
4
B.
Branch migration
Processing of dHJ in CO mode
C
Mlh1-independent conversion-type repair
1
4
C.
HJ dissolution
C
Mlh1-independent conversion-type repair
3
2

Fig.10

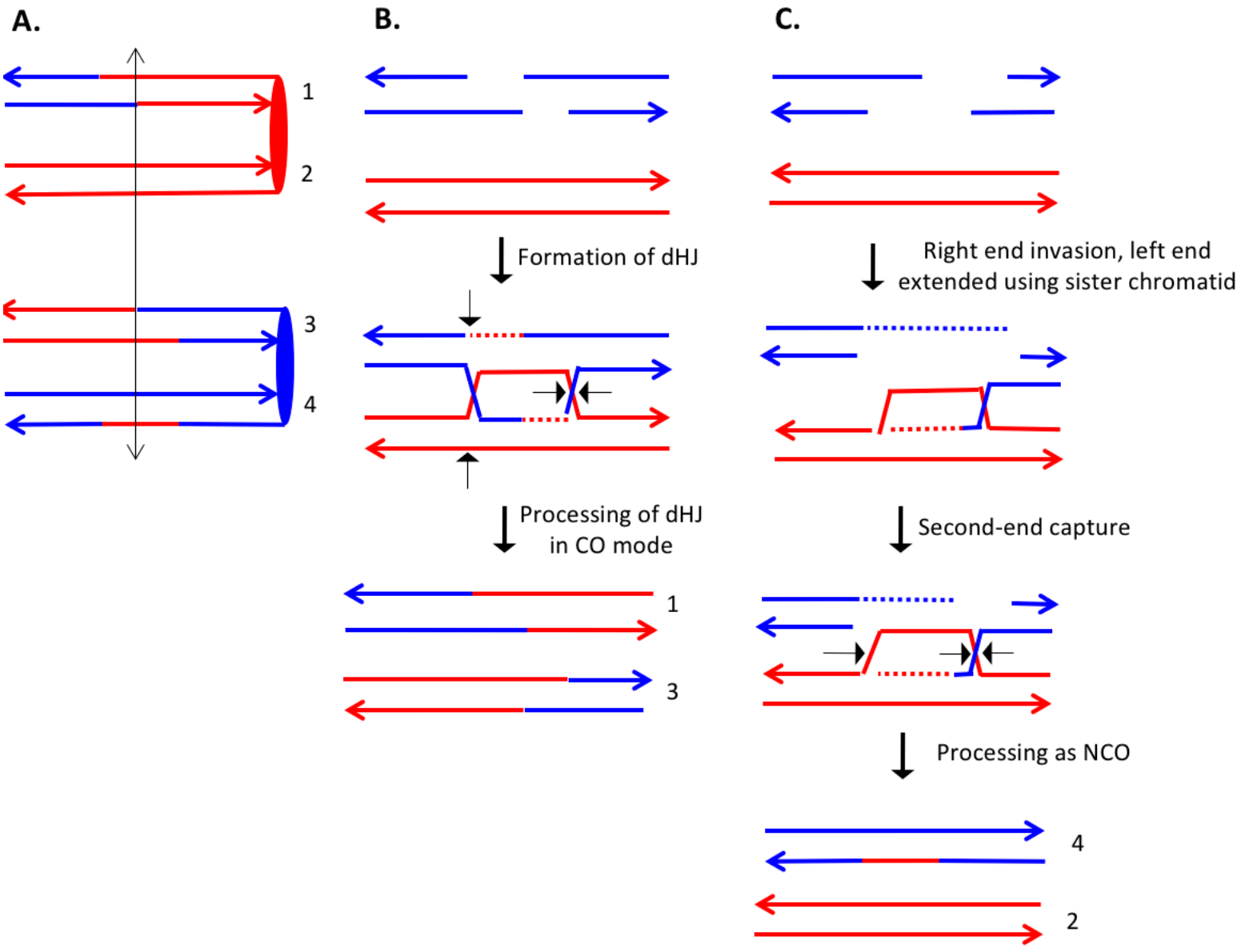
A.
1
2
3
4
B.
Formation of dHJ
Processing of dHJ
in CO mode
1
3
C.
Right end invasion, left end
extended using sister chromatid
Second-end capture
Processing as NCO
4
2

Fig.11

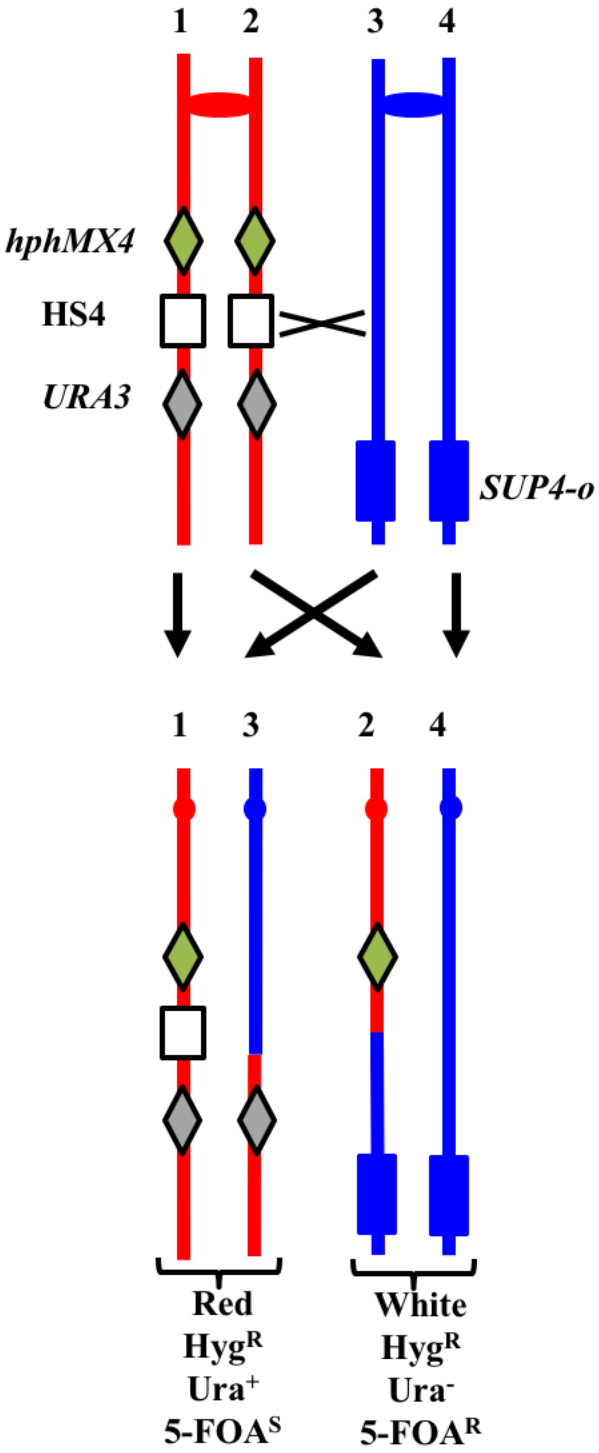
1
2
3
4
hphMX4
HS4
URA3
SUP4-o
1
3
2
4
Red
Hyg^R
Ura^+
5-FOA^S
White
Hyg^R
Ura^-
5-FOA^R

Table S1. Strain genotypes and constructions			
Strain name	Strain background	Genotype	Strain construction/reference
YYy181.3	W303-1A	*MAT***a** *ade2-1 leu2-3,112 his3-11,15 can1-100 ura3-1 trp1-1 V9229::hphMX4 V261553::LEU2 mlh1::kanMX6 RAD5*	*MLH1* in the strain PSL2 (Lee *et al* ., 2009) was replaced with *kanMX6* by transformation with an MLH1::kanMX6 fragment generated by amplifying the plasmid pFA6-KanMX4 (Longtine *et al* ., 1998) with primers MLH1::*kanMX*6 F (ATAGTGATAGTAAATGGAAGGTAAAAA TAACATAGACCTATCAATAAGCAA CGTACGCTGCAGGTCGAC) and MLH1::kanMX6 R (CTCAGGAAATAAACAAAAAACTTTGGT ATTACAGCCAAAACGTTTTAAAGT ATCGATGAATTCGAGCTCG)
YYy182.2	W303-1A	*MAT***a** *ade2-1 leu2-3,112 his3-11,15 ura3-1 trp1-1 can1-100 IV957578::hphMX4 IV1013217::URA3 mlh1::kanMX6 RAD5*	*MLH1* was replaced by *kanMX6* in the strain JSC54-1 (St. Charles and Petes, 2013) as described above for YYy181.3
YYy183.2	YJM789	*MAT*α *ade2-1 ura3 gal2 ho::hisG IV1510386::SUP4-o mlh1::kanMX6*	*MLH1* was replaced by *kanMX6* in the strain YYy136 (Yin and Petes, 2015) as described above for YYy181.3.
YYy184.3	YJM789	*MAT*α *ade2-1 URA3 gal2 ho::hisG can1::SUP4-o mlh1::kanMX6*	*MLH1* was replaced by *kanMX6* in the strain MD416-2 (Lee et al., 2009) as described above for YYy181.3
YYy302.1	W303-1A X YJM789	*MAT***a***/MAT*α *ade2-1/ade2-1 can1-100/can1::SUP4-o ura3-1/URA3 leu2-3,112/LEU2 his3-11,15/HIS3 trp1-1/TRP1 V9229::hphMX4/V9229 V261553::LEU2/V261663 GAL2/gal2 mlh1::kanMX6/mlh1::kanMX6*	Diploid formed by cross between YYy181.3 and YYy184.3.
YYy306.1	W303-1A X YJM789	*MAT***a***/MAT*α *ade2-1/ade2-1 can1-100/CAN1 ura3-1/ura3 trp1-1/TRP1 IV957578::hphMX4/IV957578 IV1013217::URA3/IV1013217 IV1510386/IV1510386::SUP4-o leu2-3,112/LEU2 his3-11,15/HIS3 GAL2/gal2 mlh1::kanMX6/mlh1::kanMX6*	Diploid formed by cross between YYy182.2 and YYy183.2.

YYy310.9	W303-1A X YJM789	*MAT***a**/*MAT*α*::natMX4 ade2-1/ade2-1 can1-100/can1::SUP4-o ura3-1/URA3 trp1-1/TRP1 leu2-3,112/LEU2 his3-11,15/HIS3 V9229::hphMX4/V9229 V261553::LEU2/V261663 GAL2/gal2 mlh1::kanMX6/mlh1::kanMX6*	Isogenic with YYy302.1 with replacement of *MAT*α with *natMX4* . The fragment to generate this replacement was obtained by amplifying the plasmid pAG25 (Goldstein and McCusker, 1999) with the primers MATALPHA natMX4 F and MATALPHA natMX4 R (sequences of primers in Table S1 of Lee *et al.,* 2009). By SNP-array analysis, this strain does not have pre-existing LOH events.
YYy310.10	W303-1A X YJM789	*MAT***a**/*MAT*α*::natMX4 ade2-1/ade2-1 can1-100/can1::SUP4-o ura3-1/URA3 trp1-1/TRP1 leu2-3,112/LEU2 his3-11,15/HIS3 V9229::hphMX4/V9229 V261553::LEU2/V261663 GAL2/gal2 mlh1::kanMX6/mlh1::kanMX6*	Isogenic with YYy310.9, resulting from independent replacement of *MAT*α with *natMX4* in YYy302.1. By SNP-array analysis, this strain does not have pre-existing LOH events.
YYy311.1	W303-1A X YJM789	*MAT***a**/*MAT*α*::natMX4 ade2-1/ade2-1 can1-100/CAN1 ura3-1/ura3 trp1-1/TRP1 IV957578::hphMX4/IV957578 IV1013217::URA3/IV1013217 IV1510386/IV1510386::SUP4-o leu2-3,112/LEU2 his3-11,15/HIS3 GAL2/gal2 mlh1::kanMX6/mlh1::kanMX6*	Isogenic with YYy306.1. *MAT*α was replaced by *natMX4* in the strain YYy302.1 as described above for YYy310.9. By SNP-array analysis, this strain does not have pre-existing LOH events. We also confirmed the presence of the inverted Ty repeats contained in the spontaneous hotspot "HS4" using primers IV 980403 R, Ty2 R, Ty1.2 R, and IV 993256 F as described in St. Charles and Petes, 2013.
YYy311.3	W303-1A X YJM789	*MAT***a**/*MAT*α*::natMX4 ade2-1/ade2-1 can1-100/CAN1 ura3-1/ura3 trp1-1/TRP1 IV957578::hphMX4/IV957578 IV1013217::URA3/IV1013217 IV1510386/IV1510386::SUP4-o leu2-3,112/LEU2 his3-11,15/HIS3 GAL2/gal2 mlh1::kanMX6/mlh1::kanMX6*	Isogenic with YYy311.1, resulting from independent replacement of MATa with natMX4 in YYy306.1. By SNP-array analysis, this strain does not have pre-existing LOH events, and we also confirmed the presence of the Ty repeats within "HS4" as described above for YYy311.1.

Table S2. SGD coordinates for LOH transitions in the *mlh1* strain YYy310 induced by a UV dose of 15 J/m^2 in G1-synchronized cells (Figs. S3-S80), spontaneous sectors in YYy310 selected on the left arm of chromosome V (Figs. S81-S85) and spontaneous sectors in YYy311 selected on the right arm of chromosome IV (Figs. S86-S91).

Sector	Chromosome	Supplementary picture	Sub sector	Transition genotype		SNPs flanking transitions	
				Left	Right	Left	Right
YYy310-9-5WR	II	S3	5W1	het	S	235624	236376
UV				S	het	236383	236479
				het	Y	248647	249558
				Y	het	250304	251093
			5W2	het	het		
			5R1	het	het		
			5R2	het	Y	238664	239853
				Y	het	239940	240829
				het	Y	240829	241471
				Y	het	241471	241694
				het	Y	241694	242027
				Y	het	249558	250304
YYy310-9-5WR	III	S4	5W1	het	S	60451	64292
UV				S	het	64292	67656
			5W2	het	S	60451	64292
				S	het	64292	67656
			5R1	het	het		
			5R2	het	het		
YYy310-9-5WR	IV	S5	5W1	het	het		
UV			5W2	het	het		
			5R1	het	S	325063	327230
				S	het	330624	331783
			5R2	het	S	325063	327230
				S	het	329222	330624
YYy310-9-5WR	IV	S6	5W1	het	het		
UV			5W2	het	het		
			5R1	het	het		
			5R2	het	Y	356529	360199
				Y	het	360199	361086
YYy310-9-5WR	IV	S7	5W1	het	het		
UV			5W2	het	S	505764	507165
				S	Y	507165	507960
				Y	het	512801	521609
			5R1	het	Y	505764	507165
				Y	het	509817	512801
			5R2	het	Y	505764	507165
				Y	het	509817	512801
YYy310-9-5WR	V	S8	5W1	Y	HET	51915	53692
UV				HET	S	54198	56117
				S	het	57170	60701
			5W2	Y	HET	45587	48837
				HET	het	51915	53692
				het	S	54198	56117
				S	het	57170	60701
			5R1	S	het	57170	60701
			5R2	S	het	51915	53692
YYy310-9-5WR	VI	S9	5W1	het	S	185398	186565
UV				S	het	186912	189728
			5W2	het	S	180526	185398
				S	het	186912	189728
			5R1	het	het		
			5R2	het	S	186643	186862
				S	het	189839	191415
YYy310-9-5WR	VII	S10	5W1	het	S	157428	159699

UV				S	het	159699	162937
			5W2	het	het		
			5R1	het	het		
			5R2	het	het		
YYy310-9-5WR	VIII	S11	5W1	het	het		
UV			5W2	het	het		
			5R1	het	HET	108370	110004
			5R2	het	Y	108370	110004
				Y	HET	110004	111606
YYy310-9-5WR	X	S12	5W1	het	het		
UV			5W2	het	Y	314934	315219
				Y	het	320668	320792
			5R1	het	Y	315219	317971
				Y	het	323059	323805
			5R2	het	Y	315219	317971
				Y	het	320668	320792
YYy310-9-5WR	XI	S13	5W1	het	Y	46433	46576
UV				Y	het	51547	52577
			5W2	het	het		
			5R1	het	Y	50384	51547
				Y	het	51547	52577
			5R2	het	Y	46123	46433
				Y	het	47424	50384
YYy310-9-5WR	XII	S14	5W1	het	S	897133	897352
UV				S	het	901814	902318
			5W2	het	S	890066	893936
				S	het	901814	902318
			5R1	het	het		
			5R2	het	S	897133	897352
				S	het	898548	899569
YYy310-9-5WR	XV	S15	5W1	het	S	1019448	1022697
UV				S	het	1023392	1024031
			5W2	het	het		
			5R1	het	S	1014379	1018892
				S	het	1023392	1024031
			5R2	het	het		
YYy310-9-5WR	XVI	S16	5W1	HET	S	162425	165200
UV				S	het	165200	171020
			5W2	HET	S	158225	162425
				S	het	162425	165200
			5R1	het	S	158225	162425
				S	het	165200	171020
			5R2	het	het		
YYy310-9-12WR	II	S17	12W1	het	S	407335	410831
UV				S	het	410985	411148
			12W2	het	S	403952	406262
				S	het	410985	411148
			12R1	het	het		
			12R2	het	S	407335	410831
				S	het	411214	420497
YYy310-9-12WR	IV	S18	12W1	het	Y	29689	31400
UV				Y	het	33241	37025
			12W2	het	het		
			12R1	het	het		
			12R2	het	het		
YYy310-9-12WR	IV	S19	12W1	het	het		
UV			12W2	het	het		
			12R1	het	Y	426766	427154
				Y	het	427315	427981
			12R2	het	Y	426766	427154

				Y	het	427315	427981
YYy310-9-12WR	IV	S20	12W1	het	het		
UV			12W2	het	S	454186	455000
				S	het	458195	469765
			12R1	het	het		
			12R2	het	het		
YYy310-9-12WR	V	S21	12W1	Y	het	50196	50295
UV			12W2	Y	het	51768	53692
			12R1	S	het	50196	50295
			12R2	S	het	50196	50295
YYy310-9-12WR	VII	S22	12W1	het	Y	481769	482414
UV				Y	het	482414	484837
			12W2	het	Y	481769	482414
				Y	het	482414	484837
			12R1	het	het		
			12R2	het	het		
YYy310-9-12WR	VIII	S23	12W1	het	Y	13263	13512
UV				Y	het	16312	17106
			12W2	het	Y	13263	13512
				Y	het	16312	17106
			12R1	het	het		
			12R2	het	het		
YYy310-9-12WR	VIII	S24	12W1	het	HET	388782	393258
UV			12W2	het	HET	388782	393258
			12R1	het	HET	388782	393258
			12R2	het	S	378185	378225
				S	het	382724	388782
				het	S	388782	393258
				S	HET	397033	399358
YYy310-9-12WR	X	S25	12W1	het	Y	76156	77570
UV				Y	het	77717	78260
			12W2	het	Y	76156	77570
				Y	het	77717	78260
			12R1	het	het		
			12R2	het	het		
YYy310-9-12WR	XI	S26	12W1	het	HET	74554	76907
UV				HET	het	78118	78701
				het	S	78701	79174
				S	HET	79174	79722
				HET	S	79722	80717
				S	het	81237	83093
				het	S	83992	84050
				S	het	84071	84394
			12W2	het	S	78701	79174
				S	het	79174	79722
				het	S	79722	80717
				S	het	84426	84604
				het	S	84604	85461
				S	het	85830	87504
			12R1	HET	S	84604	85461
				S	het	85830	87504
			12R2	HET	het	85830	87504
YYy310-9-12WR	XII	S27	12W1	het	Y	188741	190430
UV				Y	het	190736	191599
			12W2	het	Y	188741	190430
				Y	het	190736	191599
			12R1	het	het		
			12R2	het	het		
YYy310-9-12WR	XII	S28	12W1	het	S	249041	249624
UV				S	HET	249888	250394

			12W2	het	HET	249041	249624
			12R1	het	S	249041	249624
				S	het	250968	253263
			12R2	het	S	249041	249624
				S	het	250968	253263
YYy310-9-12WR	XII	S29	12W1	het	het		
UV			12W2	het	S	665333	665741
				S	het	665742	677689
			12R1	het	Y	657904	665226
				Y	het	665742	677689
			12R2	het	Y	657904	665226
				Y	het	665742	677689
YYy310-9-12WR	XII	S30	12W1	het	het		
UV			12W2	het	het		
			12R1	het	S	693776	694201
				S	het	706779	706956
			12R2	het	S	693776	694201
				S	het	696985	697188
YYy310-9-12WR	XII	S31	12W1	het	S	834095	835000
UV				S	het	835000	835184
			12W2	het	S	834095	835000
				S	het	835000	835184
			12R1	het	S	833747	833877
				S	het	835000	835184
			12R2	het	S	833877	833970
				S	het	835000	835184
YYy310-9-12WR	XIII	S32	12W1	het	het		
UV			12W2	het	Y	296414	303742
				Y	het	303910	307056
			12R1	het	het		
			12R2	het	het		
YYy310-9-12WR	XIII	S33	12W1	het	het		
UV			12W2	het	het		
			12R1	het	Y	370211	370688
				Y	het	371928	378717
			12R2	het	Y	370211	370688
				Y	het	371928	378717
YYy310-9-12WR	XVI	S34	12W1	het	Y	99390	101743
UV				Y	het	105255	105779
			12W2	het	Y	99390	101743
				Y	het	105941	108288
			12R1	het	Y	99390	101743
				Y	het	104035	104416
			12R2	het	Y	105255	105779
				Y	het	105941	108288
YYy310-9-12WR	XVI	S35	12W1	het	het		
UV			12W2	het	het		
			12R1	het	S	635100	637439
				S	het	639408	644553
			12R2	het	S	635100	637439
				S	het	639408	644553
YYy310-9-17WR	I	S36	17W1	het	het		
UV			17W2	het	Y	124574	124635
				Y	het	125371	125782
			17R1	het	het		
			17R2	het	het		
YYy310-9-17WR	II	S37	17W1	Y	het	74904	79448
UV			17W2	Y	het	74904	79448
			17R1	S	het	74904	79448
			17R2	S	het	68229	69213

YYy310-9-17WR	II	S38	17W1	het	S	173854	174748
UV				S	het	175099	175399
			17W2	het	S	173854	174748
				S	het	175099	175399
			17R1	het	S	173854	174748
				S	het	175099	175399
				het	Y	179400	180245
				Y	het	180245	182118
			17R2	het	het		
YYy310-9-17WR	II	S39	17W1	het	het		
UV			17W2	het	S	420548	427526
				S	het	429164	431460
			17R1	het	het		
			17R2	het	het		
YYy310-9-17WR	IV	S40	17W1	het	het		
UV			17W2	het	Y	173405	184716
				Y	het	184727	188296
			17R1	het	het		
			17R2	het	het		
YYy310-9-17WR	IV	S41	17W1	HET	Y	409879	410333
UV				Y	het	417000	420543
			17W2	HET	Y	409879	410333
				Y	het	417000	420543
			17R1	het	HET	409879	410333
				HET	S	414508	415063
				S	het	417000	420543
			17R2	het	HET	409879	410333
				HET	het	410349	413580
				het	S	413580	414508
				S	het	414508	415063
YYy310-9-17WR	IV	S42	17W1	het	Y	1040924	1044556
UV				Y	het	1046711	1053213
			17W2	het	Y	1040924	1044556
				Y	het	1044648	1046711
			17R1	het	het		
			17R2	het	het		
YYy310-9-17WR	V	S43	17W1	Y	het	78080	80291
UV			17W2	Y	het	78080	80291
			17R1	S	HET	48837	49044
				HET	S	60913	61808
				S	HET	62013	62494
				HET	Y	76261	77288
				Y	S	78080	80291
				S	het	80291	81264
			17R2	S	het	72490	75719
				het	S	78080	80291
				S	het	80291	81264
YYy310-9-17WR	V	S44	17W1	het	het		
UV			17W2	het	Y	501972	502134
				Y	het	502978	504162
				het	Y	507136	507433
				Y	het	507627	508392
			17R1	het	Y	504309	504693
				Y	het	504917	506853
				het	Y	507433	507484
				Y	het	507627	508392
			17R2	het	Y	504309	504693
				Y	het	504917	506853
				het	Y	507136	507433
				Y	het	507627	508392

YYy310-9-17WR	IX	S45	17W1	S	het	132136	132892
UV			17W2	S	HET	119675	122608
				HET	het	122608	129791
			17R1	Y	het	119675	122608
				het	Y	122608	129791
				Y	het	132136	132892
			17R2	Y	het	122608	129791
YYy310-9-17WR	XV	S46	17W1	het	Y	182373	186468
UV				Y	het	196650	198759
			17W2	het	Y	182373	186468
				Y	het	196650	198759
			17R1	het	Y	182373	186468
				Y	het	196650	198759
			17R2	het	Y	182373	186468
				Y	het	196650	198759
YYy310-10-14WR	II	S47	14W1	het	S	584379	584616
UV				S	het	586395	586943
			14W2	het	S	584379	584616
				S	het	586395	586943
			14R1	het	S	584379	584616
				S	het	586395	586943
			14R2	het	S	584379	584616
				S	het	586395	586943
YYy310-10-14WR	V	S48	14W1	Y	het	94077	94339
UV				het	Y	95429	95684
				Y	het	95906	96550
			14W2	Y	het	91739	93200
			14R1	S	het	80291	81264
			14R2	S	het	80291	81264
				het	S	85566	86732
				S	het	90062	90200
				het	S	90215	91703
				S	het	91739	93200
YYy310-10-14WR	IX	S49	14W1	het	Y	235680	236609
UV				Y	het	239260	240253
			14W2	het	Y	235680	236609
				Y	het	239260	240253
			14R1	het	het		
			14R2	het	het		
YYy310-10-14WR	XI	S50	14W1	het	het		
UV			14W2	het	het		
			14R1	het	Y	105100	112922
				Y	het	113668	114642
			14R2	het	het		
YYy310-10-14WR	XII	S51	14W1	het	het		
UV			14W2	het	het		
			14R1	het	S	757465	757753
				S	het	759448	760629
			14R2	het	het		
YYy310-10-14WR	XIII	S52	14W1	het	het		
UV			14W2	het	het		
			14R1	het	S	368237	368927
				S	het	369406	370211
			14R2	het	S	367185	367797
				S	het	369406	370211
YYy310-10-14WR	XIII	S53	14W1	het	Y	612380	613145
UV				Y	het	613247	613271
			14W2	het	Y	612380	613145
				Y	het	613247	613271
			14R1	het	Y	613271	613724

				Y	het	613724	614157
			14R2	het	Y	613271	613724
				Y	het	613724	614157
YYy310-10-14WR	XV	S54	14W1	het	Y	1004852	1009367
UV				Y	het	1009367	1014379
			14W2	het	het		
			14R1	het	Y	1004852	1009367
				Y	het	1009367	1014379
			14R2	het	Y	1004852	1009367
				Y	het	1009367	1014379
YYy310-10-14WR	XVI	S55	14W1	het	S	901548	907111
UV				S	het	912806	918183
			14W2	het	S	901548	907111
				S	het	911222	912157
			14R1	het	S	901548	907111
				S	het	909996	911222
			14R2	het	S	901548	907111
				S	het	912806	918183
YYy310-10-17WR	IV	S56	17W1	het	Y	248076	249496
UV				Y	het	249496	251661
			17W2	het	Y	248076	249496
				Y	het	249496	251661
			17R1	het	Y	232819	233059
				Y	het	244267	246953
			17R2	het	Y	242167	244267
				Y	het	244267	246953
				het	Y	248076	249496
				Y	het	249496	251661
YYy310-10-17WR	IV	S57	17W1	het	het		
UV			17W2	het	het		
			17R1	het	Y	526934	540214
				Y	het	540214	543869
			17R2	het	Y	526934	540214
				Y	het	540214	543869
YYy310-10-17WR	IV	S58	17W1	het	HET	608319	611611
UV				HET	Y	611611	618459
			17W2	het	Y	608319	611611
			17R1	het	S	608319	611611
			17R2	het	S	608319	611611
YYy310-10-17WR	V	S59	17W1	Y	HET	121397	124190
UV				HET	Y	124505	124754
				Y	HET	127038	128941
				HET	het	131261	132281
			17W2	Y	het	131261	132281
			17R1	S	het	126304	127030
			17R2	S	het	124754	125129
				het	Y	126304	127030
				Y	het	127038	128941
YYy310-10-17WR	VIII	S60	17W1	het	S	139939	141697
UV				S	het	141697	144711
			17W2	het	Y	117153	117396
				Y	het	120428	139939
			17R1	het	het		
			17R2	het	het		
YYy310-10-17WR	IX	S61	17W1	HET	S	108413	110547
UV				S	het	117444	119675
			17W2	HET	Y	110547	111619
				Y	het	115879	116682
			17R1	HET	het	122608	129791
			17R2	HET	S	117444	119675

				S	het	122608	129791
YYy310-10-17WR	X	S62	17W1	S	HET	237196	238853
UV				HET	Y	241092	242667
				Y	het	242937	244592
			17W2	S	HET	237196	238853
				HET	het	242937	244592
			17R1	Y	het	242937	244592
			17R2	Y	het	237196	238853
				het	Y	240830	242667
				Y	het	242937	244592
YYy310-10-17WR	XIII	S63	17W1	het	het		
UV			17W2	het	Y	113881	114292
				Y	het	114636	117330
			17R1	het	Y	113881	114292
				Y	het	114636	117330
			17R2	het	Y	113881	114292
				Y	het	114636	117330
YYy310-10-18WR	II	S64	18W1	het	het		
UV			18W2	het	Y	398295	399516
				Y	het	400808	401593
			18R1	het	Y	400808	401593
				Y	het	401882	403262
			18R2	het	S	400808	401593
				S	het	401882	403262
YYy310-10-18WR	V	S65	18W1	Y	het	44506	45284
UV				het	Y	45587	48837
				Y	het	49385	49896
				het	Y	50295	51183
				Y	het	51183	51567
			18W2	Y	het	37492	38068
			18R1	S	HET	34235	34481
				HET	het	34481	37492
				het	Y	37492	38068
				Y	het	41533	44506
			18R2	S	Y	38068	41126
				Y	het	41533	44506
YYy310-10-18WR	VII	S66	18W1	het	Y	263911	264645
UV				Y	het	275506	275695
				het	HET	277103	278627
				HET	het	281296	284849
			18W2	het	Y	262989	263911
				Y	het	264645	267678
				het	Y	268082	269269
				Y	het	272660	273402
				het	Y	277103	278627
				Y	het	281296	284849
			18R1	het	S	263911	264645
				S	het	269529	272660
			18R2	het	het		
YYy310-10-18WR	X	S67	18W1	het	S	690840	696274
UV				S	het	696274	697635
			18W2	het	S	690840	696274
				S	het	696274	697635
			18R1	het	Y	690840	696274
				Y	het	696274	697635
			18R2	het	het		
YYy310-10-18WR	XII	S68	18W1	het	S	25673	27102
UV				S	het	27102	28812
			18W2	het	S	25673	27102
				S	het	29402	29600

			18R1	het	het		
			18R2	het	het		
YYy310-10-18WR	XIV	S69	18W1	het	S	306383	310719
UV				S	het	310719	316099
			18W2	het	S	301637	304112
				S	het	310719	316099
			18R1	het	het		
			18R2	het	het		
YYy310-10-18WR	XIV	S70	18W1	het	Y	540177	540710
UV				Y	het	541005	542559
			18W2	het	Y	537970	538761
				Y	het	539355	539640
			18R1	het	het		
			18R2	het	het		
YYy310-10-18WR	XV	S71	18W1	het	Y	105667	108932
UV				Y	het	139346	140733
			18W2	Y	het	141843	143584
			18R1	het	Y	80436	86804
				Y	het	108932	111280
			18R2	het	Y	105667	108932
				Y	het	108932	111280
YYy310-10-18WR	XV	S72	18W1	het	het		
UV			18W2	het	Y	252032	253952
				Y	het	253952	254189
				het	Y	254189	255004
				Y	het	255254	259077
			18R1	het	het		
			18R2	het	het		
YYy310-10-18WR	XV	S73	18W1	het	S	288101	288801
UV				S	het	288906	289639
			18W2	het	het		
			18R1	het	het		
			18R2	het	het		
YYy310-10-23WR	I	S74	23W1	S	het	92538	93104
UV				het	S	95179	96036
				S	het	99216	99918
			23W2	S	het	92538	93104
				het	S	95179	96036
				S	het	98625	98874
			23R1	Y	het	88734	90376
				het	S	90970	92053
				S	het	92521	92538
			23R2	Y	het	92538	93104
YYy310-10-23WR	IV	S75	23W1	het	S	1468302	1468543
UV				S	het	1469944	1471442
			23W2	het	S	1468302	1468543
				S	het	1468701	1469252
			23R1	het	S	1468302	1468543
				S	het	1468543	1468701
			23R2	het	S	1468302	1468543
				S	het	1469944	1471442
YYy310-10-23WR	V	S76	23W1	Y	het	75719	76261
UV				het	Y	78080	80069
				Y	het	80291	81264
			23W2	Y	het	80291	81264
			23R1	S	het	75719	76261
				het	Y	78080	80069
				Y	het	82770	84997
			23R2	S	het	72490	75719
YYy310-10-23WR	VIII	S77	23W1	het	het		

UV			23W2	het	het		
			23R1	het	Y	95306	96110
				Y	het	96638	97583
			23R2	het	S	95306	96110
				S	HET	96110	96638
				HET	het	96638	97583
YYy310-10-23WR	XII	S78	23W1	het	Y	234494	235321
UV				Y	HET	240616	241709
				HET	Y	243415	243631
			23W2	het	Y	235686	236112
				Y	HET	240616	241709
				HET	Y	255725	256514
			23R1	het	S	227845	228409
			23R2	het	HET	228409	234166
				HET	S	234494	235321
YYy310-10-23WR	XII	S79	23W1	Y	het	400760	401521
UV				het	Y	403077	407394
				Y	het	407394	407628
				het	Y	408418	412592
			23W2	Y	het	400760	401521
				het	Y	403077	407394
				Y	het	407394	407628
				het	Y	408418	412592
			23R1	S	S		
			23R1	S	S		
YYy310-10-23WR	XVI	S80	23W1	het	S	676134	677039
UV				S	het	677039	677701
			23W2	het	S	676134	677039
				S	het	677039	677701
			23R1	het	het		
			23R2	het	het		
YYy310-1WR	V	S81	1W1	Y	het	78080	80069
spontaneous				het	S	80069	80291
				S	het	80291	81264
			1W2	Y	het	78080	80069
				het	S	80069	80291
				S	Y	82770	84997
				Y	het	84997	85566
			1R1	S	het	78080	80069
			1R2	S	Y	78080	80069
				Y	het	80291	81264
YYy310-4WR	V	S82	4W1	Y	HET	90215	91703
spontaneous				HET	Y	95906	97221
				Y	het	97792	98369
				het	Y	98369	98736
				Y	HET	100439	101353
				HET	S	104257	104636
				S	het	105481	105830
			4W2	Y	HET	90215	91703
				HET	Y	91739	93200
				Y	het	97792	98369
				het	HET	100201	100439
				HET	S	100439	101353
				S	het	105481	105830
			4R1	S	het	104257	104636
			4R2	S	HET	90215	91703
				HET	S	95906	97221
				S	het	104636	105299
YYy310-6WR	V	S83	6W1	Y	het	39153	41126
spontaneous			6W2	Y	HET	34799	37492

				HET	het	39153	41126
			6R1	S	het	34799	37492
			6R2	S	het	33770	34235
				het	S	34799	37492
				S	het	39153	41126
YYy310-9WR	V	S84	9W1	Y	HET	94077	94339
spontaneous				HET	het	100439	101353
				het	S	107912	109029
				S	het	109050	111741
			9W2	Y	HET	90215	91703
				HET	S	91739	93200
				S	HET	93407	94077
				HET	S	96550	97221
				S	HET	98369	98736
				HET	S	100439	101353
				S	het	107912	109029
			9R1	S	het	118782	119505
			9R2	S	het	118605	118782
YYy310-38WR	V	S85	38W1	Y	het	38068	41126
spontaneous			38W2	Y	het	34481	37492
				het	S	41533	44506
				S	Y	44506	45284
				Y	het	45587	45951
			38R1	S	het	45587	45951
			38R2	S	het	46371	48837
YYy311-10WR	IV	S86	10W1	het	Y	968316	968451
spontaneous				Y	het	971058	971688
				het	Y	973167	973779
				Y	het	976159	977291
				het	Y	977470	977752
			10W2	het	Y	969369	969944
				Y	het	970646	971058
				het	Y	971889	972525
			10R1	het	S	973167	973779
			10R2	het	S	968316	968451
				S	het	971058	971688
				het	S	976159	977291
YYy311-21WR	IV	S87	21W1	het	Y	973959	974614
spontaneous			21W2	het	Y	973959	974614
				Y	het	993347	993964
				het	Y	996000	996527
			21R1	het	Y	978621	979477
				Y	het	996527	996677
				het	S	1017595	1022402
			21R2	het	S	977470	977752
				S	HET	978621	979477
				HET	het	980838	992782
				het	Y	993347	993964
				Y	het	995883	996527
				het	S	1017595	1022402
YYy311-25WR	IV	S88	25W1	het	Y	967772	968451
spontaneous			25W2	het	Y	978763	979777
			25R1	het	Y	950685	950745
				Y	het	978763	979777
				het	Y	980838	992782
				Y	S	993964	995822
				S	Y	997558	997989
				Y	S	999715	1002104
				S	Y	1004465	1005641
				Y	S	1011955	1013221

				S	Y	1036164	1036844
				Y	S	1037332	1039370
			25R2	het	Y	950685	950745
				Y	het	978763	979777
				het	Y	980838	992782
				Y	S	993964	995822
				S	Y	997558	997989
				Y	S	999715	1002104
				S	het	1004465	1005641
				het	S	1011955	1013221
				S	het	1036164	1036844
				het	S	1037332	1039370
YYy311-27WR	IV	S89	27W1	het	Y	975687	976159
spontaneous			27W2	het	Y	974716	974975
			27R1	het	Y	968451	969369
				Y	het	995622	995822
				het	Y	995883	996000
				Y	het	1000365	1001602
				het	S	1004465	1005641
			27R2	het	Y	968451	969369
				Y	het	993964	994215
				het	S	1004465	1005641
YYy311-30WR	IV	S90	30W1	het	Y	974674	974716
spontaneous			30W2	het	Y	974674	974716
				Y	HET	980838	992782
				HET	Y	1000365	1001602
			30R1	het	Y	980838	992782
				Y	het	992897	993113
				het	Y	996000	996527
				Y	het	997989	998469
				het	S	1000365	1001602
			30R2	het	Y	980838	992782
				Y	het	992897	993113
				het	Y	994215	994598
				Y	het	994598	995622
				het	Y	996000	996527
				Y	het	997989	998469
				het	S	1000365	1001602
YYy311-32WR	IV	S91	32W1	het	Y	973959	974614
spontaneous			32W2	het	Y	964391	965936
			32R1	het	Y	953272	955278
				Y	S	993964	994598
			32R2	het	Y	968451	969944
				Y	HET	978358	978583
				HET	Y	980838	992782
				Y	S	993964	994598

In this table, we show the SGD coordinates (2009 version) for the LOH transitions that are given in Figs.S3-S91. "S" means homozygous for W303 (red) in the specified sub sector, "Y" means homozygous for YJM789 (blue), "het" means heterozygous with the same coupling relation as the heterozygous SNPs located centromere-proximal to the event. "HET" means heterozygous with a linkage switch relative to the SNPs located centromere-proximal to the event.

Table S3. Classification of UV-induced mitotic recombination events in YYy310 (derivatives YYy310-9 and YYy310-10); Figs. S3-S80), spontaneous events in YYy310 (Figs. S81-S85), and spontaneous crossovers on chromosome IV in YYy311 (Figs. 86-91). Details of the positions of the transitions are given in Table S2. The table headings are described in the table legend.

Sector	Chromosome	Type of break	Break 1				Break 2				Figure
			NCO or	Chromatids	Homolog broken	Class	NCO or	Chromatids	Homolog broken	Class	
YYy310-9-5WR	II	DSCB	NCO	1 & 4	S	1	NCO	2 & 3	S	Complex	S3
	III	SCB	NCO	1 & 3	Y	2					S4
	IV-1	SCB	NCO	1 & 4	Y	3					S5
	IV-2	SCB	NCO	2 & 3	S	1					S6
	IV-3	DSCB	NCO	1 & 4	S	1	NCO	2 & 3	S	Complex	S7
	V	DSCB	CO	1 & 4	Y	Complex	NCO	2 & 3	Y	Complex	S8
	VI	DSCB	NCO	1 & 3	Y	3	NCO	2 & 4	Y	1	S9
	VII	SCB	NCO	2 & 3	Y	1					S10
	VIII	SCB	CO	2 & 4	S	4					S11
	X	DSCB	NCO	1 & 3	S	1	NCO	2 & 4	S	5	S12
	XI	DSCB	NCO	1 & 3	S	Complex	NCO	2 & 4	S	Complex	S13
	XII	DSCB	NCO	1 & 3	Y	5	NCO	2 & 4	Y	1	S14
	XV	DSCB	NCO	1 & 3	Y	1	NCO	2 & 4	Y	1	S15
	XVI	DSCB	CO	1 & 3	Y	6	NCO	2 & 4	Y	Complex	S16
YYy310-9-12WR	II	DSCB	NCO	1 & 3	Y	5	NCO	2 & 4	Y	1	S17
	IV-1	SCB	NCO	1 & 3	S	1					S18
	IV-2	SCB	NCO	2 & 3	S	2					S19
	IV-3	SCB	NCO	2 & 3	Y	1					S20
	V	SCB	CO	1 & 4	S	4					S21
	VII	SCB	NCO	1 & 3	S	2					S22
	VIII-1	SCB	NCO	1 & 3	S	2					S23
	VIII-2	DSCB	CO	1 & 3	Y	7	CO	2 & 4	Y	Complex	S24
	X	SCB	NCO	1 & 3	S	2					S25
	XI-1	DSCB	NCO	1 & 3	Y	Complex	CO	2 & 4	Y	4	S26
	XI-2	SCB	NCO	1 & 3	S	2					S27
	XII-1	DSCB	CO	1 & 3	Y	4	NCO	2 & 4	Y	Complex	S28
	XII-2	SCB	NCO	2 & 3	S	8					S29
	XII-3	SCB	NCO	1 & 4	Y	3					S30
	XII-4	DSCB	NCO	1 & 3	Y	2	NCO	2 & 4	Y	3	S31
	XIII-1	SCB	NCO	1 & 3	S	1					S32
	XIII-2	SCB	NCO	2 & 3	S	2					S33
	XVI-1	DSCB	NCO	1 & 3	S	5	NCO	2 & 4	S	Complex	S34
	XVI-2	SCB	NCO	2 & 4	Y	2					S35
YYy310-9-17WR	I	SCB	NCO	1 & 3	S	1					S36
	II-1	SCB	CO	1 & 4	S	4					S37
	II-2	DSCB	NCO	2 & 3	S	Complex	NCO	3 & 4	Y	Complex	S38
	II-3	SCB	NCO	1 & 3	Y	1					S39
	IV-1	SCB	NCO	1 & 3	S	1					S40
	IV-2	DSCB	CO	1 & 3	S	Complex	NCO	2 & 4	S	Complex	S41
	IV-3	SCB	NCO	1 & 3	S	3					S42
	V-1	DSCB	CO	1 & 4	S	Complex	NCO	2 & 3	S	Complex	S43
	V-2	DSCB	NCO	1 & 3	S	Complex	NCO	2 & 4	S	Complex	S44
	IX	DSCB	NCO	1 & 4	S	1	CO	2 & 3	S	Complex	S45
	XV	DSCB	NCO	1 & 3	S	2	NCO	2 & 4	S	2	S46
YYy310-10-14WR	II	DSCB	NCO	1 & 3	Y	2	NCO	2 & 4	Y	2	S47
	V	SCB	CO	1 & 4	S	Complex					S48
	IX	SCB	NCO	1 & 3	S	2					S49
	XI	SCB	NCO	2 & 3	S	1					S50
	XII	SCB	NCO	1 & 4	Y	1					S51
	XIII-1	SCB	NCO	1 & 4	Y	3					S52
	XIII-2	DSCB	NCO	1 & 3	S	Complex	NCO	2 & 4	S	Complex	S53
	XV	DSCB	NCO	1 & 3	S	1	NCO	2 & 4	S	2	S54
	XVI	DSCB	NCO	1 & 3	Y	3	NCO	2 & 4	Y	3	S55

YYy310-10-17WR	IV-1	DSCB	NCO	1 & 3	S	Complex	NCO	2 & 4	S	Complex	S56
	IV-2	SCB	NCO	2 & 3	S	2					S57
	IV-3	DSCB	CO	1 & 4	Y	7	NCO	2 & 3	Y	1	S58
	V	DSCB	CO	1 & 4	S	Complex	NCO	2 & 3	S	Complex	S59
	VIII	2SCBs	NCO	1 & 4	S	1	NCO	2 & 3	Y	1	S60
	IX	DSCB	CO	1 & 4	Y	Complex	CO	2 & 3	S	6	S61
	X	DSCB	NCO	1 & 4	S	Complex	CO	2 & 3	S	Complex	S62
	XIII	DSCB	NCO	1 & 3	S	1	NCO	2 & 4	S	2	S63
YYy310-10-18WR	II	DSCB	NCO	1 & 3	S	1	NCO	2 & 4	S	Complex	S64
	V	DSCB	CO	1 & 4	S	Complex	NCO	2 & 3	S	Complex	S65
	VII	DSCB	NCO	2 & 3	Y	Complex	NCO	1 & 4	Y	Complex	S66
	X	SCB	NCO	2 & 3	Y	8					S67
	XII	SCB	NCO	2 & 3	Y	3					S68
	XIV-1	SCB	NCO	2 & 3	Y	3					S69
	XIV-2	SCB	NCO	1 & 3	S	Complex					S70
	XV-1	See table legend.									S71
	XV-2	SCB	NCO	1 & 3	S	Complex					S72
	XV-3	SCB	NCO	1 & 3	Y	1					S73
YYy310-10-23WR	I	DSCB	NCO	1 & 4	Y	Complex	CO	2 & 3	Y	Complex	S74
	IV	DSCB	NCO	1 & 3	Y	3	NCO	2 & 4	Y	3	S75
	V	DSCB	CO	1 & 4	S	Complex	NCO	2 & 3	S	Complex	S76
	VIII	SCB	NCO	2 & 4	S	Complex					S77
	XII-1	DSCB	CO	1 & 4	Y	Complex	NCO	2 & 3	Y	Complex	S78
	XII-2	SCB	NCO	1 & 3	Y	Complex					S79
	XVI	SCB	NCO	2 & 3	Y	2					S80
YYy310-1WR	V	DSCB	CO	1 & 4	Y	Complex	NCO	2 & 3	Y	Complex	S81
YYy310-4WR	V	DSCB	CO	1 & 4	Y	Complex	NCO	2 & 3	Y	Complex	S82
YYy310-6WR	V	DSCB	CO	1 & 4	S	Complex	NCO	2 & 3	S	Complex	S83
YYy310-9WR	V	DSCB	CO	1 & 4	Y	Complex	NCO	2 & 3	Y	Complex	S84
YYy310-38WR	V	DSCB	CO	1 & 4	Y	Complex	NCO	2 & 3	Y	1	S85
YYy311-10WR	IV	SCB	CO	1 & 4	S	Complex					S86
YYy311-21WR	IV	DSCB	CO	1 & 4	S	Complex	NCO	2 & 3	S	Complex	S87
YYy311-25WR	IV	DSCB	CO	1 & 4	S	Complex	NCO	2 & 3	S	Complex	S88
YYy311-27WR	IV	DSCB	CO	1 & 4	S	Complex	NCO	2 & 3	S	Complex	S89
YYy311-30WR	IV	DSCB	CO	1 & 4	S	Complex	NCO	2 & 3	S	Complex	S90
YYy311-32WR	IV	DSCB	CO	1 & 4	S	Complex	NCO	2 & 3	S	Complex	S91

Column A shows the identifying number of the specific sectored colony examined. Column B shows the chromosome with the event. Column C indicates whether the event reflects a single chromatid break (SCB) or a double sister-chromatid break (DSCB). Columns D and H show whether the event is a crossover (CO) or non-crossover (NCO), and columns E and I indicate which chromatids were involved. For NCO events in which only a single chromatid is recombinant the non-recombinant chromatid served as a donor is ambiguous. Columns F and J show which chromatid or chromosome received the initiating double-strand break (S=W303-1A and Y=YJM789). Column L indicates the supplemental figure that depicts the event. Columns G and K list the classes of events as defined below. **Class 1.** NCO. Simple continuous heteroduplex with no interrupting homoduplexes. Unidirectional from putative DSB site. **Class 2.** NCO. Simple conversion tract, unidirectional from putative DSB site. **Class 3.** NCO. Hybrid conversion and heteroduplex tract with mismatches. Unidirectional on one side of DSB. **Class 4.** CO. Heteroduplex on only one of recombinant chromosomes. **Class 5**. NCO. Conversion on one side of DSB, heteroduplex on the other. **Class 6**. CO. Uni-directional heteroduplexes on the two recombinant chromosomes propagated in opposite directions.**Class 7.** CO with no evident heteroduplexes or conversion tracts. **Class 8**. NCO with two recombinant chromosomes, one with homoduplex tract and one with heteroduplex tract. Most of the Classes 1-8 are consistent with the DSBR model as described in the text. More complex patterns of recombination are listed as "Complex" and are described in Table S4 and in the text. All samples labeled YYy310-9 or YYy310-10 represent sectored colonies induced by UV; in addition to events on chromosome V, these strains have many unselected recombination events. The five strains labeled YYy310-1WR to YYy310-38WR were red/white sectors that formed spontaneously. The strains labeled YYy311-10WR to YYy311-32WR have spontaneous sectors that were selected to occur at a hotspot previously identified (details in main text). The event described in Fig. S71 appeared to have a BIR event that occurred in one of the daughter cells, preventing an unambiguous description of the types of heteroduplexes.

Table S4. Summary of complex patterns of recombination.

Supp. Fig. #	CO or NCO	Observations	Interpretations
S3	NCO1	Simple heteroduplex. DSB on blue chromatid.	SDSA
	NCO2	Simple heteroduplex. DSB on red chromatid.	SDSA
	NCO3	Long heteroduplex with regions of homoduplex. DSB on red chromatid.	Standard DSBR event except Mlh1-independent MMR. Two independent DSBs.
S7	NCO1	Large homoduplex region separating DSB site from heteroduplex tract (chromatids 2 and 3).	Repair of double-stranded DNA gap
	NCO2	Simple heteroduplex on chromatid 1	SDSA
S8	CO	Symmetric heteroduplexes	Branch migration following formation of double Holliday junction (dHJ)
	NCO	Strand switches of heteroduplexes on NCO chromatid, region of conversion at junction of heteroduplex	dHJ dissolution and region of Mlh1-independent MMR
S13	NCO1	Heteroduplex spanning DSB site in chromatid 1	Extension of broken end by interaction with sister chromatid
	NCO2	Bi-directional heteroduplexes on chromatid 2 with strand switch, separated by homoduplex	Dissolution of dHJ followed by Mlh1-independent MMR
S16	CO	Heteroduplexes in *trans* flanking DSB site	Standard CO according to DSBR model
	NCO	Heteroduplex spanning DSB site on NCO chromatid 4	Extension of broken end by interaction with sister chromatid
S17	NCO1	Heteroduplex with interspersed conversion and restoration tracts (chromatid 3)	SDSA with Mlh1-independent MMR
	NCO2	Simple heteroduplex (chromatid 4)	SDSA
S24	CO1	CO between chromatids 1 and 3 with no heteroduplex	Standard DSBR model with limited strand invasion and limited DNA synthesis
	CO2	CO between chromatids 2 and 4 with restoration tract between *trans* heteroduplexes	Standard DSBR model with tract of Mlh1-independent restoration repair
S26	NCO	Symmetric heteroduplexes; regions of homoduplex within heteroduplex; strand switch within heteroduplex	Branch migration; Mlh1-independent MMR; DSB between regions of strand switch, followed by dissolution
	CO	CO between chromatids 2 and 4 with heteroduplex on only one chromatid	Standard CO according to DSBR with one heteroduplex occurring in region without SNP
S28	NCO	Long conversion tract spanning putative DSB site	Repair of double-stranded DNA gap
	CO	Heteroduplex tract on only one side of DSB site	Standard CO according to DSBR with one heteroduplex occurring in region without SNP
S34	NCO1	Long conversion-tract on chromatid 1	Repair of double-stranded DNA gap
	NCO2	Bi-directional heteroduplex in on chromatid 2 with strand switch, separated by homoduplex	Dissolution of dHJ associated with restoration repair

S38	NCO1	Conversion tract adjacent to DSB1 site on chromatid 3	SDSA, Mlh1-independent MMR
	NCO2	Heteroduplex adjacent to DSB1 site on chromatid 4	SDSA
	NCO3	Heteroduplex adjacent to DSB2 site on chromatid 2	SDSA
S41	NCO	Symmetric heteroduplexes on chromatids 2 and 4; homoduplex regions within heteroduplex	Branch migration; Mlh1-independent MMR
	CO	Crossover between chromatids 1 and 3 associated with long conversion tract	Repair of double-stranded DNA gap
S43	CO	Restoration repair on one side of CO chromatid 4 and conversion repair on the other	Branch migration; Mlh1-independent MMR
	NCO	Long heteroduplex region with short restoration tract	SDSA with Mlh1-independent MMR
S44	NCO1	Chromatid 1 has heteroduplex region with long restoration tract in the middle	Template switch during replication to sister strand; SDSA
	NCO2	Chromatid 2 has mixture of homoduplex conversion and restoration tracts	Mlh1-independent patchy MMR
S45	NCO	Simple heteroduplex (chromatid 1)	SDSA
	CO	Regions of heteroduplex with switched strands on chromatid 3; symmetric heteroduplexes	Independent invasion of two broken ends; branch migration
S48	CO	Regions of heteroduplex interspersed with homoduplex regions	Mlh1-independent patchy MMR
S53	NCO1	Conversion tract with no heteroduplex in chromatid 1	Mlh1-independent MMR
	NCO2	Conversion and restoration tracts in chromatid 2	Mlh1-independent patchy MMR
S56	NCO1	Conversion tract with no heteroduplex in chromatid 1	Mlh1-independent MMR
	NCO2	Conversion and restoration tracts in chromatid 2	Mlh1-independent patchy MMR
S59	CO	Long conversion tract between heteroduplex and putative DSB site on chromatid 4	Repair of double-stranded DNA gap
	NCO	Regions of conversion/restoration and heteroduplex on same side of putative DSB site in chromatids 3 and 4	Branch migration; NCO resolution of dHJ; Mlh1-independent patchy repair
S60	NCO1	Simple heteroduplex. DSB on red chromatid.	SDSA
	NCO2	Simple heteroduplex. DSB on blue chromatid.	SDSA
S61	CO1	Uni-directional heteroduplexes on chromatids 2 and 3 propagated in opposite directions	Crossover by standard DSBR model
	CO2	DSB on blue chromatid, large conversion tract	Repair of double-stranded DNA gap; followed by cleavage of dHJ to yield a CO
S62	NCO	Conversion tract spanning putative DSB site in chromatid 1	Repair of double-stranded DNA gap; dissolution

	CO	Uni-directional heteroduplexes on chromatids 2 and 3; propagated in opposite directions; interspersed conversion and restoration tracts	Mlh1-independent MMR
S64	NCO1	Simple heteroduplex (chromatid 1)	SDSA
	NCO2	Heteroduplexes on same side of DSB in chromatids 2 and 4	Branch migration; NCO mode of dHJ resolution
S65	CO	Heteroduplex on same side of DSB site in chromatids 1 and 4; heteroduplex spans DSB site in chromatid 4; tracts of restoration within heteroduplex in chromatid 2	Extension of broken end by interaction with sister chromatid; Mlh1-independent patchy repair; CO resolution of dHJ
	NCO	Heteroduplex spans DSB site in chromatid 2; tracts of conversion and restoration interspersed with heteroduplex regions	Extension of broken end by interaction with sister chromatid; Mlh1-independent patchy repair; SDSA
S66	NCO1	Heteroduplex on chromatid 3 separated from putative DSB site by long region of homoduplex	Extension of broken end by interaction with sister chromatid, followed by SDSA
	NCO2	Heteroduplexes on both chromatids 1 and 4; chromatid 1 has trans heteroduplexes flanking the DSB site in addition to regions of homoduplex within the heteroduplex	Invasion of right end, followed by cleavage of junction and invasion of left end; branch migration; Mlh1-independent patchy repair
S67	NCO	Uni-directional heteroduplexes on chromatids 2 and 3 propagated in opposite directions	NCO mode of dHJ resolution with limited synthesis
S70	NCO	Bi-directional heteroduplex with strand switch separated by restoration tract on chromatid 1	Formation of dHJ event; dissolution followed by Mlh1-independent repair
S72	NCO	Heteroduplex tract with an internal restoration tract	Mlh1-independent MMR, SDSA
S74	NCO	Region of restoration repair separating DSB site from heteroduplex on chromatid 4	Mlh1-independent MMR, SDSA
	CO	Long regions of restoration and conversion repair separating DSB site from heteroduplex tract	Mlh1-independent MMR or template switching
S76	CO	Conversion event at the end of heteroduplex tract	Mlh1-independent MMR, resolution of dHJ in CO mode
	NCO	Displacement of heteroduplex tract from DSB site	Interaction of broken end with sister chromatid or long restoration tract by Mlh1-independent MMR
S77	NCO	Symmetric heteroduplex; conversion tract at end of heteroduplex tract	Branch migration; Mlh1-independent MMR; NCO processing of dHJ
S78	NCO	Regions of homoduplex separating heteroduplex region from DSB site	Mlh1-independent MMR or template switching; resolution of dHJ in NCO mode
	CO	Region of conversion separating heteroduplex region from DSB site on chromatid 4	Mlh1-independent MMR or gap repair; resolution of dHJ in CO mode

S79	NCO	In regions centromere-proximal to event, both homologs in white sector derived from one parental homolog and both in red sector derived from the other; regions of conversion and restoration homoduplexes on chromatid 1	Crossover on same chromosomes located centromere-proximal to the event in S79 (described in S78) produced centromere-proximal regions. Homoduplex regions produced by template switching or by Mlh1-independent MMR
S81	CO	Long tracts of homoduplex on chromatids 1 and 4.	Extension of broken end by interaction with sister chromatid; Mlh1-independent restoration repair; resolution of dHJ in CO mode
	NCO	Heteroduplex DNA on same side of DSB site in NCO chromatids	Branch migration followed by processing of dHJ in CO mode
S82	CO	Heteroduplex with interspersed conversion and restoration tracts (chromatid 1); initiated at DSB1	Mlh1-independent MMR; processing of dHJ in CO mode
	NCO	Symmetric heteroduplex tracts; heteroduplex tract interspersed with homoduplex regions; strand switch on chromatid 3; initiated at DSB2	Branch migration; Mlh1-independent MMR; dissolution of dHJ
S83	CO	Strand switch of heteroduplex in CO chromatid 4	Invasion of the right broken end, followed by processing of junction; extension of right end by sister-chromatid interaction; invasion of the left end and processing dHJ in crossover mode
	NCO	DSB on red chromatid, but red chromatid acts as donor	Following strand invasion, junction cleaved before initiating DNA synthesis
S84	CO	Long conversion tract spanning DSBs in both CO chromatids 1 and 4; heteroduplex in chromatid 1 interrupted by restoration tracts	Gap repair; Mlh1-independent MMR; resolution of dHJ in CO mode
	NCO	NCO chromatid 3 has strand switch of heteroduplexes; conversion event within heteroduplex	Resolution of dHJ by dissolution; Mlh1-independent MMR
S85	CO	Strand switch in CO chromatid 1; heteroduplexes in trans on chromatids 1 and 4; long conversion tract adjacent to heteroduplex region in chromatid 1	Invasion of right end, followed by branch migration and cutting of junction. Extension of right end by interaction with sister chromatid; invasion of left end and resolution of dHJ in CO mode
	NCO	Simple heteroduplex	SDSA
S86	CO	Strand switches in heteroduplexes in both CO chromatids 1 and 4; both chromatids have homoduplex regions interspersed with heteroduplex	Invasion of right broken end, followed by branch migration; resolution of junctions in NCO mode, followed by left end invasion and branch migration; cleavage in CO mode and Mlh1-independent MMR

S87	CO	Large region of conversion spanning putative DSB site; uni-directional heteroduplexes on chromatids 1 and 4 propagated in opposite directions;; conversion tract distal to heterodupex tract on chromatid 4	Repair of large gap associated with HS4 hotspot; processing dHJ in CO mode; Mlh1-independent MMR
	NCO	Region of conversion spanning putative DSB site; conversion tract adjacent to heteroduplex	Repair of large gap; SDSA; Mlh1-independent MMR
S88	CO	Region of conversion spanning putative DSB site; uni-directional heteroduplex tracts in on chromatids 1 and 4 propagated in different directions; multiple homoduplex tracts within heteroduplex tract on chromatid 4	Repair of large gap; patchy Mlh1-independent MMR; resolution of dHJ in CO mode
	NCO	Large conversion tract spanning putative DSB site; chromatid 3 has a pattern of heteroduplex and homoduplex tracts that is very similar to that of chromatid 4	Repair of large gap; chromatid 4 CO chromatid used as template for part of repair; also, switch of repair templates to sister chromatid
S89	CO	Very large conversion tract spanning putative DSB site; heteroduplex on chromatid 1 but not 4	Repair of large gap; resolution of dHJ in CO mode
	NCO	Very large conversion tract spanning putative DSB site; restoration tract in middle of heteroduplex	Repair of large gap; resolution of dHJ in NCO mode; Mlh1-independent MMR
S90	CO	Very large conversion tract spanning DSB site; no heteroduplexes observed	Repair of large double-stranded DNA gap, resolution of dHJ in CO mode
	NCO	Heteroduplexes in both NCO chromatids 2 and 3 on same side of DSB site; homoduplex tracts in heteroduplex	Invasion of broken end, followed by branch migration; resolution of dHJ structure in NCO mode with regions of Mlh1-independent MMR
S91	CO	Heteroduplexes on both chromatids 1 and 4 on same side of putative DSB site; large conversion tract flanking DSB site	Invasion of right broken end, followed by synthesis off of homolog; template switch to sister chromatid, and then re-invasion of sister chromatid; resolution of dHJ in CO mode
	NCO	Large conversion tract spanning putative DSB site	Repair of large gap; SDSA

Table S5. Primers and enzymes used in PCR and restriction enzyme analysis.							
SNP position	Primer pairs	Primer Sequences	PCR fragment size (bp)	Restriction fragment size for W303-1A	Restriction fragment size for YJM789	Enzyme used	Purpose
108382	V-108306F	CCCTCGTCCTGCCTTATCCTT	268	164+76+28	240+28	*Hpy* 188III	1
	V-108574R	GGGATAGTAATTCCTGGACAGAT					
108750	V-108509F	GCGATTCATCTTGCTGTAGGTA	463	463	222+241	*Taq* aI	1
	V-108972R	CCCCATTGGAATACGAATGGA					
109461	V-109162F	CTCACTCCTAGTAGGGAACAT	555	256+299	555	*Sty*I	1
	V-109717R	CAACTTCTAATGCATTAATGCGT					
109718	V-109550F	GGTCCAACAGCAACTCTGTA	476	476	308+168	*Hinc* II	1
	V-110026R	CGCAGCCTAATGAATTACA					
110830	V-110540F	TGAAGCTATCCATCTAATGGAT	496	206+296	496	*Mfe* I	1
	V-111036R	AACCTGCAGTTTCCTGTA					
104269	V-104109F	GGTAAGGAAGGAATCGTATCCA	277	117+160	277	*Dde* I	1
	V-104386R	GTCATTTACTTGGACGGTGTGT					
105087	V-104896F	CTGTCCCCTTGTTTCCAAT	413	191+222	413	*Hind* III	1
	V-105309R	GGCTTACAAACGGGGCTT					
105842	V-105555F	CATGTGGCGTCGTCAAGCA	439	439	152+287	*Dra* I	1
	V-105994R	GGATTGTATACCGGAACGTCCAA					
Multiple SNPs	V- 45888F (38R)	GTATGAACCTACACAAGGC	702			Seq	2 (310-38WR)
	V- 46590R (38R)	CGATTGACGTAAACGGT					Spontaneous
Multiple SNPs	V-118435F (9R)	GGCAGATCTTTAACTCGGCT	606			Seq	2 (310-9WR)
	V-119041R (9R)	CTATGGGGATTGGGCTCGGA					Spontaneous
Multiple SNPs	V-34122F	CAAGGCTAATAAGGGACAAGAGTTC	775			Seq	2 (310-6WR)

	V-34897R	GGTGTGGTGTTA CTACTAGGA					Spontaneous
Multiple SNPs	V-37344F	CGCTAATATCAG AAAGATTCTCGG	807			Seq	2 (310-6WR)
	V-38151R	GAAACCTGCAGT ACATTAGAG					Spontaneous
Multiple SNPs	V-38495F	GTGGACGCTACT TGCCTATGC	799			Seq	2 (310-6WR)
	V-39294R	GCTCAAATGAAT GCCAAGAG					Spontaneous
Multiple SNPs	V-44890F	GACGAAGTGGTG GAGCAC	811			Seq	2 (310-6WR)
	V-45701R	GAGGAATGACAA CAGAAAGG					Spontaneous
Multiple SNPs	V-45781F	GAATATAAGCTT GGGCTTGCCG	573			Seq	2 (310-6WR)
	V-46354R	CTTGAGGCGCCG TTAAAGAGAG					Spontaneous
1002467	IV-1002341F	TGCAGGGATATG TATAACGAG	337	126+211	337	*Hpy* CH4I II	3
	IV-1002678R	CTATGAAGAAGT AGACGGAGA					
999930	IV-999739F	CATGAGTGATCC TAGCTGC	350	350	159+191	*Hpy* 188III	3
	IV-1000089R	CTAACCTGTAACT GACAATAGCA					
997278	IV-997153F	CACCGGATAACA AAGGTGAC	341	341	216+!25	*Hpy* CH4 V	3
	IV-997494R	CGGATACCGGAA AAGATTGC					
994719	IV-994468F	GCCATATCTACA GGGTGCA	561	260+301	561	*Bsp* MI	3
	IV-995029R	CAGAAGATTCTG ATTTGTTGGTCT					
993060	IV-992915F	CTATTAGCGATC AATATGAAGGGT	308	163+145	308	*Hpy* 188III	3
	IV-993223R	GACGACGTTCTT ACCTCTTAC					
980873	IV-980667F	CCGAAATGCGAT AAGTCGTGAT	397	397	19+206	*Hae* III	3
	IV-981064R	GTAAATTGAGGC AACTTGGCCGA					
978636	IV-978353F	GTGTTGTCACTC GAATTCTGA	440	283+157	440	*Bgl* II	3
	IV-978793R	CATCGGATATTG GGCGTGGAA					
975702	IV-975536F	CAGACGGACCAG ATAGATGCA	229	63+166	229	*Hinf* I	3

	IV-975765R	GATTCGTCCCGA TATGTATAATCA					
973794	IV-973660F	CGTTCTTCGAATT CACCTCT	460	134+326	460	*Aci* I	3
	IV-974120R	GCAAGACCTCGA GTAGCCAA					
971073	IV-970892F	GCATTTCCAAATC AAAGGAGT	246	65+181	246	*Dra* I	3
	IV-971138R	GTTTGGAACAAA CCAAGCGA					
968331	IV-968094F	GTCGTGGAAACA ACGCCACT	440	238+202	440	*Aci* I	3
	IV-968534R	CCCGCTATCAGA GATGGA					
965754	IV-965469F	CGTAGTAAAGCT CCAACCTG	524	283+239	524	*Hinc* II	3
	IV-965993R	CCAGTAAGGCCT TGGTGCT					
963747	IV-963536F	CCAAGTTACAAG CTGAACTTC	406	406	211+195	*Hpy* 188III	3
	IV-963942R	CTGCAACATTAAT GTGATAGCA					
85522	XI-85323F	GTGCCGCATTTA CTGCACA	307	307	199+108	*Hpy* 188III	4 (9-12R)
	XI-85630R	TGACTTCCTTGG GTTTGCT					UV
250697	XII-250483F	CACACTTGCACT TCCCTCCA	375	375	214+161	*Eco* RV	4 (9-12R)
	XII-250858R	GGAGAAACACCA GCAGCACA					UV
694318	XII-694140F	GAGGTCGATTTA CCACTGA	423	178+245	423	*Hha* I	4 (9-12R)
	XII-694563R	GGACATTGGACC ATGTTTGAA					UV
705704	XII-705448F	CTCAGGGCAATG GATTGA	471	256+215	471	*Xba* I	4 (9-12R)
	XII-705919R	CCCAGTATCTTG GTTTGAATCT					UV
74853	II-74609F	CAATGCATATTCC GGCCTGA	473	244+229	473	*Dra* I	4 (9-17W)
	II-75082R	CGTGCAACACGA TATAGAGTA					UV
410359	IV-410040F	GGCACAAGGTAG TACATGGTA	555	555	319+236	*Hpa* I	4 (9-17W)
	IV-410595R	GACCACCTCGTC TTGCTAGA					UV
1044571	IV-1044334F	GGCTGCATCTTC ATGATTCA	536	536	237+299	*Hpy* 188I	4 (9-17W)

	IV-1044870R	GTTGCAAACGCA AATACAGAC					UV
130876	IX-130598F	GGATGCCATATT ATGAAGCA	561	278+283	561	*Hpy* CH4I V	4 (9-17W)
	IX-131159R	CTGACACTGTAG GTATATCAGA					UV
233551	IV-233330F	GAGCAACAAGAA GAAGAGACC	584	497+88	221+363	*Hpy* CH4 V	4 (10-17R)
	IV-233914R	GGTGAATTTCTG CGCTACT					UV
543883	IV-543676F	GTAGAAAGATGA CACTGCCA	404	207+197	404	*Hpy* CH4I II	4 (10-17R)
	IV-544080R	GTCTTCGCATAG TTCCCCT					UV
117417	VIII-117100F	CATGAGAAGCGC ACATGT	451	317+134	451	*Ase*I	4 (10-17R)
	VIII-117551R	GCGTTCAGAACC TCCATTA					UV
117456	IX-117174F	GTCTGTGTTCGC AGTGGA	551	282+269	551	*Hpy* CH4I V	4 (10-17R)
	IX-117725R	GCTGGCAACTGT GGAAA					UV
240695	X-240472F	CGAACTAGCATT AGGCGT	510	223+287	510	*Aci*I	4 (10-17R)
	X-240982R	CCATCCCAATTG TTTGCC					UV
269535	VII-269286F	GTGCAAGCTAGT CGAGTAGGA	531	531	249+282	*Aat*II	4 (10-18R)
	VII-269817R	GAATCGAGTACG ATACCCA					UV
306393	XIV-306096F	CGTGCTTATGGA AACTGTCG	574	297+277	574	*Bgl*II	4 (10-18R)
	XIV-306670R	GTTCCCAATATG ACCCAGCT					UV
255192	XIV-255000F	GGCGGTTCACGT TGGTGAA	498	498	192+306	*Rsa*I	5 (10-18WR)
	XIV-255498R	GTTCCGGACTGC GATCTCA					UV
306393	XIV-306096F	CGTGCTTATGGA AACTGTCG	574	297+277	574	*Bgl*II	5 (10-18WR)
	XIV-306670R	GTTCCCAATATG ACCCAGCT					UV
345154	XIV-344911F	GGTCCGATATTC GTCCT	418	243+175	418	*Bts*CI	5 (10-17WR)
	XIV-345329R	CTTGTTGTTTCTA CTGAACAC					UV
540228	IV-540035F	CTTTGCCCACGA GAAGAGA	348	C	T	Seq	5 (10-17WR)

	IV-540383R	GGGCTATCCAATAGTTCC					UV
615114	IV-614880F	CCATCGTCGTTGTGCGA	563	234+329	563	*Eco*RI	5 (10-17WR)
	IV-615443R	TACCCTGACCAGCTTGC					UV
509831	IV-509611F	GCACGGTGCCTGCTTTG	416	220+196	416	*Alu*I	5 (10-17WR)
	IV-510027R	GAGTCAAGTACCATTCAACAAG					UV
543883	IV-543676F	GTAGAAAGATGACACTGCCA	404	207+197	404	*Hpy* CH4III	5 (10-17WR)
	IV-544080R	GTCTTCGCATAGTTCCCCT					UV
611625	IV-611375F	GGACATCAGCAAAGTCAAAC	494	494	250+244	*Hpy* CH4IV	5 (10-17WR)
	IV-611869R	CCATACCATTCTTCGGATC					UV
143895	VIII-143600F	TGAGGACCCAGCACCGA	496	295+201	496	*Hind*III	5 (10-17WR)
	VIII-144096R	GGAGTCTTTGGTTTGAAGACC					UV
197728	VIII-197553F	GACCGCCCACTTCTTTC	412	175+237	412	*Nde*I	5 (10-17WR)
	VIII-197965R	CTGTACCTCTCTTGGGC					UV
901435	XVI-901137F	GCATTGACAAGGACTGGC	415	415	298+117	*Ssp*I	5 (10-14WR)
	XVI-901552R	GACCAAATGGTATAGCTGG					UV
918448	XVI-918233F	GAGGTCTTTGGATCAACCG	440	215+225	440	*Eco*RV	5 (10-14WR)
	XVI-918673R	CGAGGAAGGGATACACA					UV
644833	XII-644574F	GACTGGGTAACGACCTGGTG	475	475	259+216	*Xho*I	5 (9-12WR)
	XII-645049R	CGGCCGAAAGAACAATCCTC					UV
694318	XII-694140F	GAGGTCGATTTACCACTGA	423	178+245	423	*Hha*I	5 (9-12WR)
	XII-694563R	GGACATTGGACCATGTTTGAA					UV
122948	XVI-122659F	CGGCGAACGATTTATTGGAAC	574	289+285	574	*Dra*I	5 (9-12WR)
	XVI-123233R	GTCCTTGAGGTGATCAAGTAAG					UV
126095	XVI-125869F	CCGGGTAAGAGGTTGTACTAG	479	479	226+253	*Bsr*I	5 (9-12WR)

	XVI-126348R	GACCATACTCGG CTGAAGCG					UV

The primers listed in this table were used to diagnose loss of heterozygosity for SNPs in several different ways. The purposes for each analysis (column H) were: Purpose 1: separating granddaughter cells with a crossover on the left arm of chromosome V. Note that most of the SNPs used for this purpose are also listed in Table S2 of Lee *et al.* (2009). Purpose 2: primers used for DNA sequencing to detect granddaughter cells in strains with a crossover on the left arm of chromosome V; the strain analyzed is shown in parentheses. Purpose 3: primers used to detect granddaughter cells in strains with a crossover the right arm of chromosome IV near HS4. Purpose 4: primers used to detect granddaughter cells based on unselected events (strains examined shown in parantheses). Purpose 5: primers used to detect segregation of markers in meiotic products (strains targeted shown in parantheses).

Table S6. Numbers of SCB and DSCBs induced by UV in G1-synchronized *mlh1* strains				
	# selected SCB	# selected DSCB	# unselected SCB	# unselected DSCB
WT	5	12	76	106
mlh1	2	5	37	33

Table S7. Median lengths of conversion or heteroduplex tracts for UV-induced mitotic recombination events.							
Genotype	Treatment	Length of NCO tracts in kb (95% CI)	Length of CO tracts in kb (95% CI)	Length of all tracts in kb (95% CI)	# NCO	# CO	Total #
WT	15 J/m^2	5.7 (4.5-6.6)	8.2 (6.6-10.3)	6.4 (5.8-7.3)	141	68	209
mlh1	15 J/m^2	5.4 (3.6-7.2)	10 (5.7-17)	6.1 (4.8-8.5)	65	13	78
WT	spontaneous, HS4	NA	49.5 (35.8-118.3)	NA	NA	9	NA
mlh1	spontaneous, HS4	NA	40 (26.2-87.6)	NA	NA	5	NA
WT	spontaneous, ch5	NA	6.1 (1.7-25.5)	NA	NA	13	NA
mlh1	spontaneous, ch5	NA	11.6 (6.1-28.2)	NA	NA	5	NA

Table S8. Numbers of unselected UV-induced events for each class in the wild-type and *mlh1* strains.					
	# Interstitial LOH events (ave. #/pair of sectors)	# Crossovers (ave. #/pair of sectors)	# BIR events (ave. #/pair of sectors)	Total LOH events (ave. #/pair of sectors)	# Sectors analyzed
WT	141 (7.1)	50 (2.5)	10 (0.5)	201 (10.1)	20
mlh1	65 (9.1)	6 (0.9)	0 (0)	71 (10.1)	7

Table S9. Median lengths of conversion or heteroduplex tracts for UV-induced and spontaneous mitotic recombination events at individual break level.

Class	Type of tract	Length of tracts in kb (95% CI)	# analyzed
Class 1	UV, simple het	4.8 (2.4-5.7)	26
Class 2	UV, conversion	2.2 (1.5-4.8)	18
Class 3 and 5	UV, conversion + simple het	6.2 (2.3-10.5)	16
Class 1-3, 5, 8, complex	UV, all NCO breaks	4.9 (3.5-5.7)	86
Class 4, 6, 7, complex	UV, all CO breaks	7.2 (5.1-10.0)	20
DSCB-NCO	UV, the break repaired as NCO in DSCB event that contains one NCO tract and one CO tract	8.2 (4.8-11.7)	14
DSCB-CO	UV, the break repaired as CO in DSCB event that contains one NCO tract and one CO tract	6.7 (1.6-10.0)	14
NCO w/o CO association	UV, all NCO breaks except those co-occurred with a CO in the 14 DSCB events in row 11 and 12	4.4 (3.1-5.4)	72
DSCB-NCO	Spontaneous HS4, the break repaired as NCO in DSCB event that contains one NCO tract and one CO tract	32.1 (14.2-87.6)	5
DSCB-CO	Spontaneous HS4, the break repaired as CO in DSCB event that contains one NCO tract and one CO tract	30.2 (26.3-70.2)	5
DSCB-NCO	Spontaneous non-HS4, the break repaired as NCO in DSCB event that contains one NCO tract and one CO tract	4.8 (1.9-17.5)	5
DSCB-CO	Spontaneous non-HS4, the break repaired as CO in DSCB event that contains one NCO tract and one CO tract	6.9 (6.1-26.7)	5

Fig.S1

A. Class 1, NCO

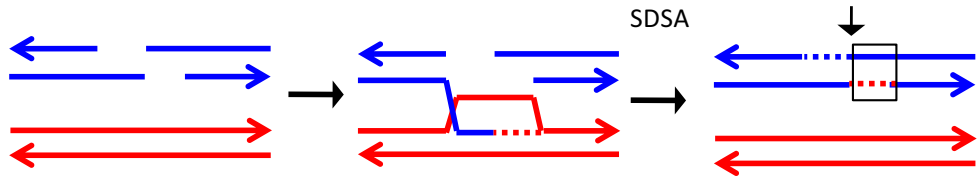

B. Class 2, NCO, mechanism 1

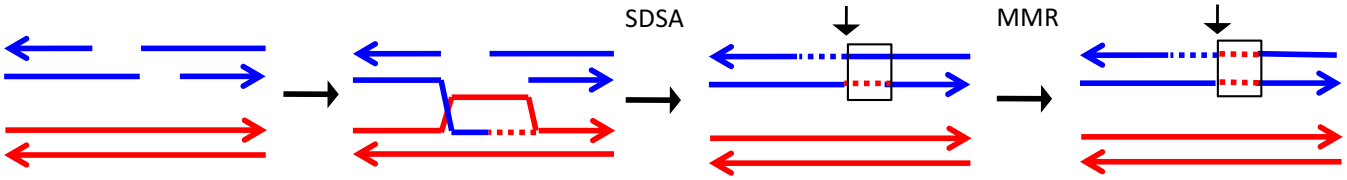

C. Class 2, NCO, mechanism 2

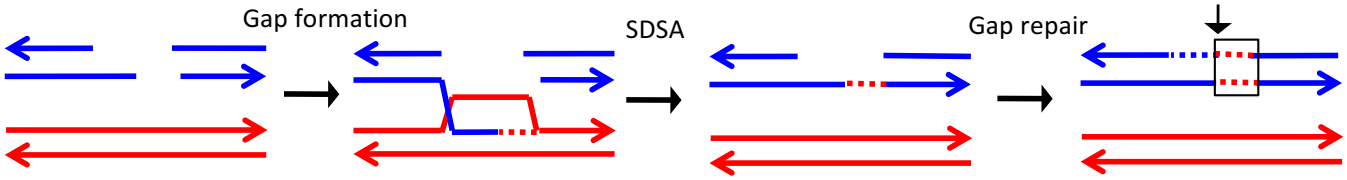

D. Class 3, NCO, mechanism 1

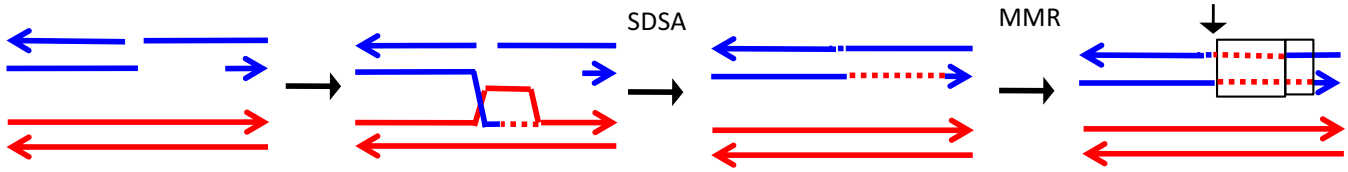

E. Class 3, NCO, mechanism 2

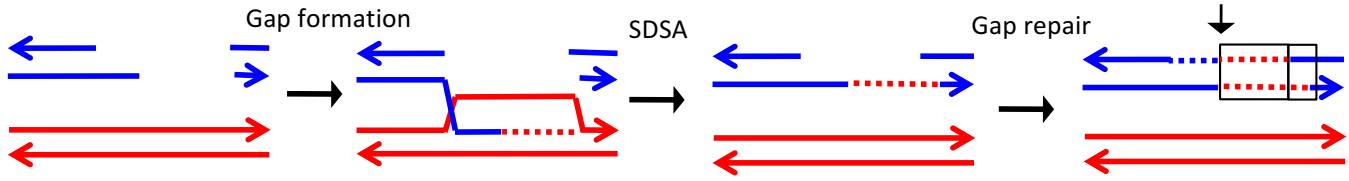

F. Class 4, CO

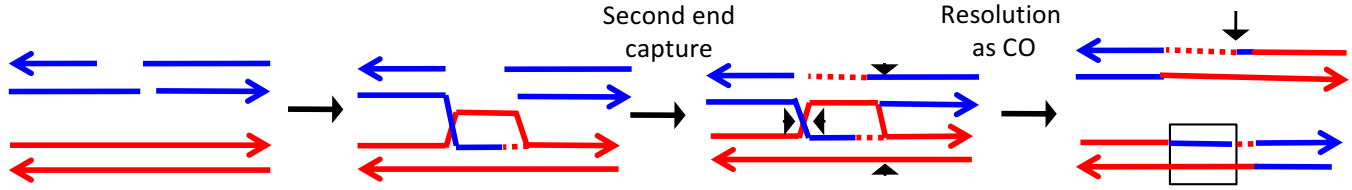

Fig.S2

A. Class 5, NCO

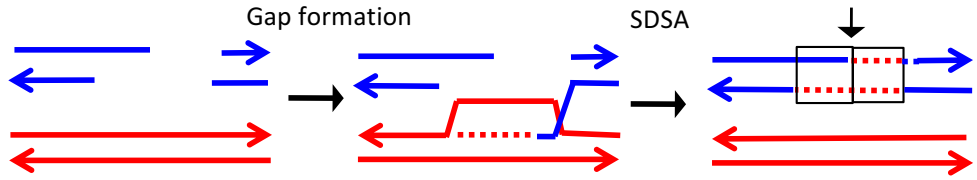

B. Class 6, CO

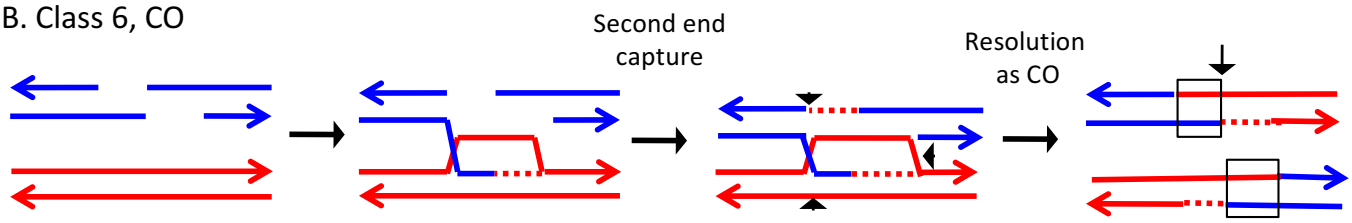

C. Class 7, CO

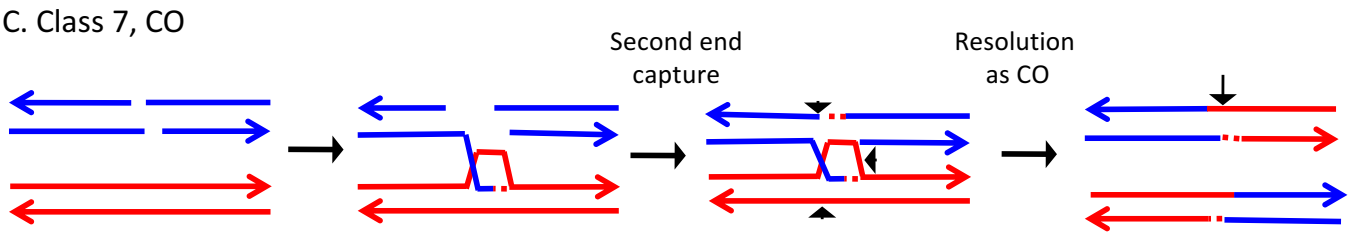

D. Class 8, NCO, mechanism 1

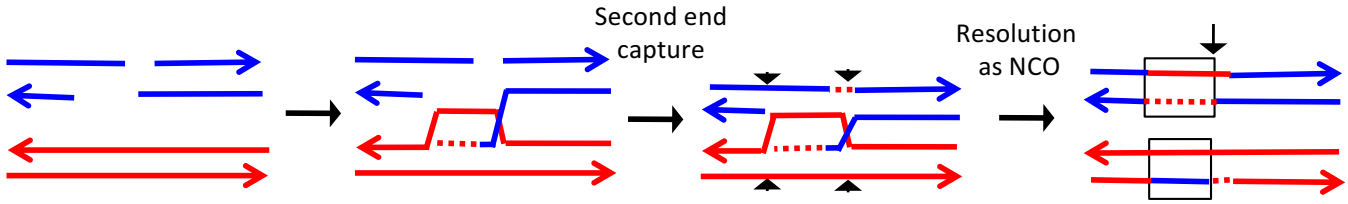

E. Class 8, NCO, mechanism 2

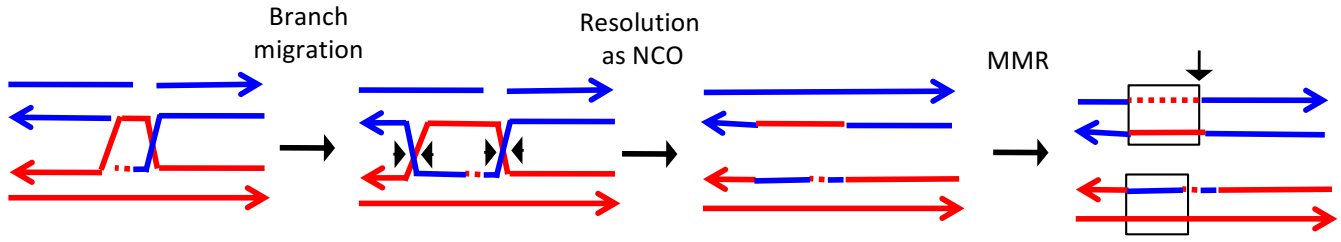

Fig.S3

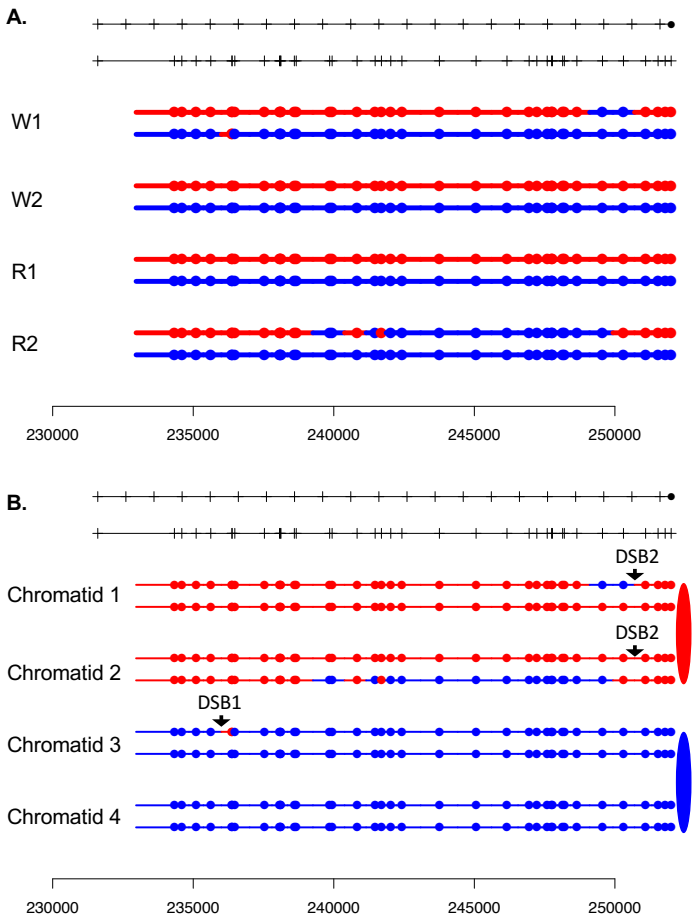

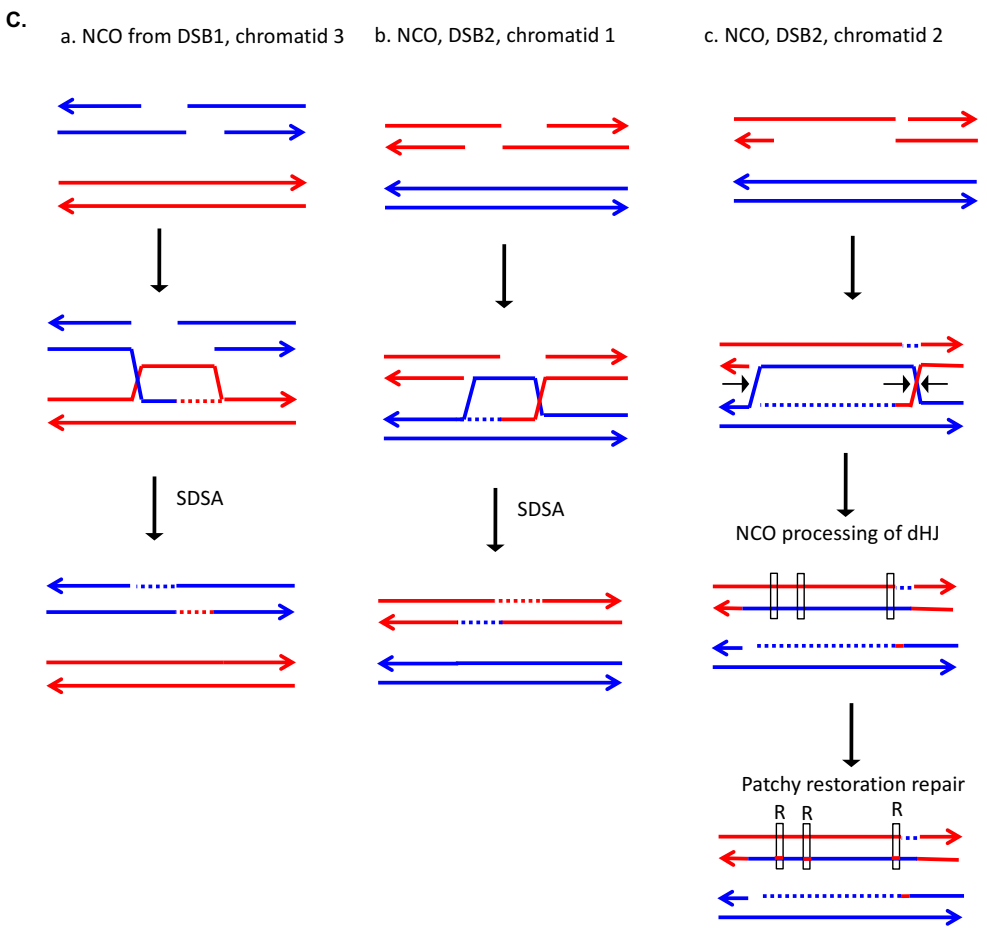

S3	NCO1	Simple heteroduplex. DSB on blue chromatid.	SDSA
	NCO2	Simple heteroduplex. DSB on red chromatid.	SDSA
	NCO3	Long heteroduplex with regions of homoduplex. DSB on red chromatid.	Standard DSBR event except Mlh1-independent MMR. Two independent DSBs.

Fig.S4

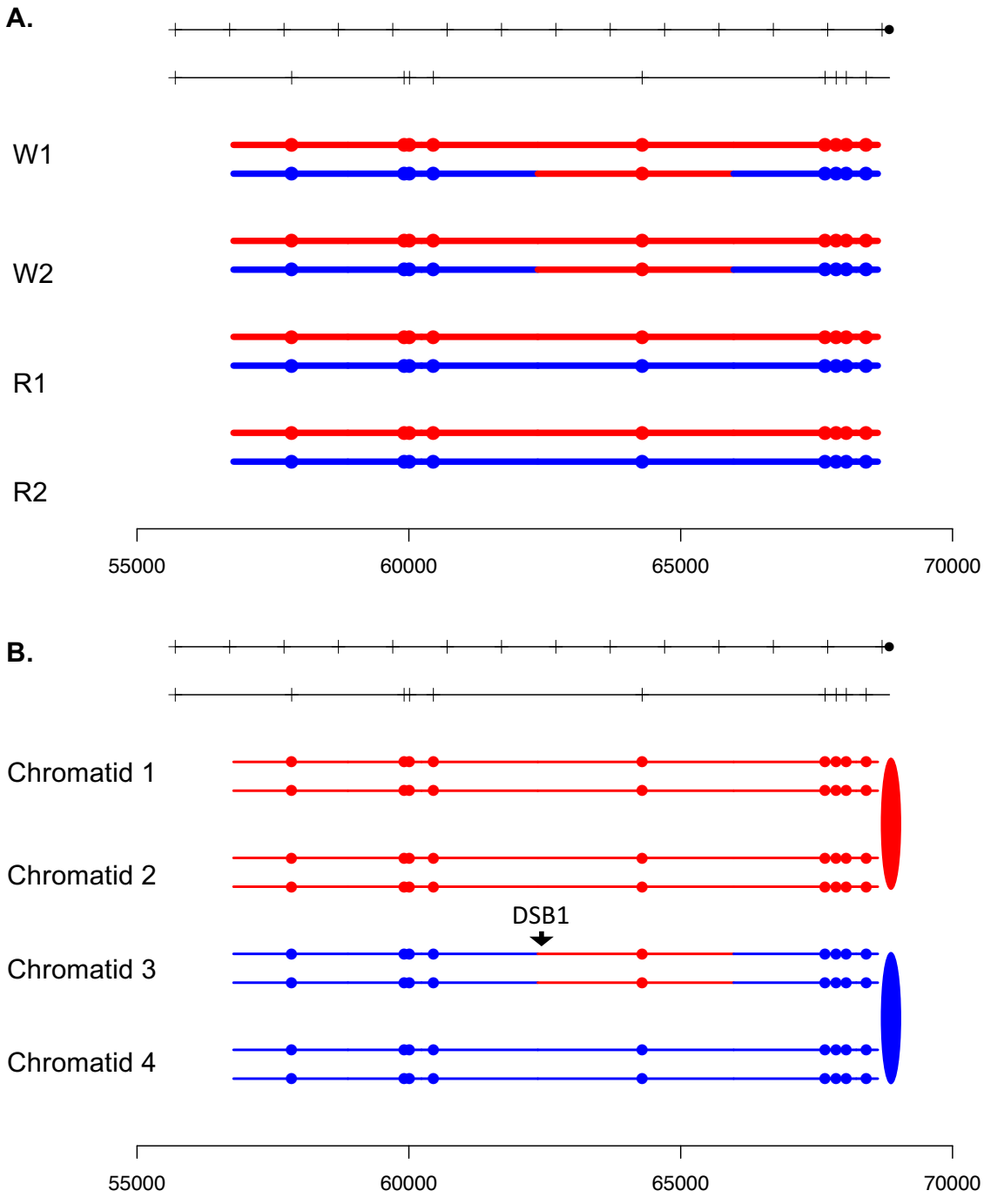
A.
W1
W2
R1
R2
55000
60000
65000
70000
B.
Chromatid 1
Chromatid 2
DSB1
Chromatid 3
Chromatid 4
55000
60000
65000
70000

Fig.S5

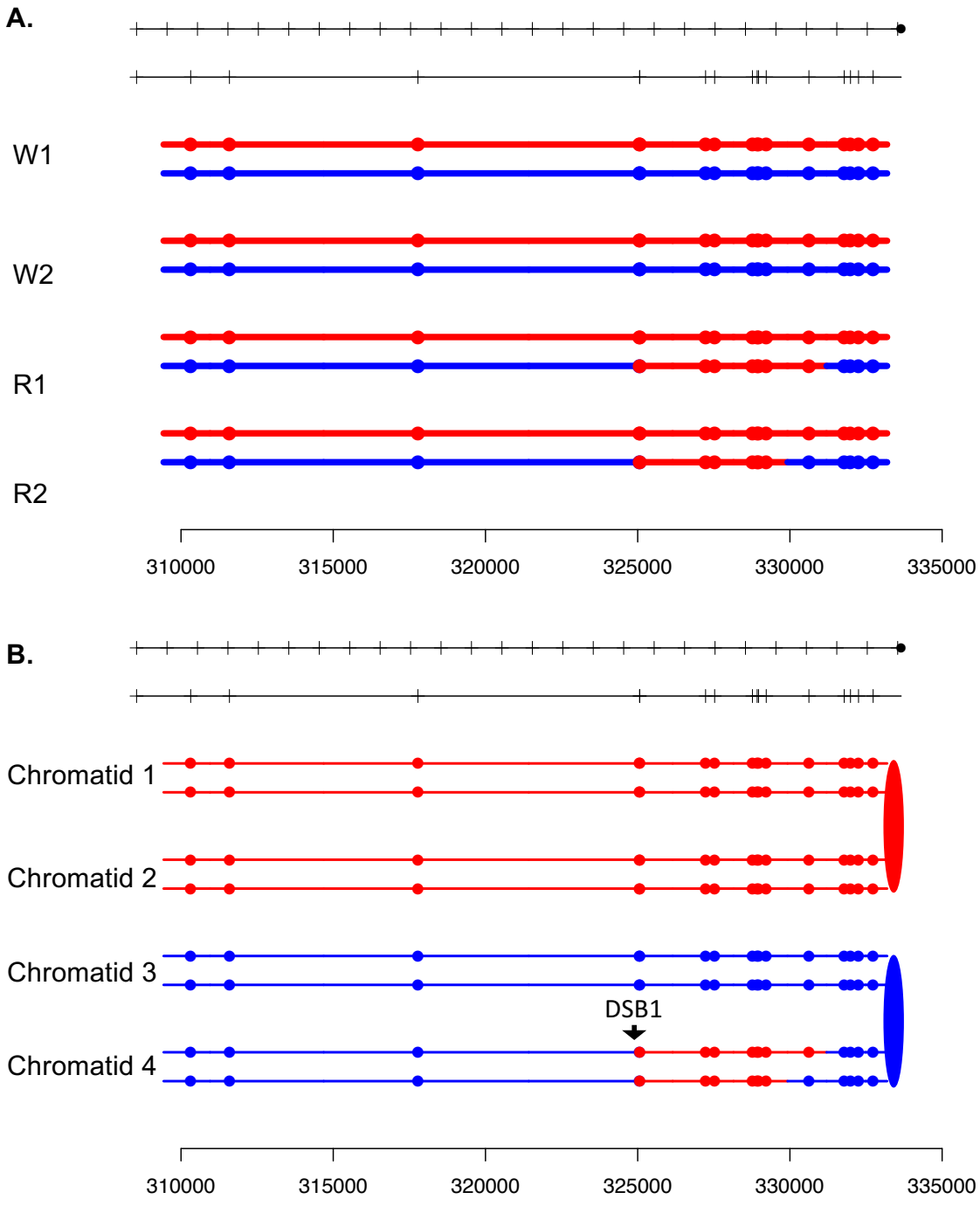
A.
W1
W2
R1
R2
310000
315000
320000
325000
330000
335000
B.
Chromatid 1
Chromatid 2
Chromatid 3
Chromatid 4
DSB1
310000
315000
320000
325000
330000
335000

Fig.S6

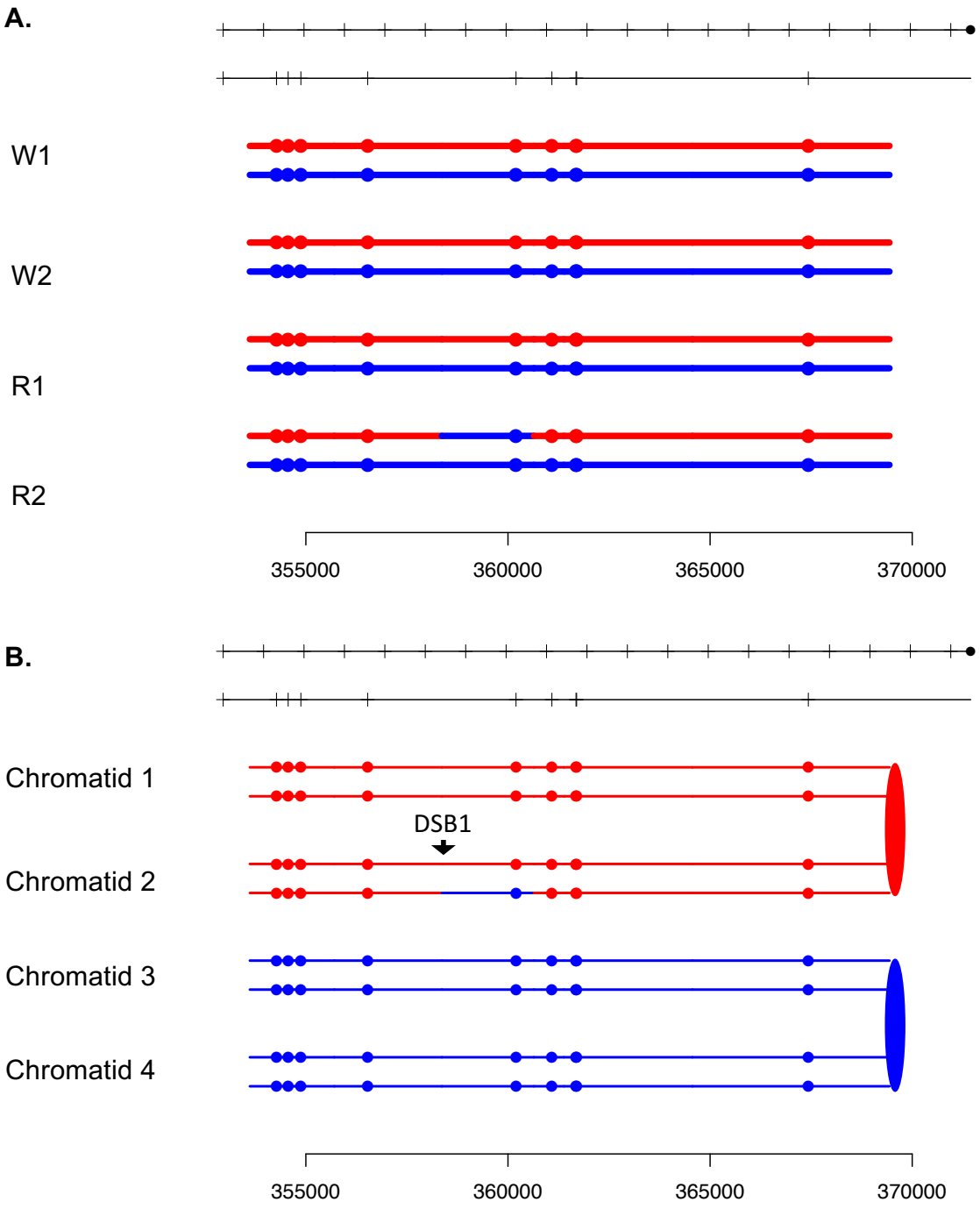
A.
W1
W2
R1
R2
355000
360000
365000
370000
B.
Chromatid 1
DSB1
Chromatid 2
Chromatid 3
Chromatid 4
355000
360000
365000
370000

Fig.S7

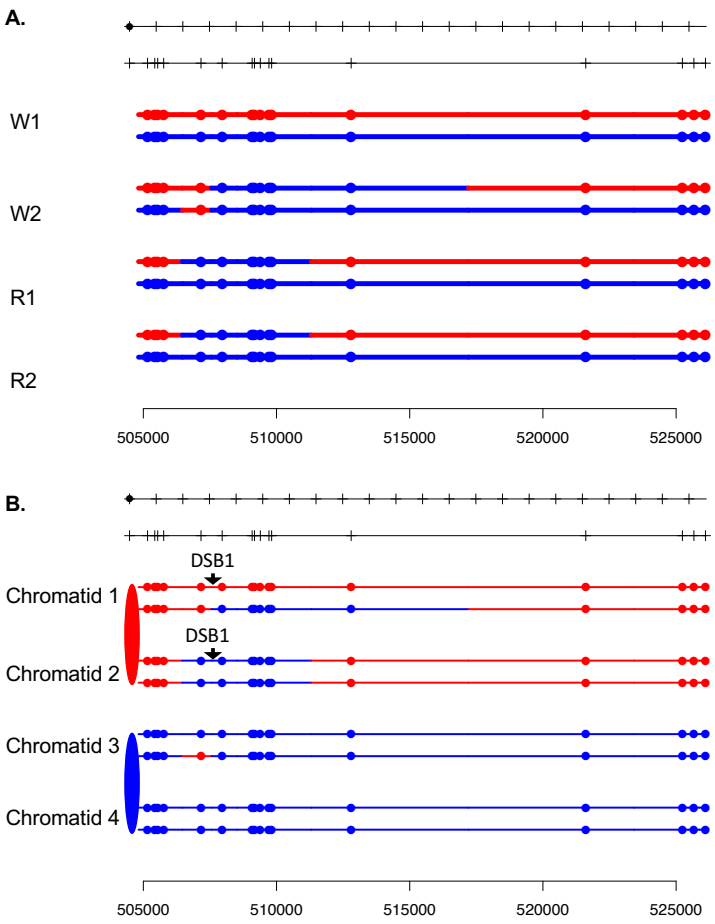

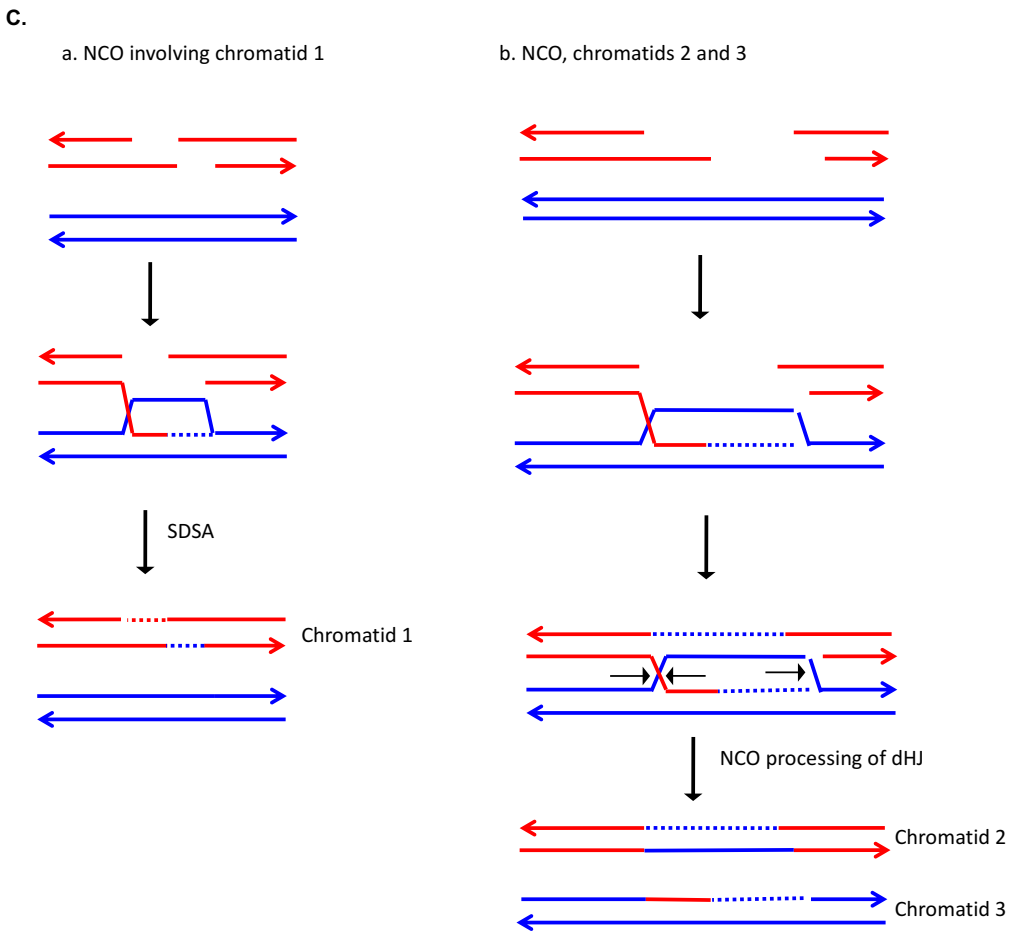

S7	NCO1	Simple heteroduplex on chromatid 1	SDSA
	NCO2	Large homoduplex region separating DSB site from heteroduplex tract (chromatids 2 and 3).	Repair of double-stranded DNA gap

Fig.S8

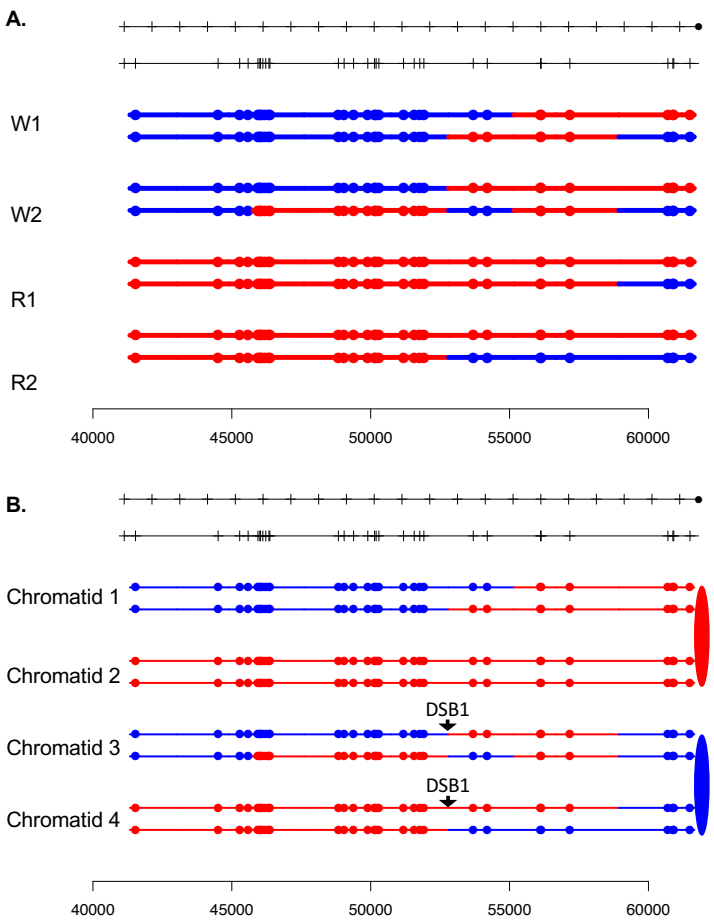

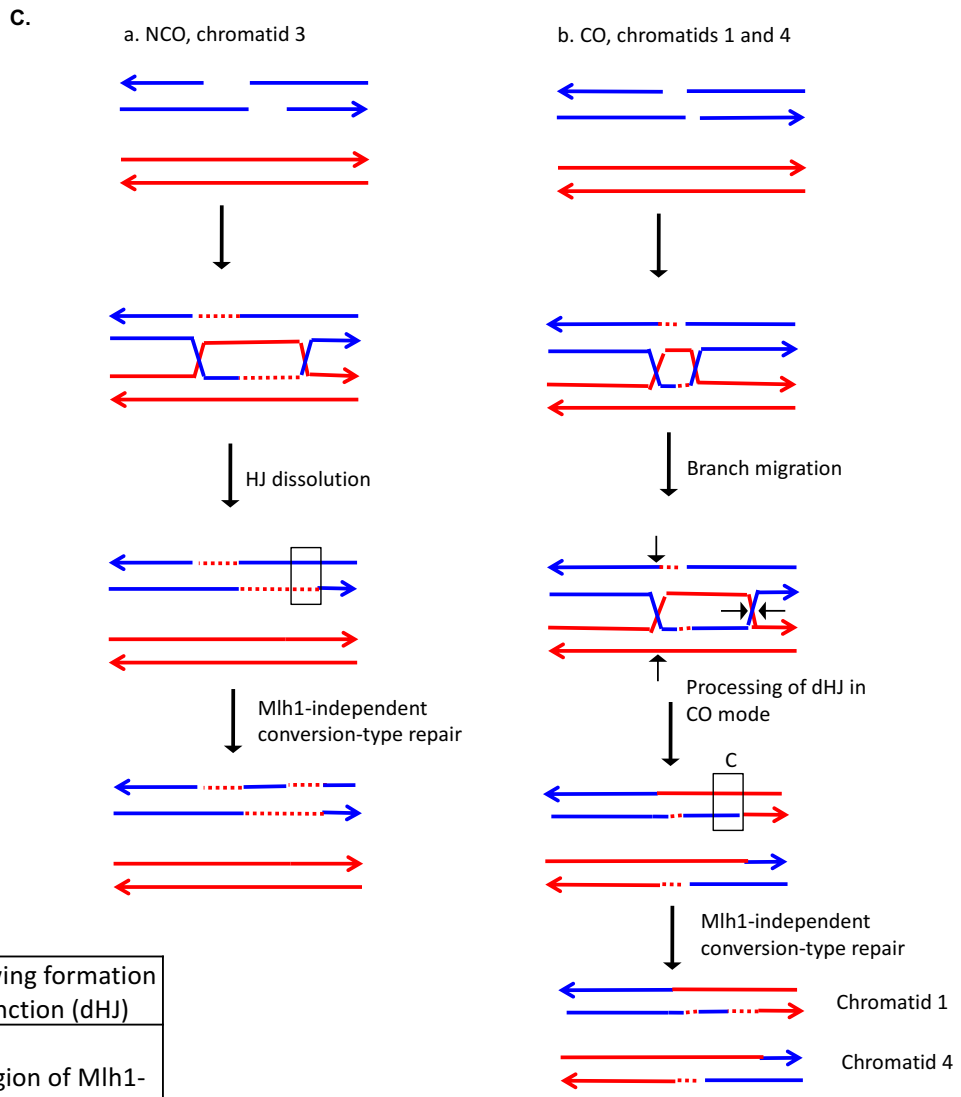

S8	CO	Symmetric heteroduplexes	Branch migration following formation of double Holliday junction (dHJ)
	NCO	Strand switches of heteroduplexes on NCO chromatid, region of conversion at junction of heteroduplex	dHJ dissolution and region of Mlh1-independent MMR

Fig.S9

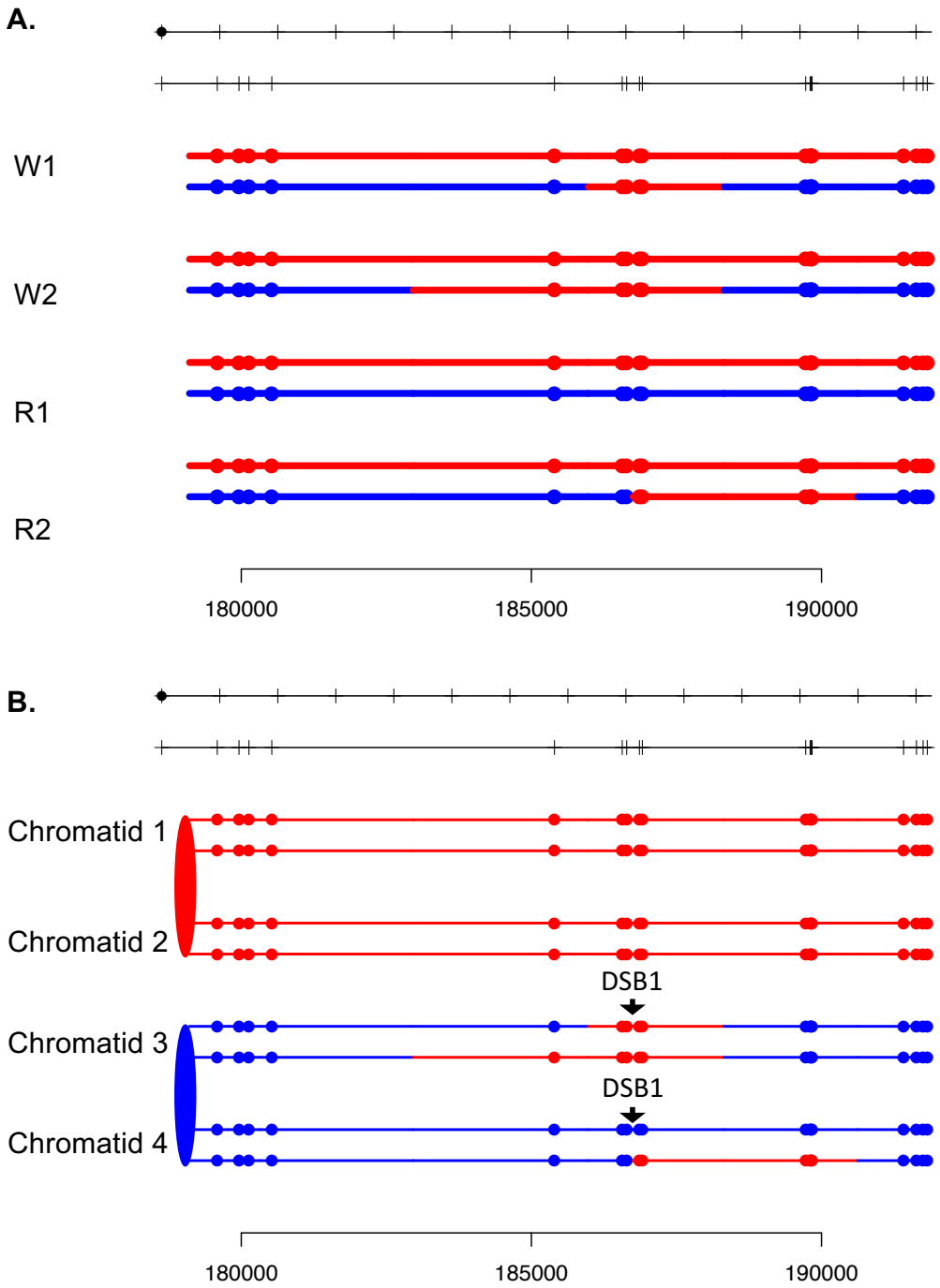
A.
W1
W2
R1
R2
180000
185000
190000
B.
Chromatid 1
Chromatid 2
DSB1
Chromatid 3
DSB1
Chromatid 4
180000
185000
190000

Fig.S10

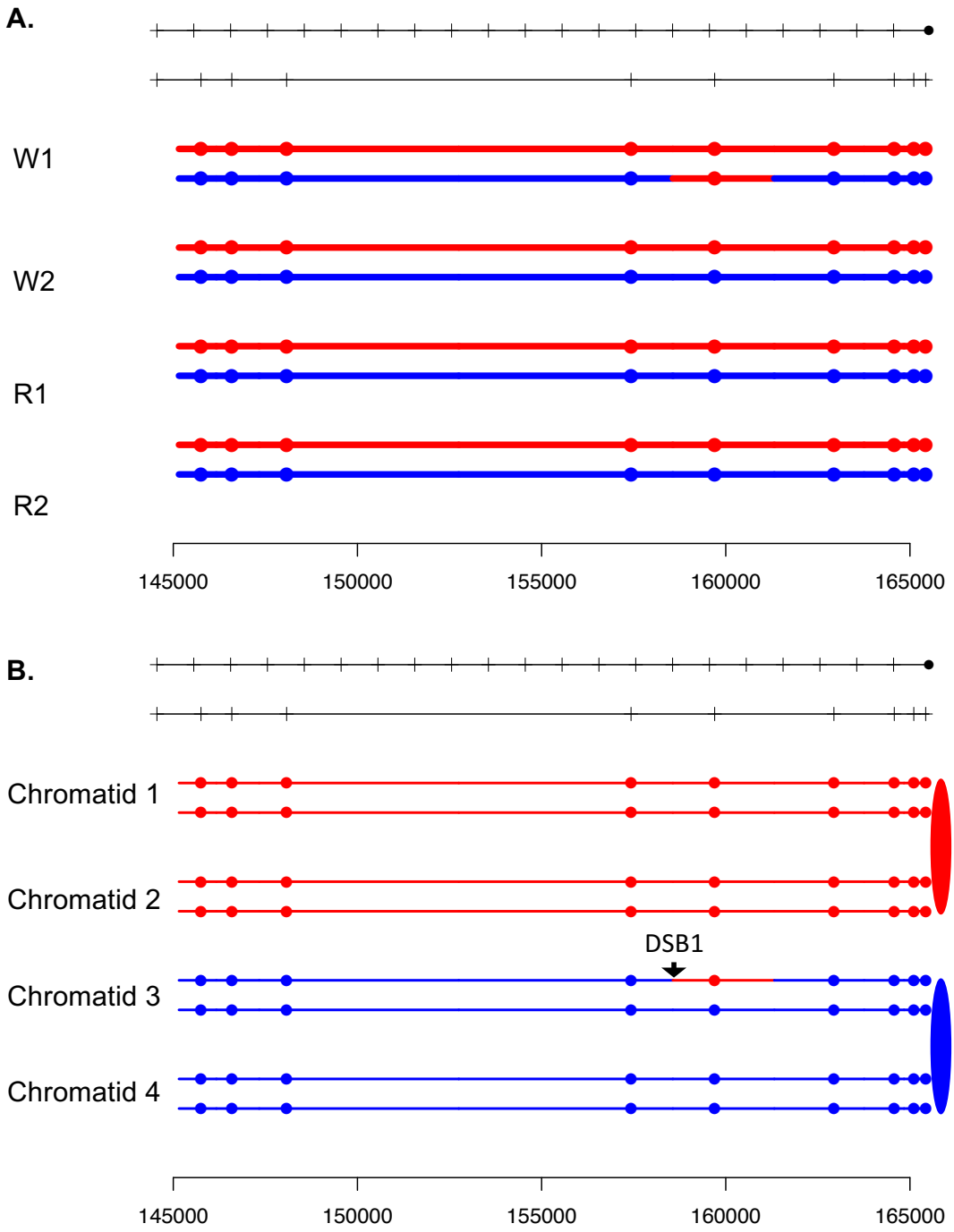
A.
W1
W2
R1
R2
145000
150000
155000
160000
165000
B.
Chromatid 1
Chromatid 2
DSB1
Chromatid 3
Chromatid 4
145000
150000
155000
160000
165000

Fig.S11

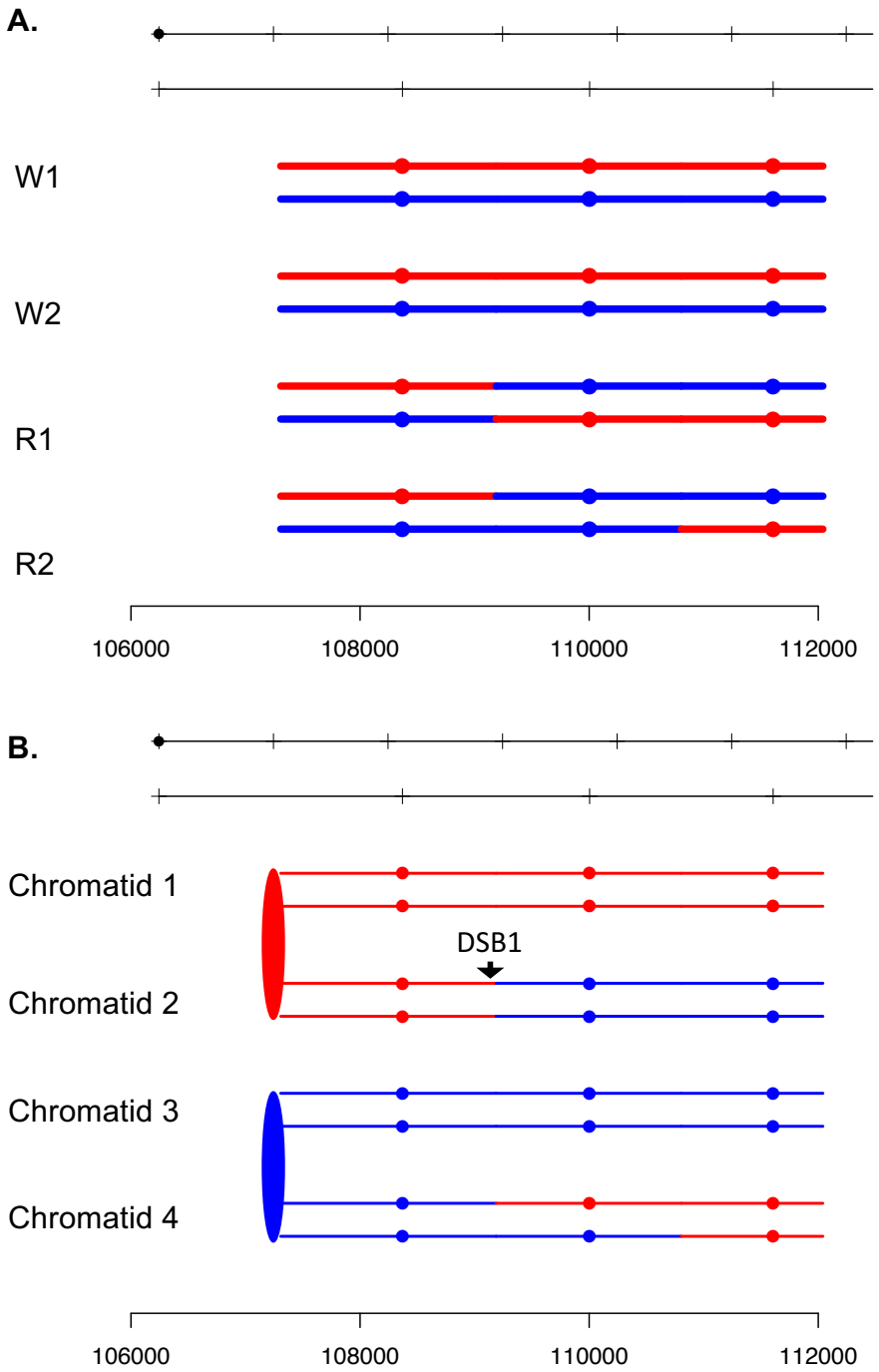
A.
W1
W2
R1
R2
106000
108000
110000
112000
B.
Chromatid 1
Chromatid 2
Chromatid 3
Chromatid 4
DSB1
106000
108000
110000
112000

Fig.S12

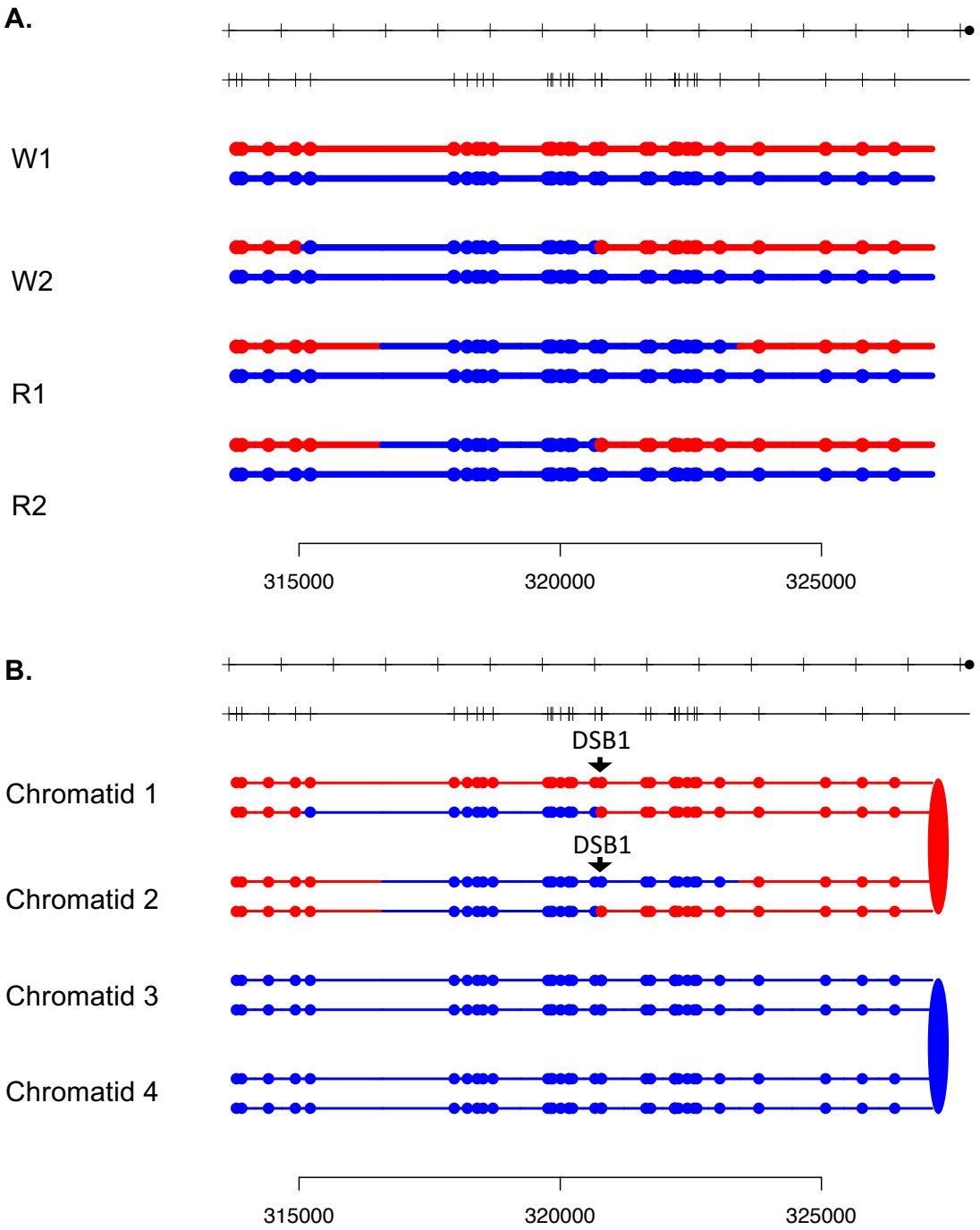
A.
W1
W2
R1
R2
315000
320000
325000
B.
DSB1
DSB1
Chromatid 1
Chromatid 2
Chromatid 3
Chromatid 4
315000
320000
325000

Fig.S13

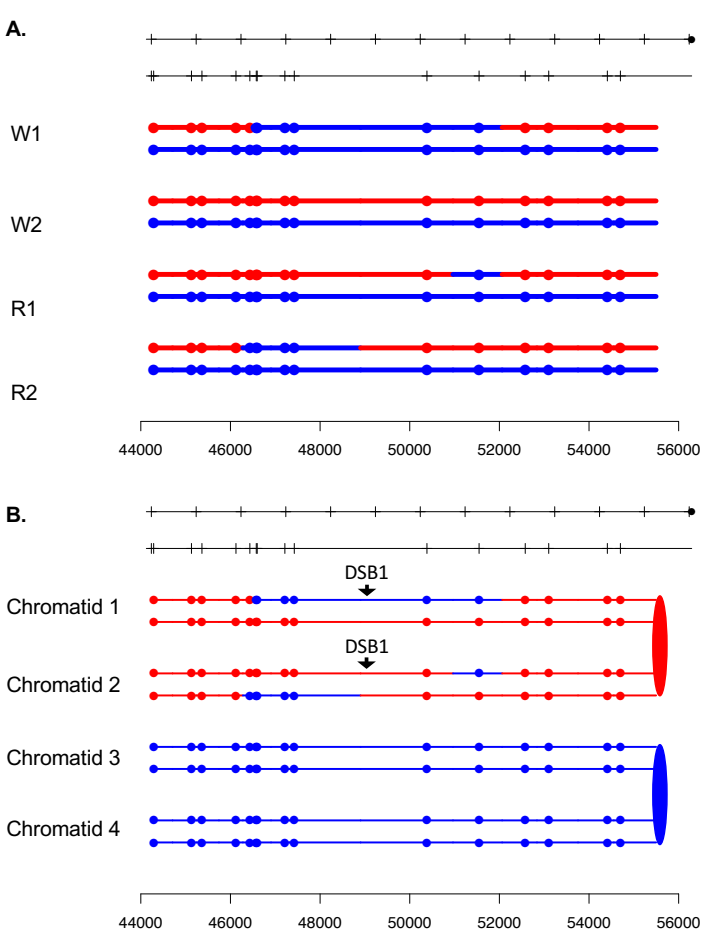

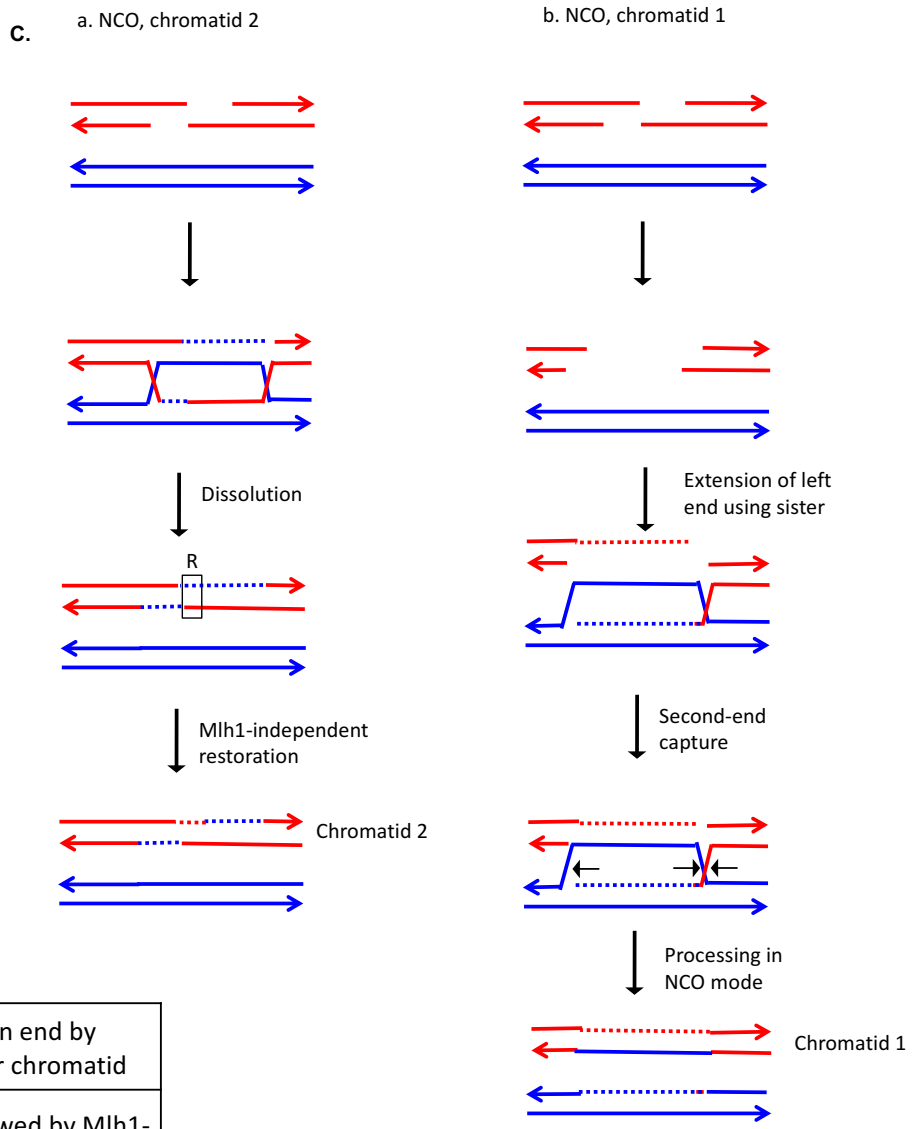

S13	NCO1	Heteroduplex spanning DSB site in chromatid 1	Extension of broken end by interaction with sister chromatid
	NCO2	Heteroduplexes in trans on chromatid 2 separated by homoduplex	Dissolution of dHJ followed by Mlh1-independent MMR

Fig.S14

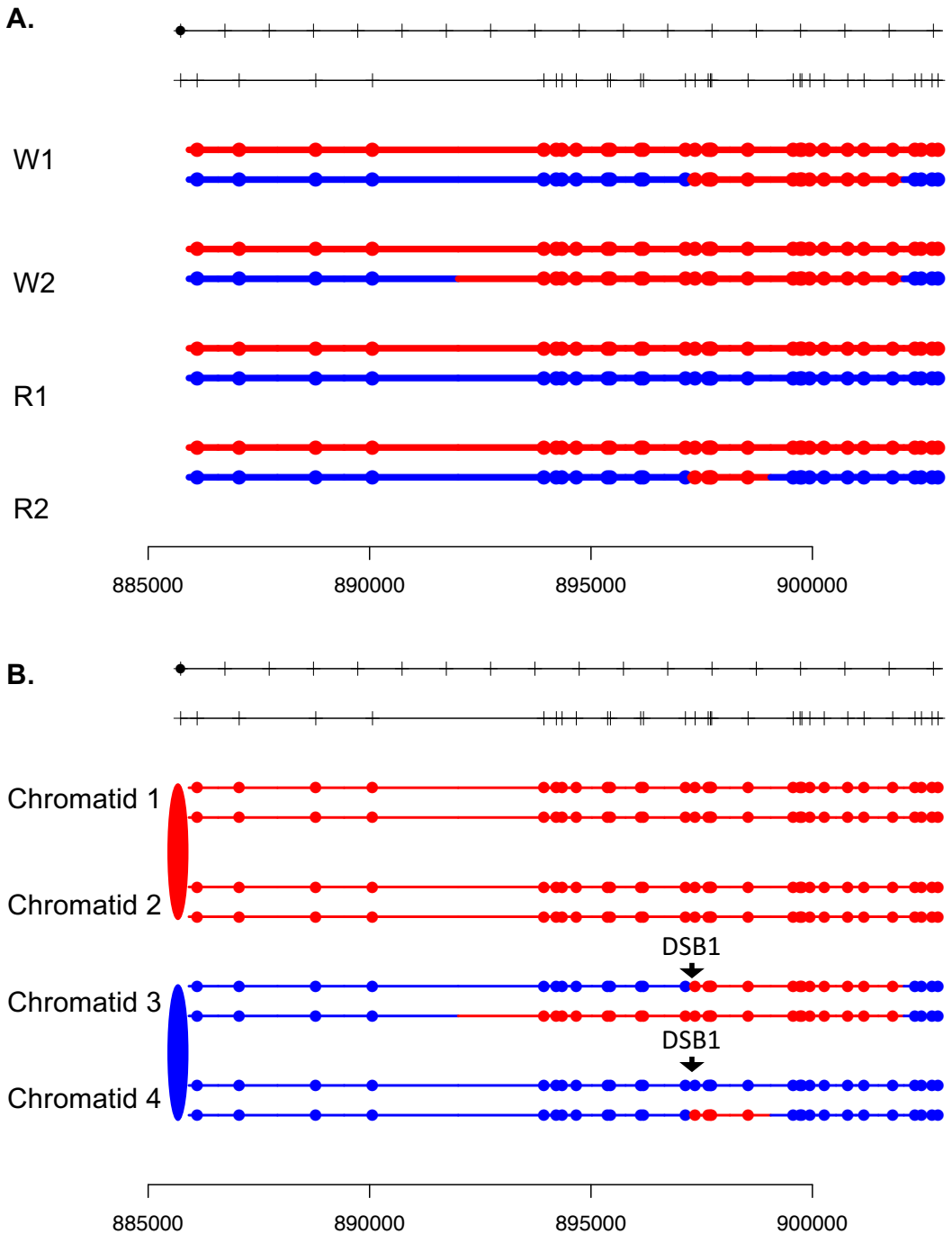
A.
W1
W2
R1
R2
885000
890000
895000
900000
B.
Chromatid 1
Chromatid 2
Chromatid 3
Chromatid 4
DSB1
DSB1
885000
890000
895000
900000

Fig.S15

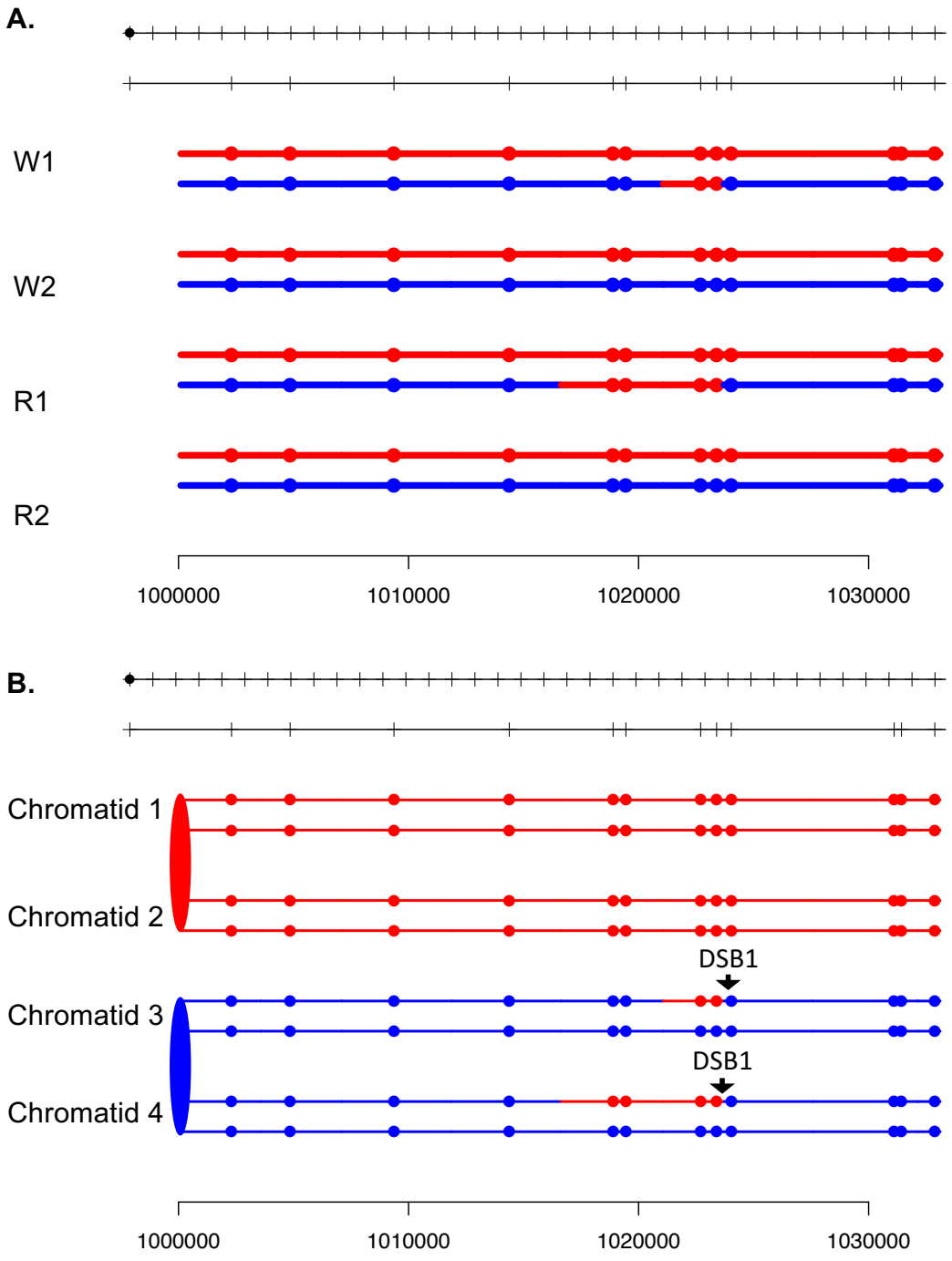
A.
W1
W2
R1
R2
1000000
1010000
1020000
1030000
B.
Chromatid 1
Chromatid 2
Chromatid 3
Chromatid 4
DSB1
DSB1
1000000
1010000
1020000
1030000

Fig.S16

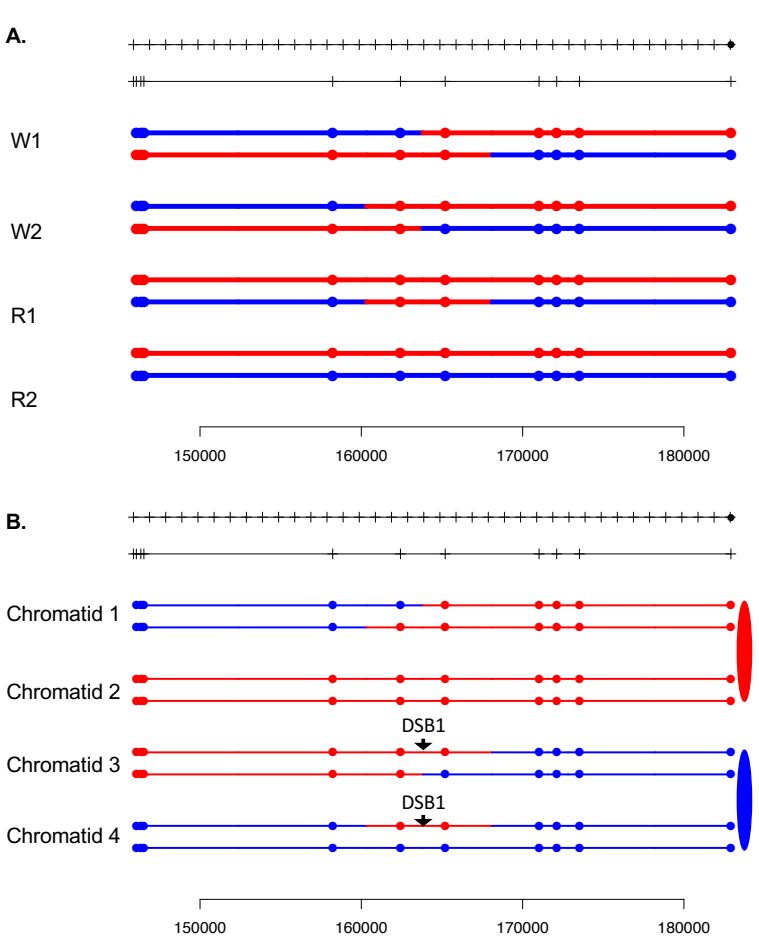

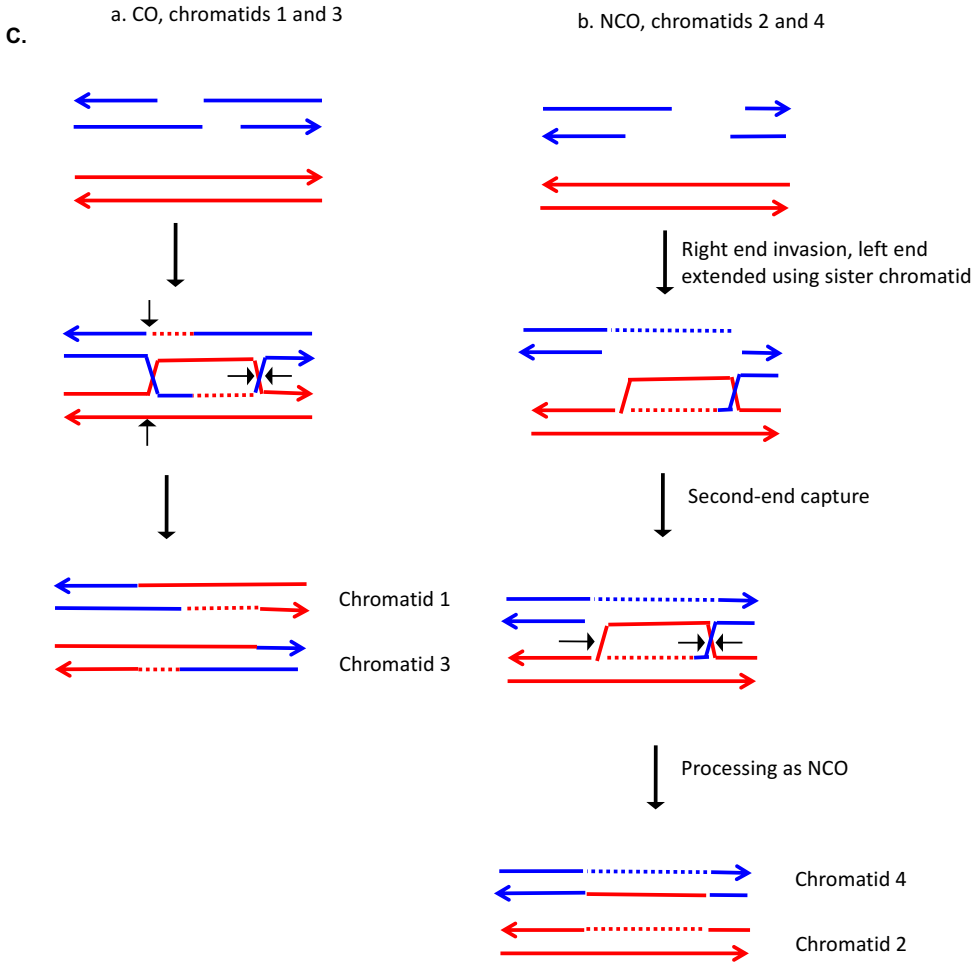

S16	CO	Heteroduplexes in *trans* flanking DSB site	Standard CO according to DSBR model
	NCO	Heteroduplex spanning DSB site on NCO chromatid 4	Extension of broken end by interaction with sister chromatid

Fig.S17

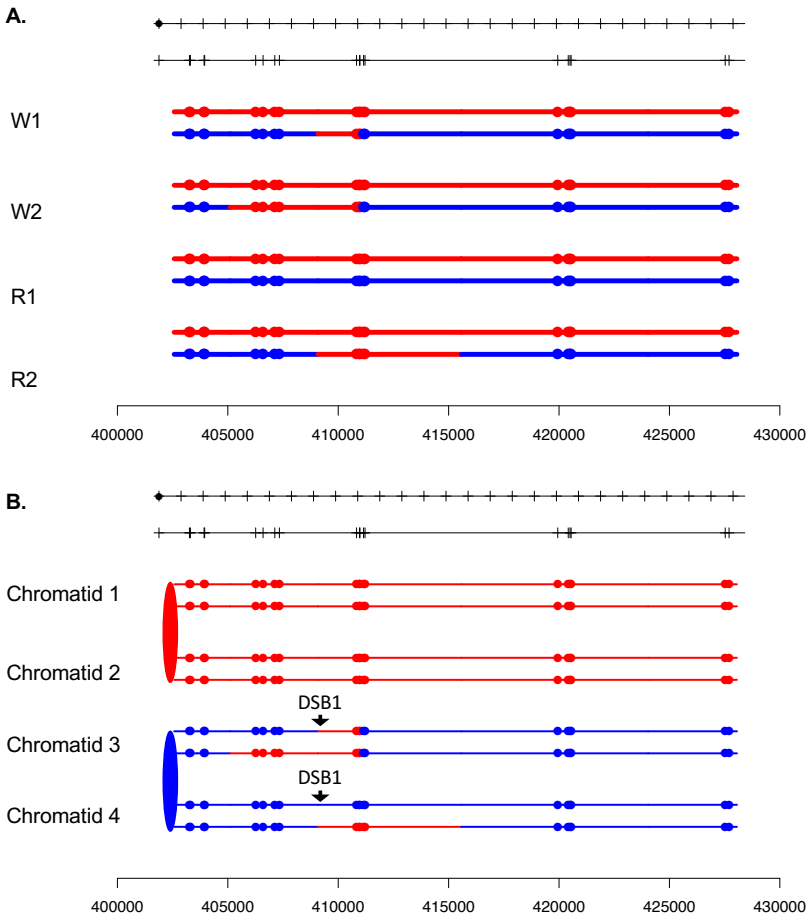

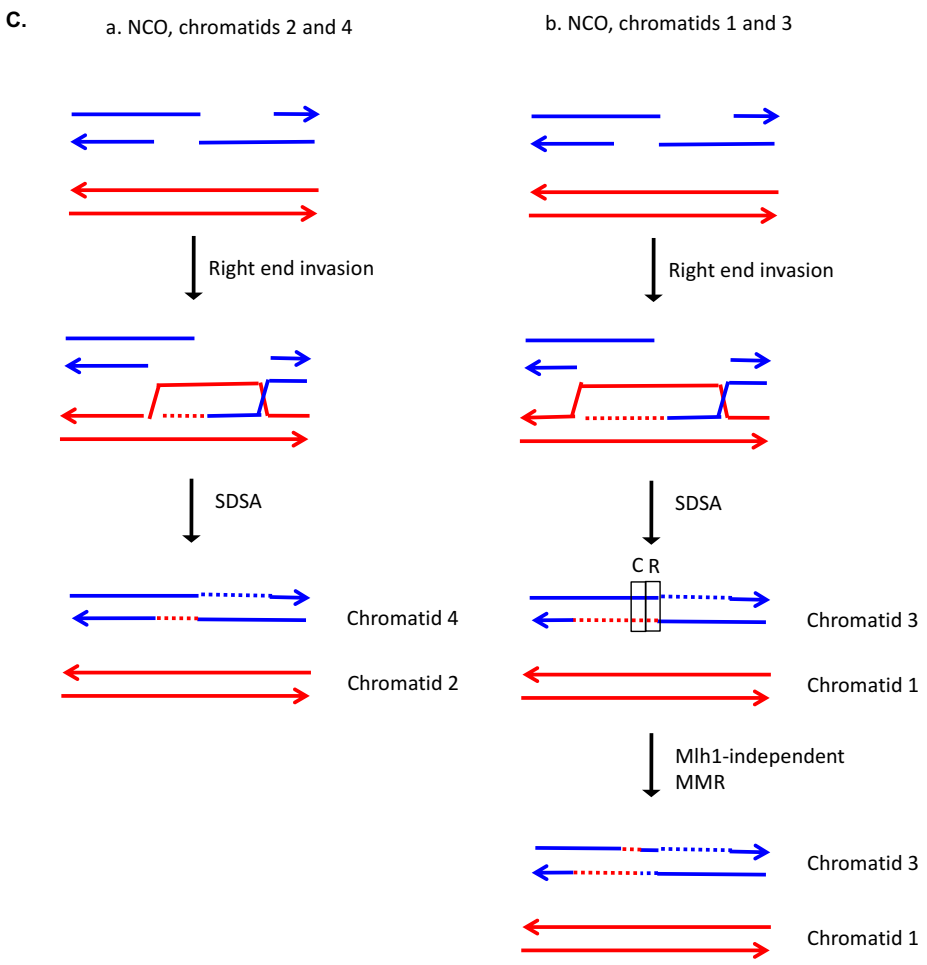

S17	NCO1	Heteroduplex with interspersed conversion and restoration tracts (chromatid 3)	SDSA with Mlh1-independent MMR
	NCO2	Simple heteroduplex (chromatid 4)	SDSA

Fig.S18

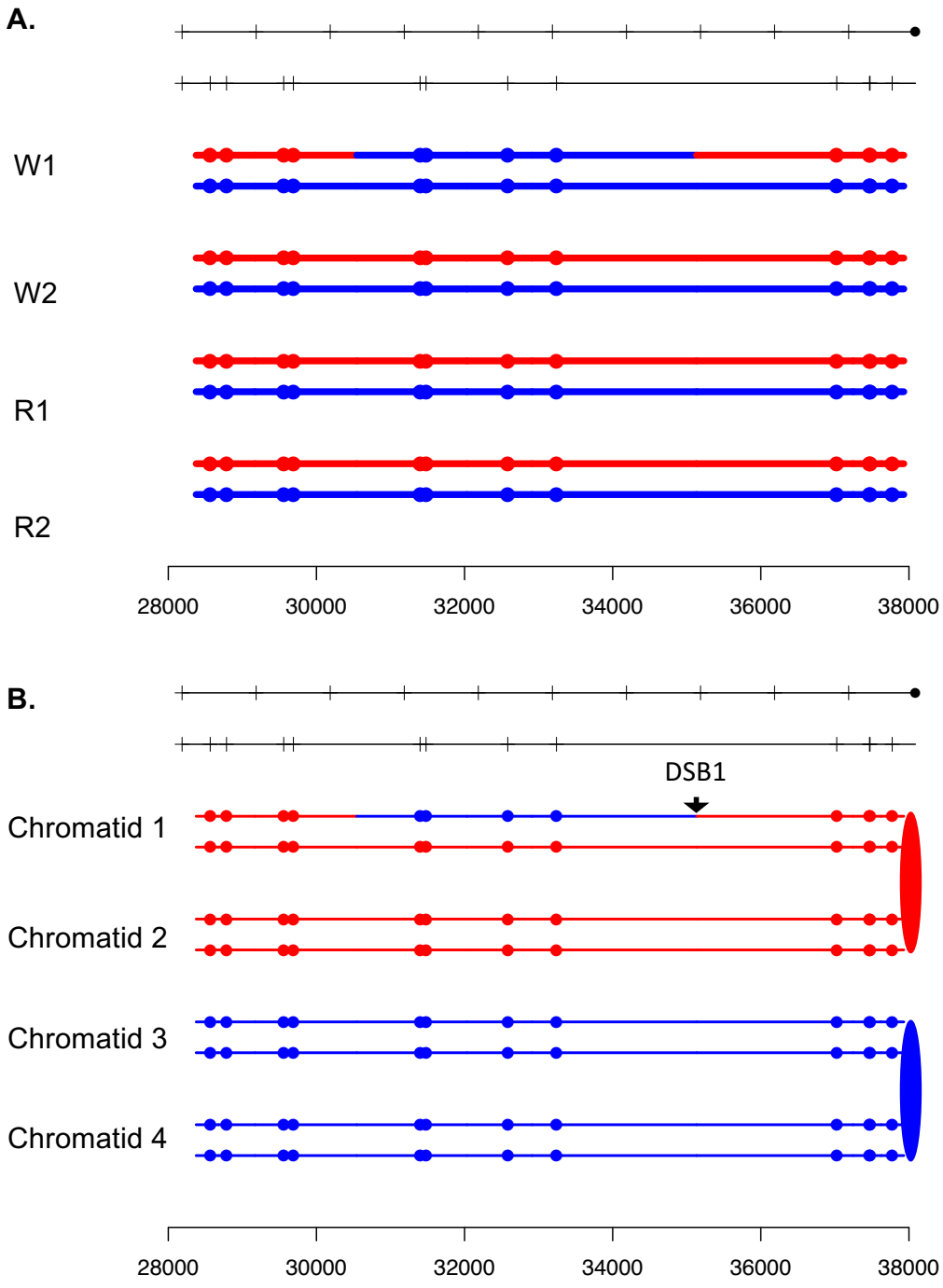
A.
W1
W2
R1
R2
28000
30000
32000
34000
36000
38000
B.
DSB1
Chromatid 1
Chromatid 2
Chromatid 3
Chromatid 4
28000
30000
32000
34000
36000
38000

Fig.S19

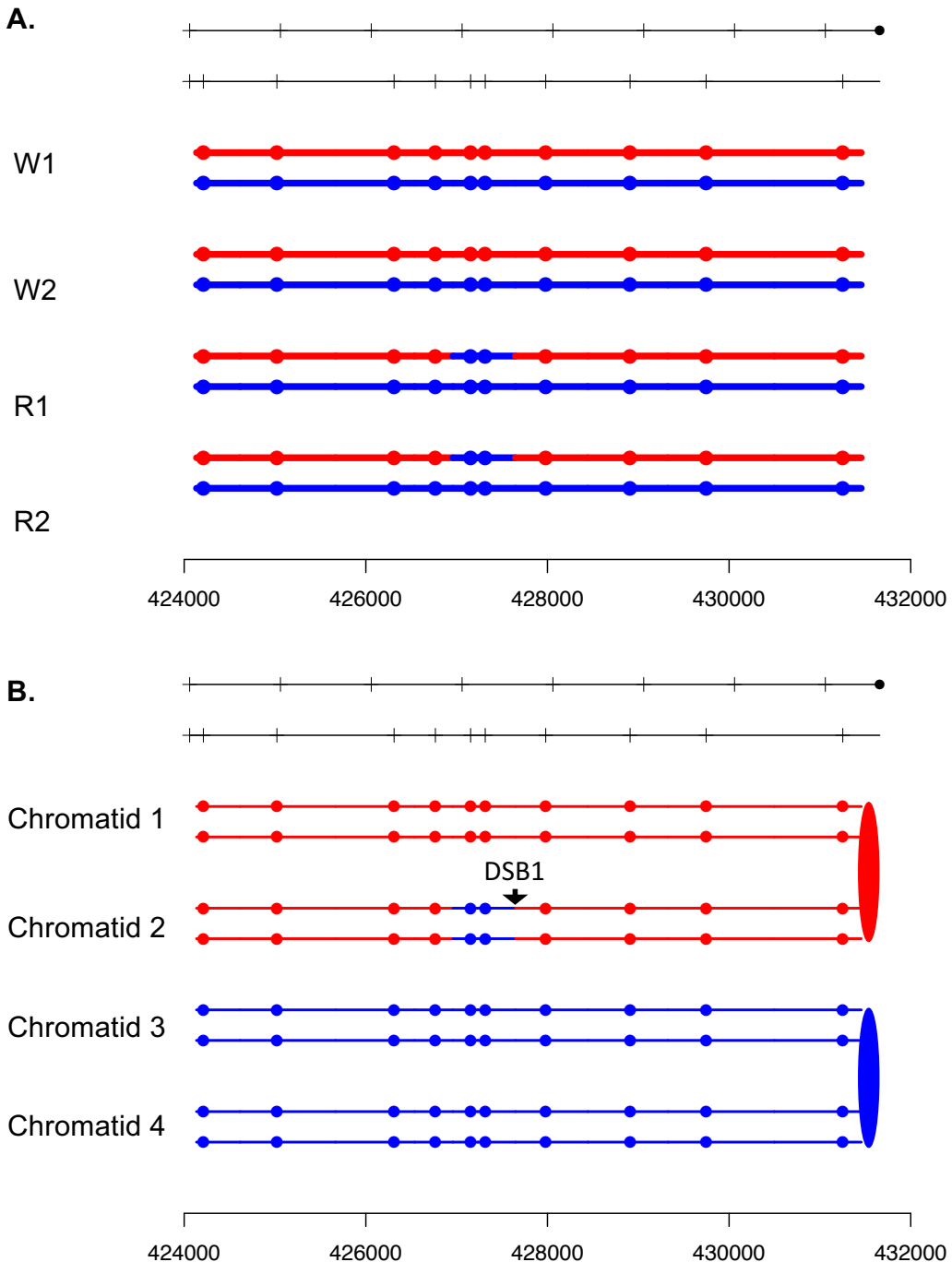
A.
W1
W2
R1
R2
424000
426000
428000
430000
432000
B.
Chromatid 1
DSB1
Chromatid 2
Chromatid 3
Chromatid 4
424000
426000
428000
430000
432000

Fig.S20

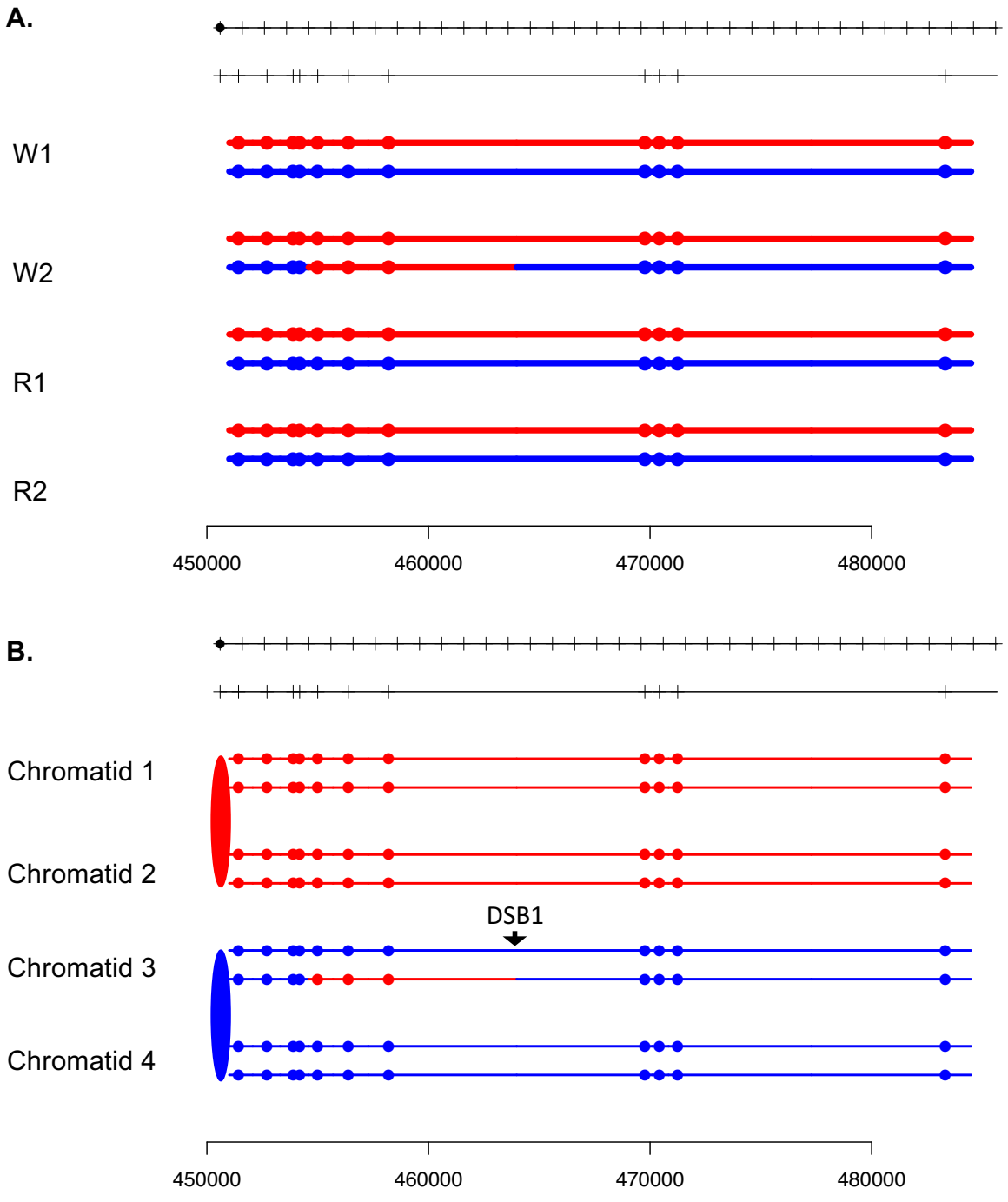
A.
W1
W2
R1
R2
450000
460000
470000
480000
B.
Chromatid 1
Chromatid 2
DSB1
Chromatid 3
Chromatid 4
450000
460000
470000
480000

Fig.S21

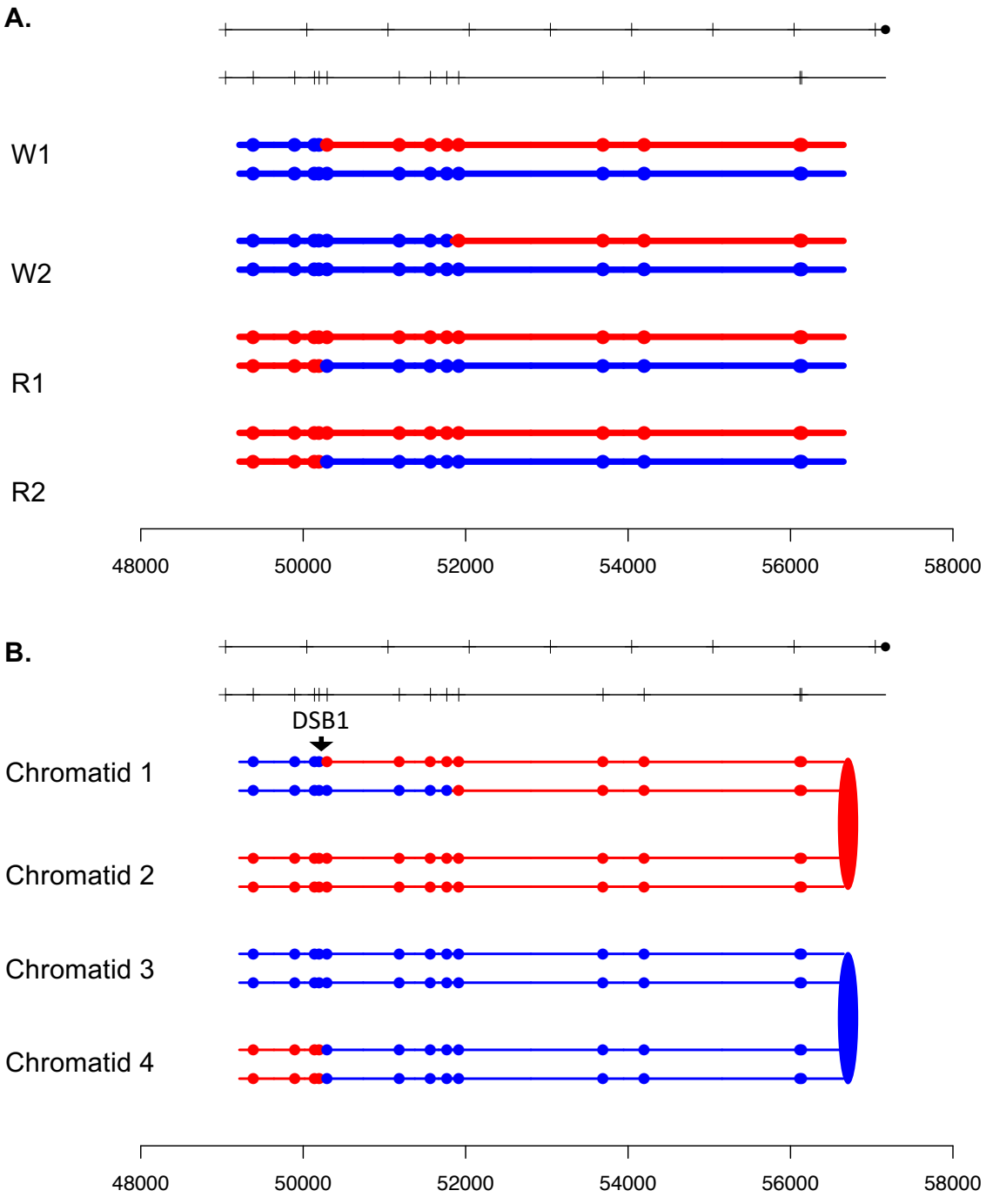
A.
W1
W2
R1
R2
48000
50000
52000
54000
56000
58000
B.
DSB1
Chromatid 1
Chromatid 2
Chromatid 3
Chromatid 4
48000
50000
52000
54000
56000
58000

Fig.S22

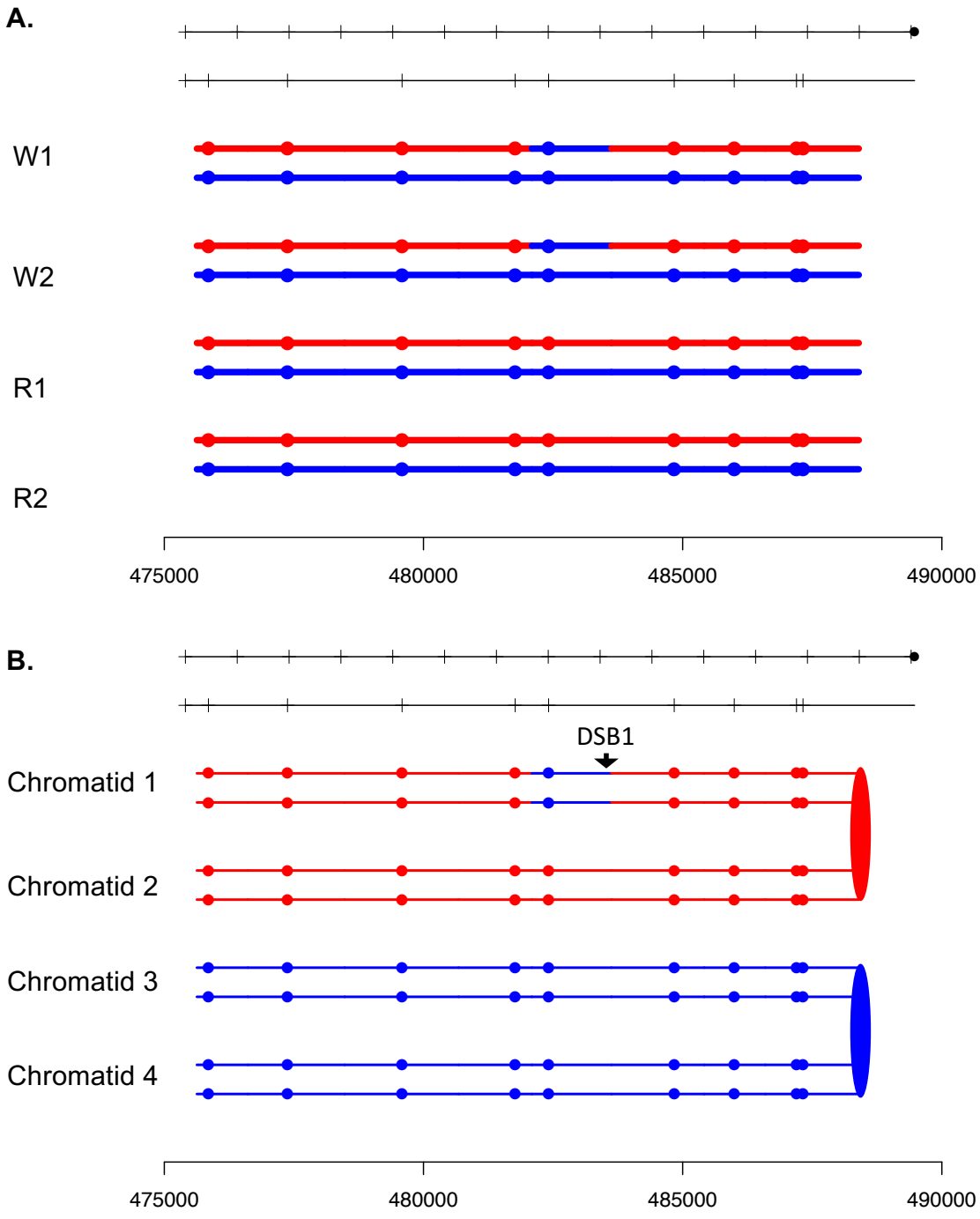
A.
W1
W2
R1
R2
475000
480000
485000
490000
B.
DSB1
Chromatid 1
Chromatid 2
Chromatid 3
Chromatid 4
475000
480000
485000
490000

Fig.S23

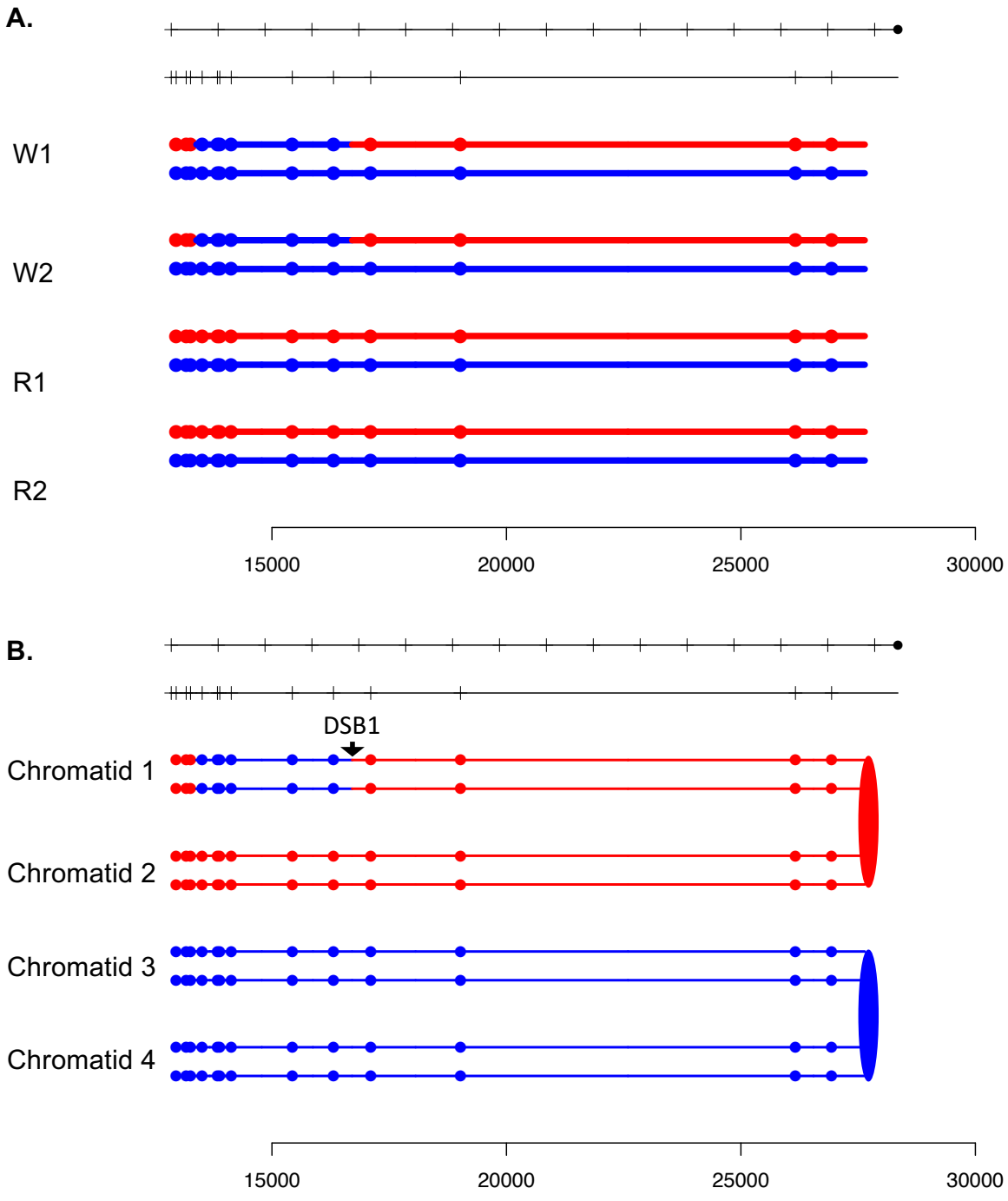
A.
W1
W2
R1
R2
15000
20000
25000
30000
B.
DSB1
Chromatid 1
Chromatid 2
Chromatid 3
Chromatid 4
15000
20000
25000
30000

Fig.S24

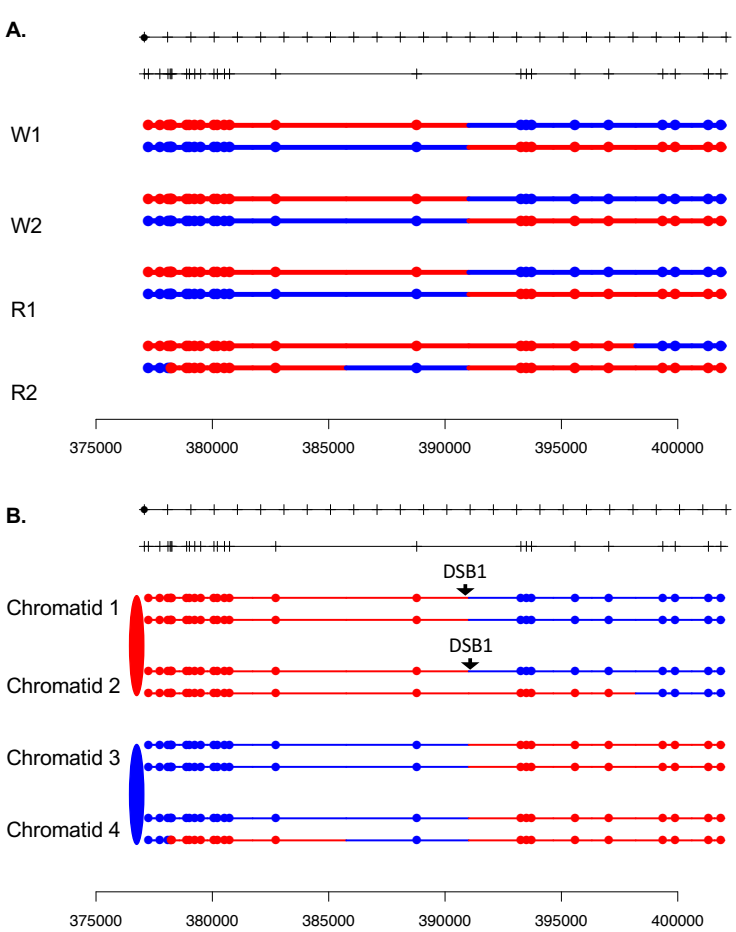

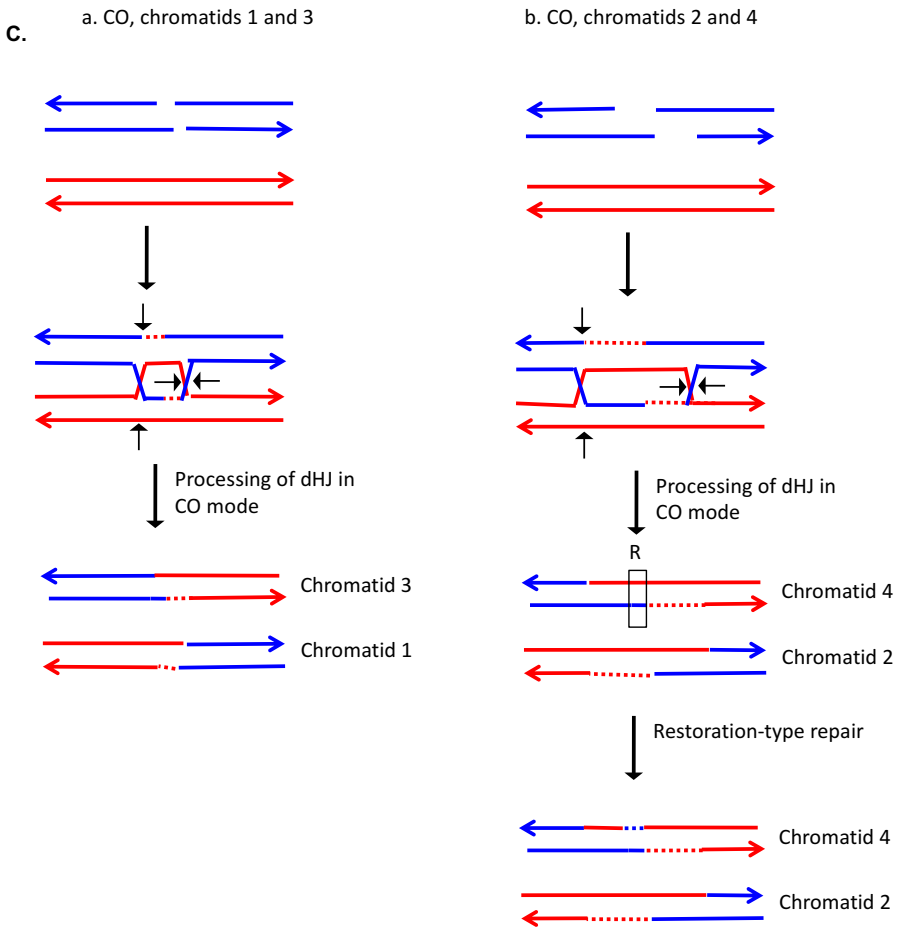

S24	CO1	CO between chromatids 1 and 3 with no heteroduplex	Standard DSBR model with limited strand invasion and limited DNA synthesis
	CO2	CO between chromatids 2 and 4 with restoration tract between *trans* heteroduplexes	Standard DSBR model with tract of Mlh1-independent restoration repair

Fig.S25

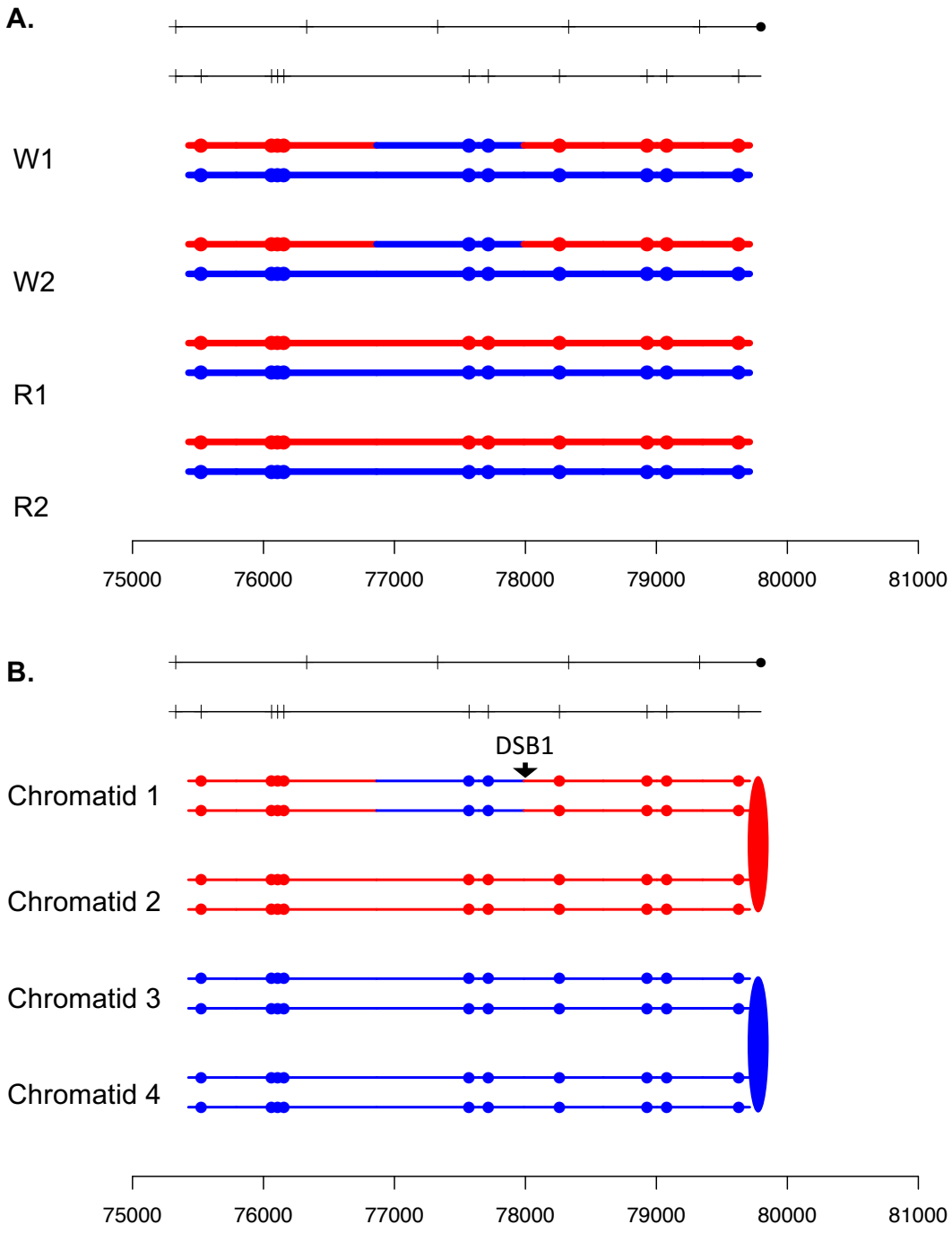
A.
W1
W2
R1
R2
75000
76000
77000
78000
79000
80000
81000
B.
DSB1
Chromatid 1
Chromatid 2
Chromatid 3
Chromatid 4
75000
76000
77000
78000
79000
80000
81000

Fig.S26

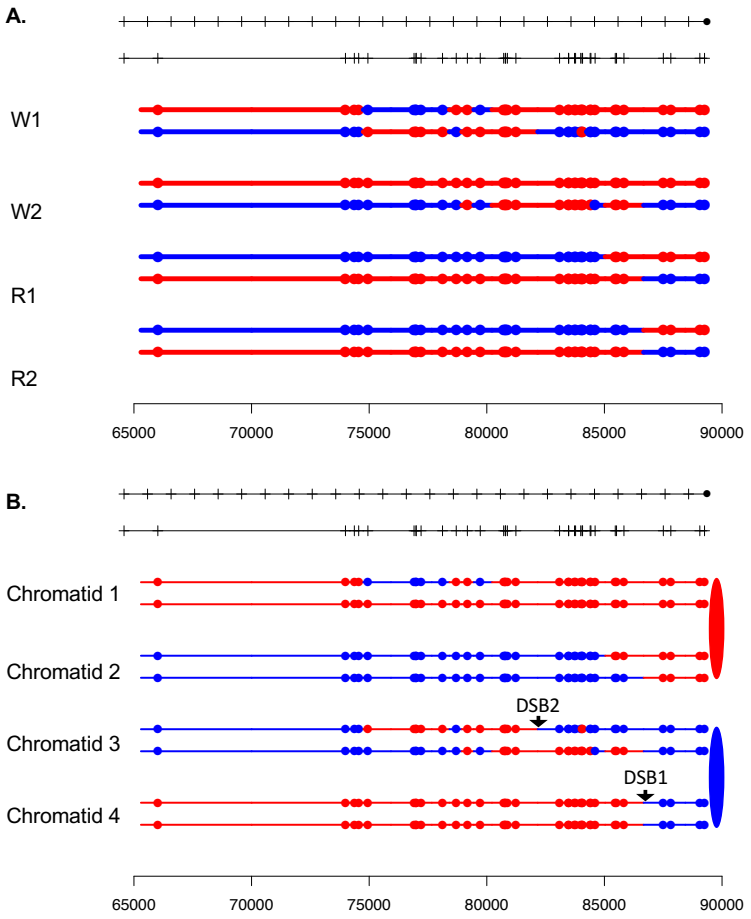

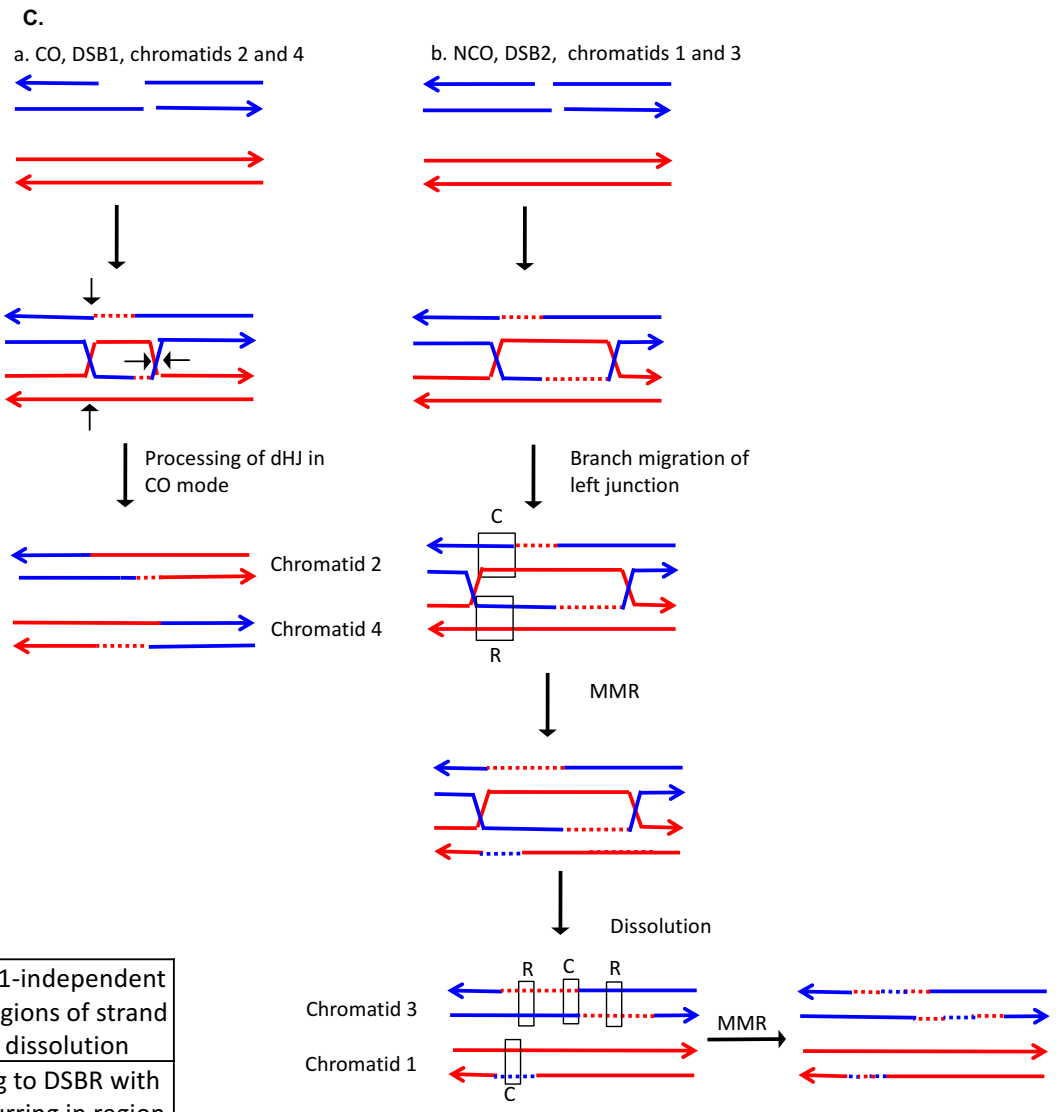

S26	NCO	Symmetric heteroduplexes; regions of homoduplex within heteroduplex; strand switch within heteroduplex	Branch migration; Mlh1-independent MMR; DSB between regions of strand switch, followed by dissolution
	CO	CO between chromatids 2 and 4 with heteroduplex on only one chromatid	Standard CO according to DSBR with one heteroduplex occurring in region without SNP

Fig.S27

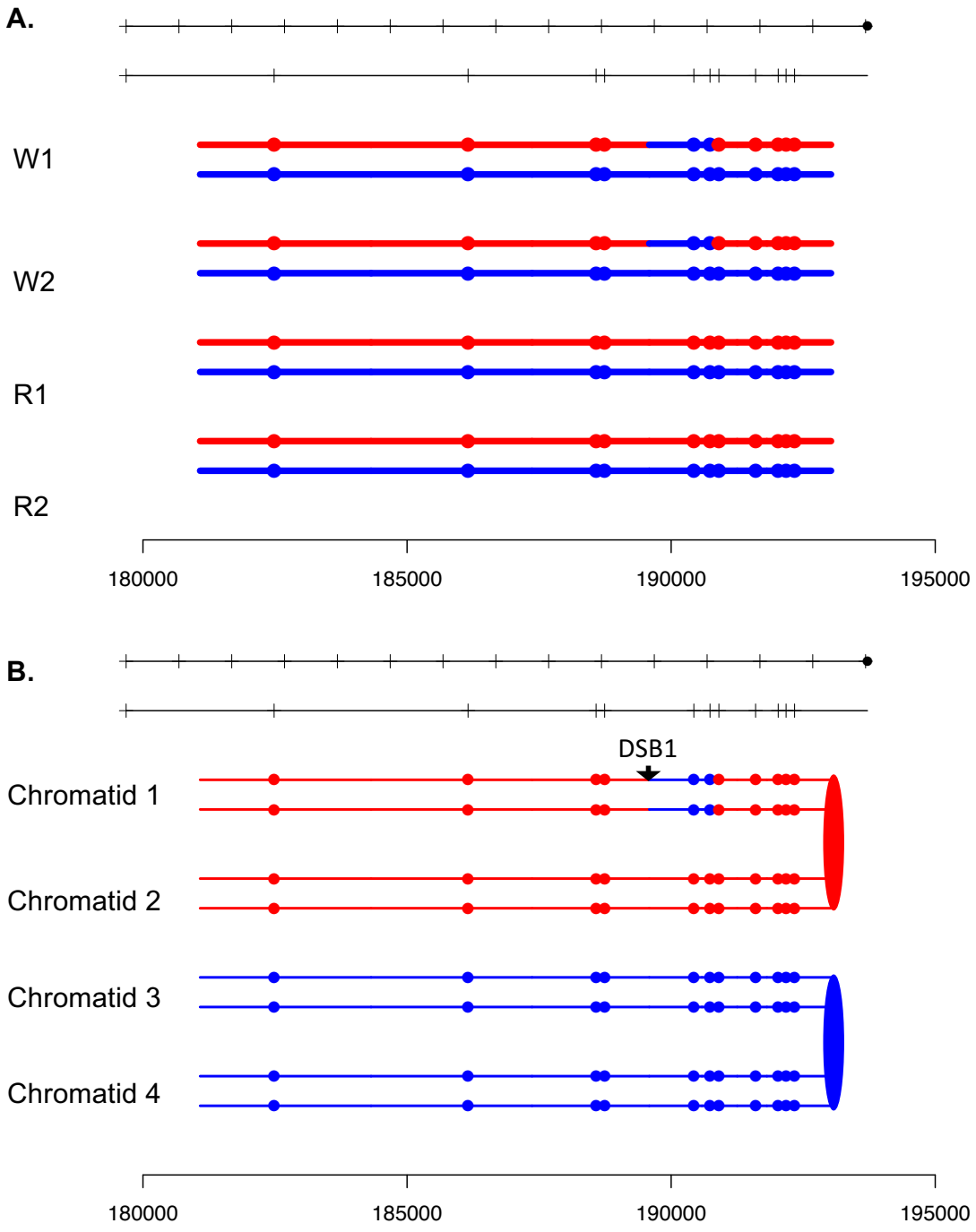
A.
W1
W2
R1
R2
180000
185000
190000
195000
B.
DSB1
Chromatid 1
Chromatid 2
Chromatid 3
Chromatid 4
180000
185000
190000
195000

Fig.S28

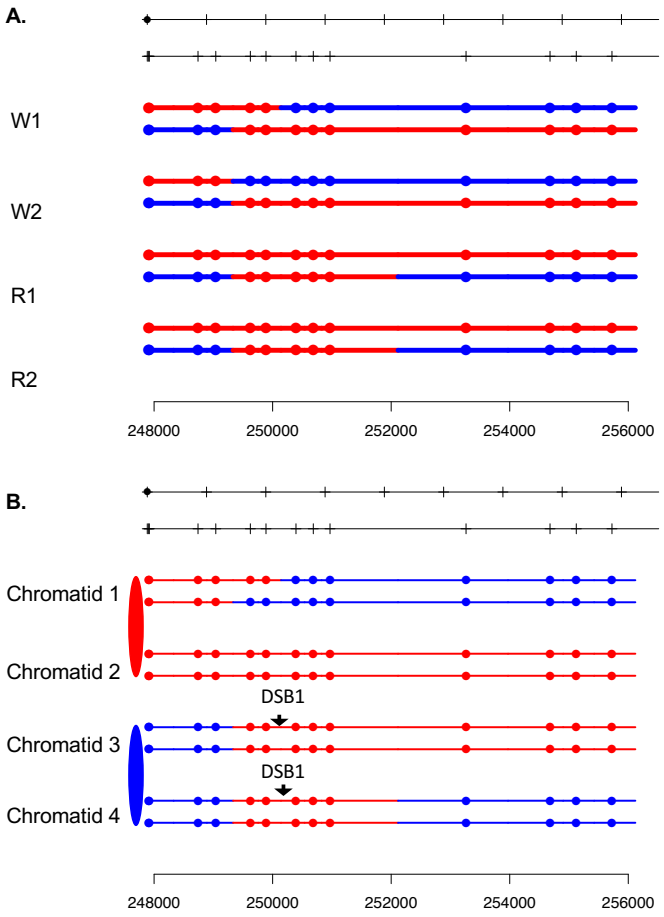

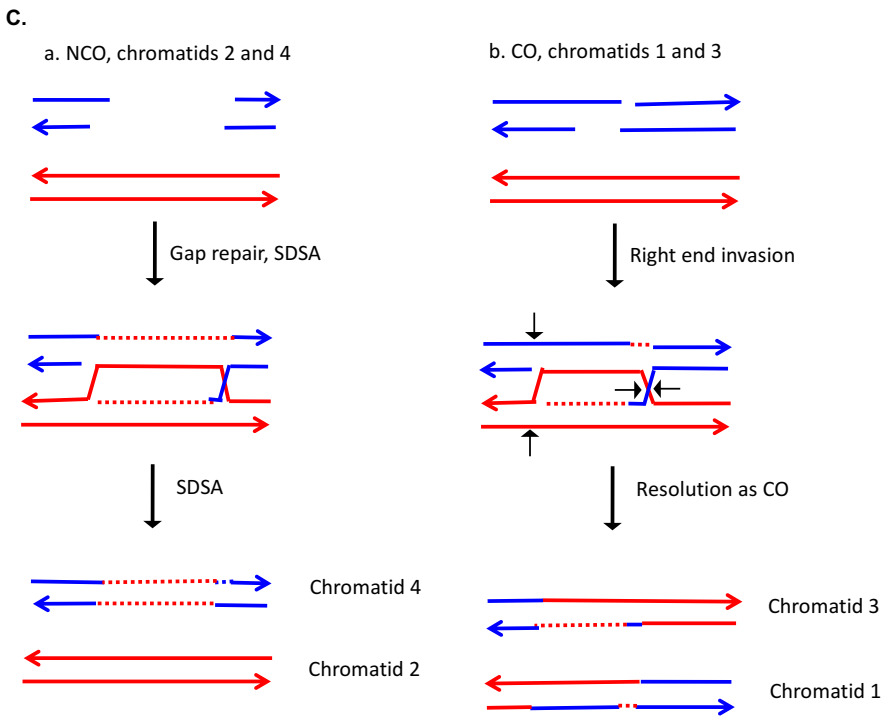

S28	NCO	Long conversion tract spanning putative DSB site	Repair of double-stranded DNA gap
	CO	Heteroduplex tract on only one side of DSB site	Standard CO according to DSBR with one heteroduplex occurring in region without SNP

Fig.S29

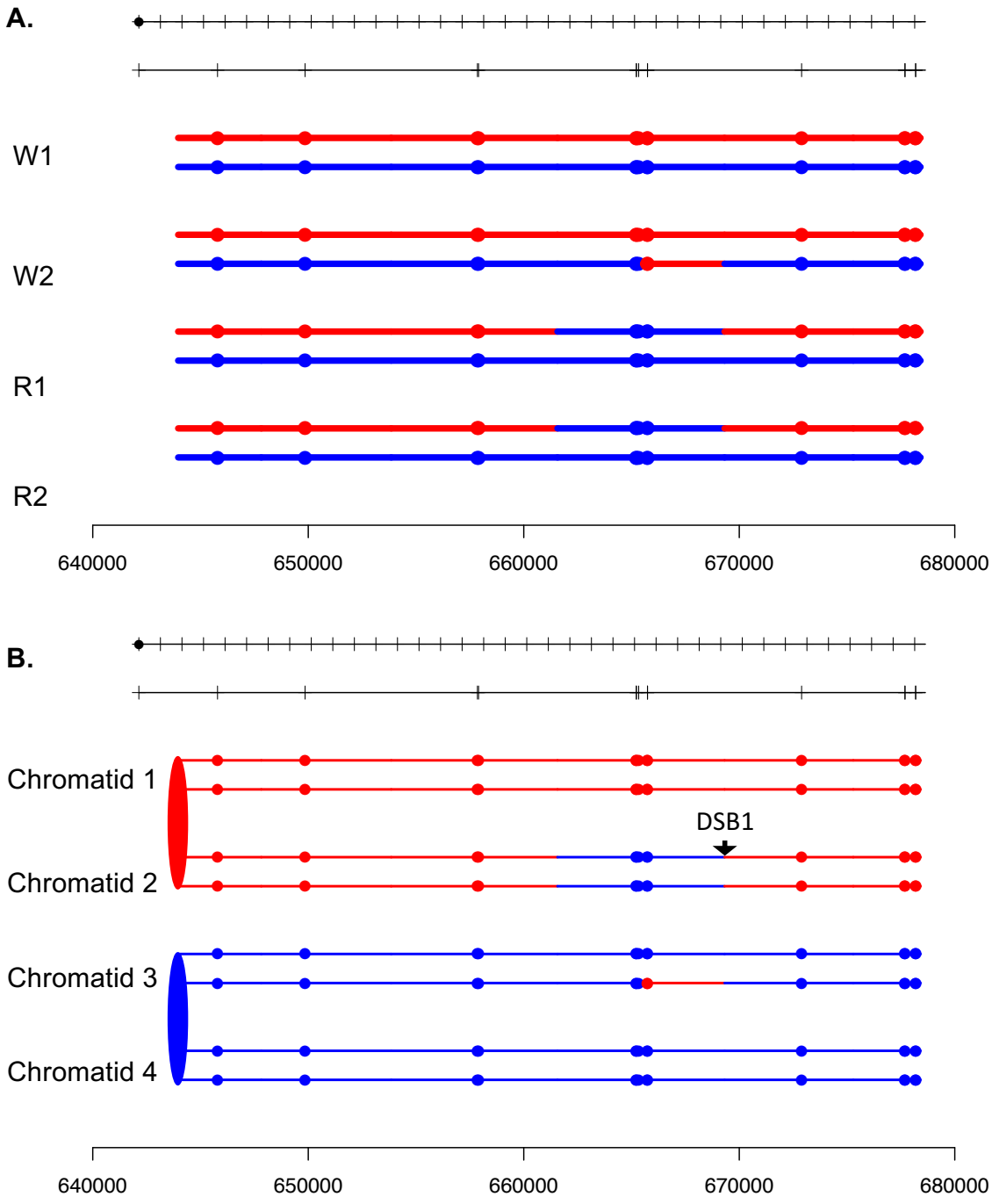
A.
W1
W2
R1
R2
640000
650000
660000
670000
680000
B.
Chromatid 1
Chromatid 2
Chromatid 3
Chromatid 4
DSB1
640000
650000
660000
670000
680000

Fig.S30

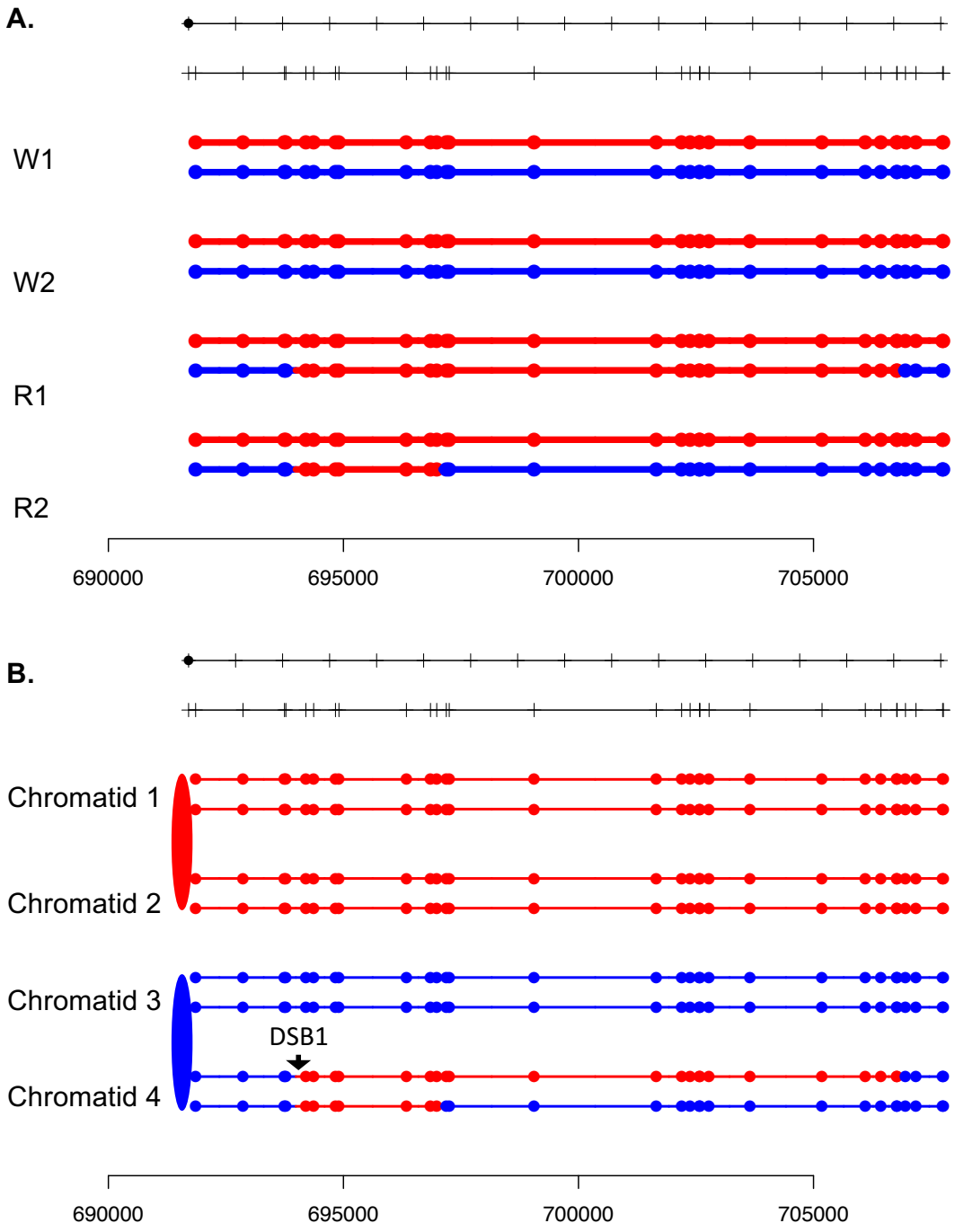
A.
W1
W2
R1
R2
690000
695000
700000
705000
B.
Chromatid 1
Chromatid 2
Chromatid 3
Chromatid 4
DSB1
690000
695000
700000
705000

Fig.S31

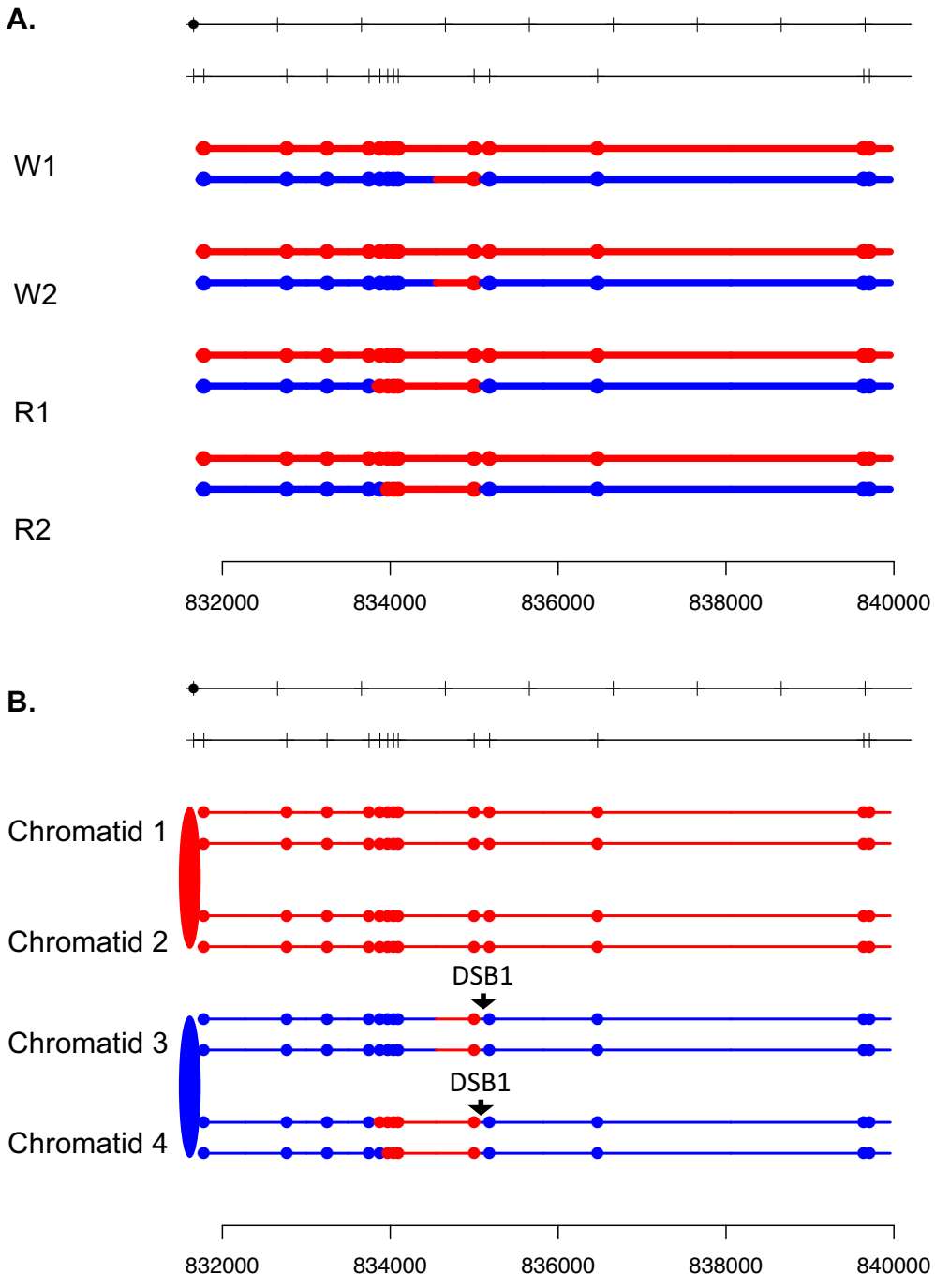
A.
W1
W2
R1
R2
832000
834000
836000
838000
840000
B.
Chromatid 1
Chromatid 2
DSB1
Chromatid 3
DSB1
Chromatid 4
832000
834000
836000
838000
840000

Fig.S32

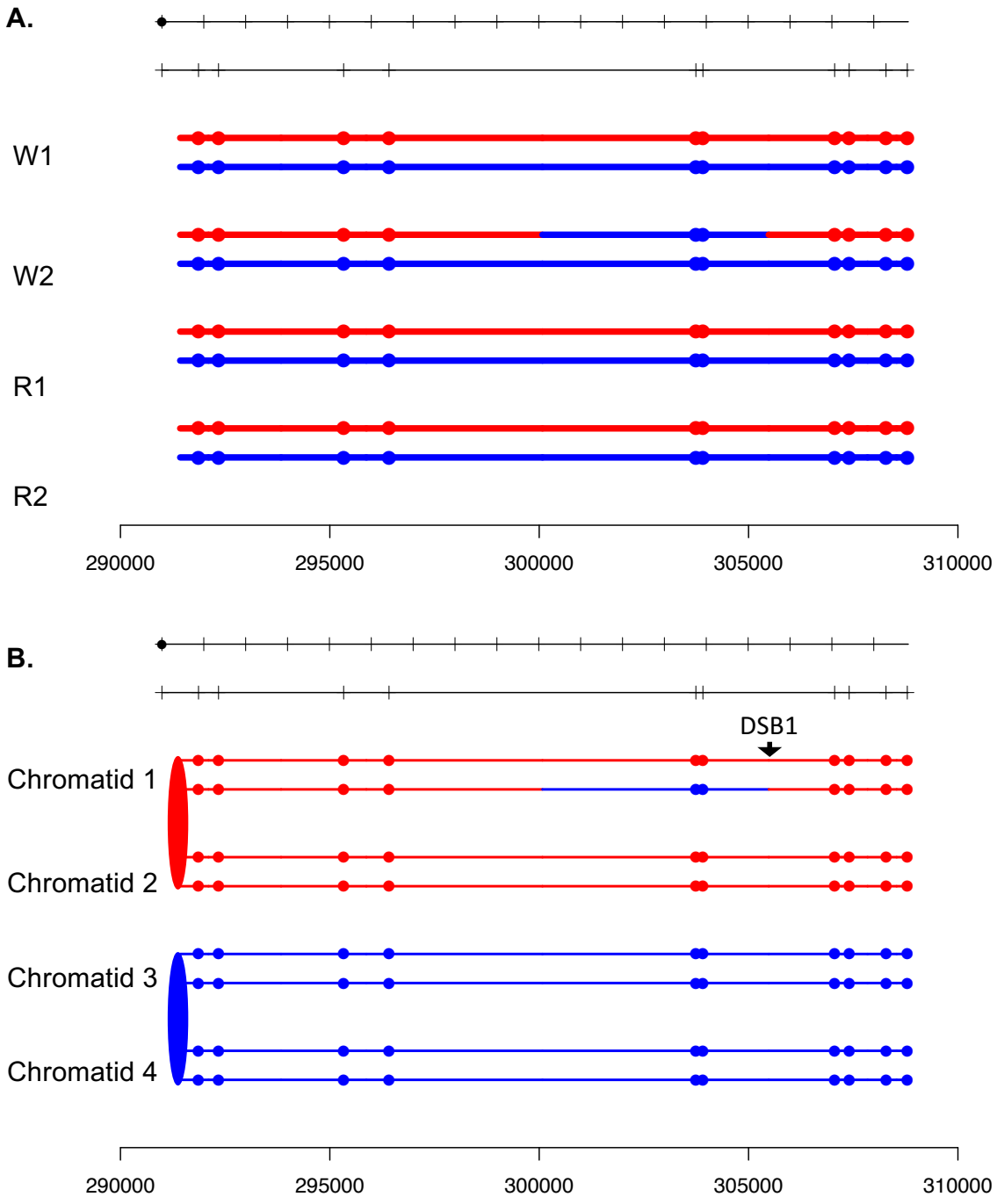
A.
W1
W2
R1
R2
290000
295000
300000
305000
310000
B.
DSB1
Chromatid 1
Chromatid 2
Chromatid 3
Chromatid 4
290000
295000
300000
305000
310000

Fig.S33

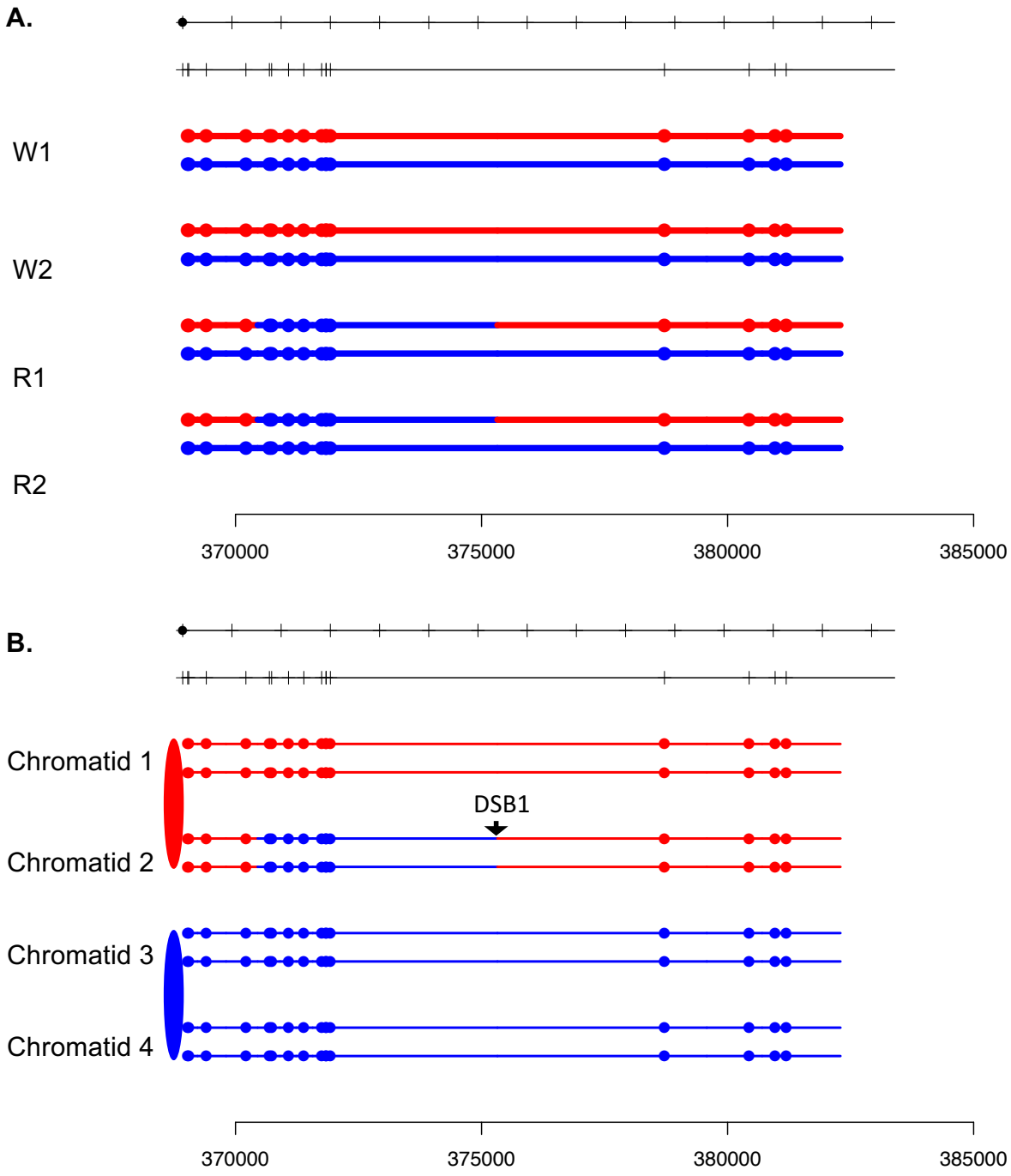
A.
W1
W2
R1
R2
370000
375000
380000
385000
B.
Chromatid 1
DSB1
Chromatid 2
Chromatid 3
Chromatid 4
370000
375000
380000
385000

Fig.S34

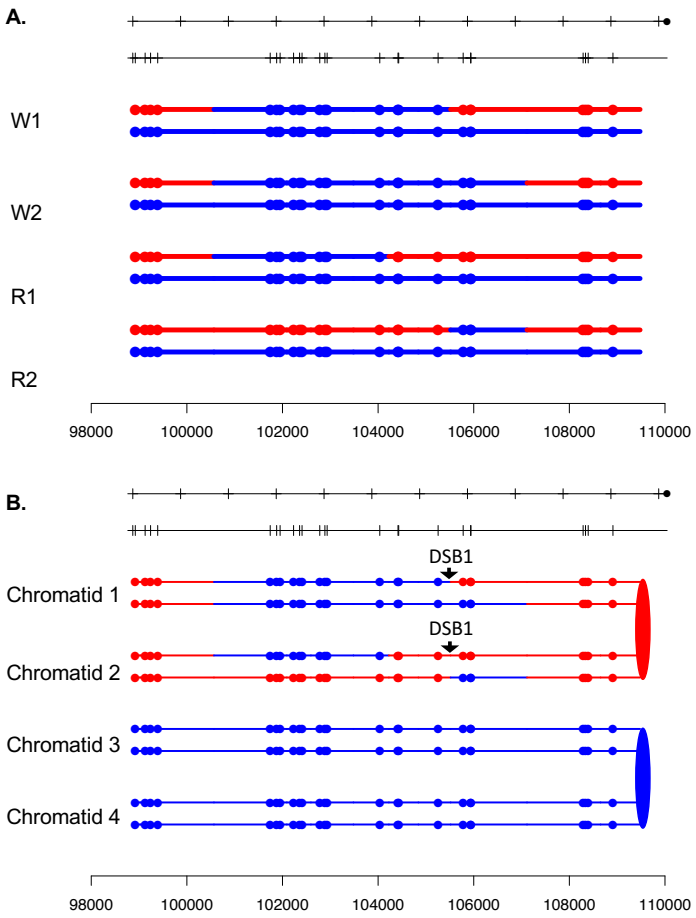

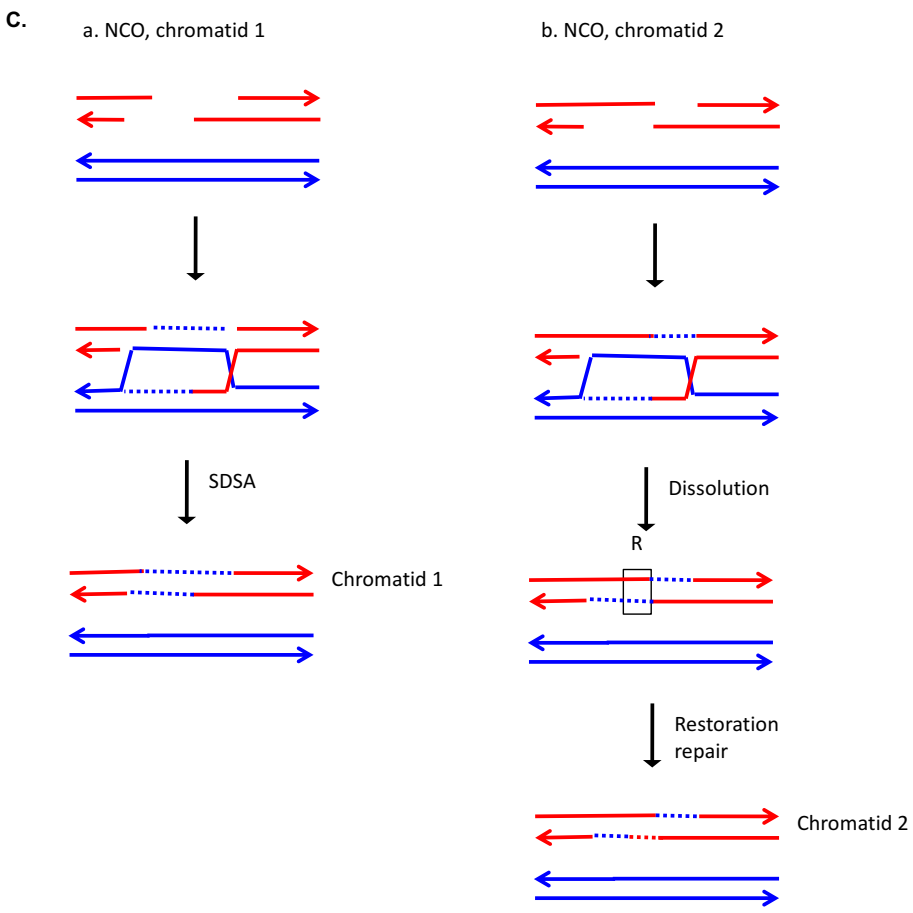

S34	NCO1	Long conversion-tract on chromatid 1	Repair of double-stranded DNA gap
	NCO2	Heteroduplexes in trans on chromatid 2 separated by homoduplex	Dissolution of dHJ associated with restoration repair

Fig.S35

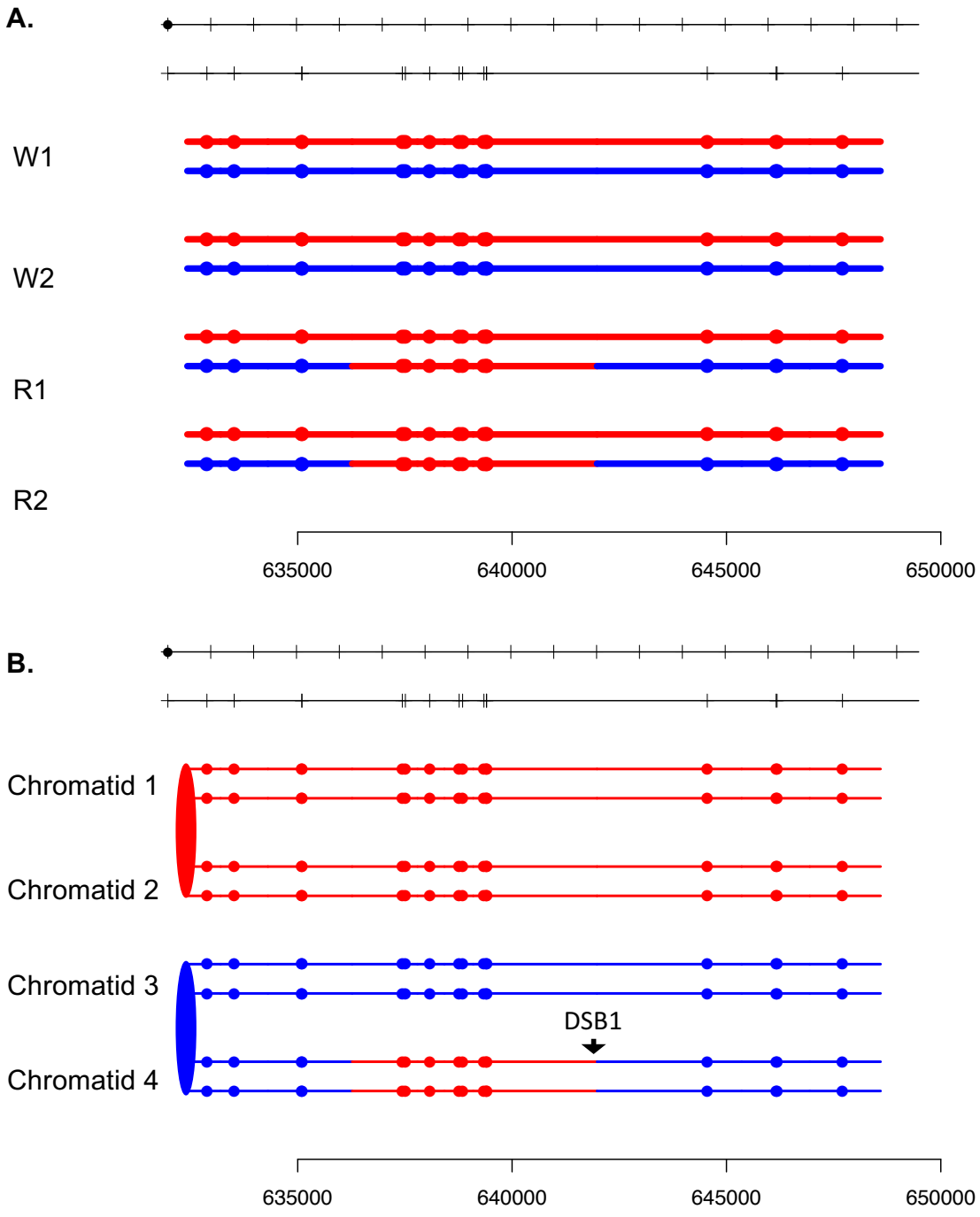
A.
W1
W2
R1
R2
635000
640000
645000
650000
B.
Chromatid 1
Chromatid 2
Chromatid 3
Chromatid 4
DSB1
635000
640000
645000
650000

Fig.S36

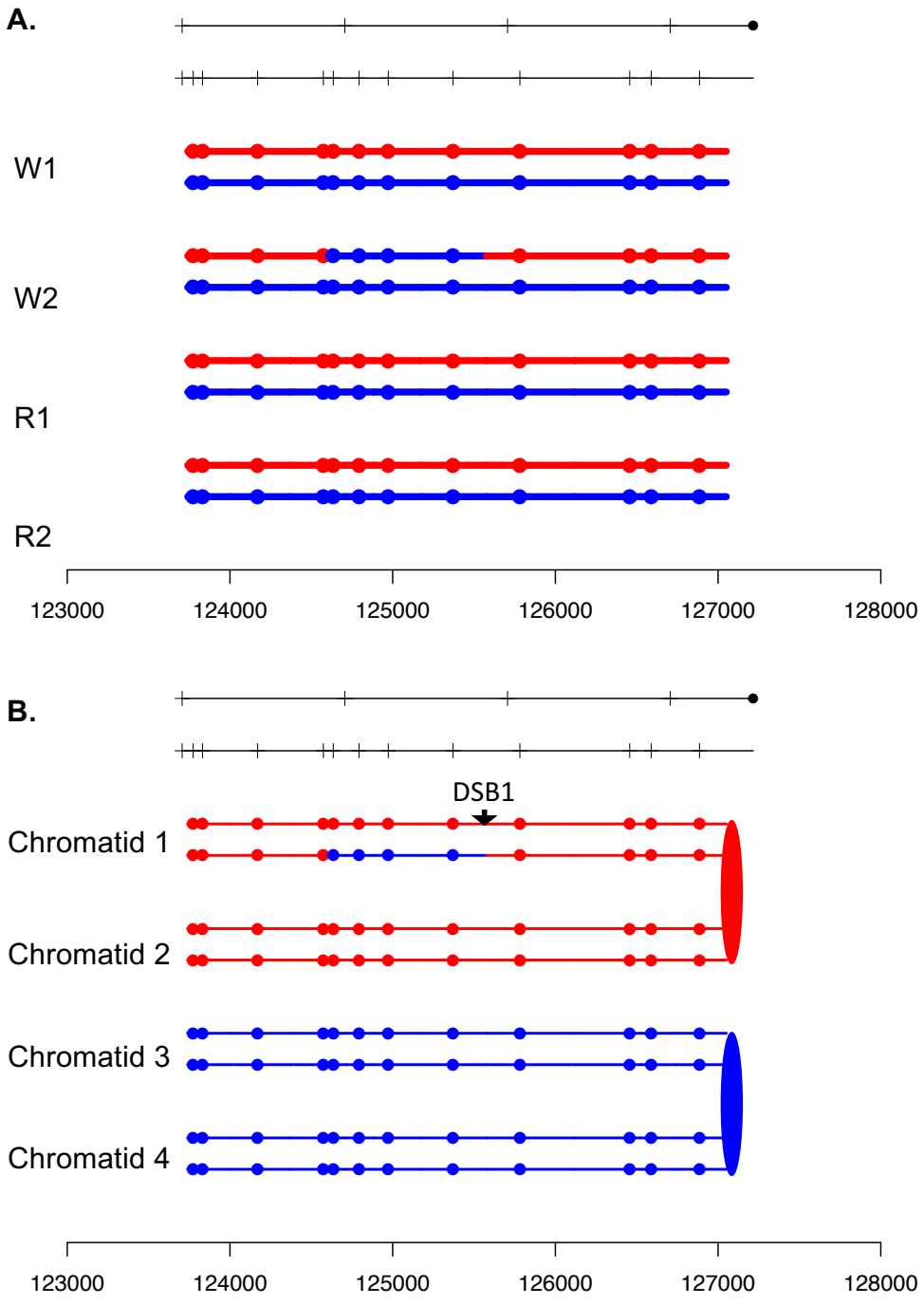
A.
W1
W2
R1
R2
123000
124000
125000
126000
127000
128000
B.
DSB1
Chromatid 1
Chromatid 2
Chromatid 3
Chromatid 4
123000
124000
125000
126000
127000
128000

Fig.S37

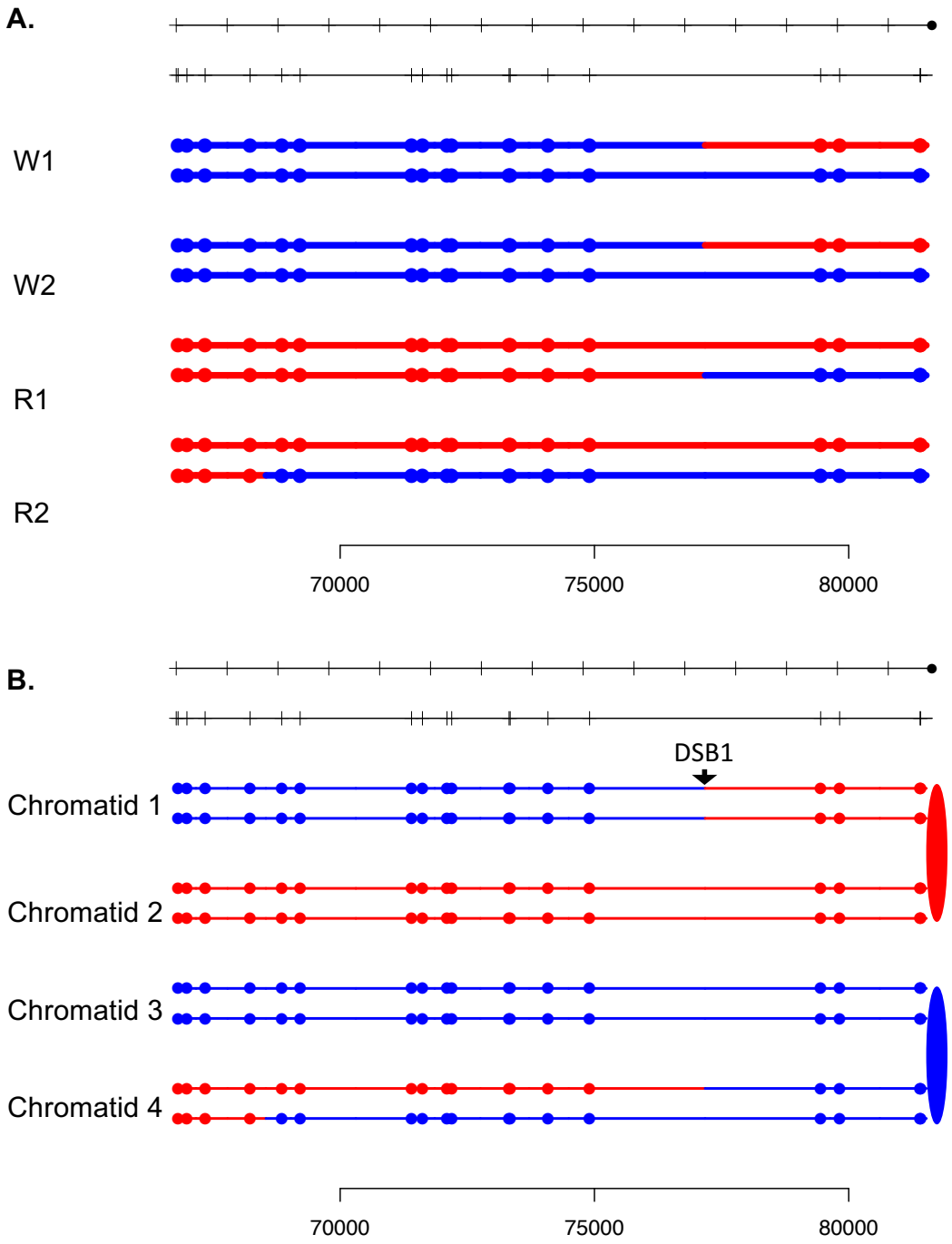
A.
W1
W2
R1
R2
70000
75000
80000
B.
DSB1
Chromatid 1
Chromatid 2
Chromatid 3
Chromatid 4
70000
75000
80000

Fig.S38

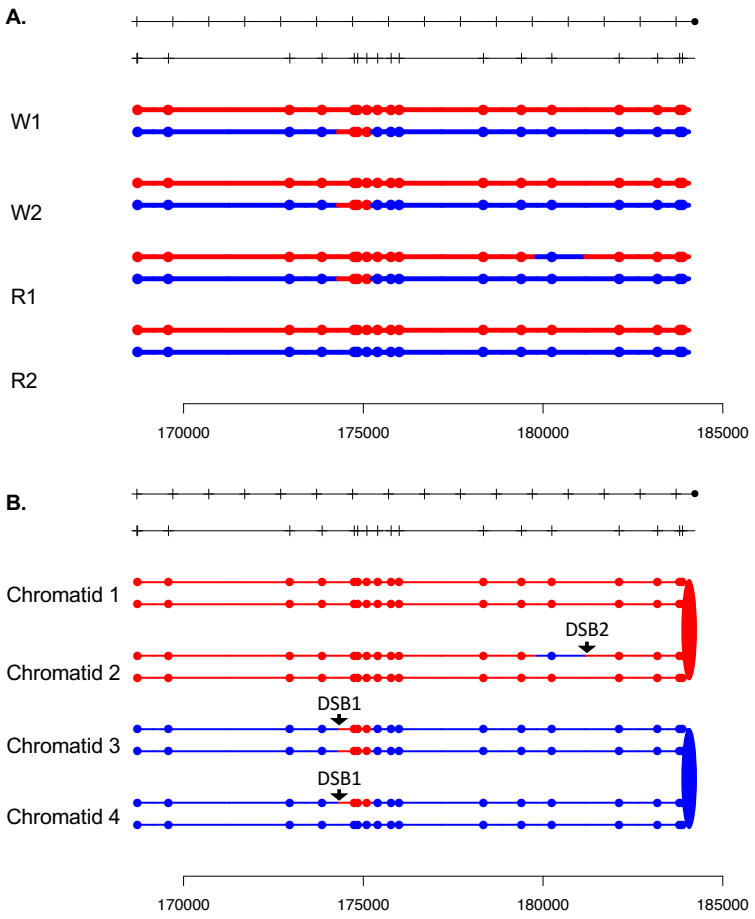

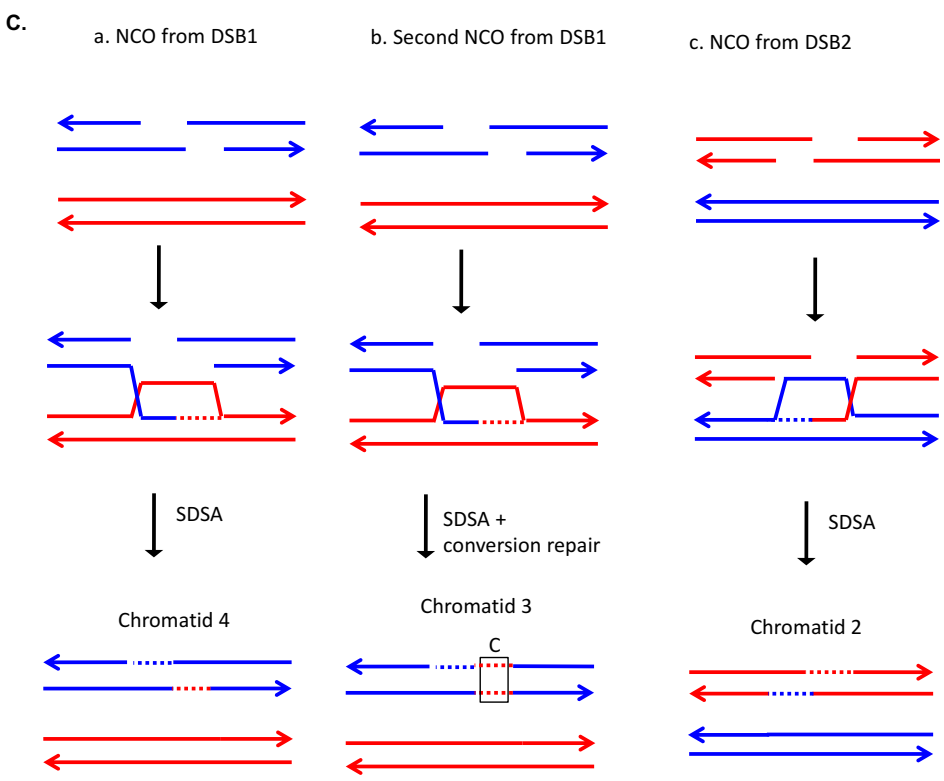

S38	NCO1	Conversion tract adjacent to DSB1 site on chromatid 3	SDSA, Mlh1-independent MMR
	NCO2	Heteroduplex adjacent to DSB1 site on chromatid 4	SDSA
	NCO3	Heteroduplex adjacent to DSB2 site on chromatid 2	SDSA

Fig.S39

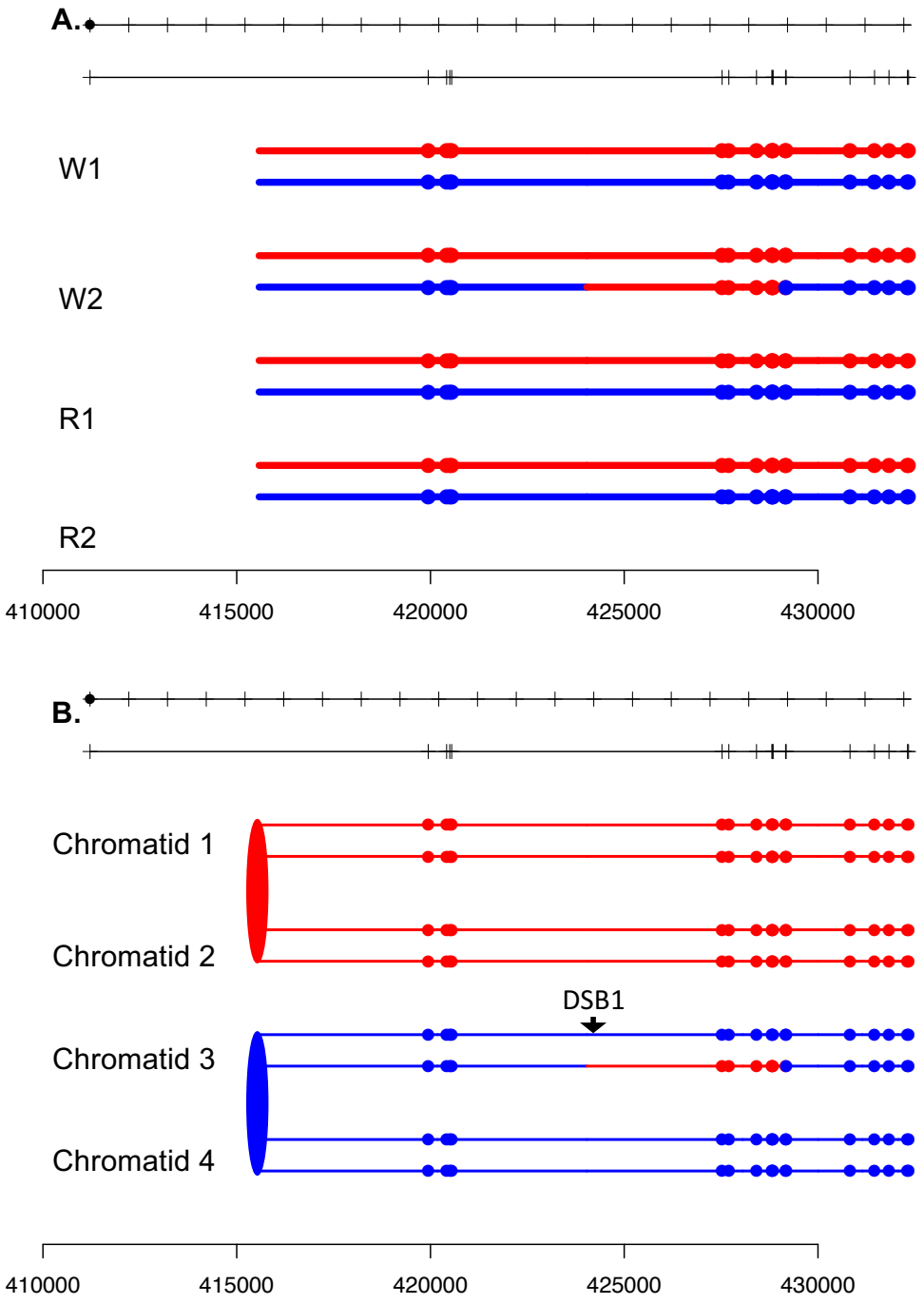
A.
W1
W2
R1
R2
410000
415000
420000
425000
430000
B.
Chromatid 1
Chromatid 2
DSB1
Chromatid 3
Chromatid 4
410000
415000
420000
425000
430000

Fig.S40

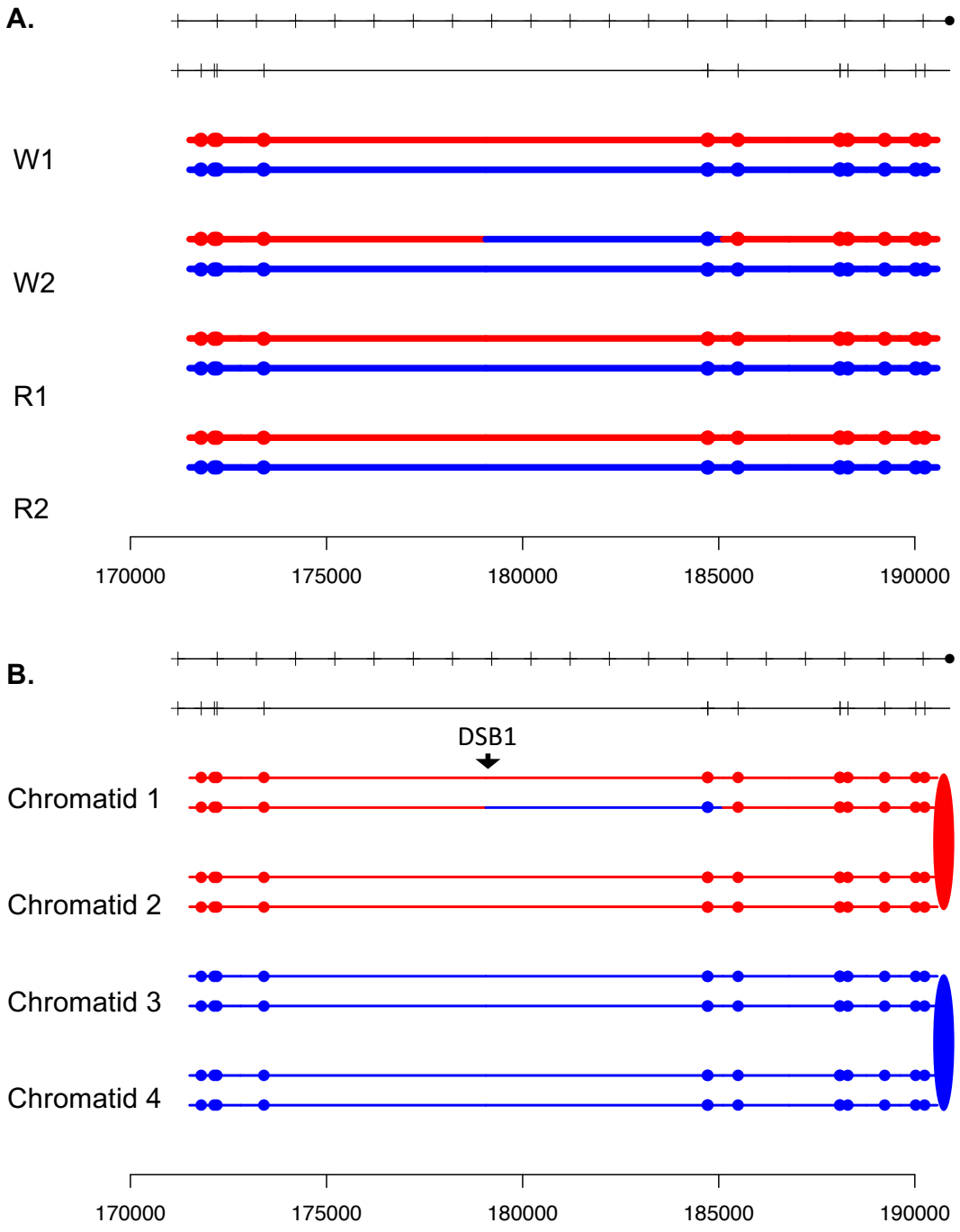
A.
W1
W2
R1
R2
170000
175000
180000
185000
190000
B.
DSB1
Chromatid 1
Chromatid 2
Chromatid 3
Chromatid 4
170000
175000
180000
185000
190000

Fig.S41

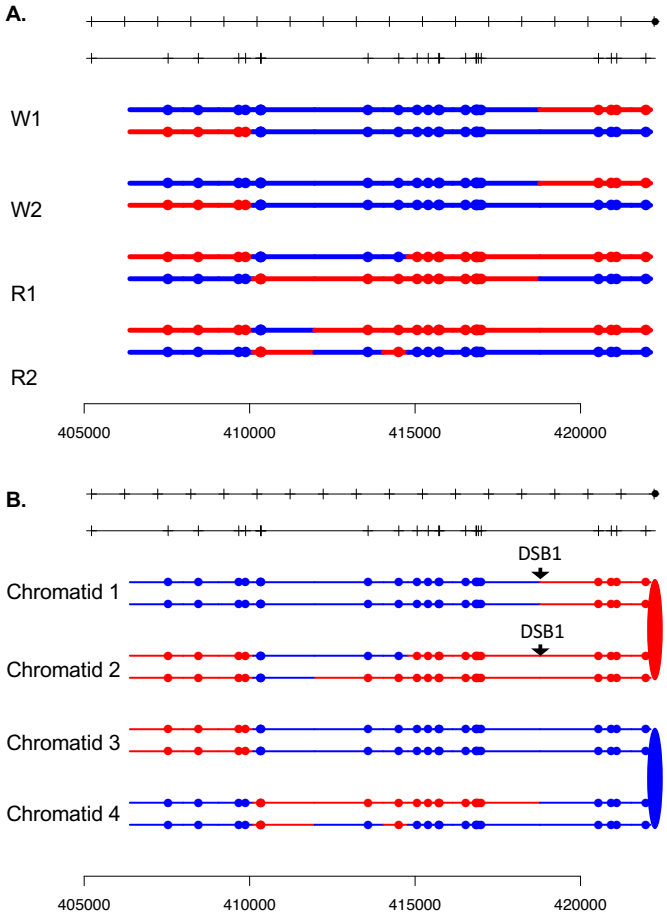

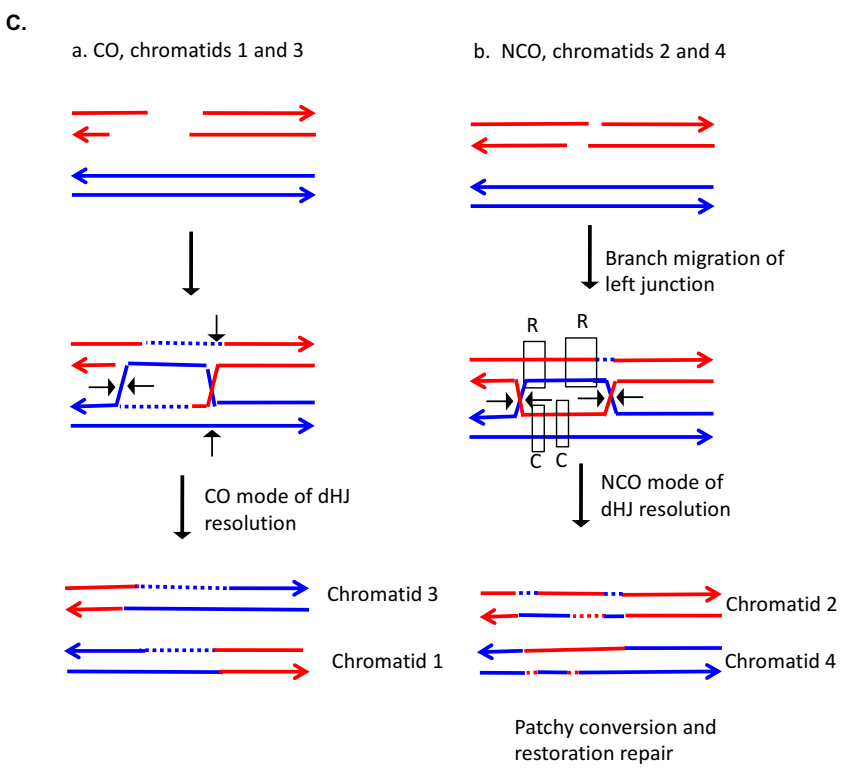

S41	NCO	Symmetric heteroduplexes on chromatids 2 and 4; homoduplex regions within heteroduplex	Branch migration; Mlh1-independent MMR
	CO	Crossover between chromatids 1 and 3 associated with long conversion tract	Repair of double-stranded DNA gap

Fig.S42

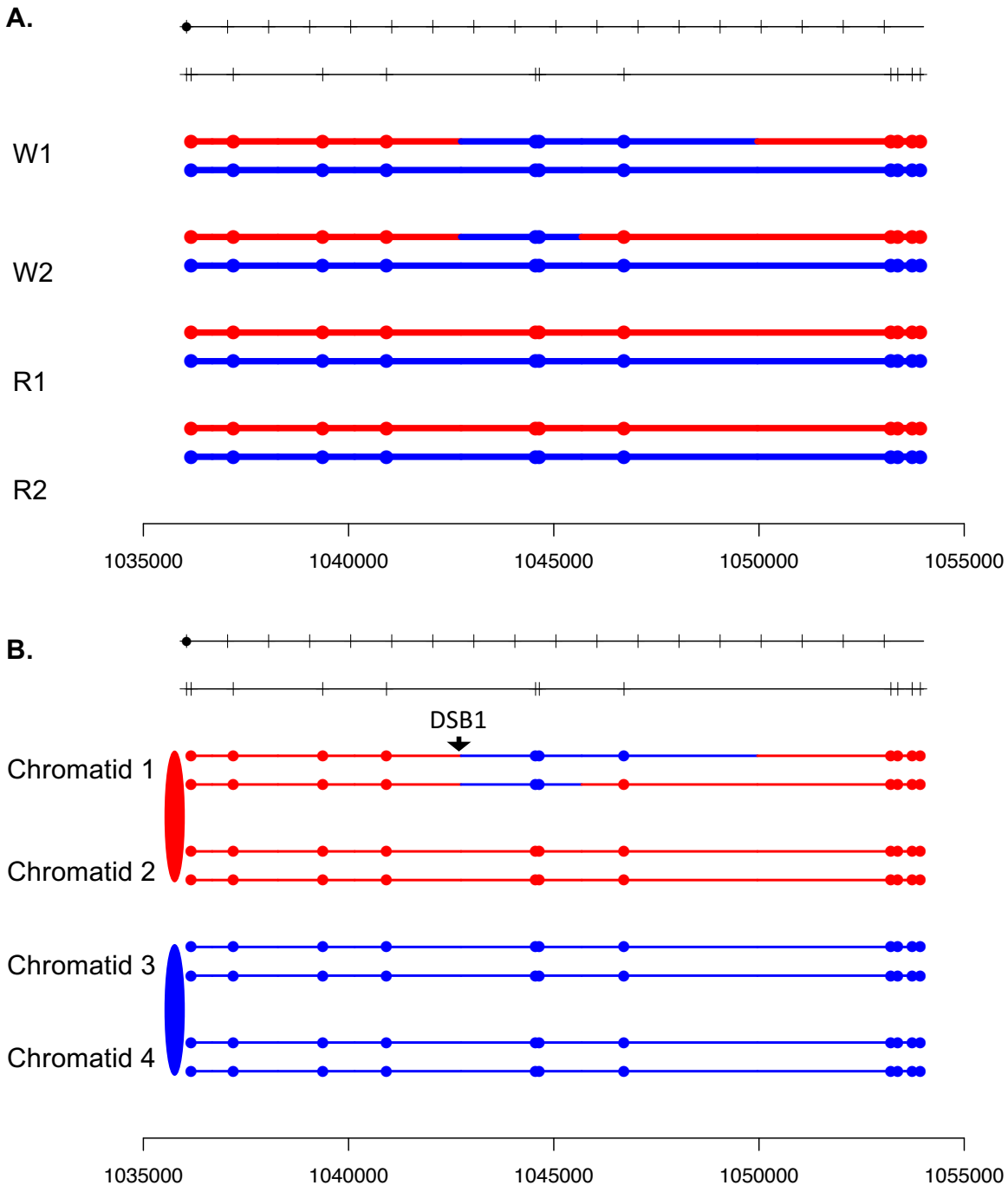
A.
W1
W2
R1
R2
1035000
1040000
1045000
1050000
1055000
B.
DSB1
Chromatid 1
Chromatid 2
Chromatid 3
Chromatid 4
1035000
1040000
1045000
1050000
1055000

Fig.S43

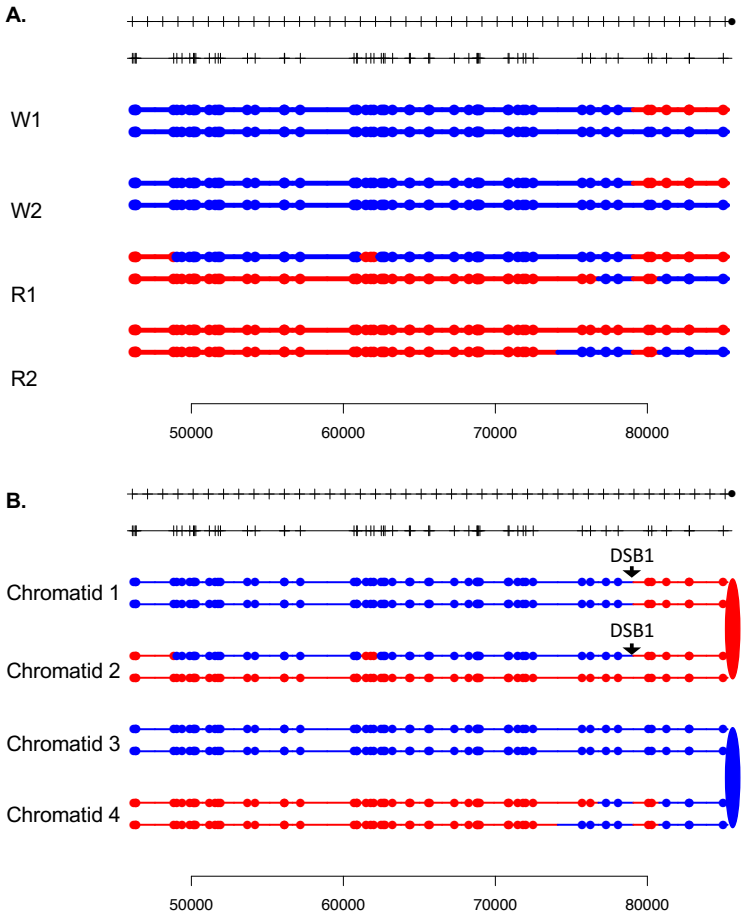

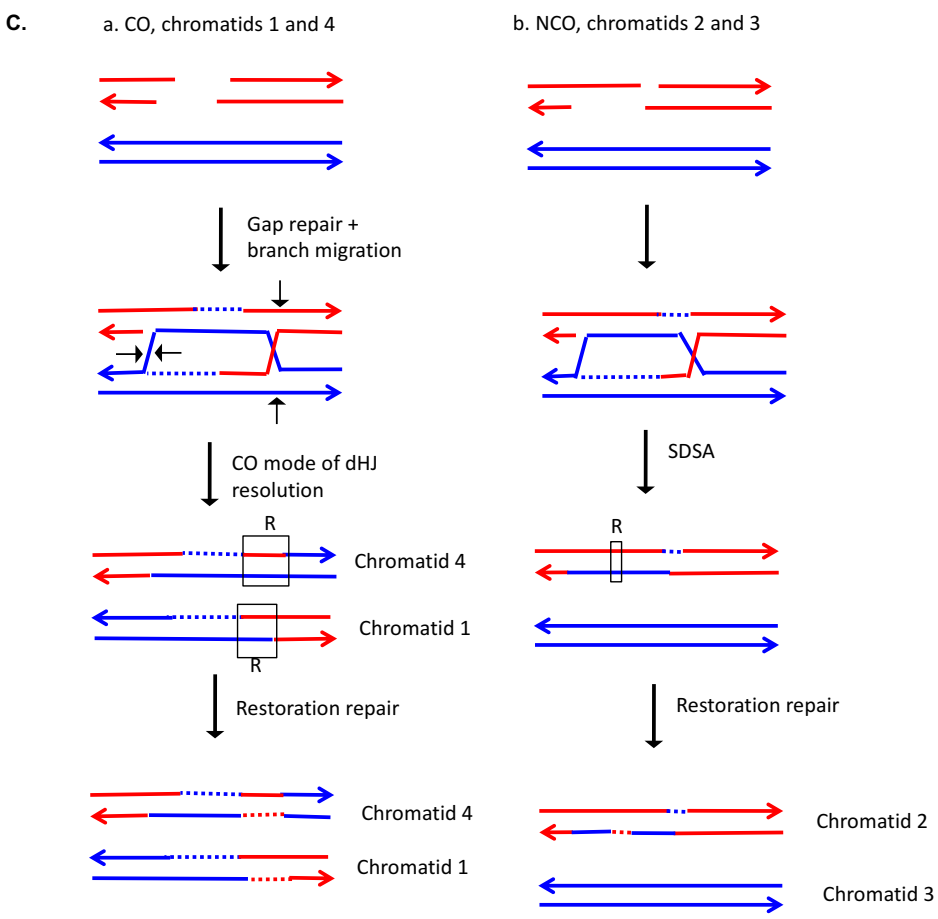

S43	CO	Restoration repair on one side of CO chromatid 4 and conversion repair on the other	Branch migration; Mlh1-independent MMR
	NCO	Long heteroduplex region with short restoration tract	SDSA with Mlh1-independent MMR

Fig.S44

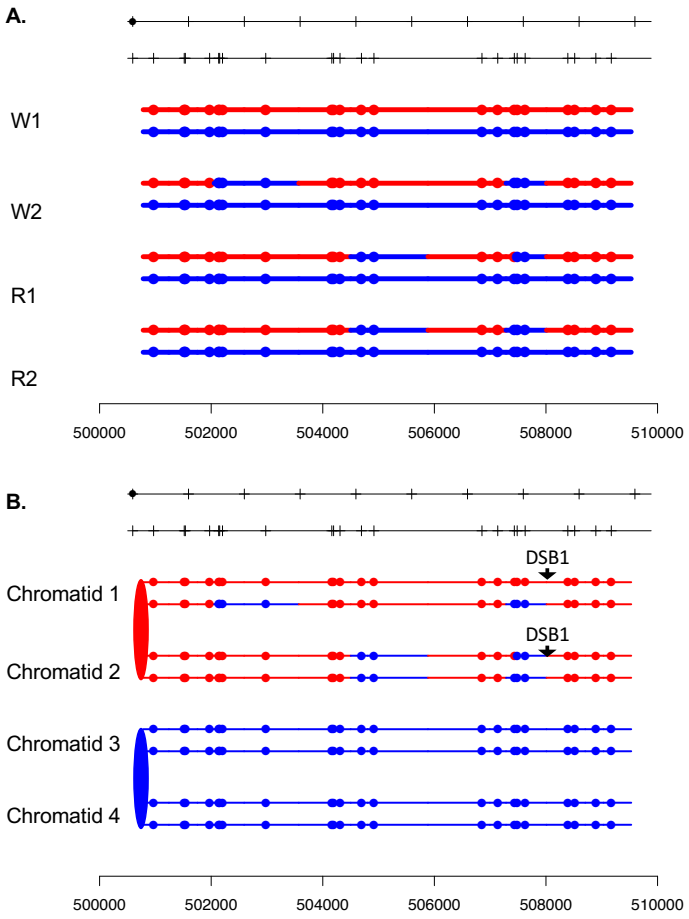

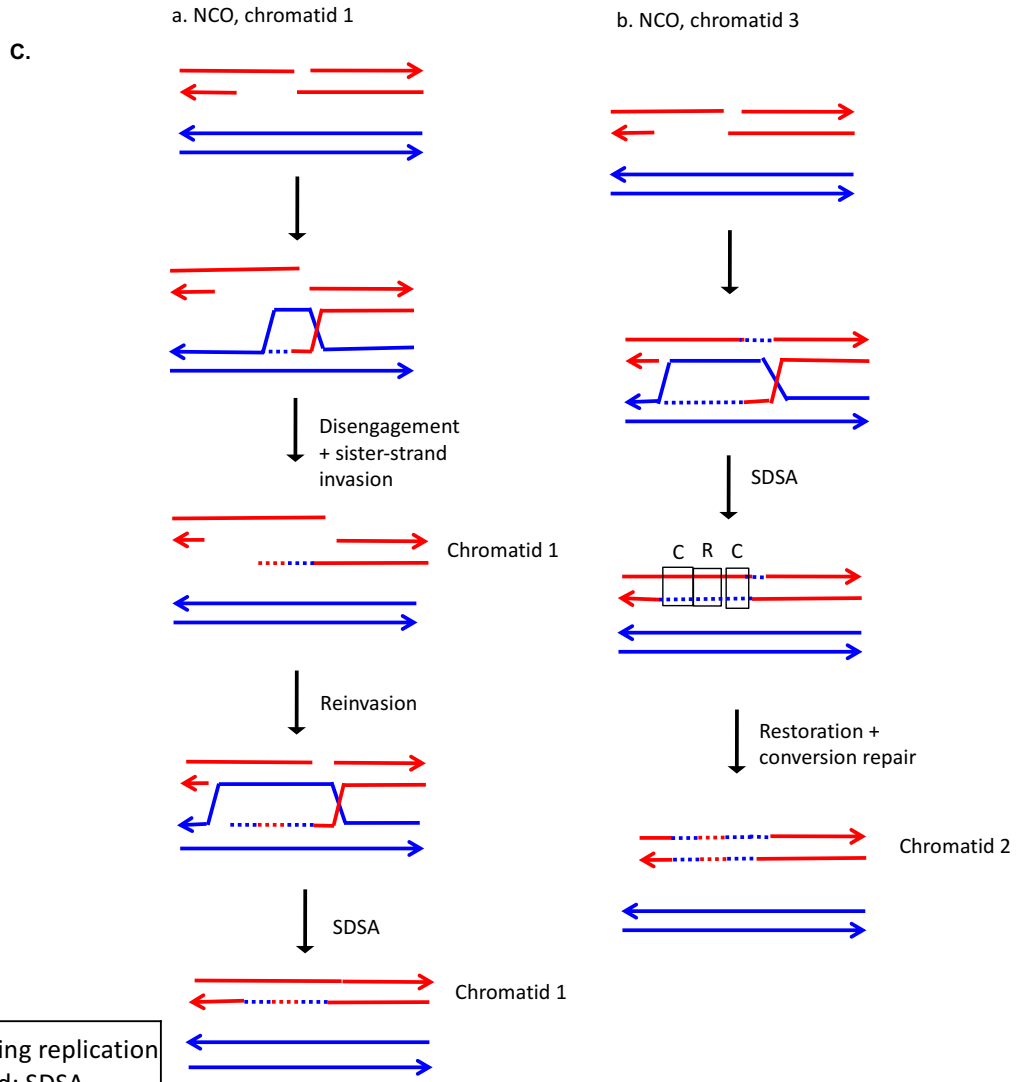

S44	NCO1	Chromatid 1 has heteroduplex region with long restoration tract in the middle	Template switch during replication to sister strand; SDSA
	NCO2	Chromatid 2 has mixture of homoduplex conversion and restoration tracts	Mlh1-independent patchy MMR

Fig.S45

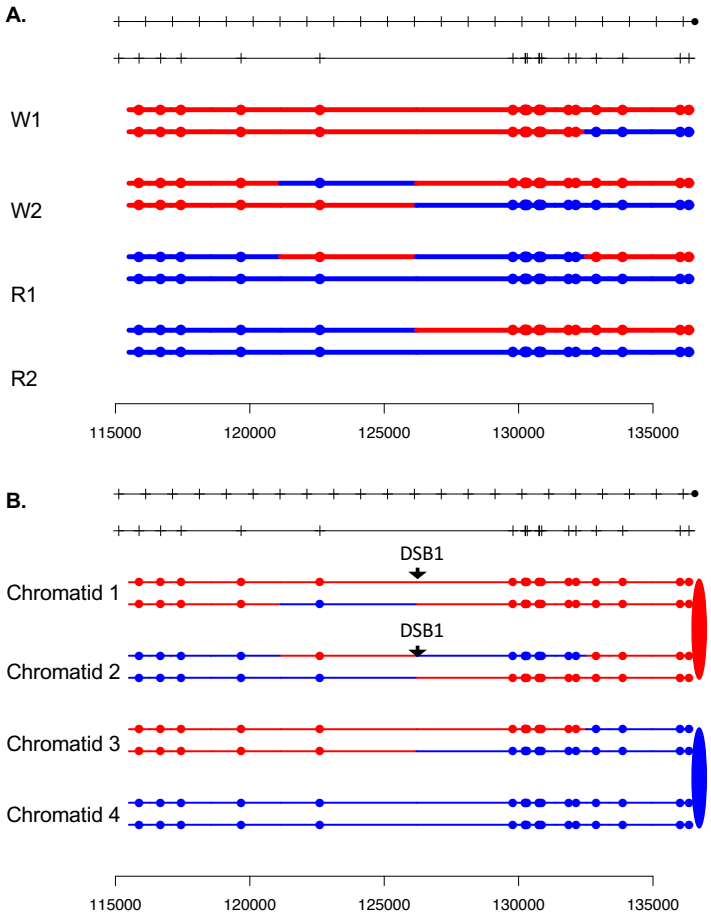

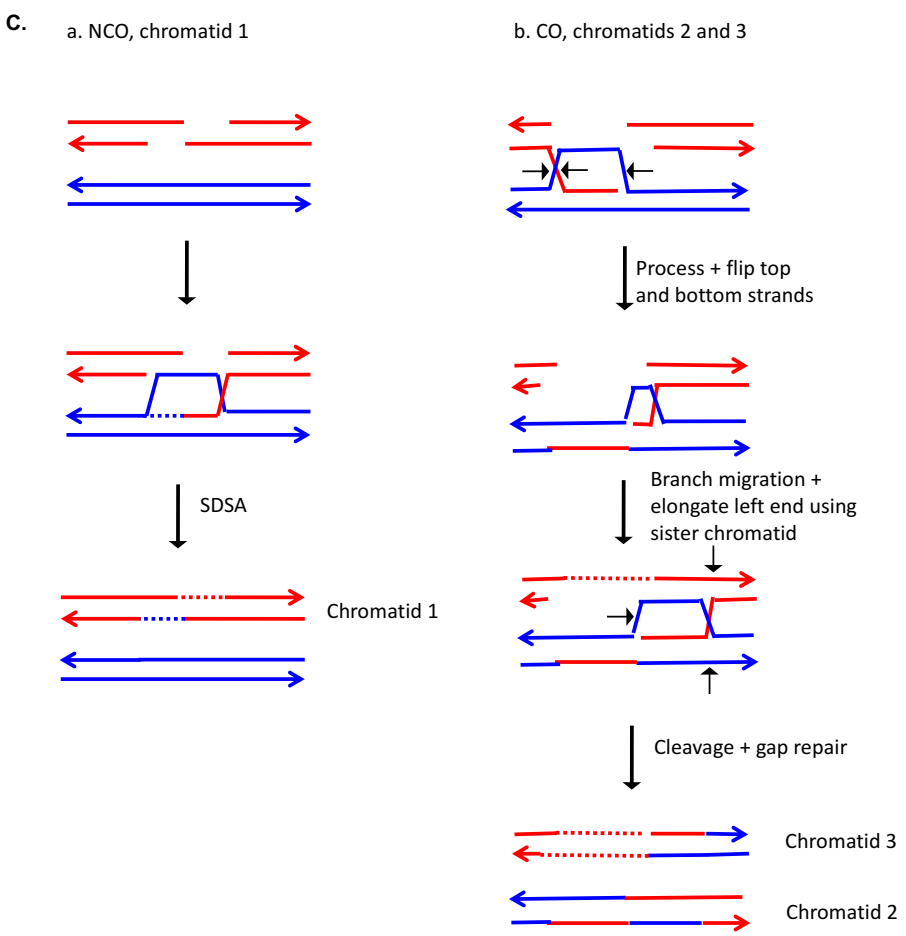

S45	NCO	Simple heteroduplex (chromatid 1)	SDSA
	CO	Regions of heteroduplex with switched strands on chromatid 3; symmetric heteroduplexes	Independent invasion of two broken ends; branch migration

Fig.S46

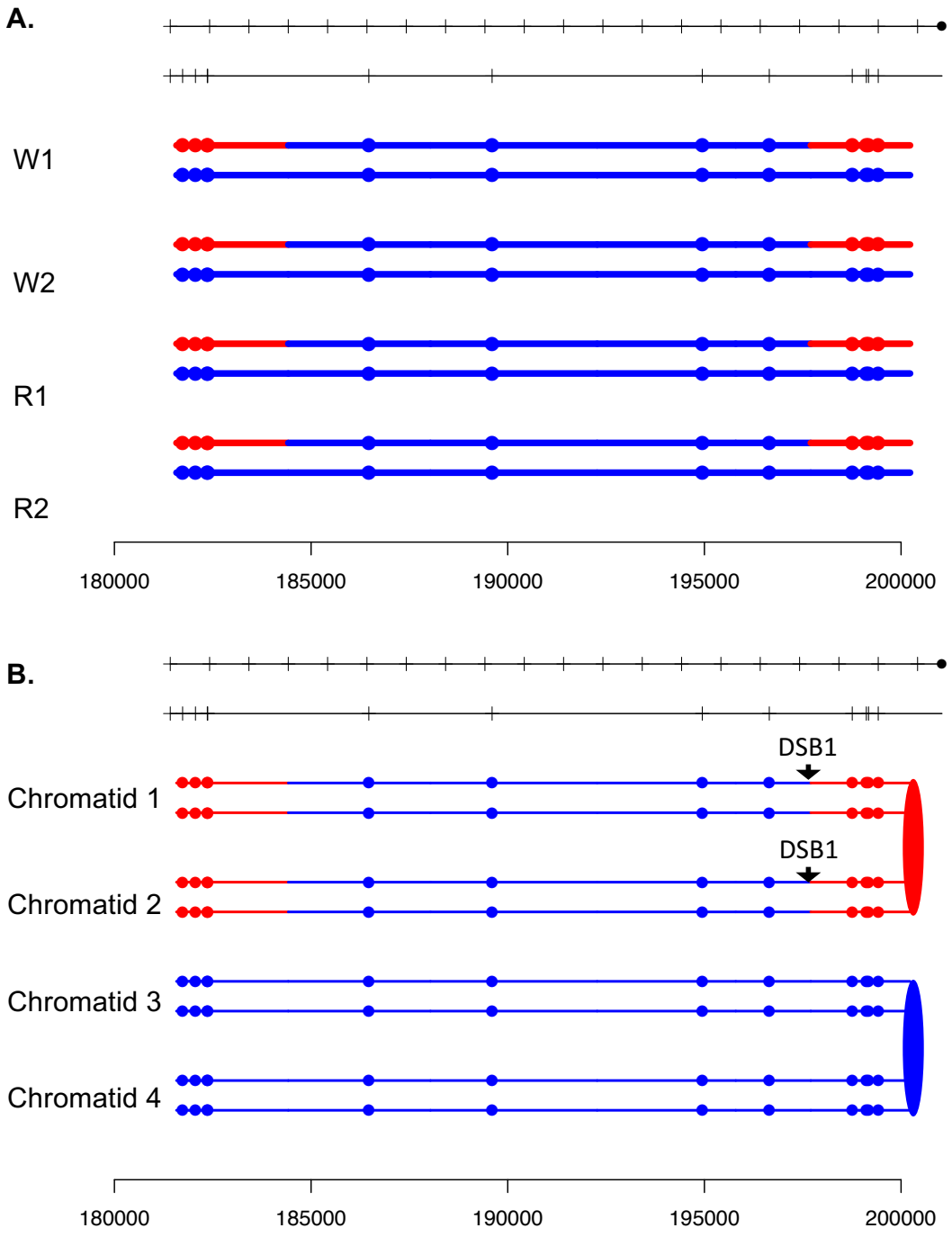
A.
W1
W2
R1
R2
180000
185000
190000
195000
200000
B.
DSB1
DSB1
Chromatid 1
Chromatid 2
Chromatid 3
Chromatid 4
180000
185000
190000
195000
200000

Fig.S47

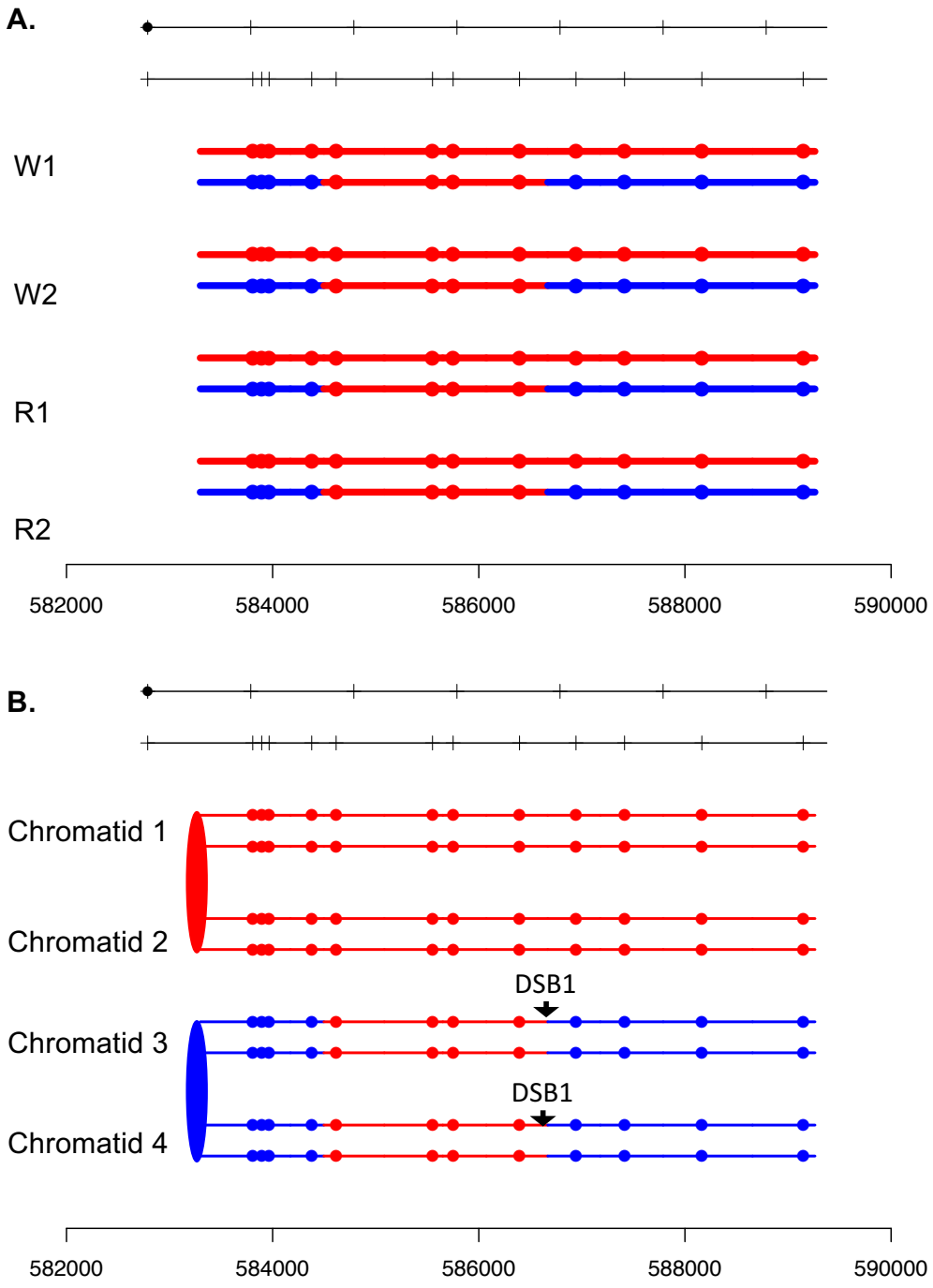
A.
W1
W2
R1
R2
582000
584000
586000
588000
590000
B.
Chromatid 1
Chromatid 2
DSB1
Chromatid 3
DSB1
Chromatid 4
582000
584000
586000
588000
590000

Fig.S48

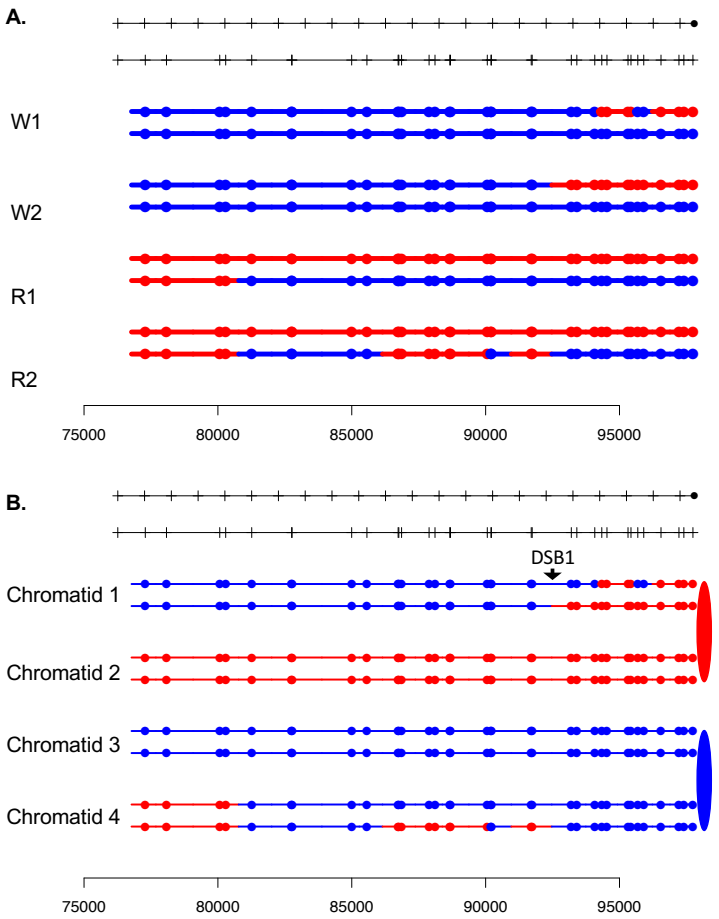

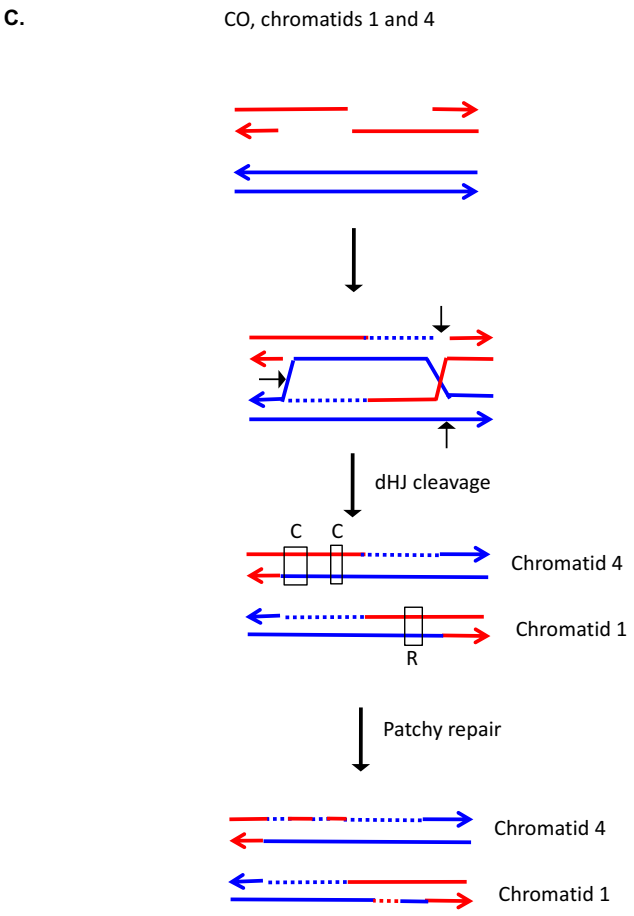

S48	CO	Regions of heteroduplex interspersed with homoduplex regions	Mlh1-independent patchy MMR

Fig.S49

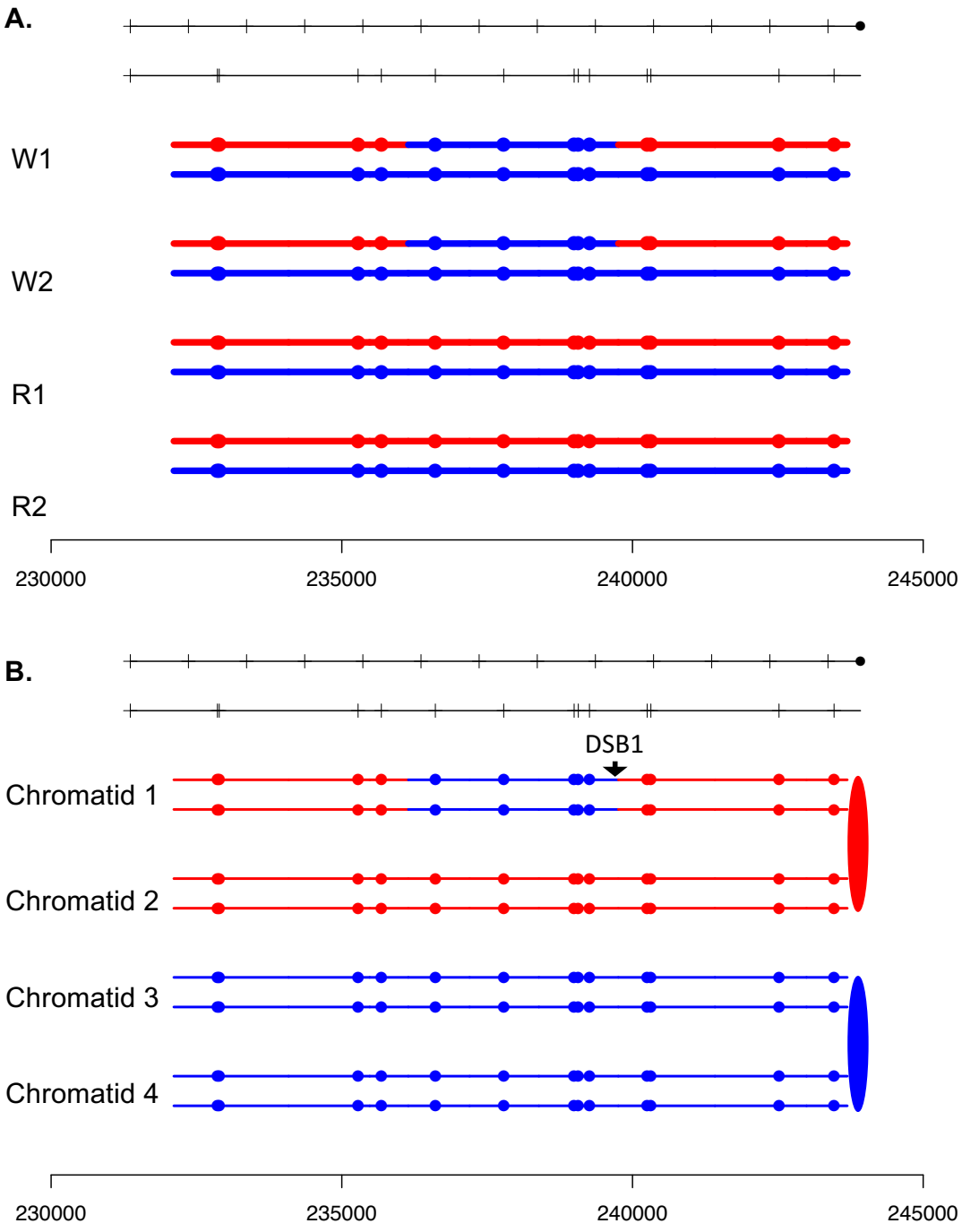
A.
W1
W2
R1
R2
230000
235000
240000
245000
B.
DSB1
Chromatid 1
Chromatid 2
Chromatid 3
Chromatid 4
230000
235000
240000
245000

Fig.S50

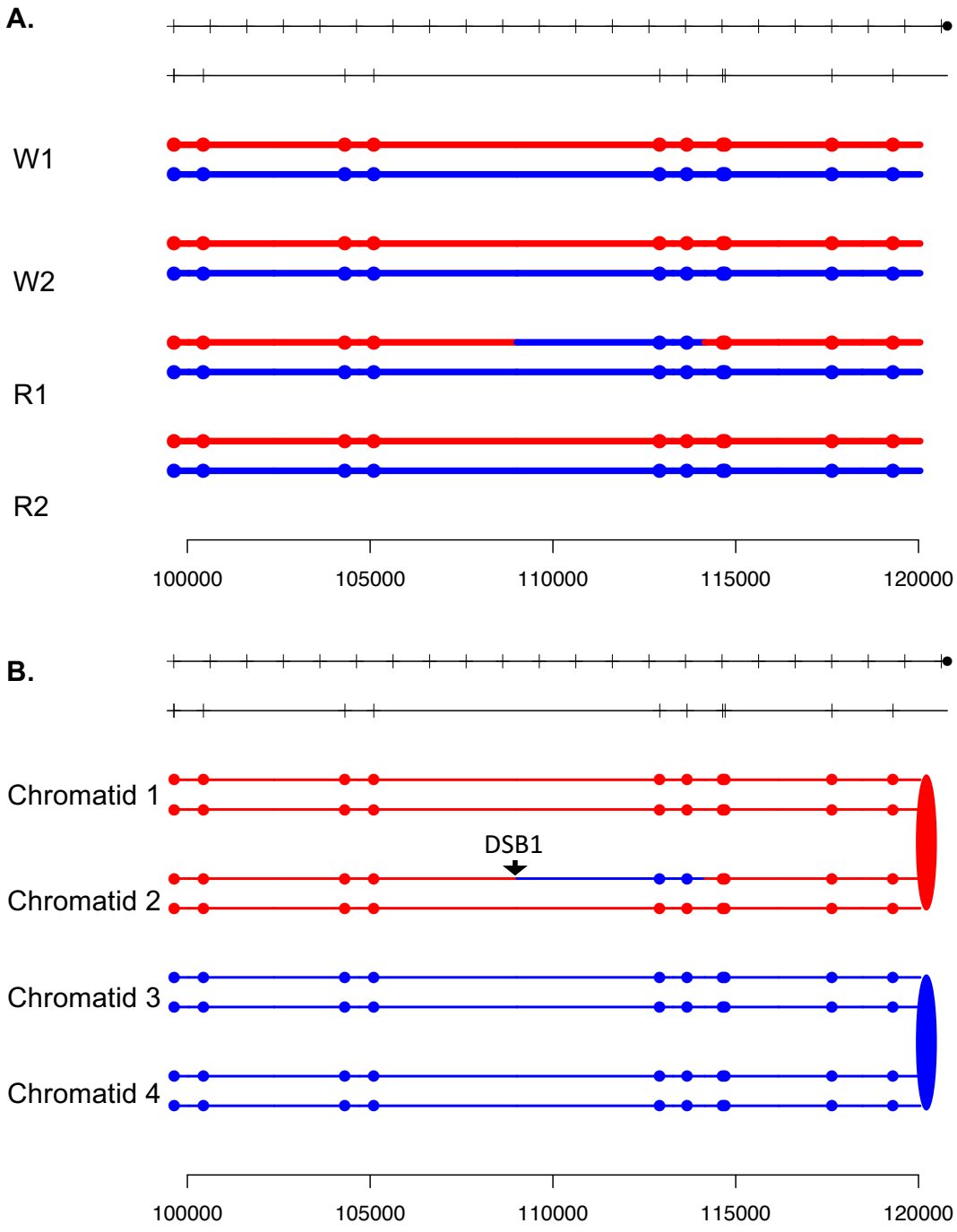
A.
W1
W2
R1
R2
100000
105000
110000
115000
120000
B.
Chromatid 1
DSB1
Chromatid 2
Chromatid 3
Chromatid 4
100000
105000
110000
115000
120000

Fig.S51

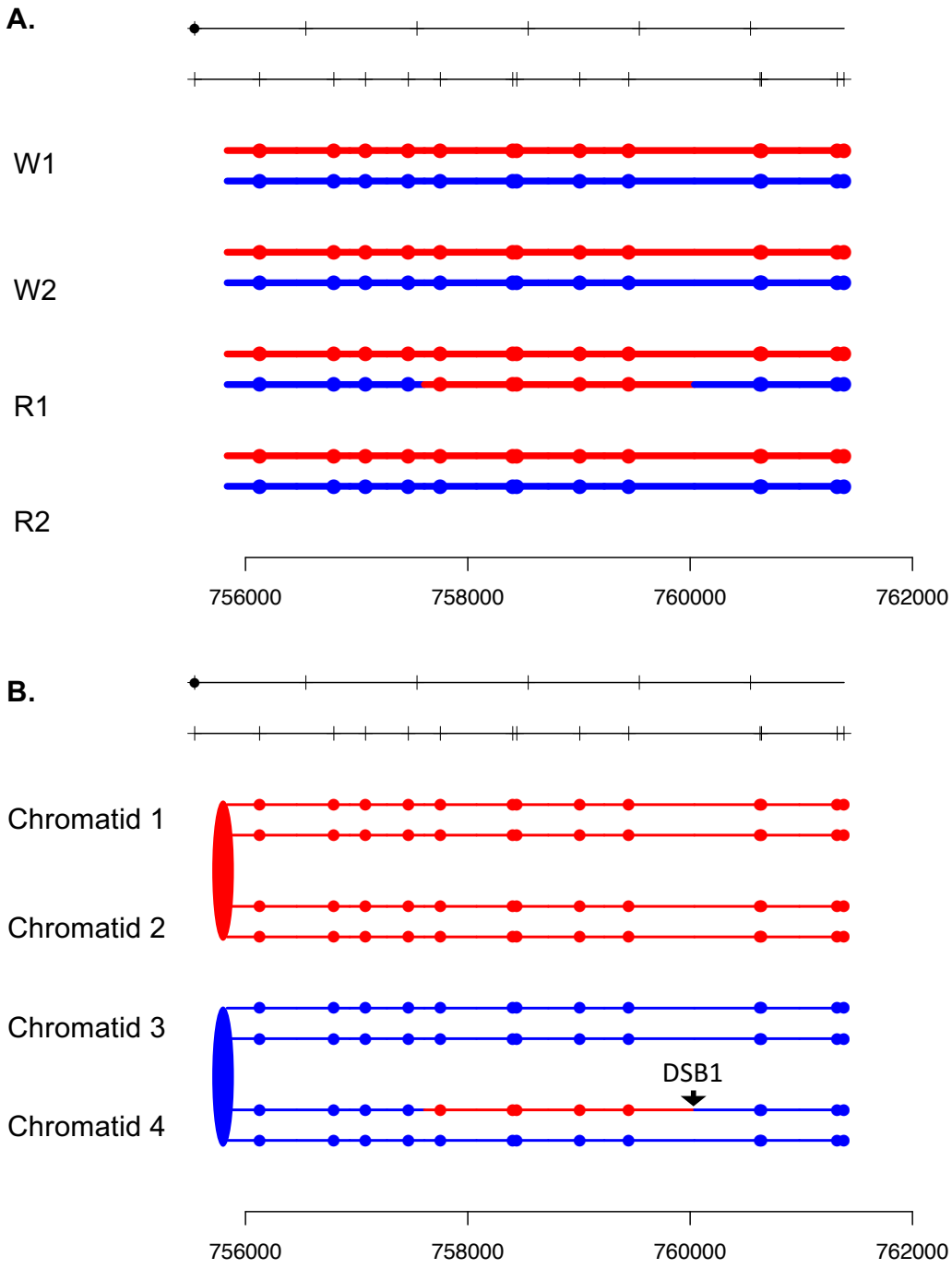
A.
W1
W2
R1
R2
756000
758000
760000
762000
B.
Chromatid 1
Chromatid 2
Chromatid 3
Chromatid 4
DSB1
756000
758000
760000
762000

Fig.S52

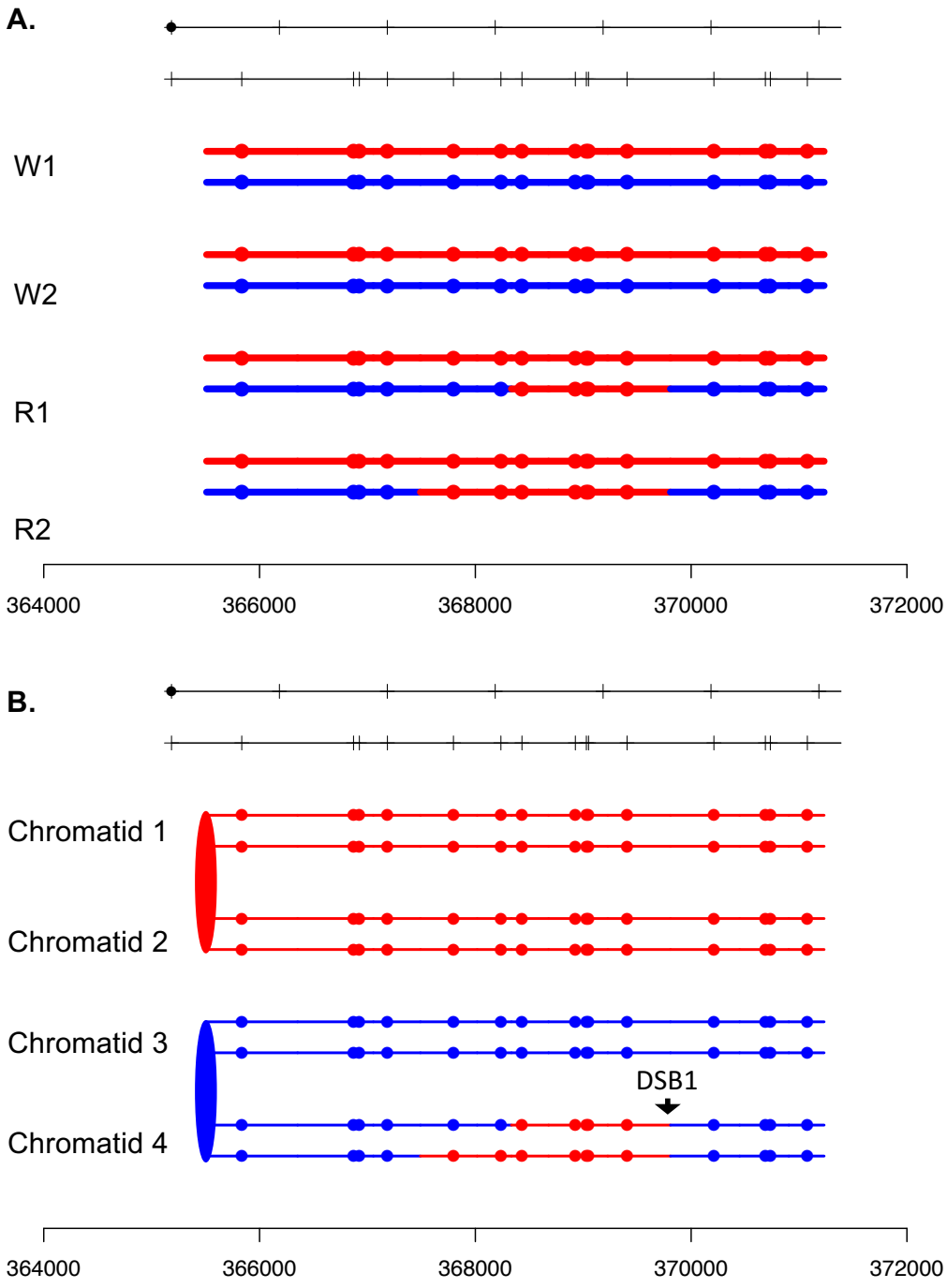
A.
W1
W2
R1
R2
364000
366000
368000
370000
372000
B.
Chromatid 1
Chromatid 2
Chromatid 3
Chromatid 4
DSB1
364000
366000
368000
370000
372000

Fig.S53

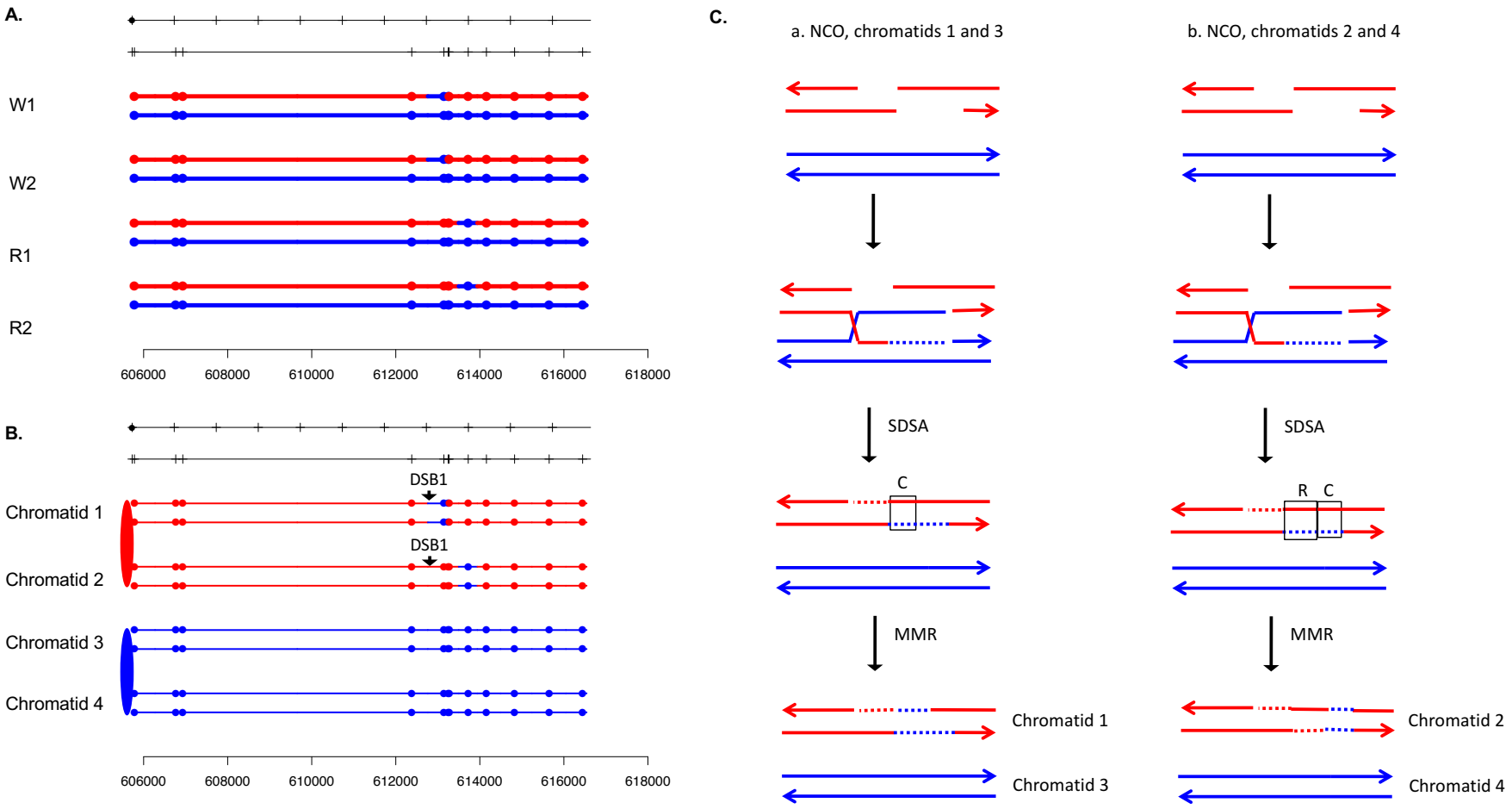

S53	NCO1	Conversion tract with no heteroduplex in chromatid 1	Mlh1-independent MMR
	NCO2	Conversion and restoration tracts in chromatid 2	Mlh1-independent patchy MMR

Fig.S54

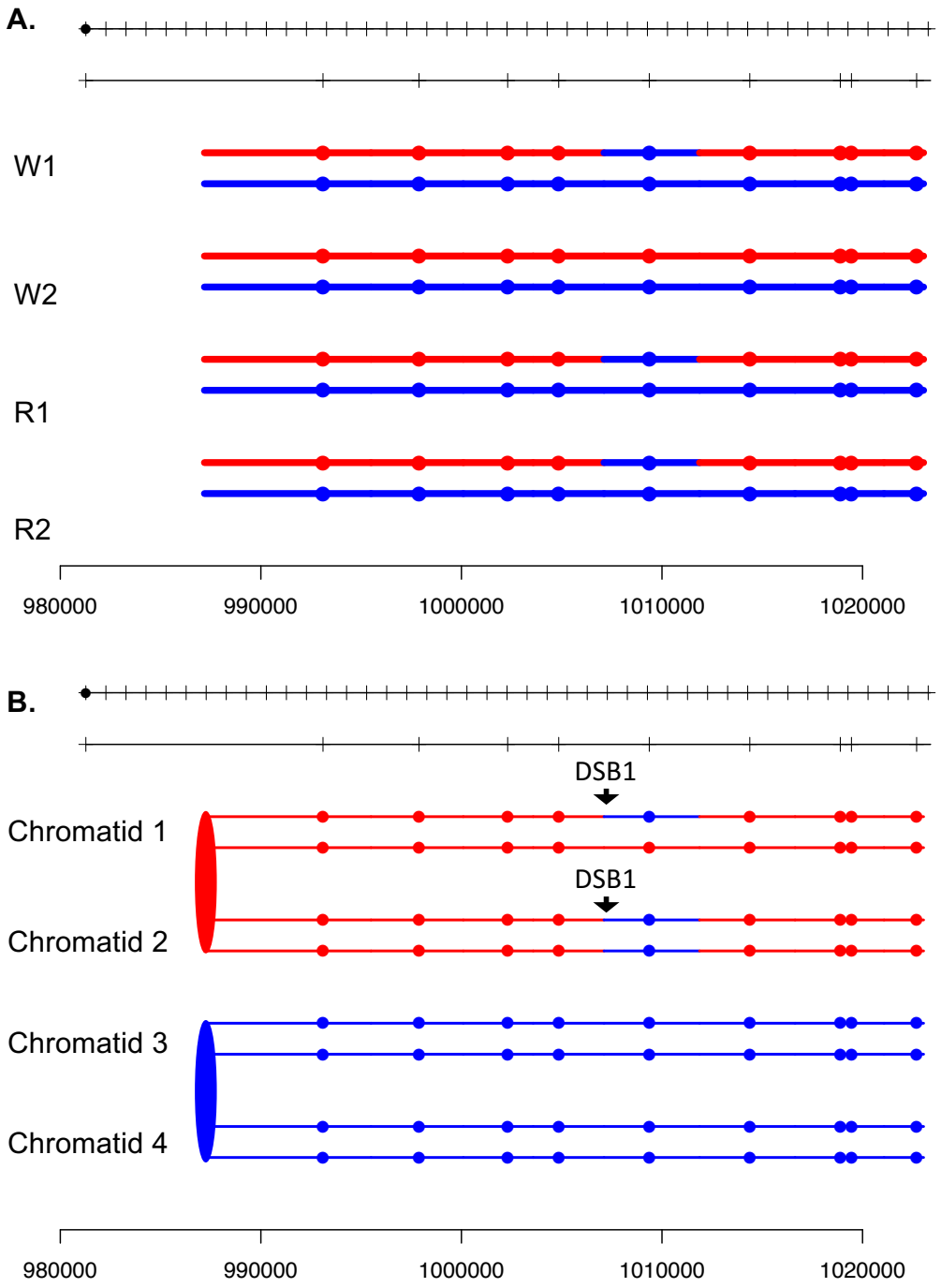
A.
W1
W2
R1
R2
980000
990000
1000000
1010000
1020000
B.
DSB1
DSB1
Chromatid 1
Chromatid 2
Chromatid 3
Chromatid 4
980000
990000
1000000
1010000
1020000

Fig.S55

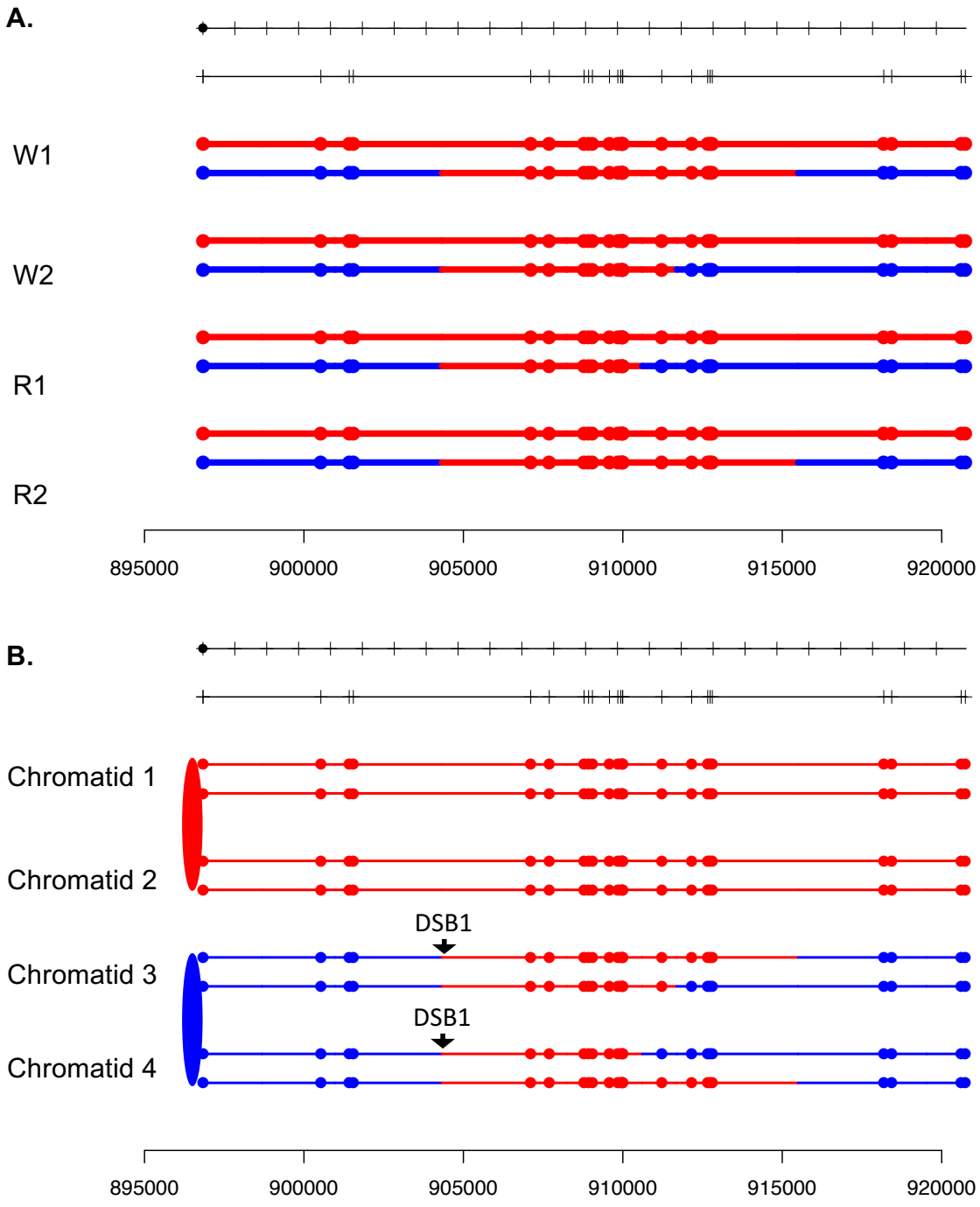
A.
W1
W2
R1
R2
895000
900000
905000
910000
915000
920000
B.
Chromatid 1
Chromatid 2
DSB1
Chromatid 3
DSB1
Chromatid 4
895000
900000
905000
910000
915000
920000

Fig.S56

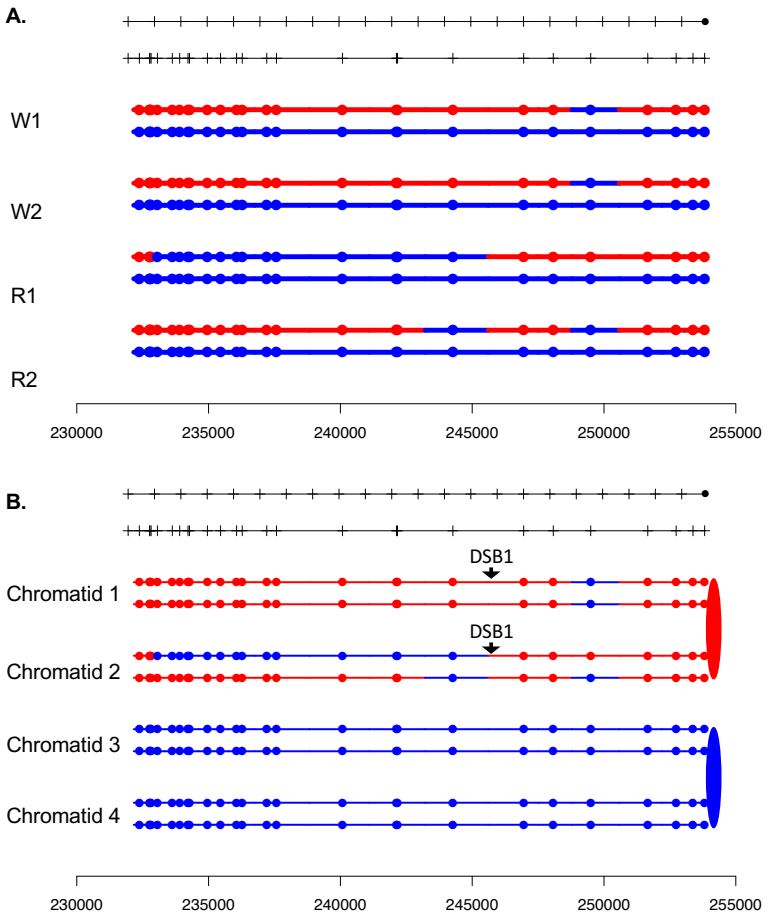

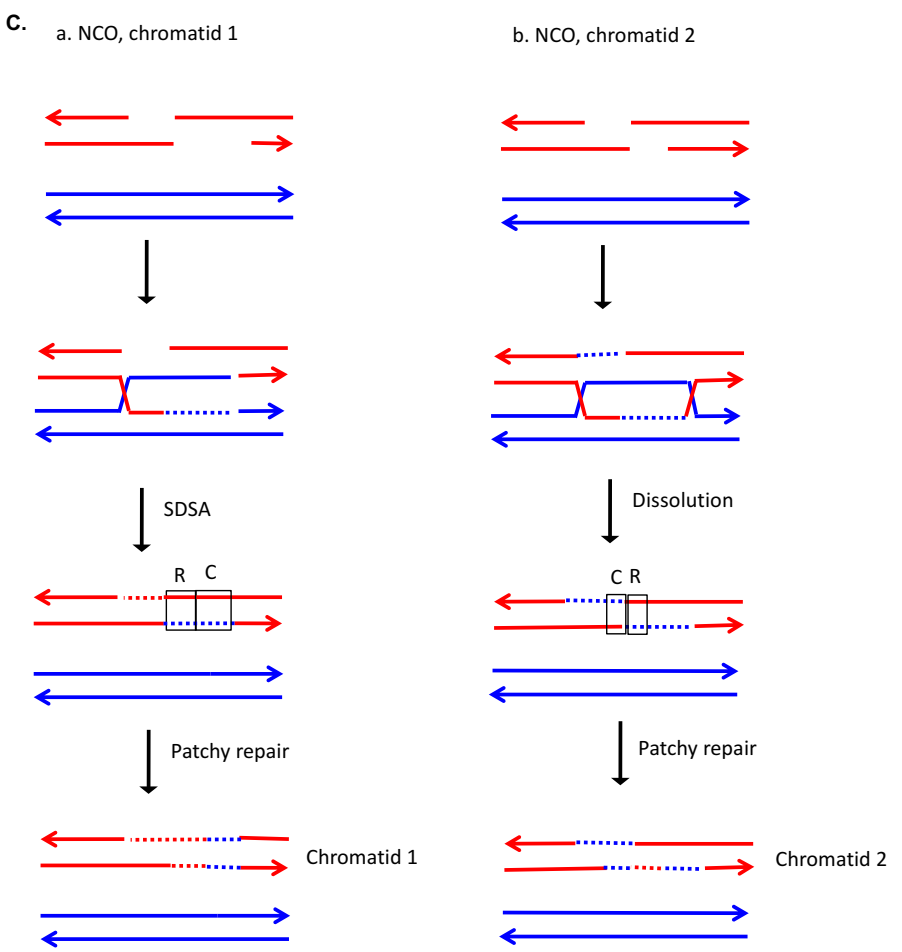

S56	NCO1	Conversion tract with no heteroduplex in chromatid 1	Mlh1-independent MMR
	NCO2	Conversion and restoration tracts in chromatid 2	Mlh1-independent patchy MMR

Fig.S57

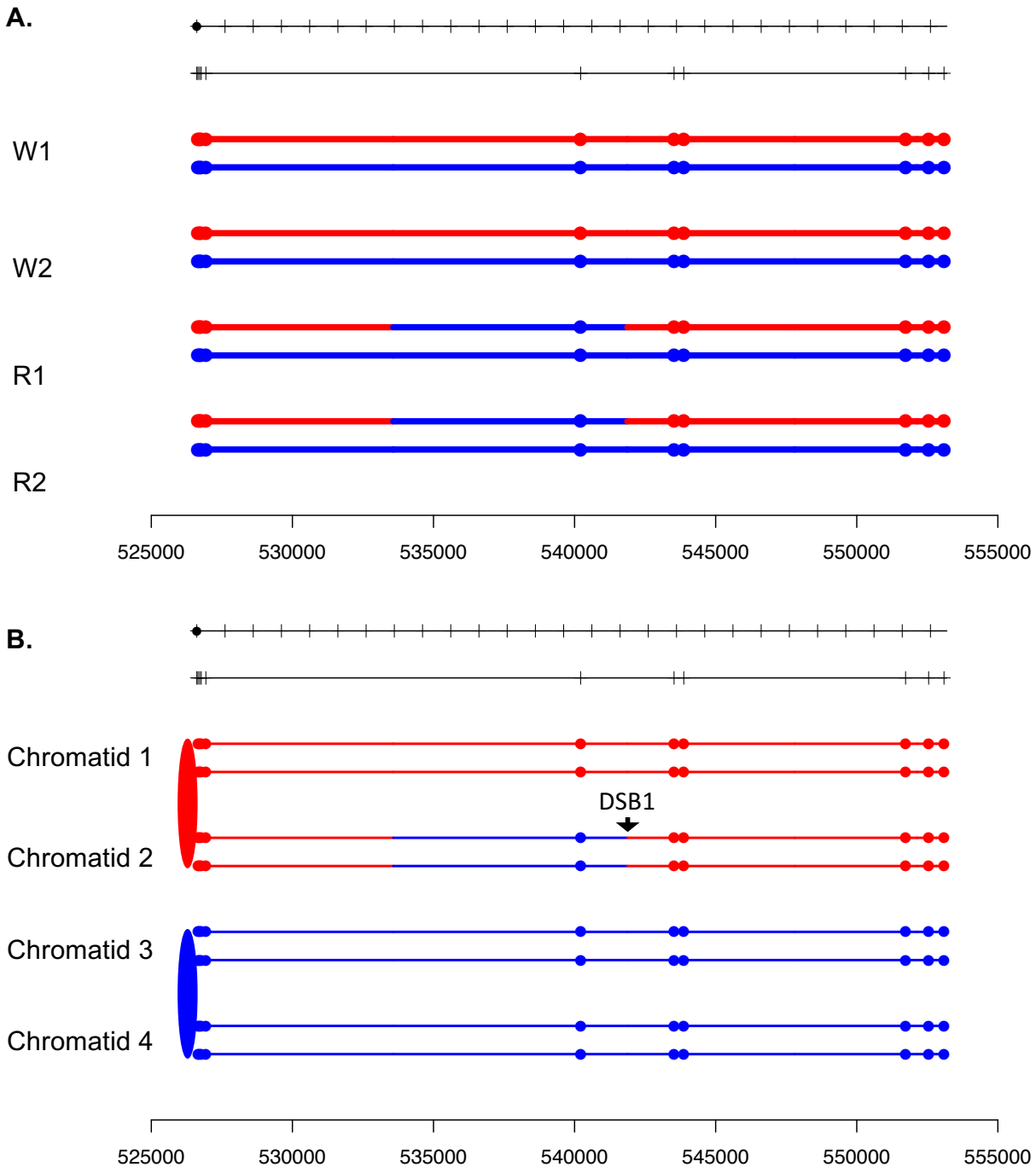
A.
W1
W2
R1
R2
525000
530000
535000
540000
545000
550000
555000
B.
Chromatid 1
Chromatid 2
Chromatid 3
Chromatid 4
DSB1
525000
530000
535000
540000
545000
550000
555000

Fig.S58

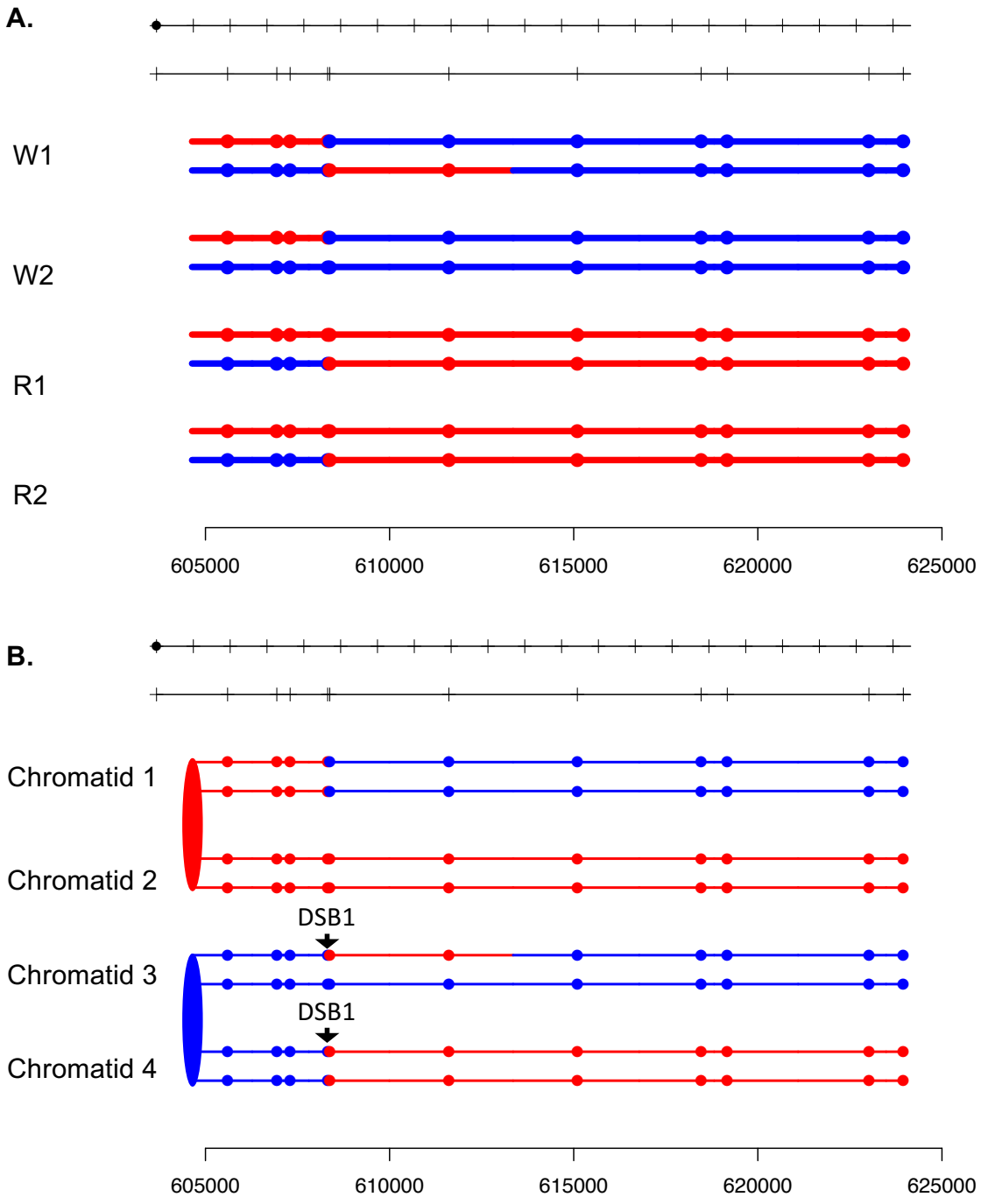
A.
W1
W2
R1
R2
605000
610000
615000
620000
625000
B.
Chromatid 1
Chromatid 2
DSB1
Chromatid 3
DSB1
Chromatid 4
605000
610000
615000
620000
625000

Fig.S59

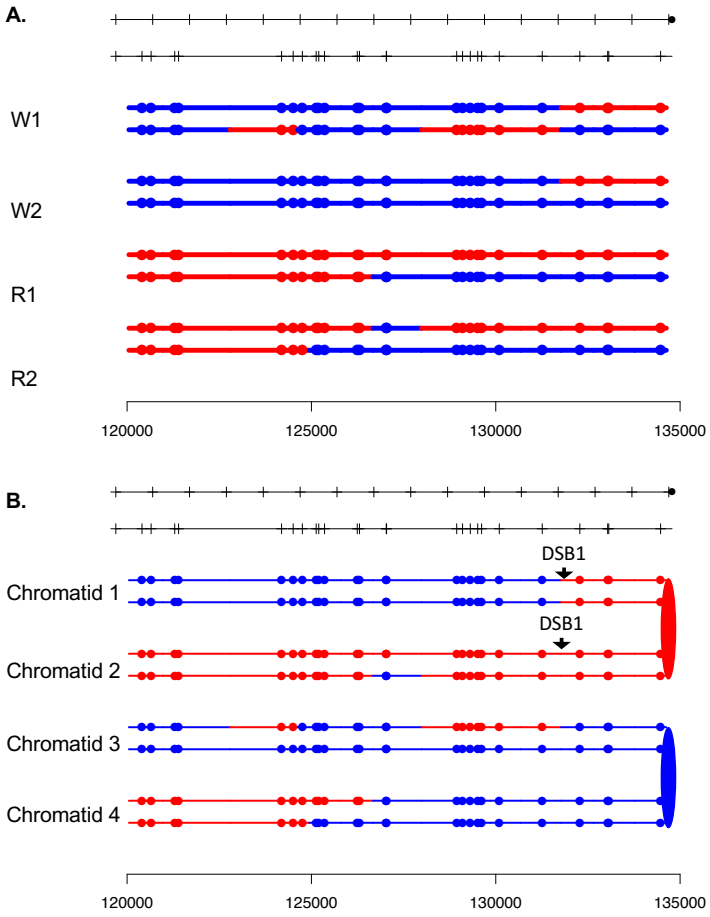

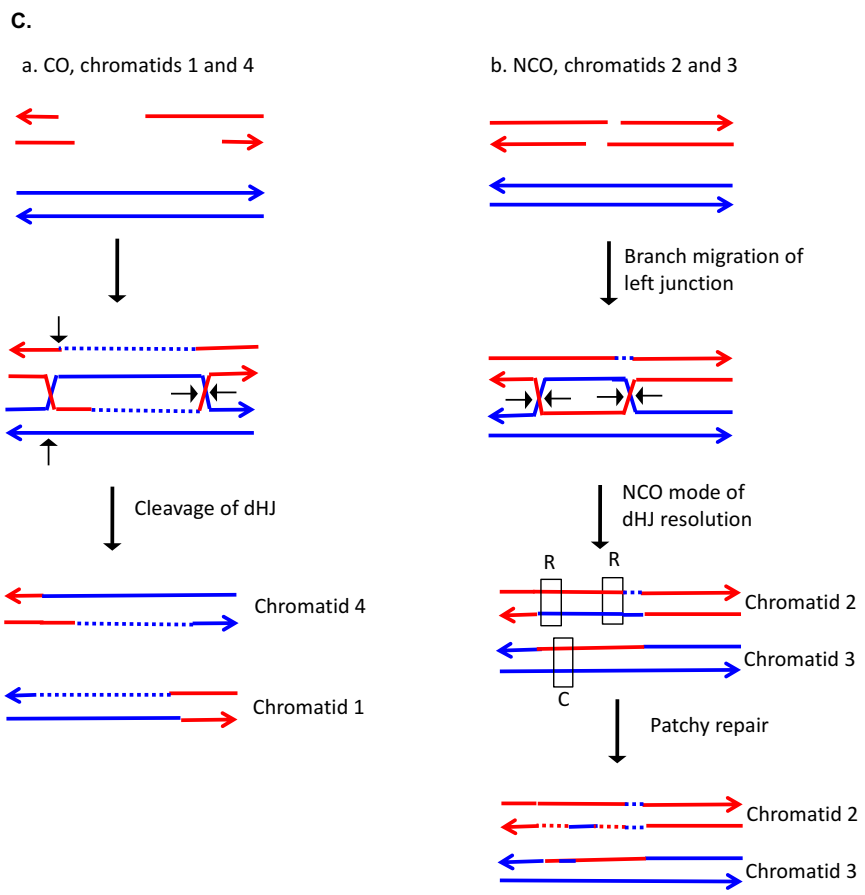

S59	CO	Long conversion tract between heteroduplex and putative DSB site on chromatid 4	Repair of double-stranded DNA gap
	NCO	Regions of conversion/restoration and heteroduplex on same side of putative DSB site in chromatids 3 and 4	Branch migration; NCO resolution of dHJ; Mlh1-independent patchy repair

Fig.S60

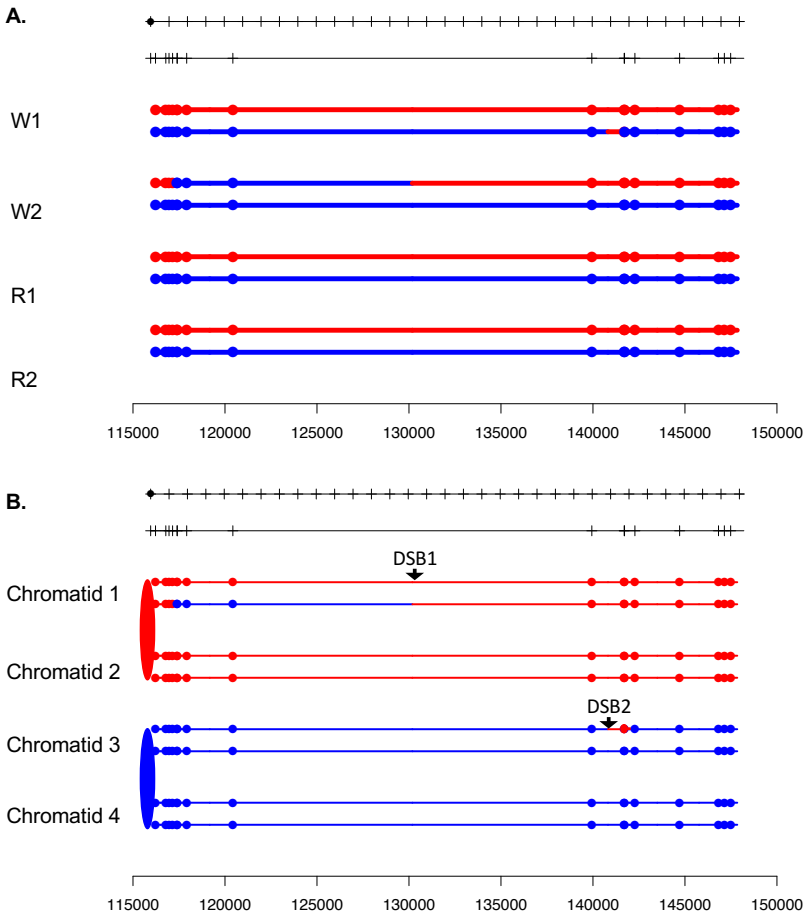

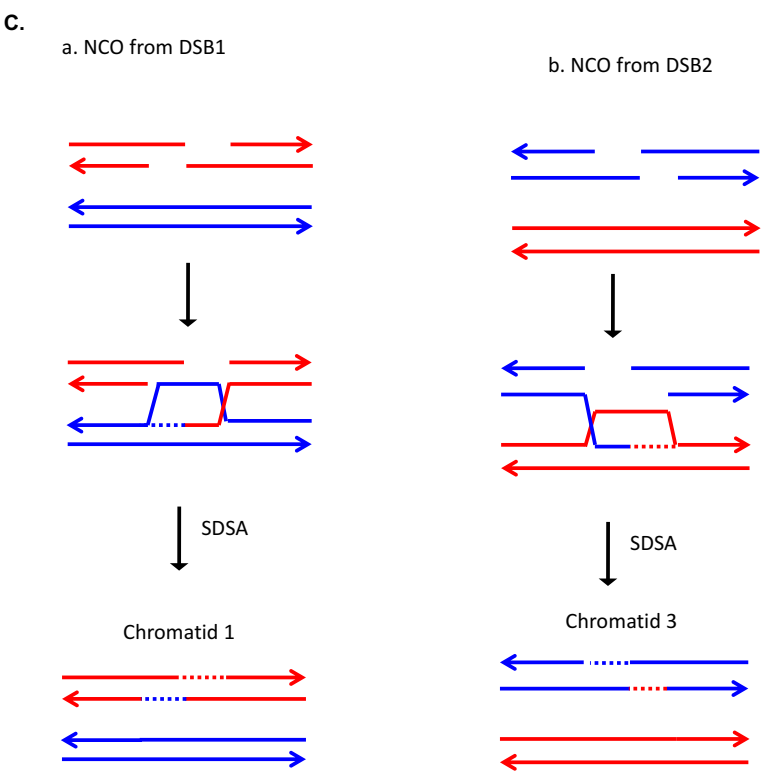

S60	NCO1	Simple heteroduplex. DSB on red chromatid.	SDSA
	NCO2	Simple heteroduplex. DSB on blue chromatid.	SDSA

Fig.S61

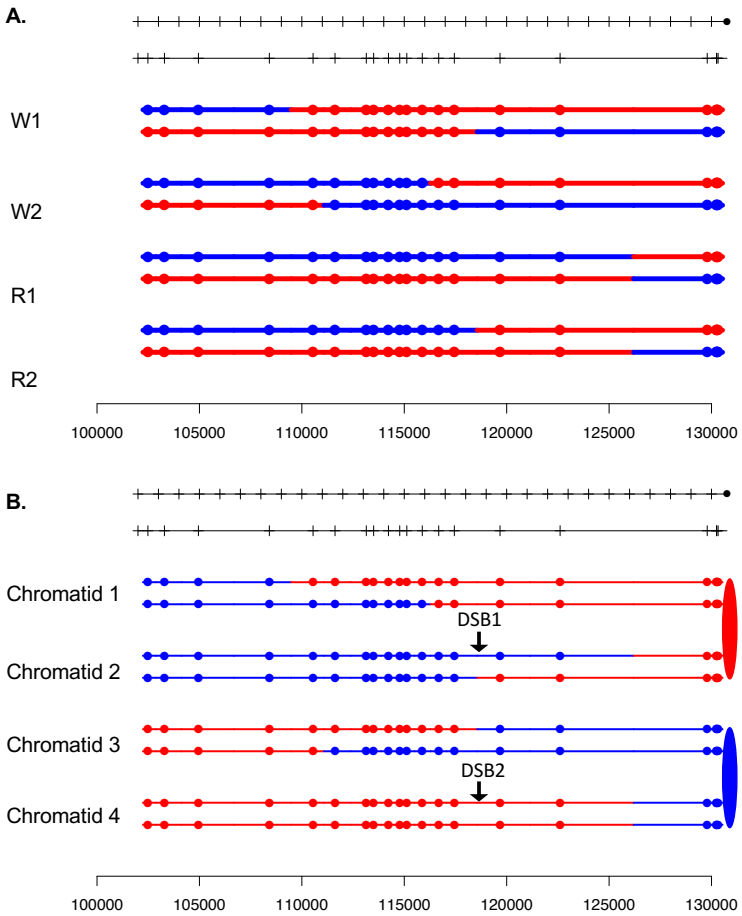

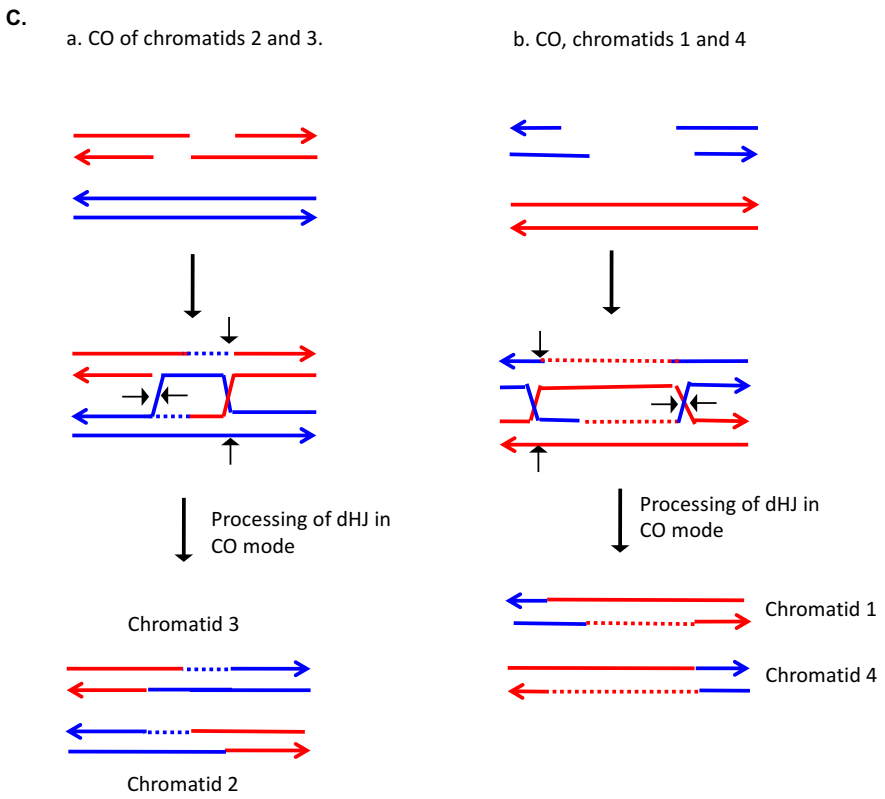

S61	CO1	Uni-directional heteroduplexes on chromatids 2 and 3 propagated in opposite directions	Crossover by standard DSBR model
	CO2	DSB on blue chromatid, large conversion tract	Repair of double-stranded DNA gap; followed by cleavage of dHJ to yield a CO

Fig.S62

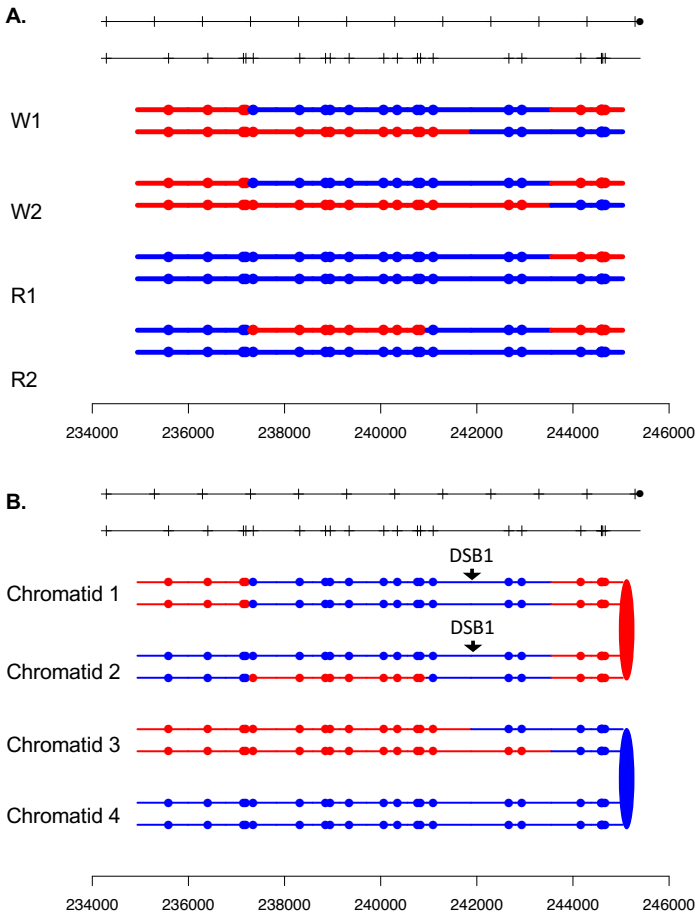

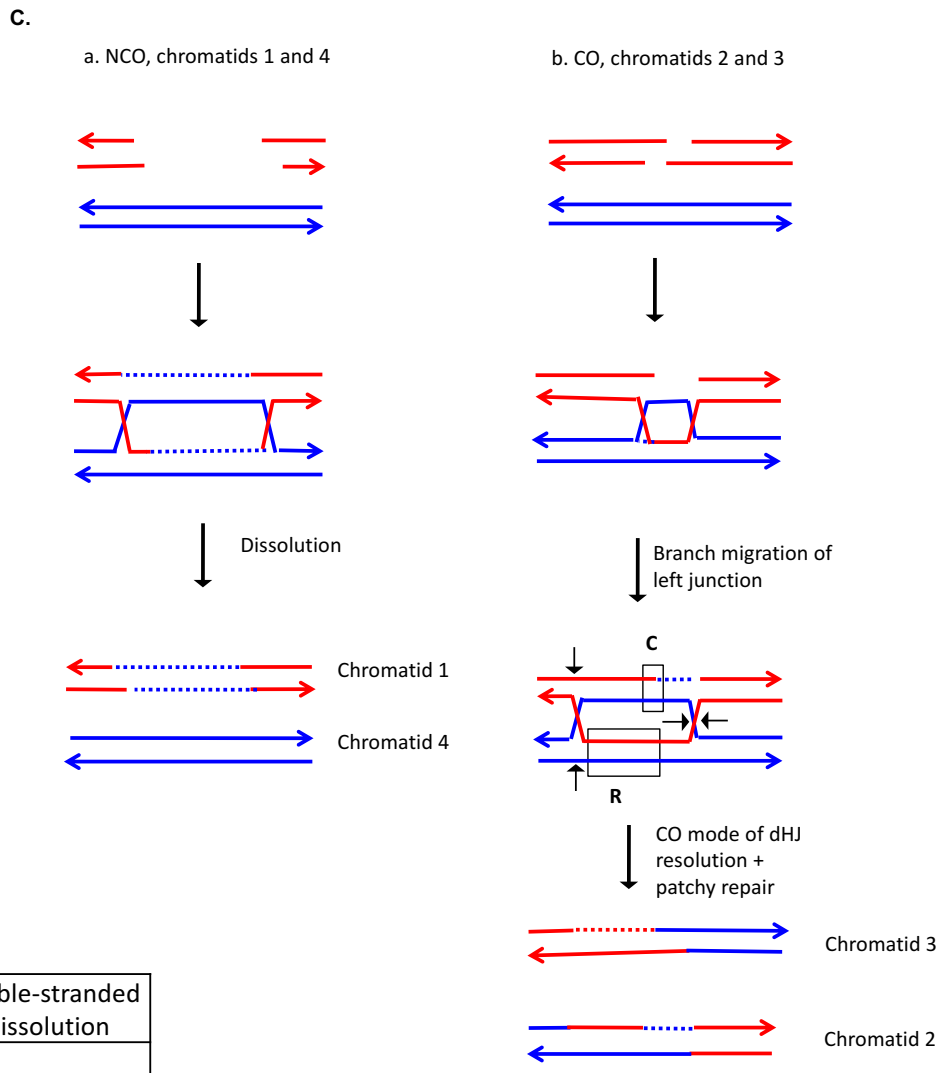

S62	NCO	Conversion tract spanning putative DSB site in chromatid 1	Repair of double-stranded DNA gap; dissolution
	CO	Uni-directional heteroduplexes on chromatids 2 and 3; propagated in opposite directions; interspersed conversion and restoration tracts	Mlh1-independent MMR

Fig.S63

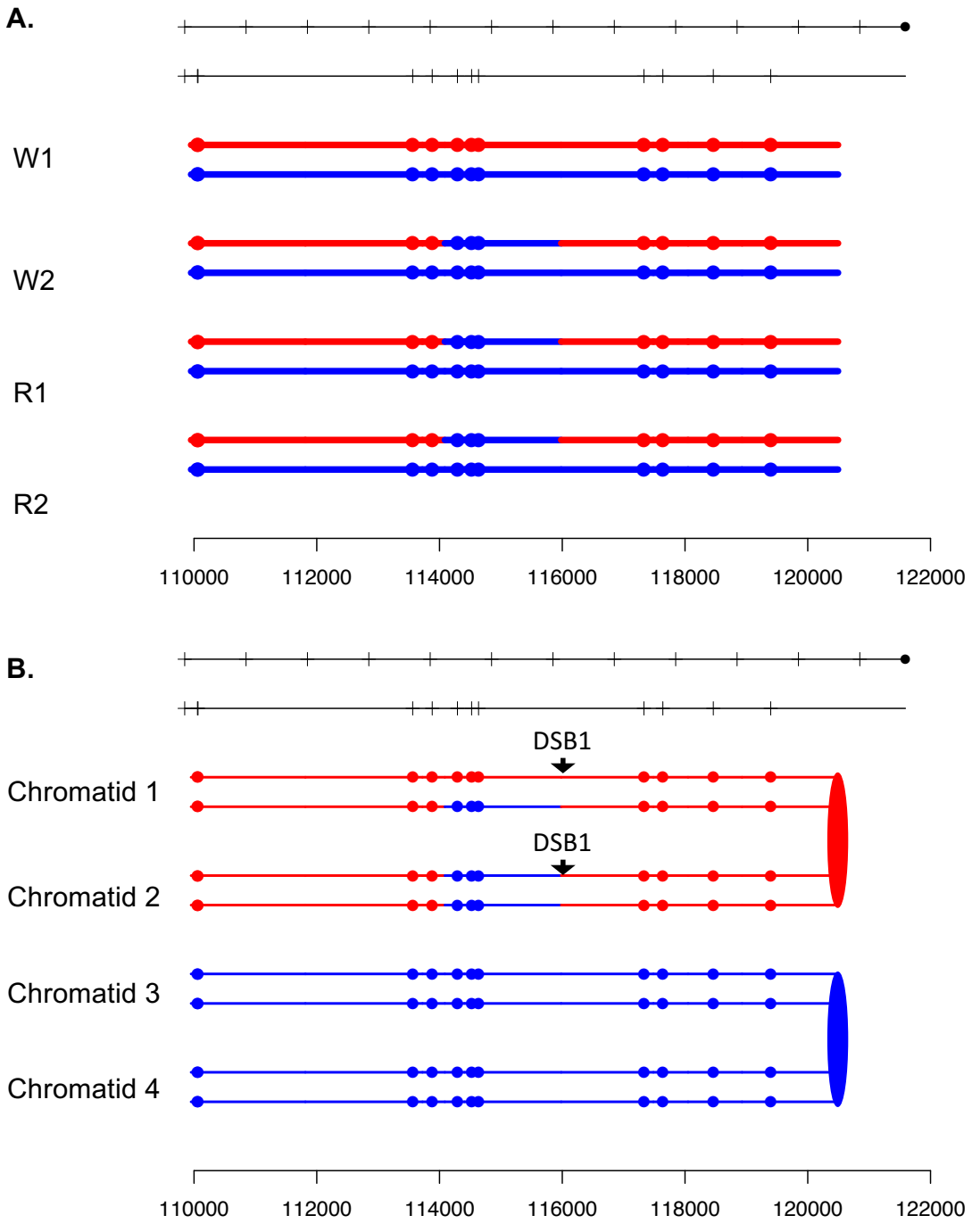
A.
W1
W2
R1
R2
110000
112000
114000
116000
118000
120000
122000
B.
DSB1
DSB1
Chromatid 1
Chromatid 2
Chromatid 3
Chromatid 4
110000
112000
114000
116000
118000
120000
122000

Fig.S64

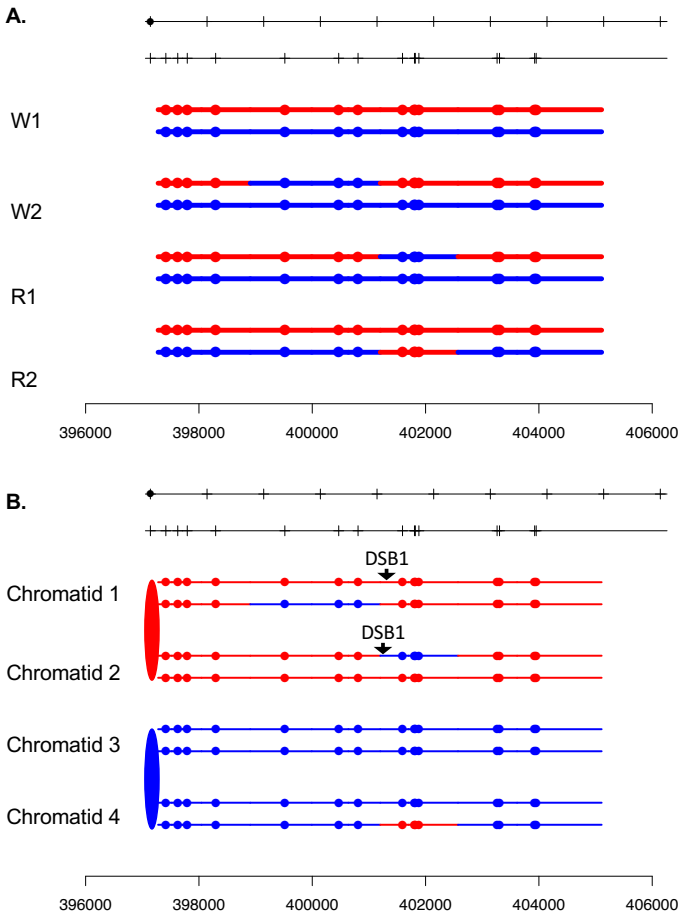

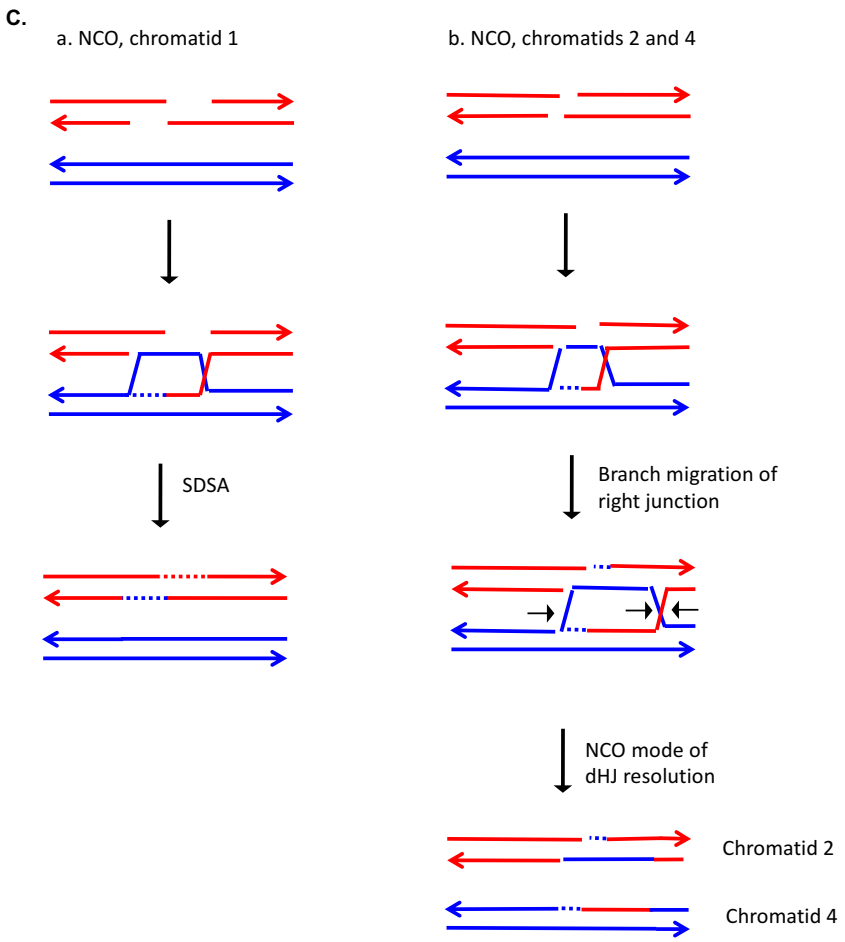

S64	NCO1	Simple heteroduplex (chromatid 1)	SDSA
	NCO2	Heteroduplexes on same side of DSB in chromatids 2 and 4	Branch migration; NCO mode of dHJ resolution

Fig.S65

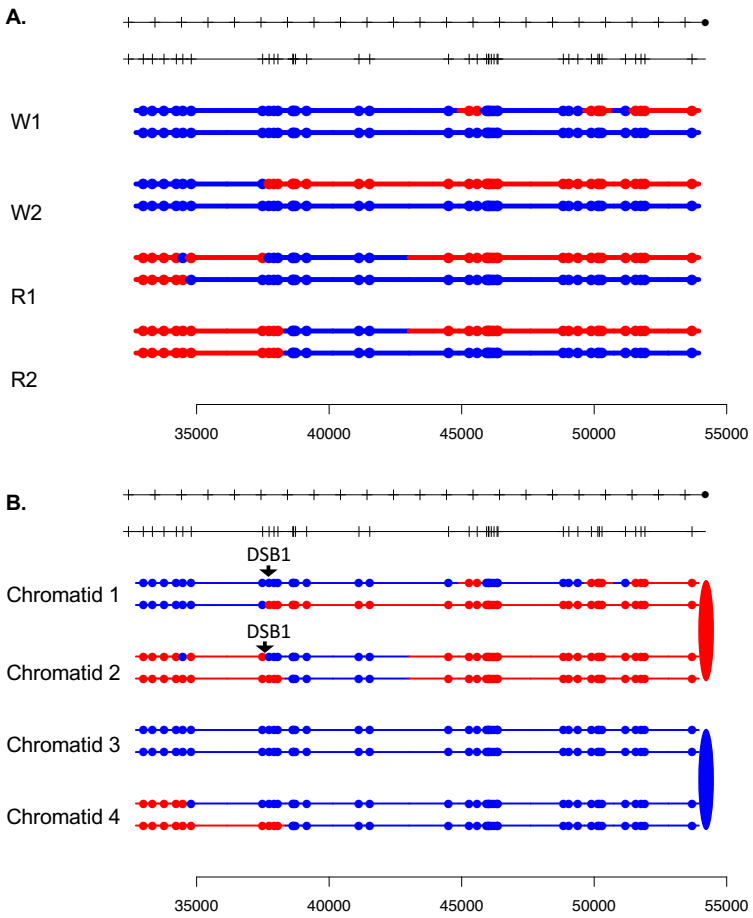

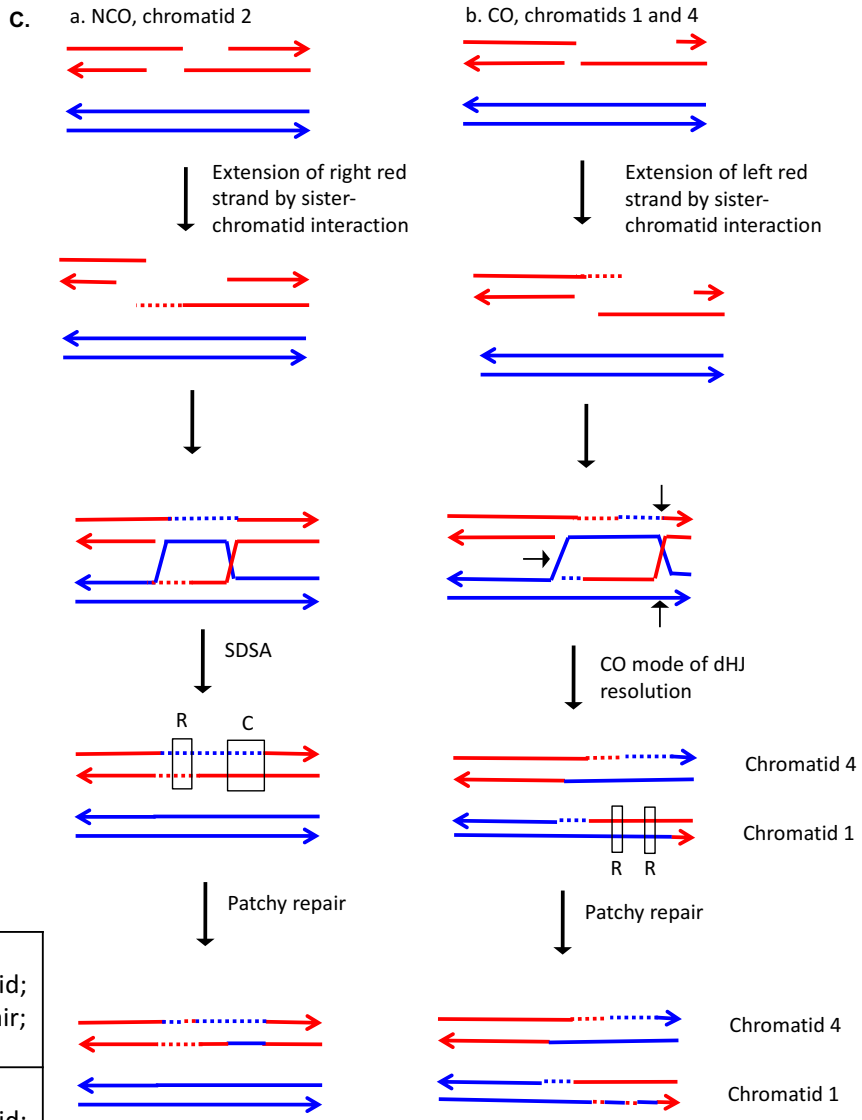

S65	CO	Heteroduplex on same side of DSB site in chromatids 1 and 4; heteroduplex spans DSB site in chromatid 4; tracts of restoration within heteroduplex in chromatid 2	Extension of broken end by interaction with sister chromatid; Mlh1-independent patchy repair; CO resolution of dHJ
	NCO	Heteroduplex spans DSB site in chromatid 2; tracts of conversion and restoration interspersed with heteroduplex regions	Extension of broken end by interaction with sister chromatid; Mlh1-independent patchy repair; SDSA

Fig.S66

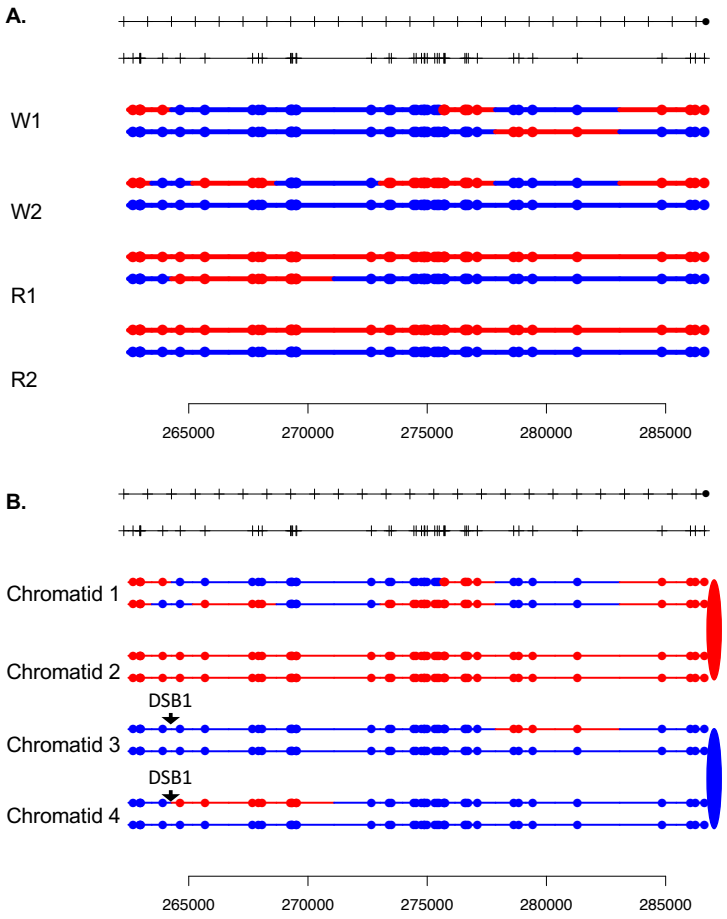

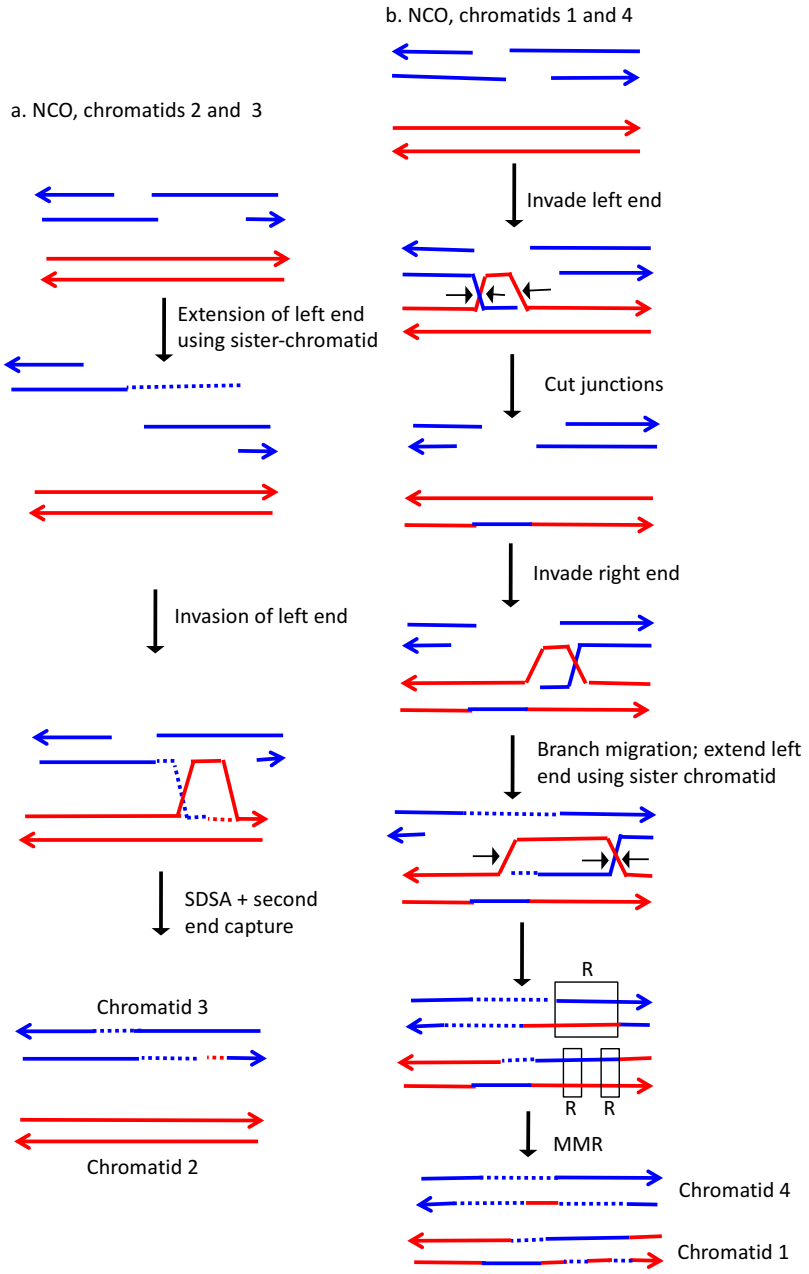

S66	NCO1	Heteroduplex on chromatid 3 separated from putative DSB site by long region of homoduplex	Extension of broken end by interaction with sister chromatid, followed by SDSA
	NCO2	Heteroduplexes on both chromatids 1 and 4; chromatid 1 has trans heteroduplexes flanking the DSB site in addition to regions of homoduplex within the heteroduplex	Invasion of right end, followed by cleavage of junction and invasion of left end; branch migration; Mlh1-independent patchy repair

Fig.S67

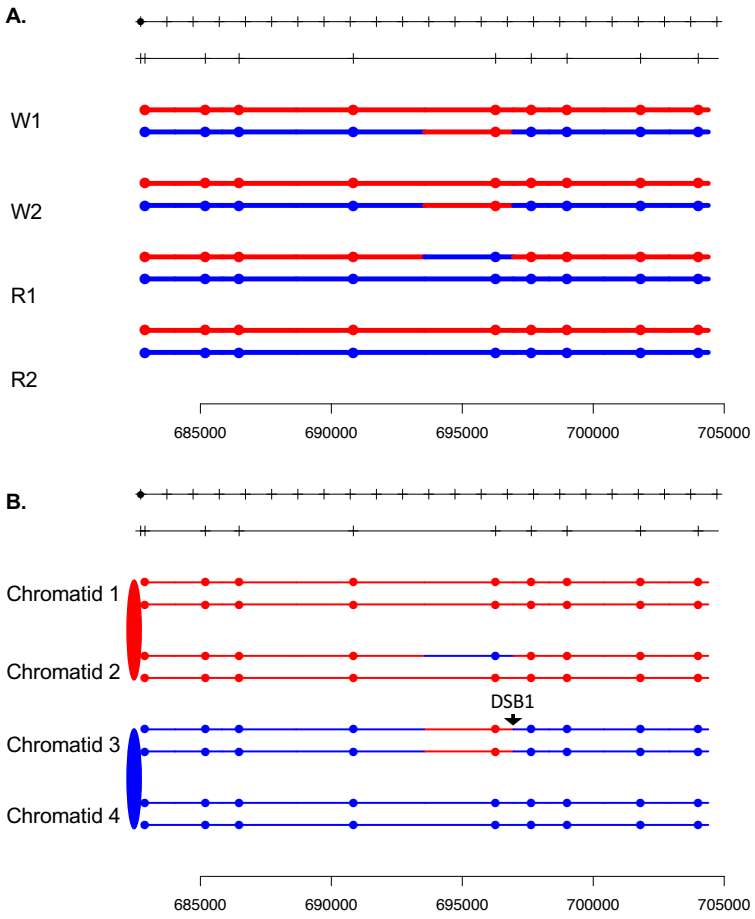

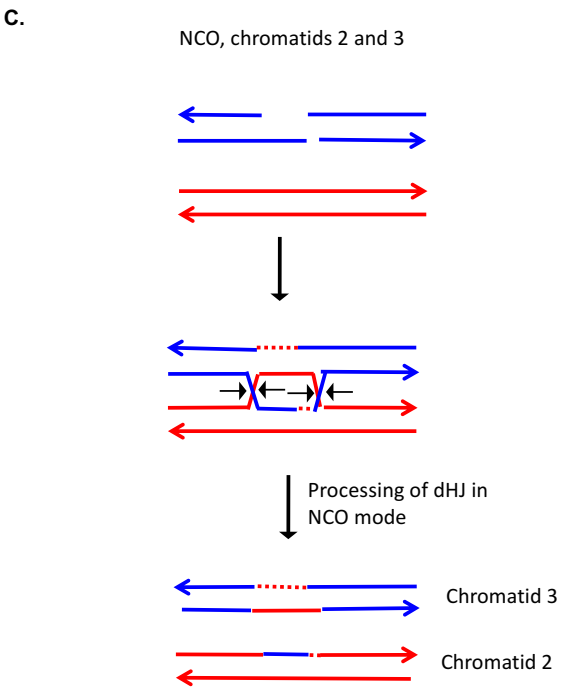

S67	NCO	Uni-directional heteroduplexes on chromatids 2 and 3 propagated in opposite directions	NCO mode of dHJ resolution with limited synthesis

Fig.S68

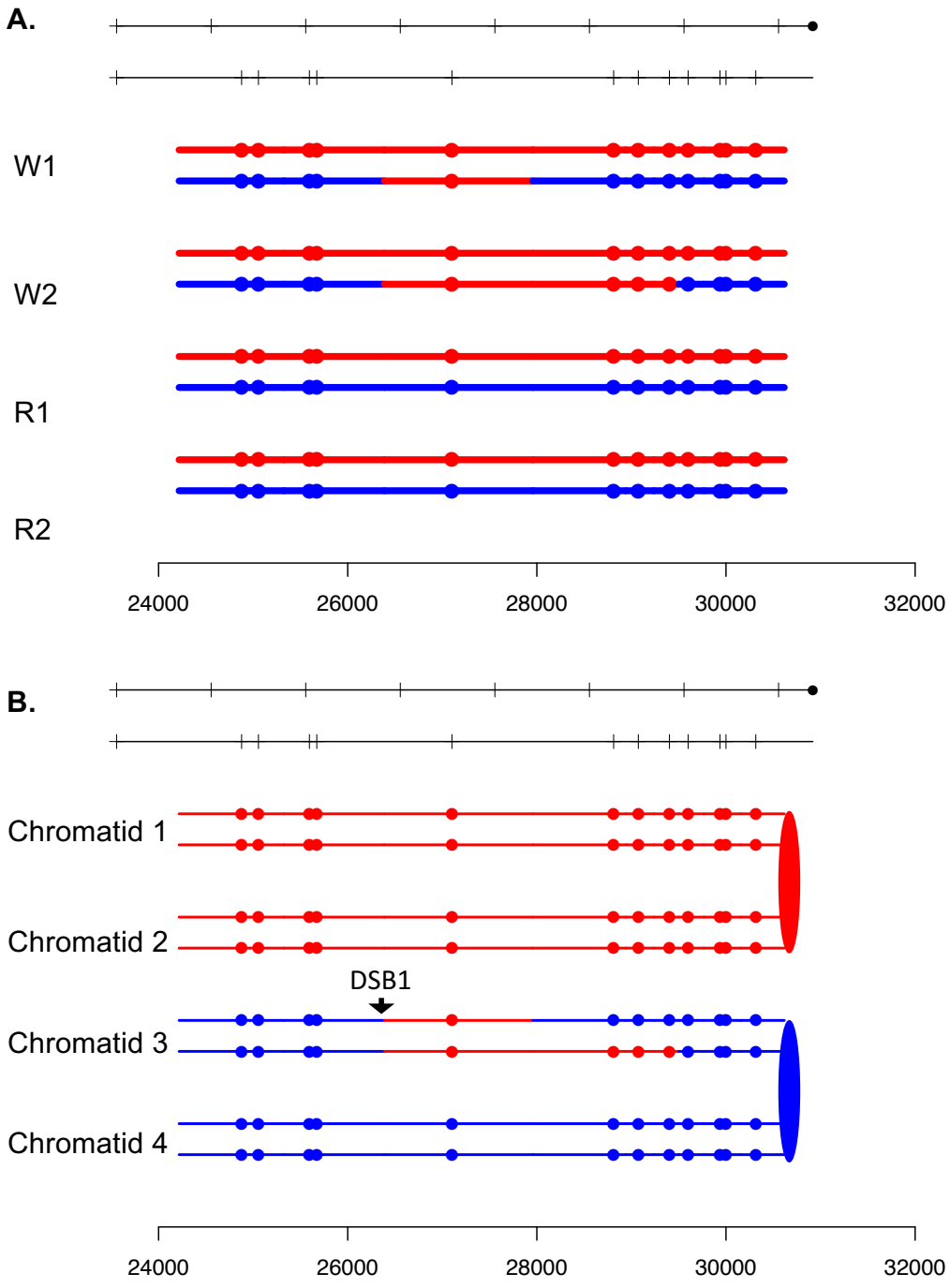
A.
W1
W2
R1
R2
24000
26000
28000
30000
32000
B.
Chromatid 1
Chromatid 2
DSB1
Chromatid 3
Chromatid 4
24000
26000
28000
30000
32000

Fig.S69

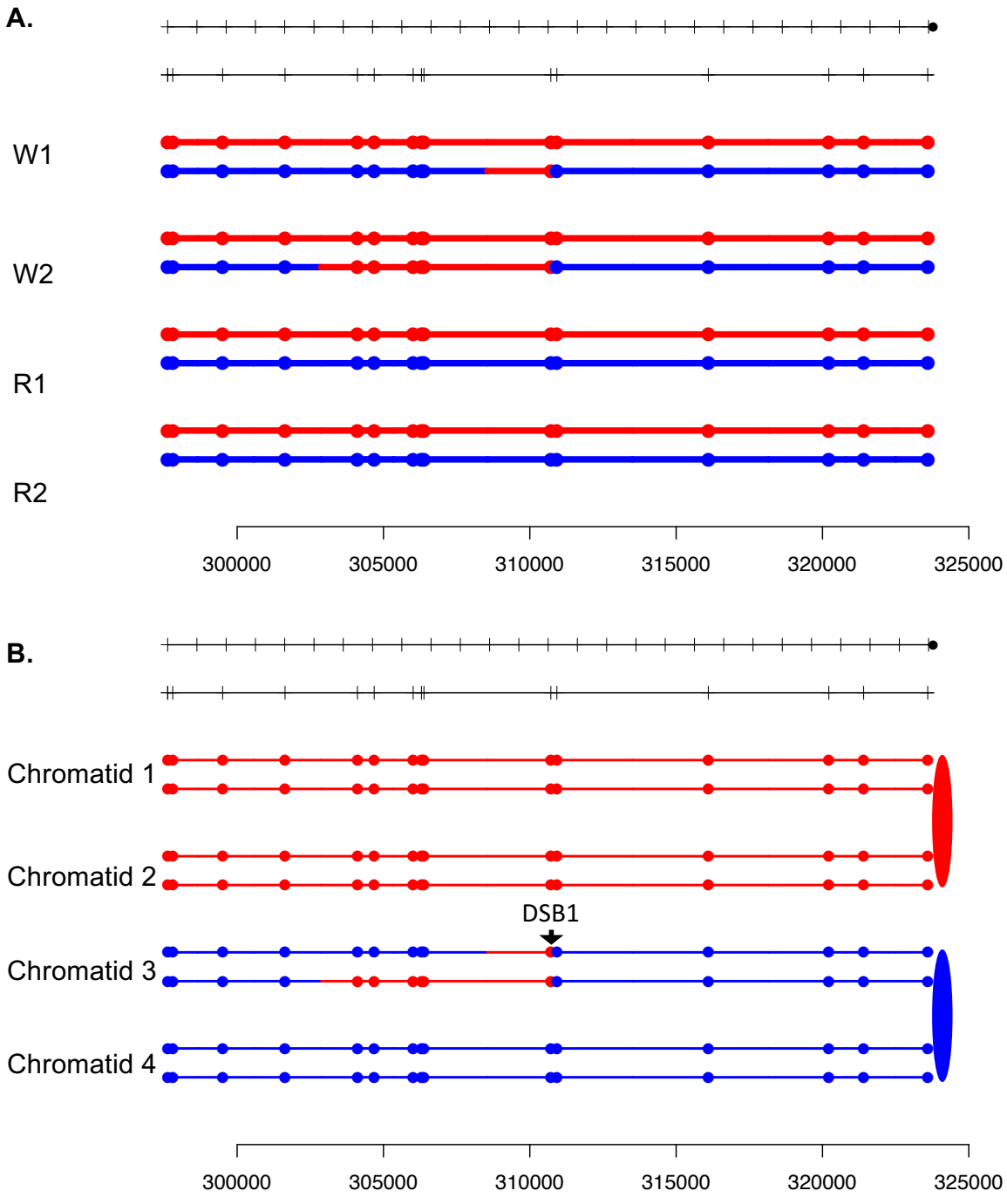
A.
W1
W2
R1
R2
300000
305000
310000
315000
320000
325000
B.
Chromatid 1
Chromatid 2
DSB1
Chromatid 3
Chromatid 4
300000
305000
310000
315000
320000
325000

Fig.S70

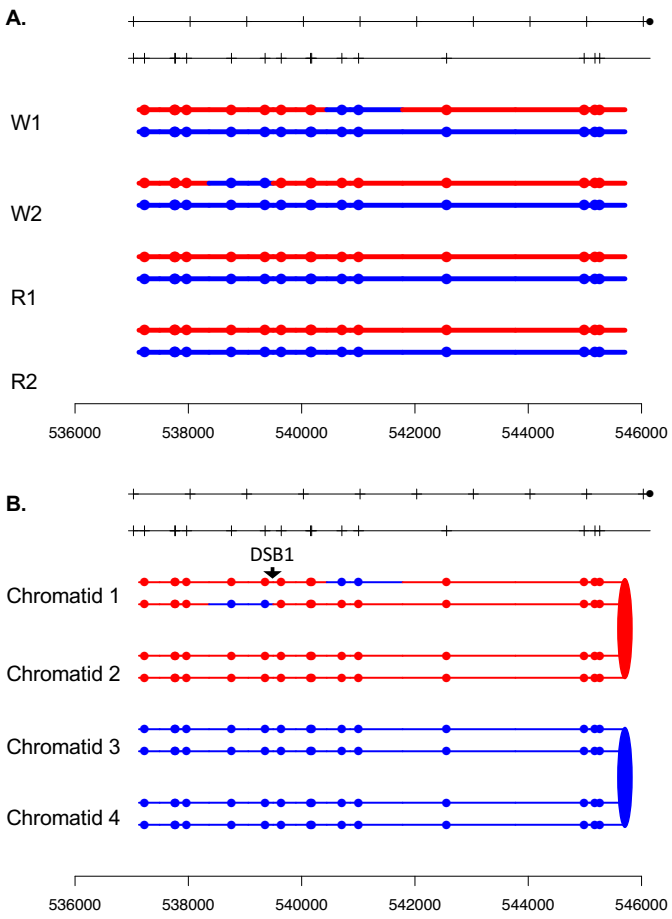

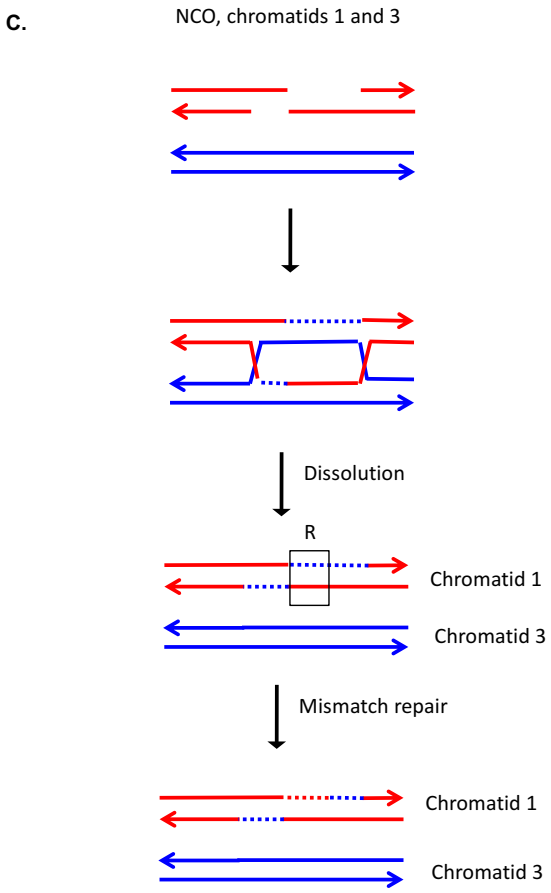

S70	NCO	*Trans* heteroduplexes separated by restoration tract on chromatid 1	Formation of dHJ event; dissolution followed by Mlh1-independent repair

Fig.S71

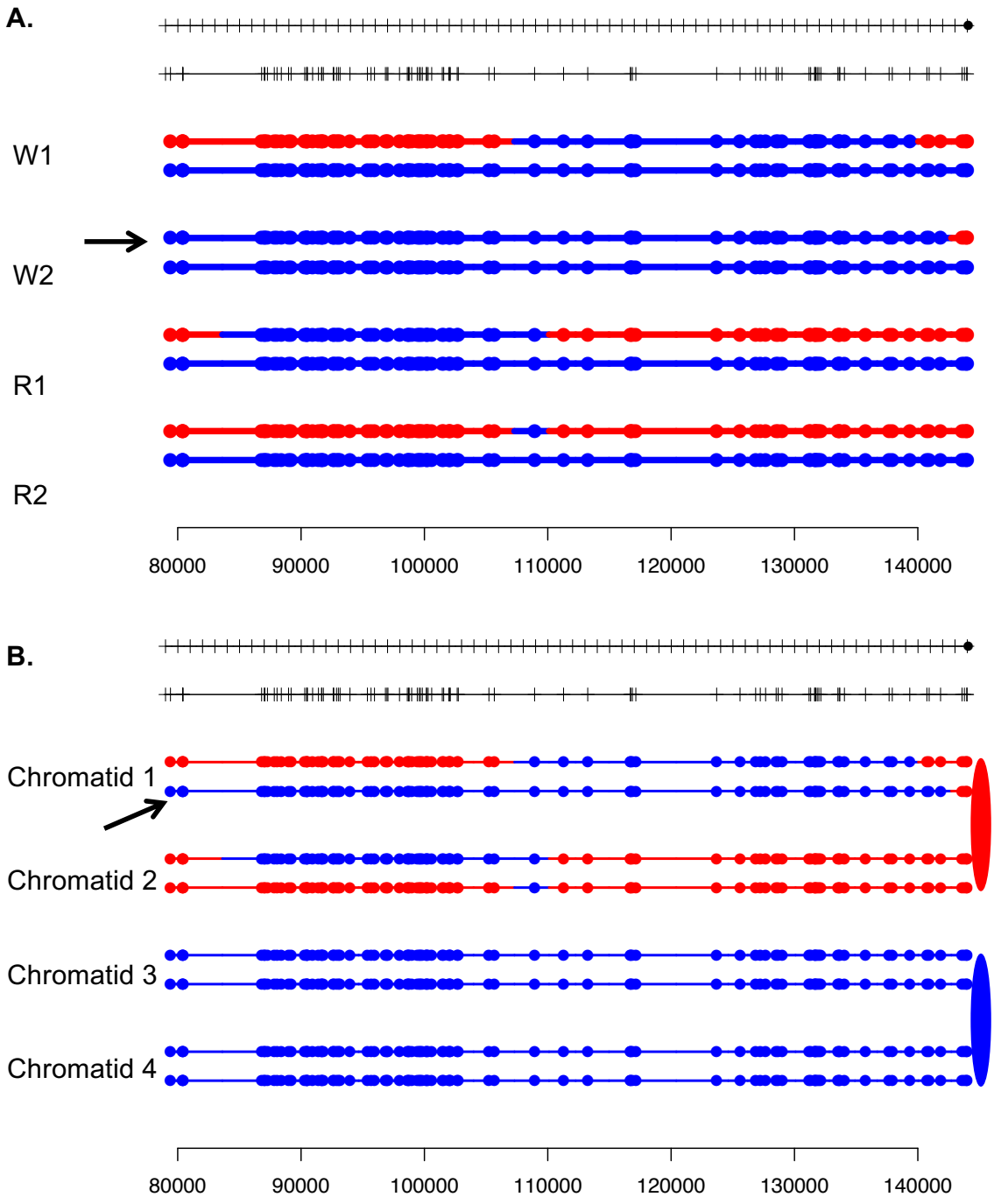
A.
W1
W2
R1
R2
80000
90000
100000
110000
120000
130000
140000
B.
Chromatid 1
Chromatid 2
Chromatid 3
Chromatid 4
80000
90000
100000
110000
120000
130000
140000

Fig.S72

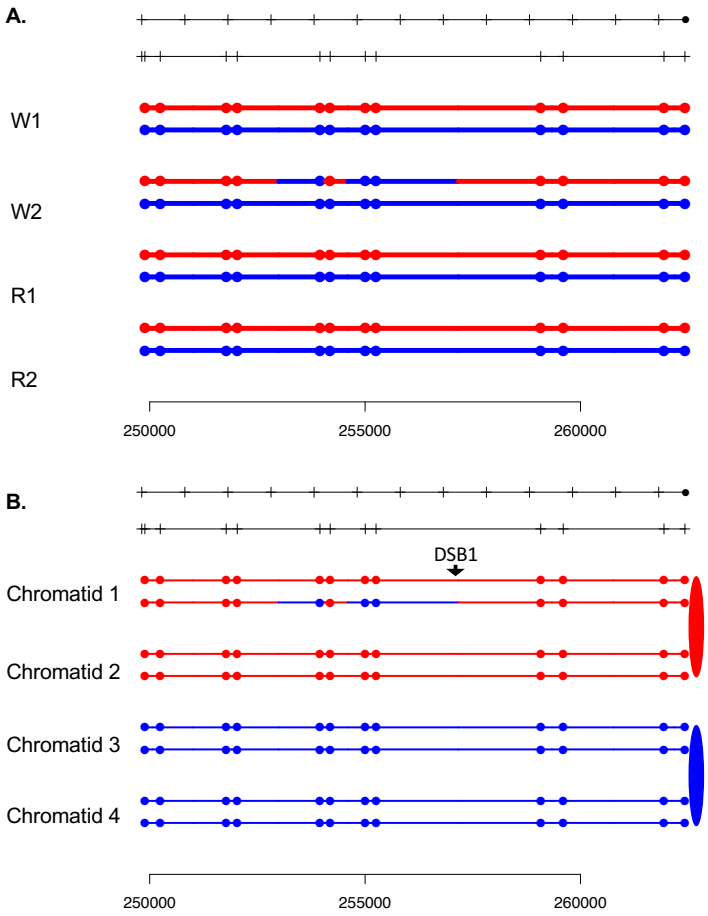

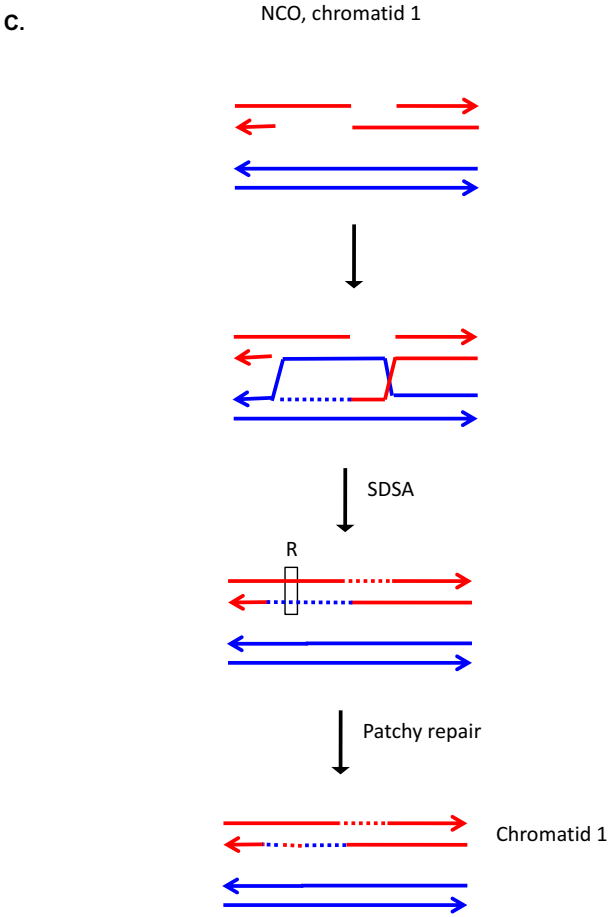

S72	NCO	Heteroduplex tract with an internal restoration tract	Mlh1-independent MMR, SDSA

Fig.S73

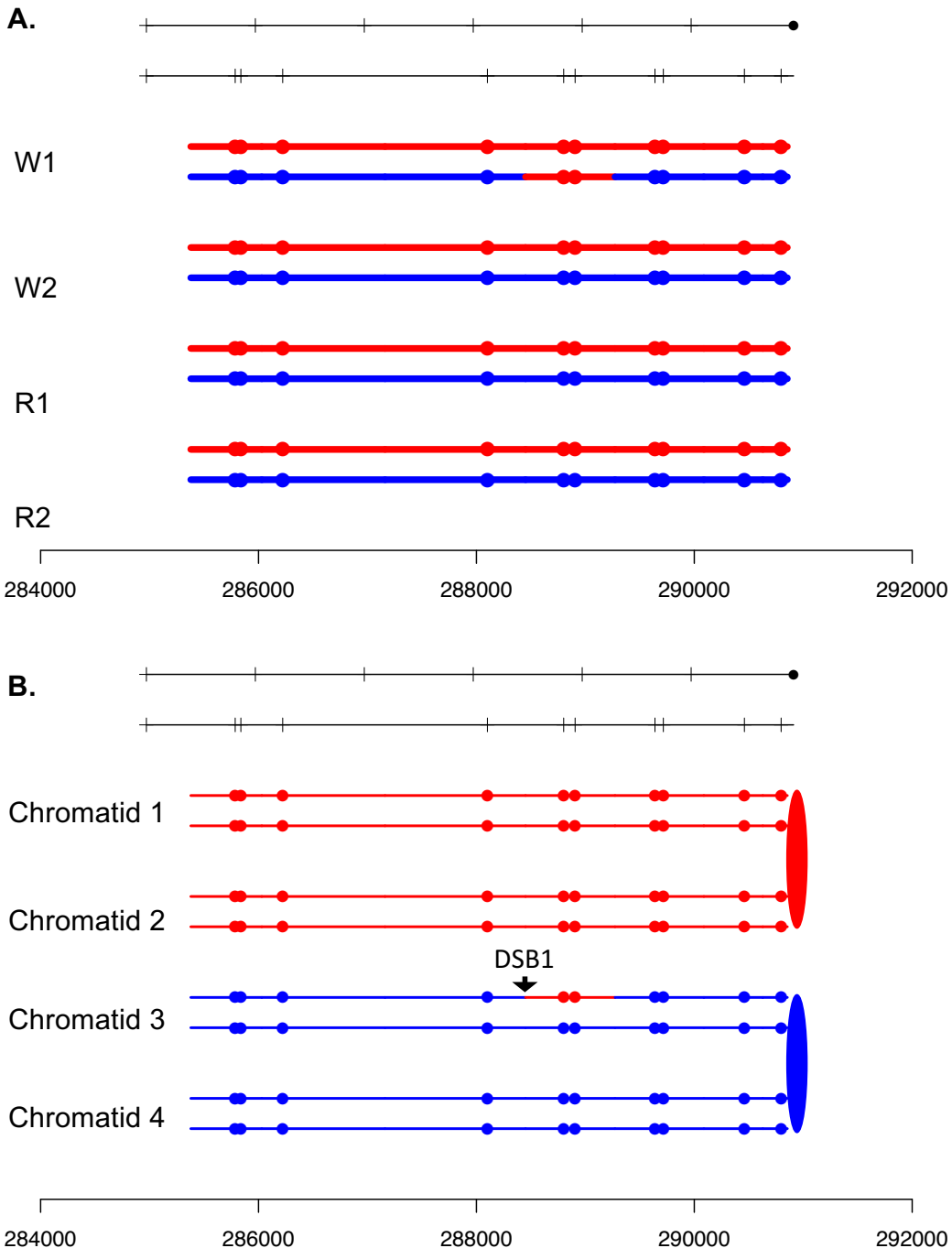
A.
W1
W2
R1
R2
284000
286000
288000
290000
292000
B.
Chromatid 1
Chromatid 2
DSB1
Chromatid 3
Chromatid 4
284000
286000
288000
290000
292000

Fig.S74

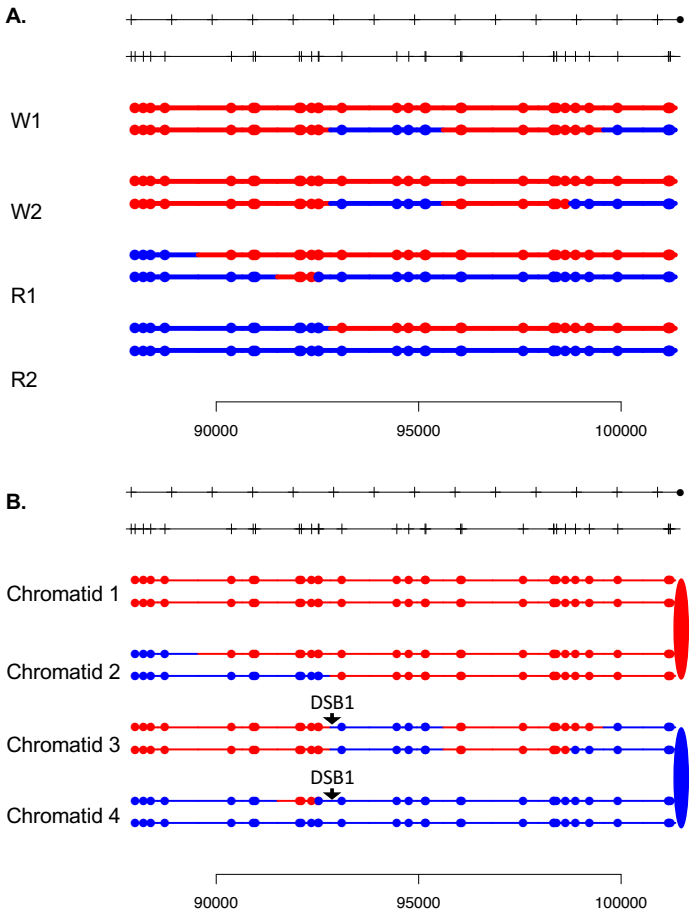

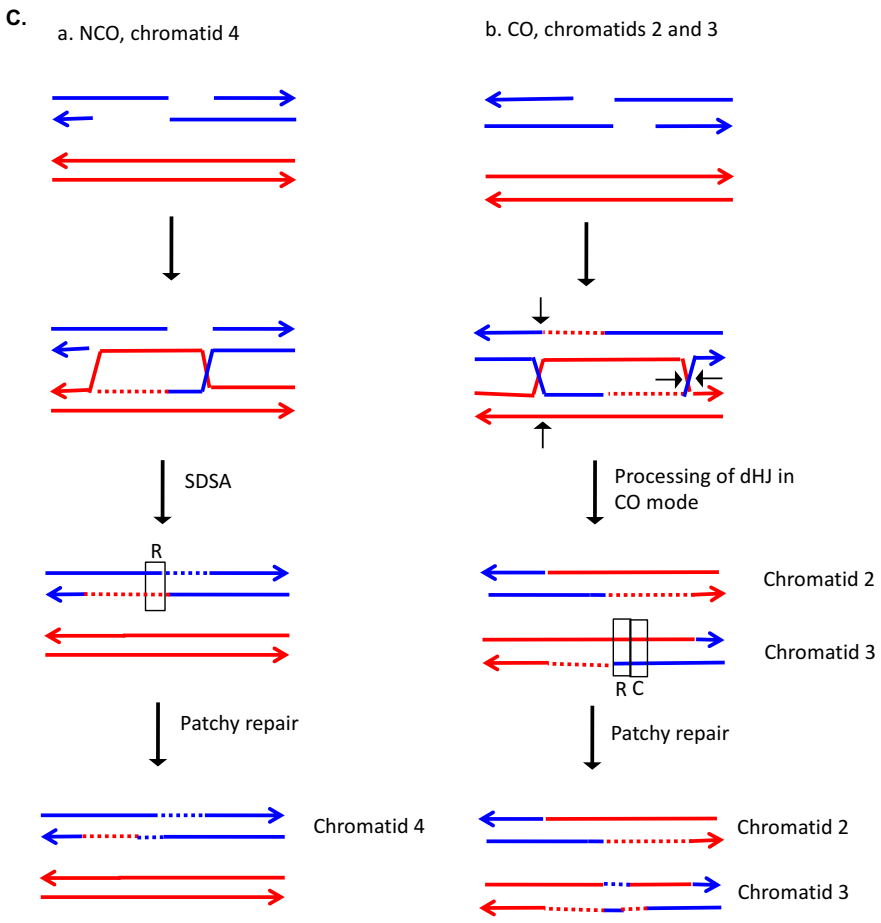

S74	NCO	Region of restoration repair separating DSB site from heteroduplex on chromatid 4	Mlh1-independent MMR, SDSA
	CO	Long regions of restoration and conversion repair separating DSB site from heteroduplex tract	Mlh1-independent MMR or template switching

Fig.S75

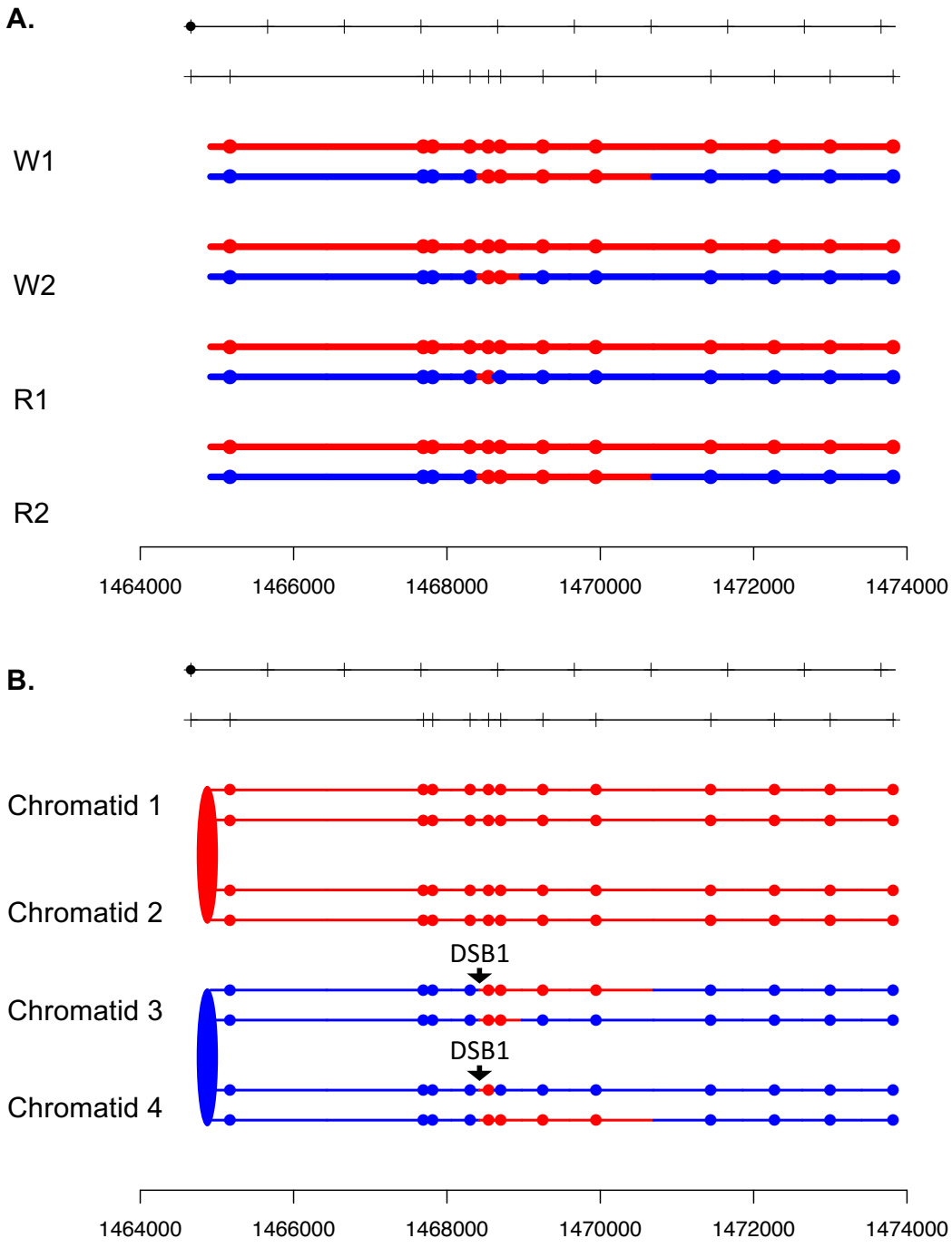
A.
W1
W2
R1
R2
1464000
1466000
1468000
1470000
1472000
1474000
B.
Chromatid 1
Chromatid 2
DSB1
Chromatid 3
DSB1
Chromatid 4
1464000
1466000
1468000
1470000
1472000
1474000

Fig.S76

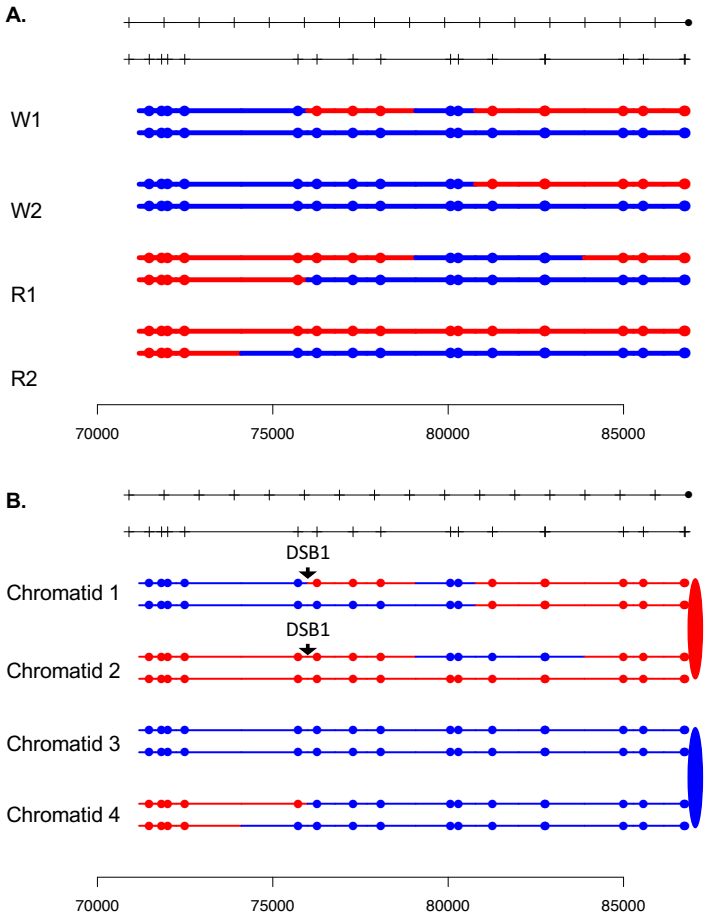

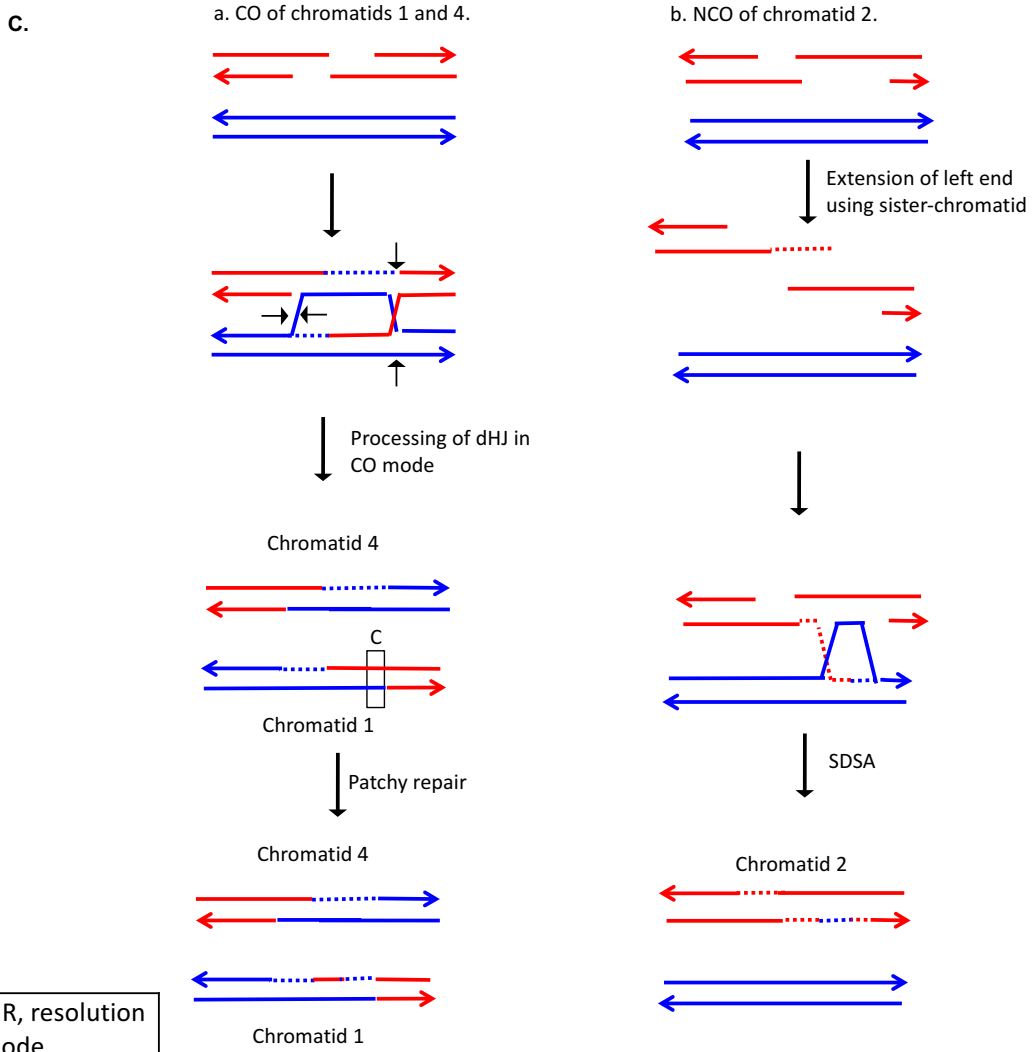

S76	CO	Conversion event at the end of heteroduplex tract	Mlh1-independent MMR, resolution of dHJ in CO mode
	NCO	Displacement of heteroduplex tract from DSB site	Interaction of broken end with sister chromatid or long restoration tract by Mlh1-independent MMR

Fig.S77

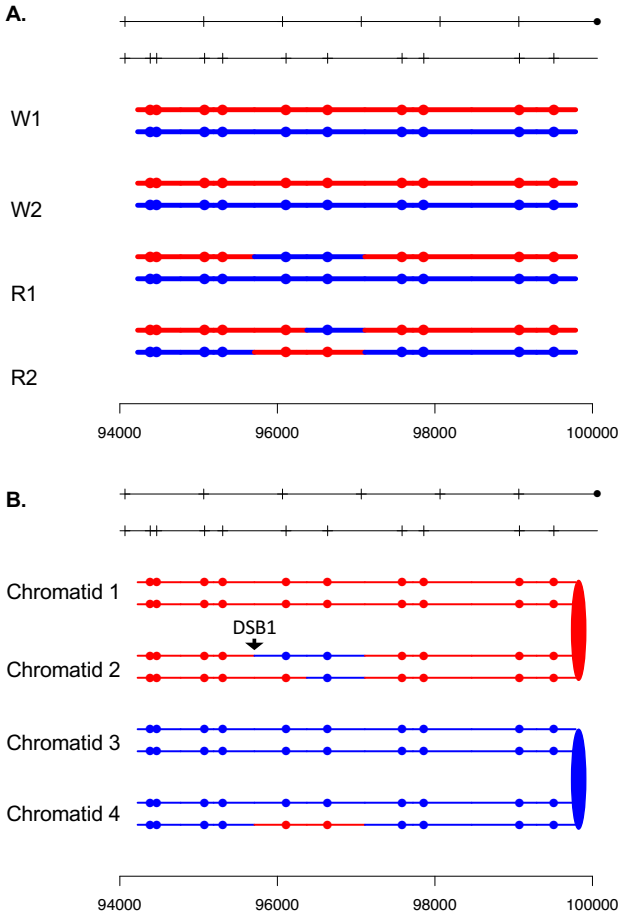

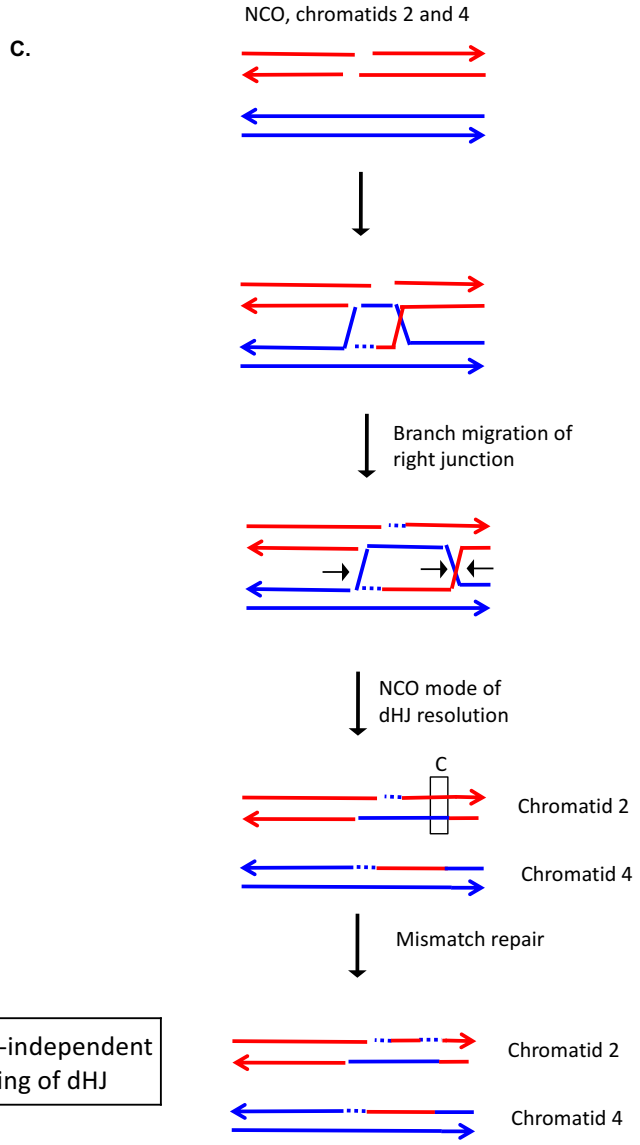

S77	NCO	Symmetric heteroduplex; conversion tract at end of heteroduplex tract	Branch migration; Mlh1-independent MMR; NCO processing of dHJ

Fig.S78

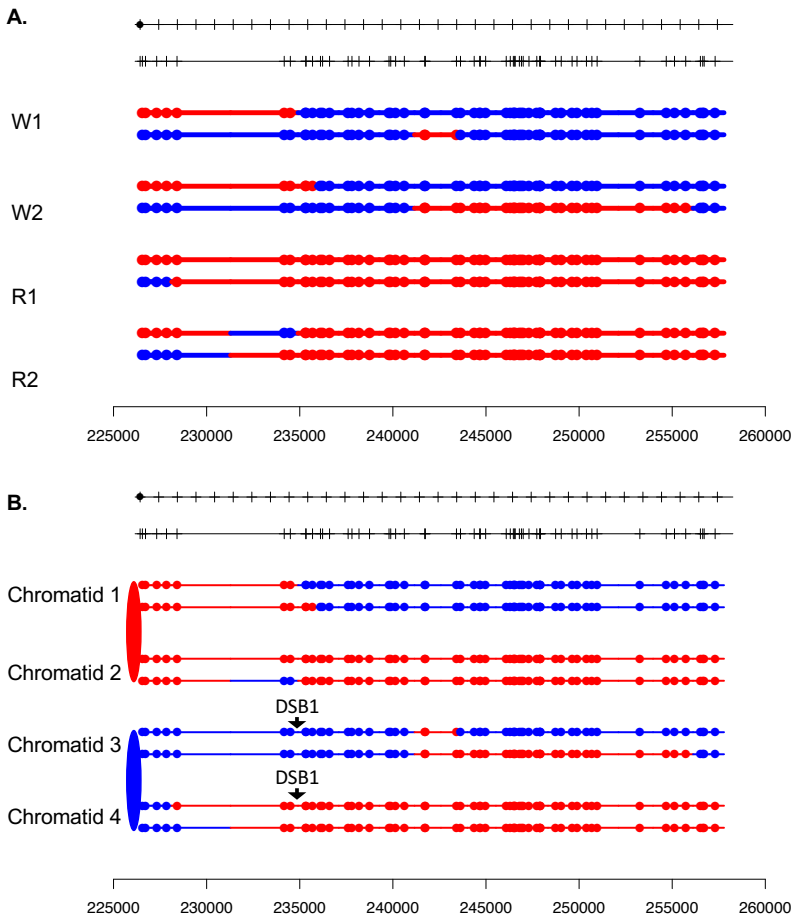

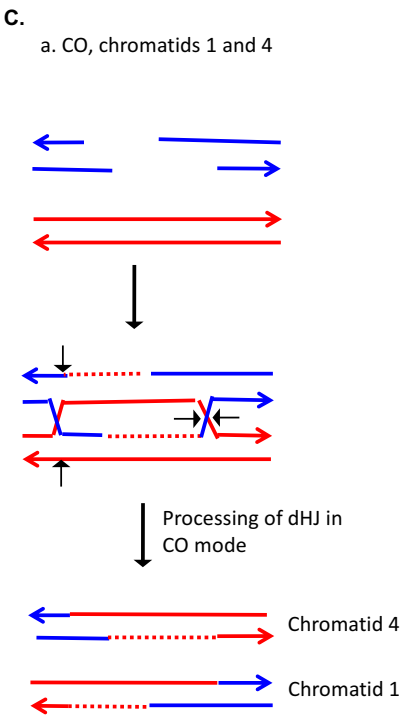

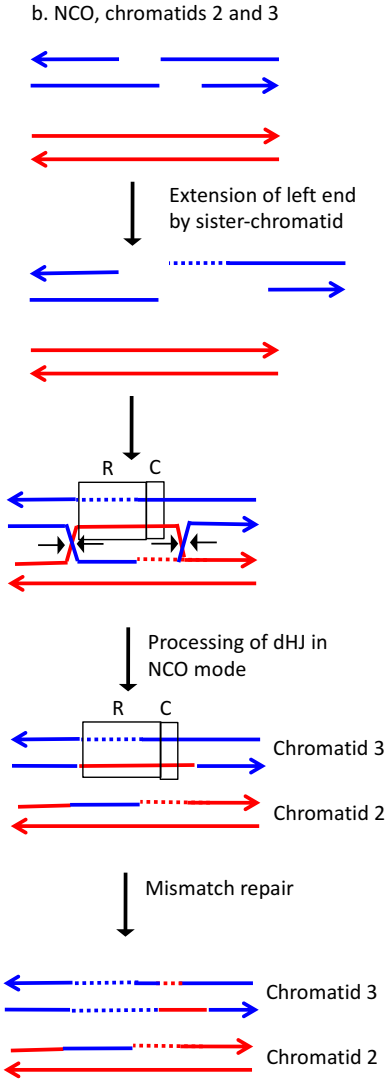

S78	NCO	Regions of homoduplex separating heteroduplex region from DSB site	Mlh1-independent MMR or template switching; resolution of dHJ in NCO mode
	CO	Region of conversion separating heteroduplex region from DSB site on chromatid 4	Mlh1-independent MMR or gap repair; resolution of dHJ in CO mode

Fig.S79

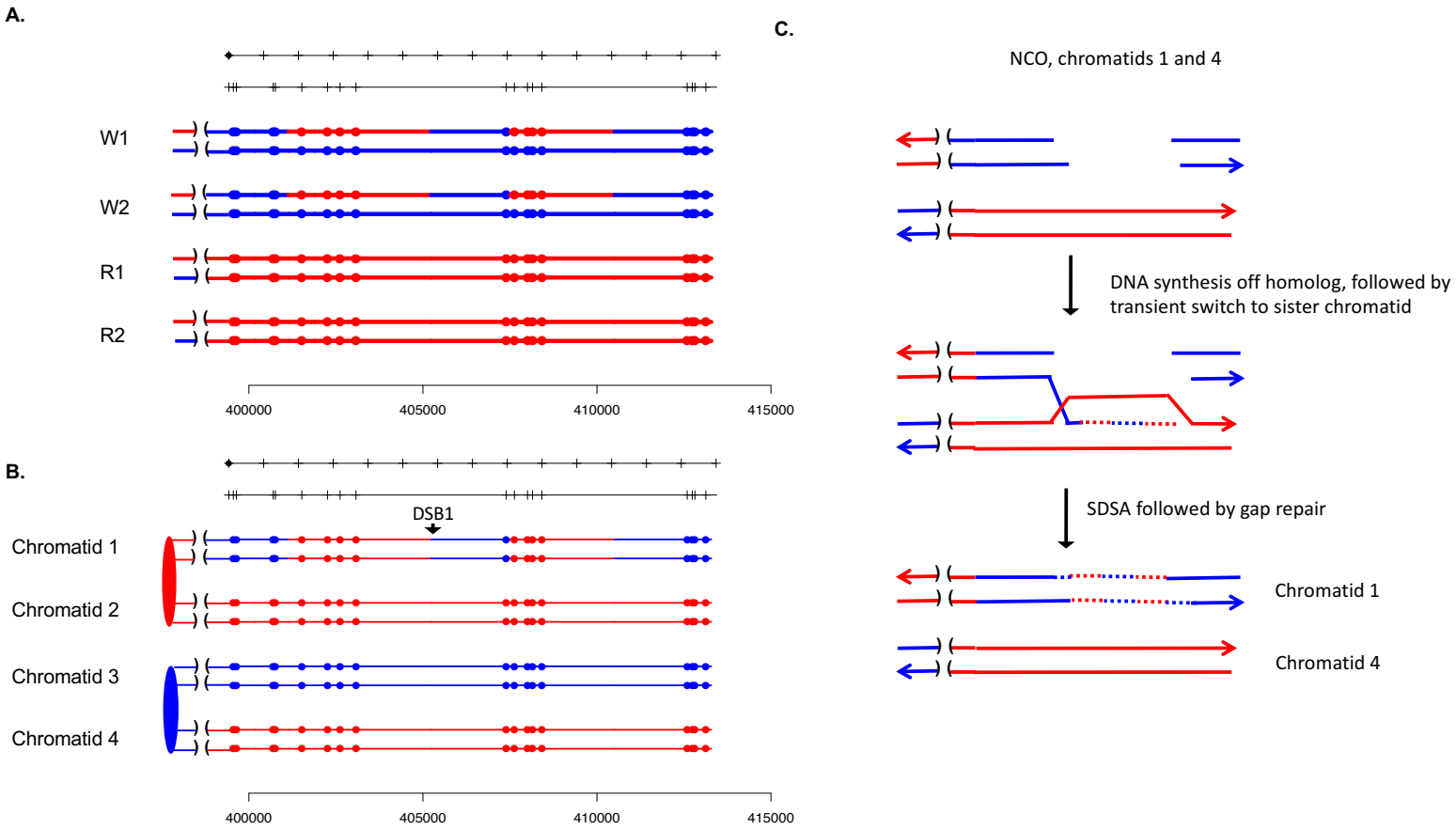

S79	NCO	In regions centromere-proximal to event, both homologs in white sector derived from one parental homolog and both in red sector derived from the other; regions of conversion and restoration homoduplexes on chromatid 1	Crossover on same chromosomes located centromere-proximal to the event in S79 (described in S78) produced centromere-proximal regions. Homoduplex regions produced by template switching or by Mlh1-independent MMR

Fig.S80

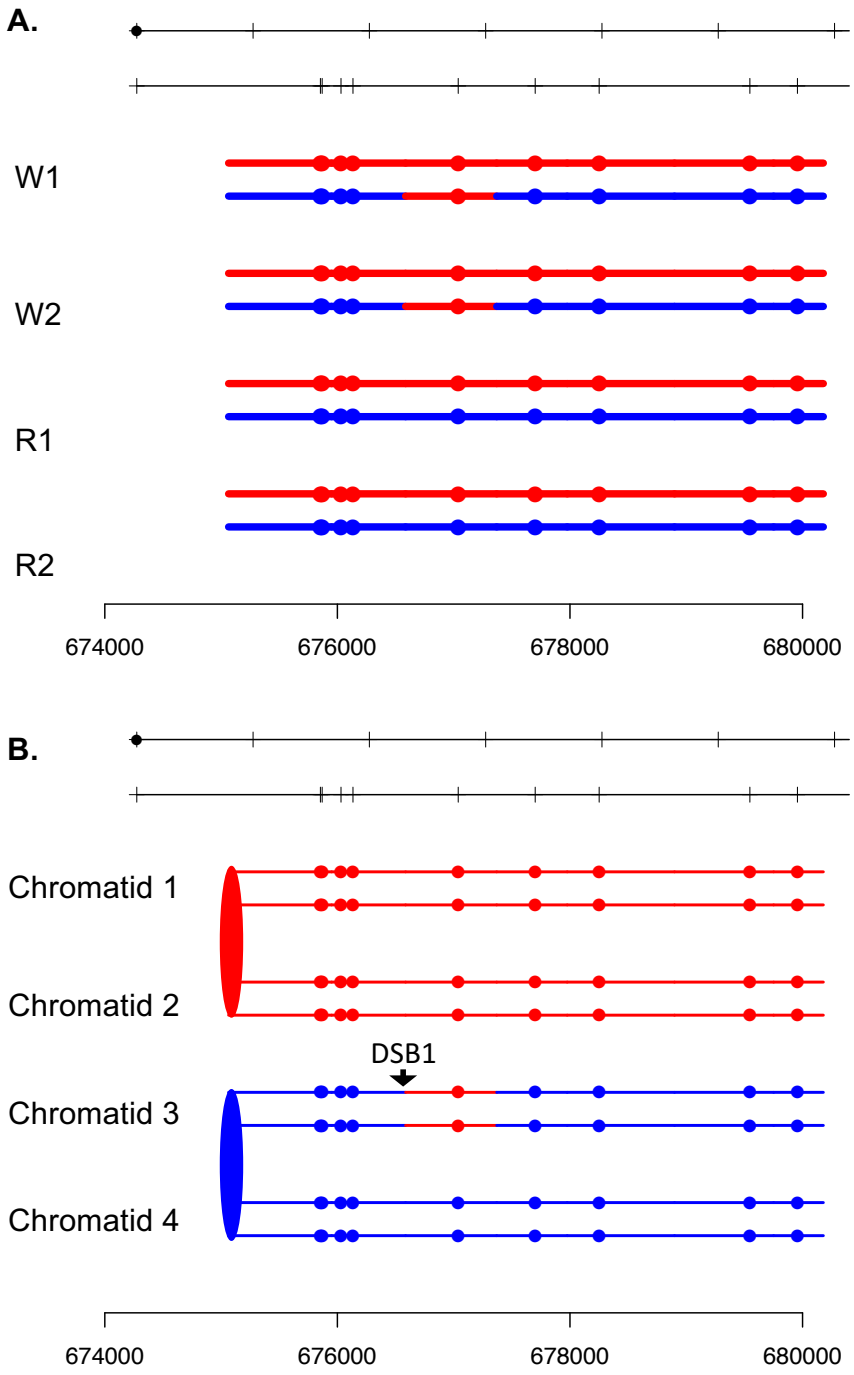
A.
W1
W2
R1
R2
674000
676000
678000
680000
B.
Chromatid 1
Chromatid 2
DSB1
Chromatid 3
Chromatid 4
674000
676000
678000
680000

Fig.S81

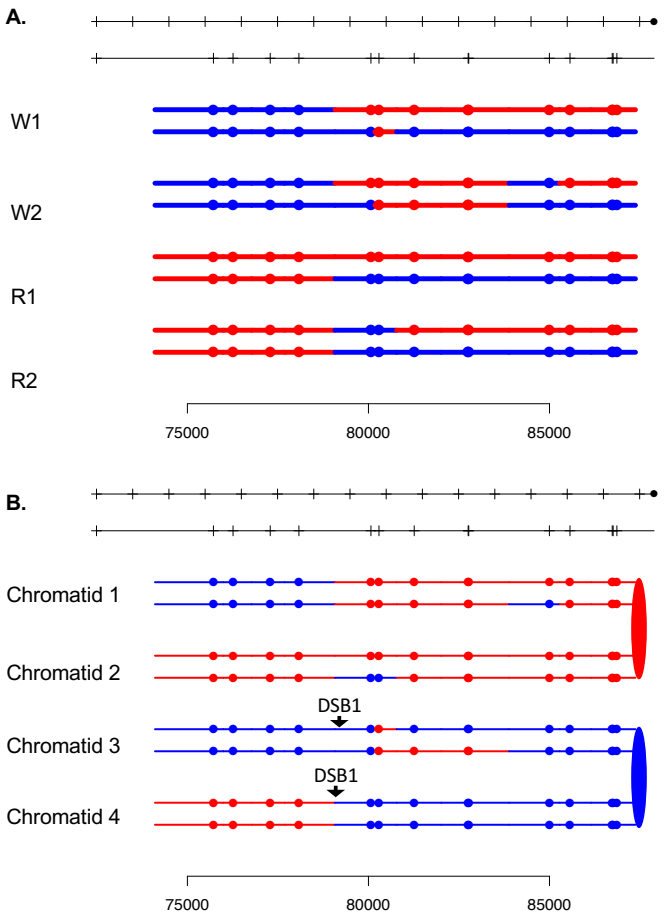

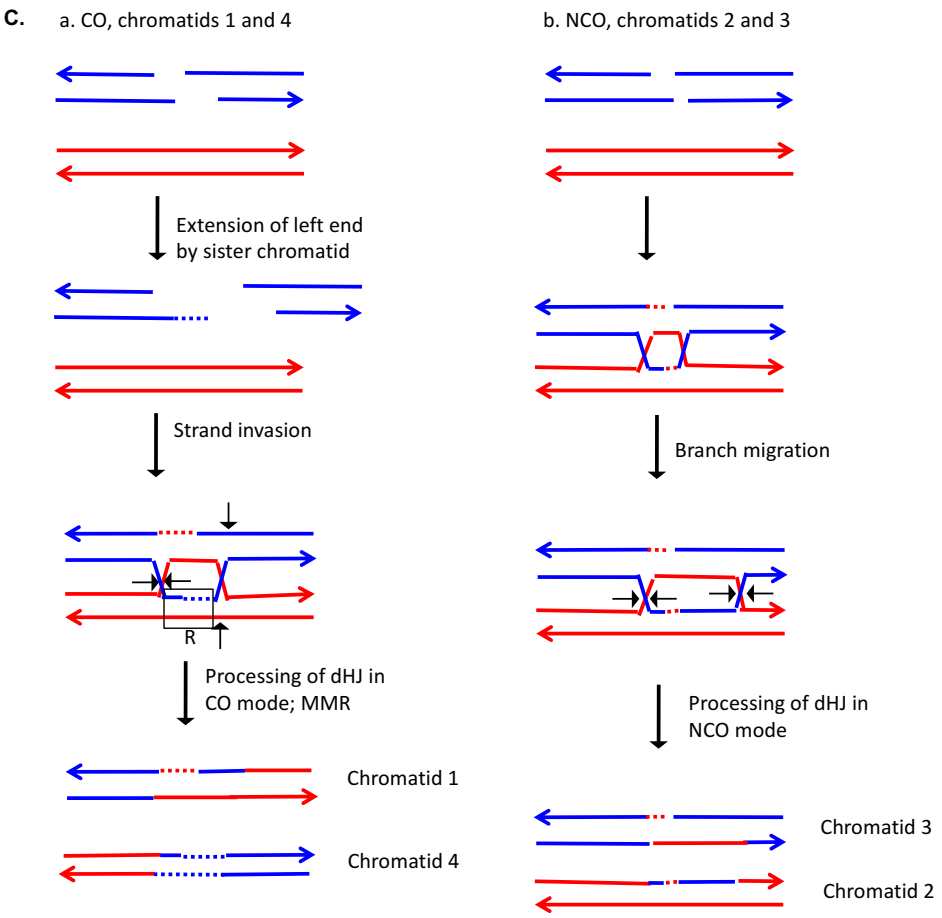

S81	CO	Long tracts of homoduplex on chromatids 1 and 4.	Extension of broken end by interaction with sister chromatid; Mlh1-independent restoration repair; resolution of dHJ in CO mode
	NCO	Heteroduplex DNA on same side of DSB site in NCO chromatids	Branch migration followed by processing of dHJ in CO mode

Fig.S82

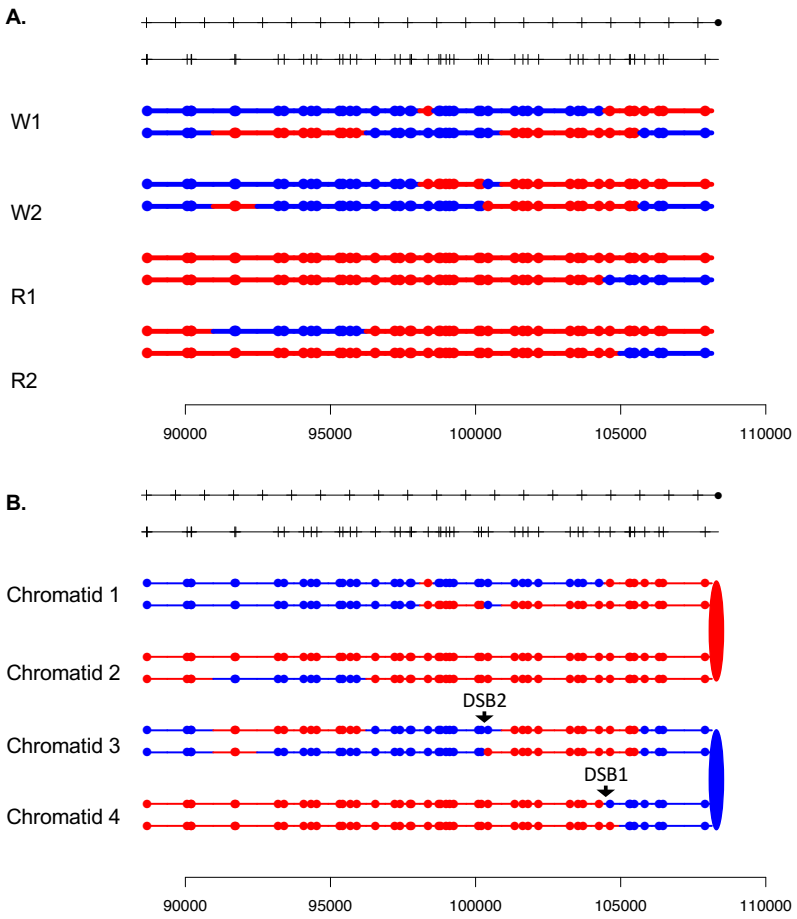

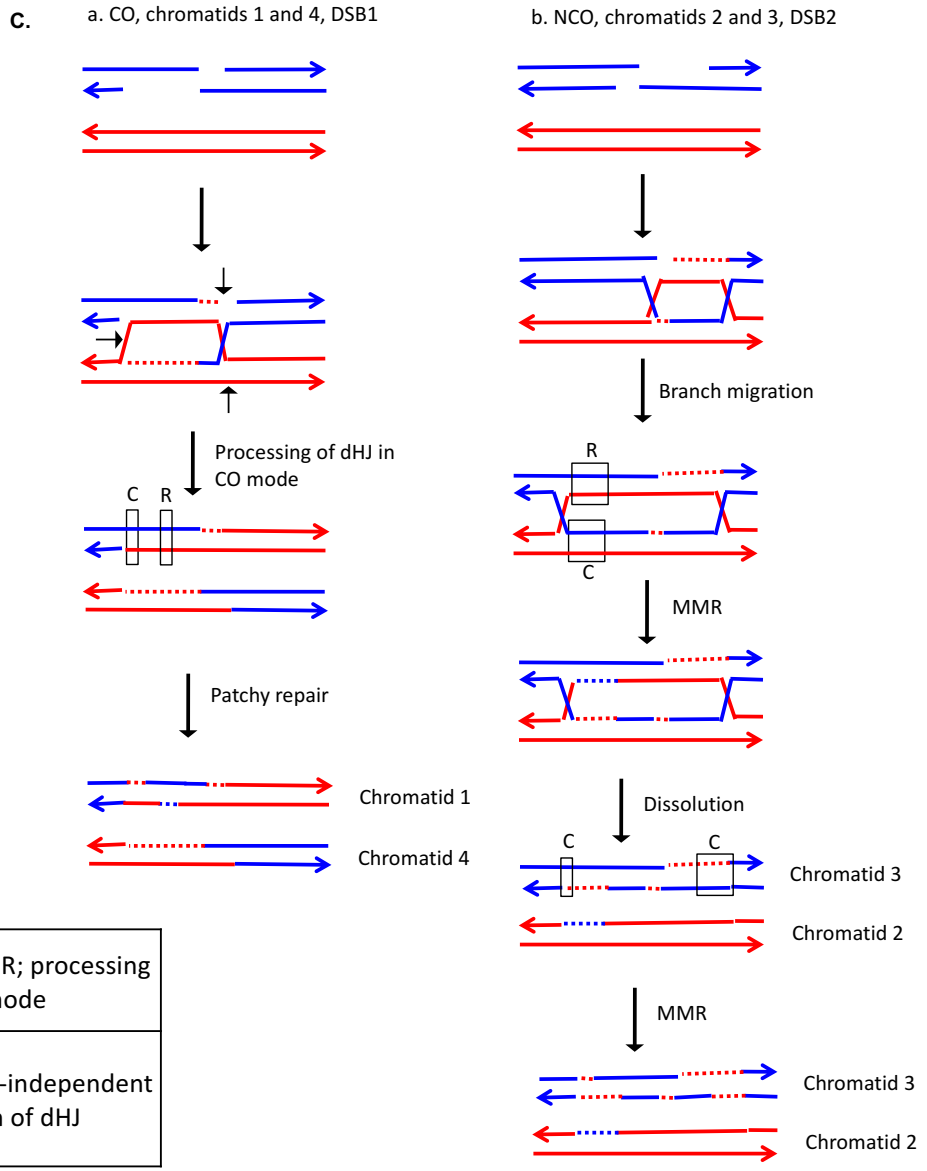

S82	CO	Heteroduplex with interspersed conversion and restoration tracts (chromatid 1); initiated at DSB1	Mlh1-independent MMR; processing of dHJ in CO mode
	NCO	Symmetric heteroduplex tracts; heteroduplex tract interspersed with homoduplex regions; strand switch on chromatid 3; initiated at DSB2	Branch migration; Mlh1-independent MMR; dissolution of dHJ

Fig.S83

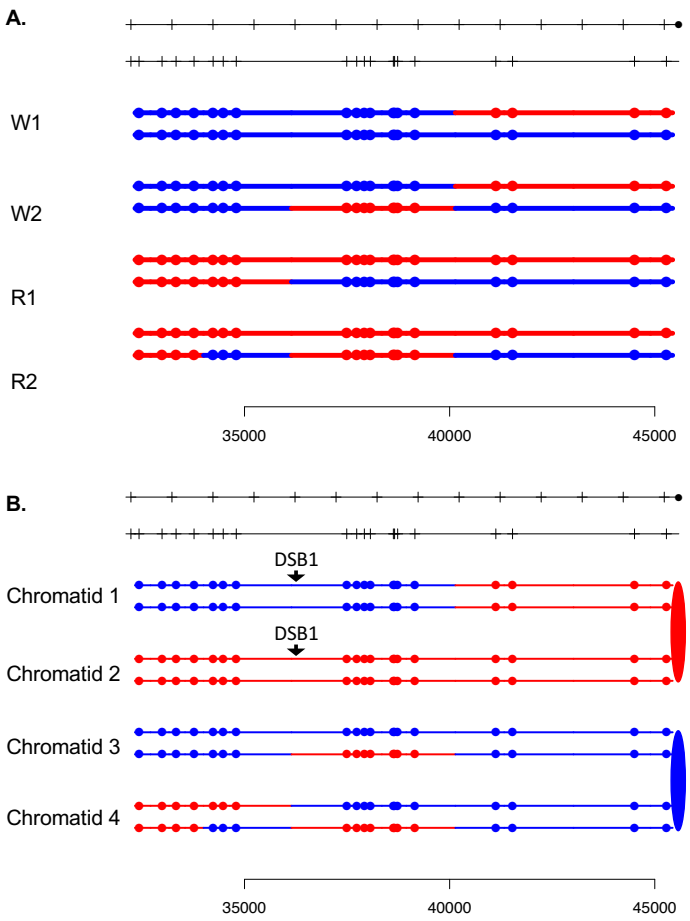

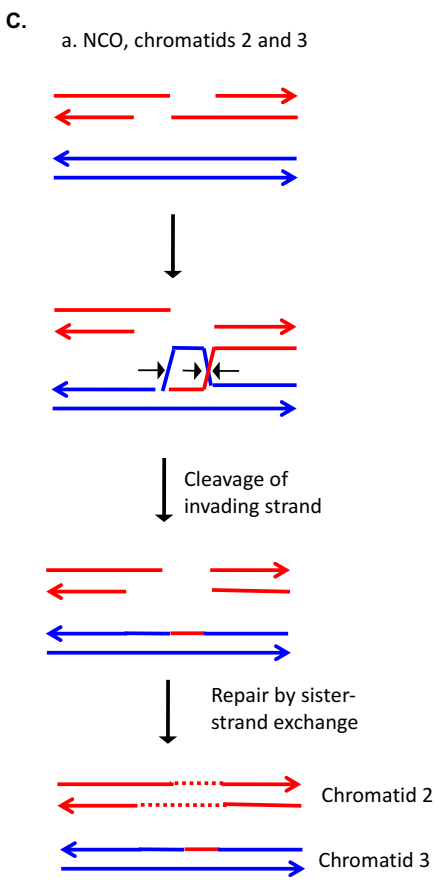

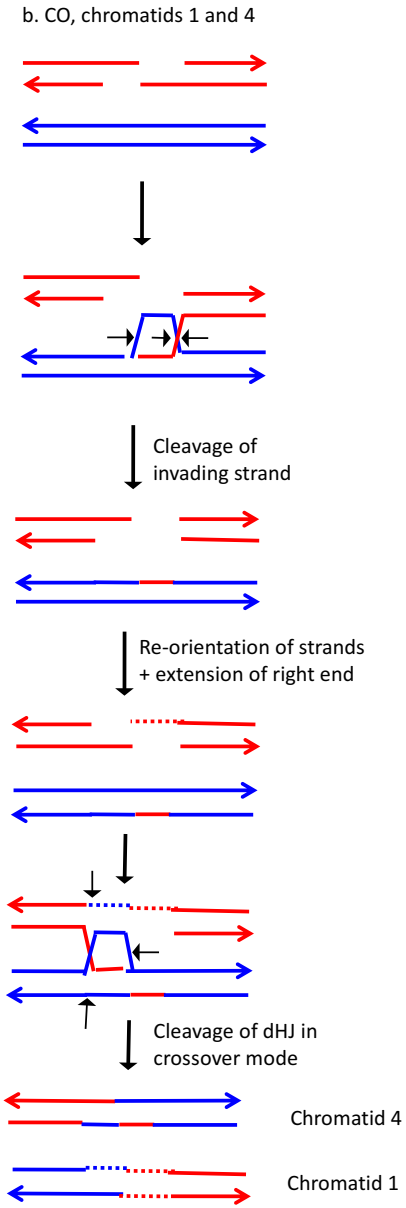

S83	CO	Strand switch of heteroduplex in CO chromatid 4	Invasion of the right broken end, followed by processing of junction; extension of right end by sister-chromatid interaction; invasion of the left end and processing dHJ in crossover mode
	NCO	DSB on red chromatid, but red chromatid acts as donor	Following strand invasion, junction cleaved before initiating DNA synthesis

Fig.S84

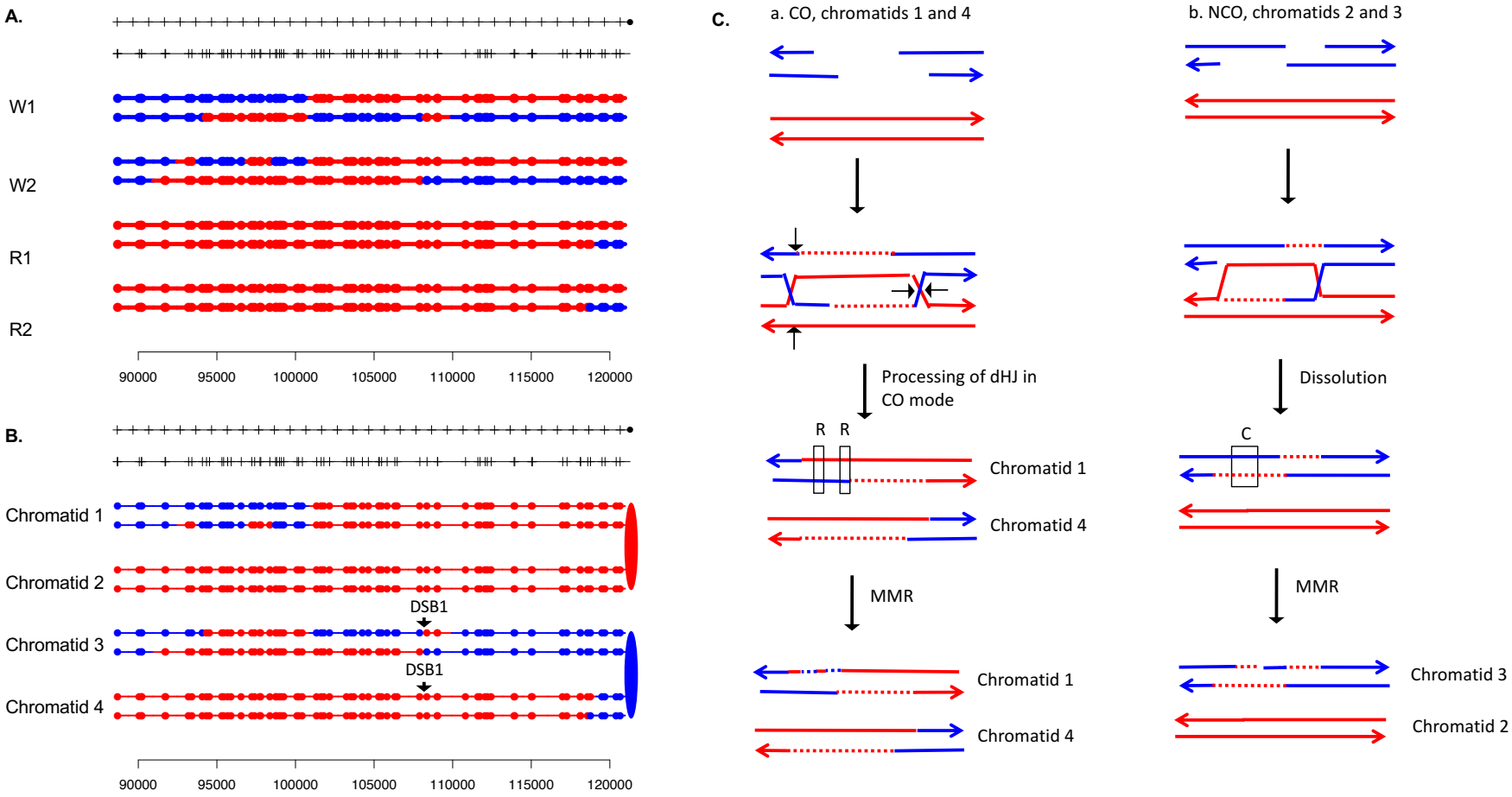

S84	CO	Long conversion tract spanning DSBs in both CO chromatids 1 and 4; heteroduplex in chromatid 1 interrupted by restoration tracts	Gap repair; Mlh1-independent MMR; resolution of dHJ in CO mode
	NCO	NCO chromatid 3 has strand switch of heteroduplexes; conversion event within heteroduplex	Resolution of dHJ by dissolution; Mlh1-independent MMR

Fig.S85

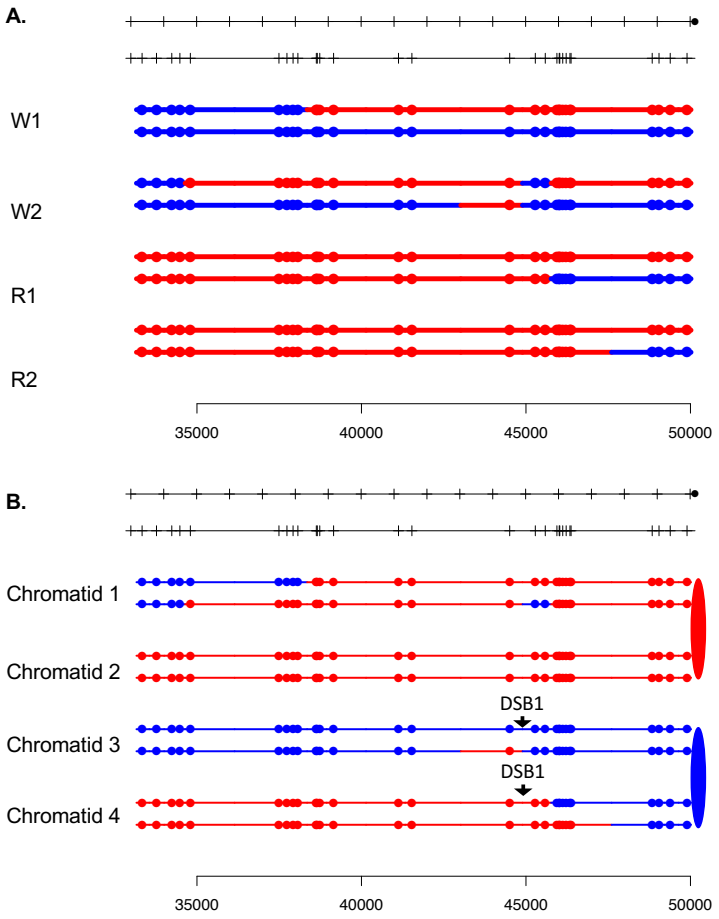

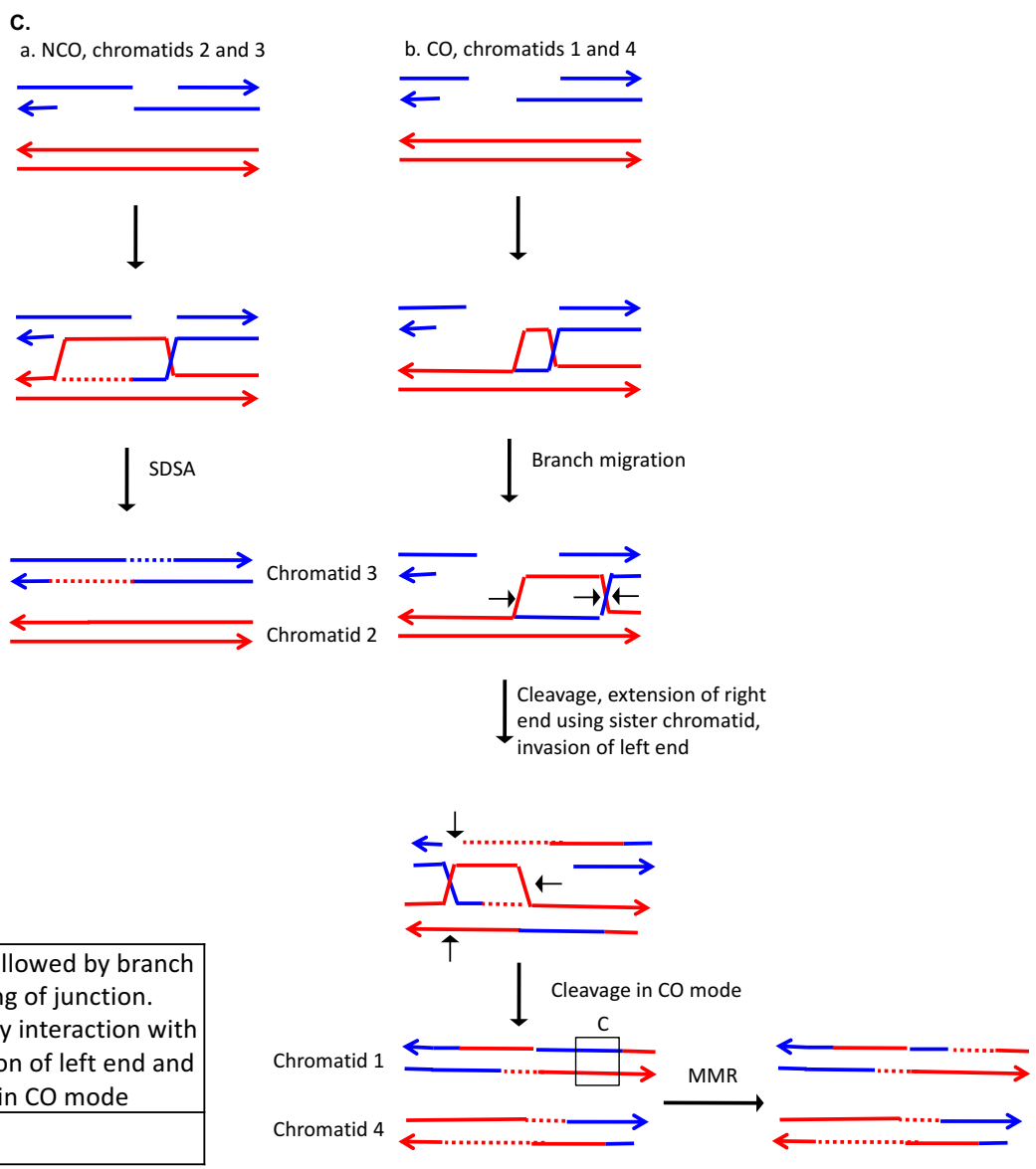

S85	CO	Strand switch in CO chromatid 1; heteroduplexes in trans on chromatids 1 and 4; long conversion tract adjacent to heteroduplex region in chromatid 1	Invasion of right end, followed by branch migration and cutting of junction. Extension of right end by interaction with sister chromatid; invasion of left end and resolution of dHJ in CO mode
	NCO	Simple heteroduplex	SDSA

Fig.S86

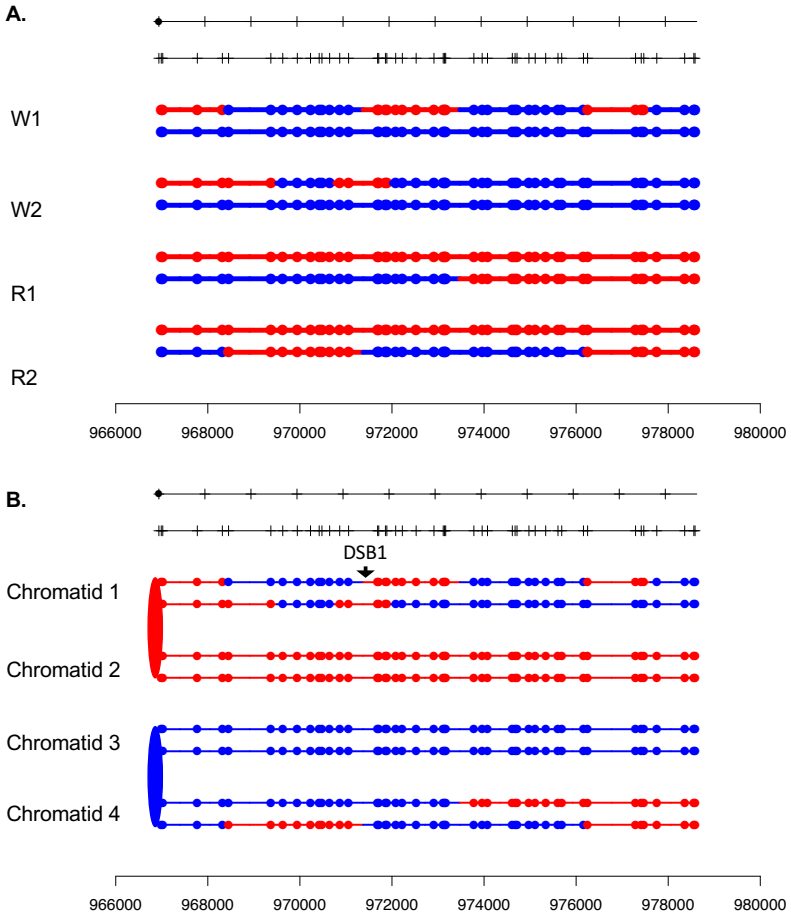

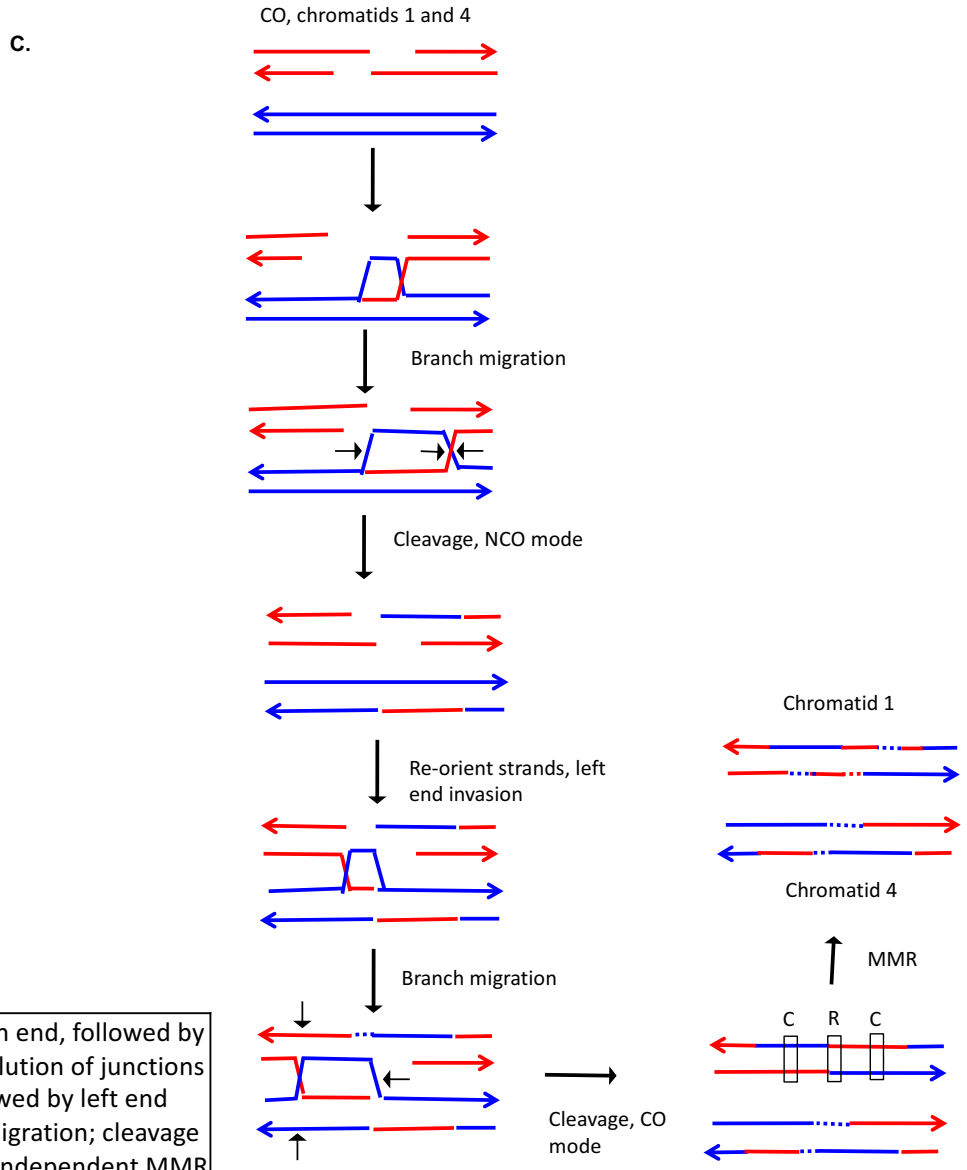

S86	CO	Strand switches in heteroduplexes in both CO chromatids 1 and 4; both chromatids have homoduplex regions interspersed with heteroduplex	Invasion of right broken end, followed by branch migration; resolution of junctions in NCO mode, followed by left end invasion and branch migration; cleavage in CO mode and Mlh1-independent MMR

Fig.S87

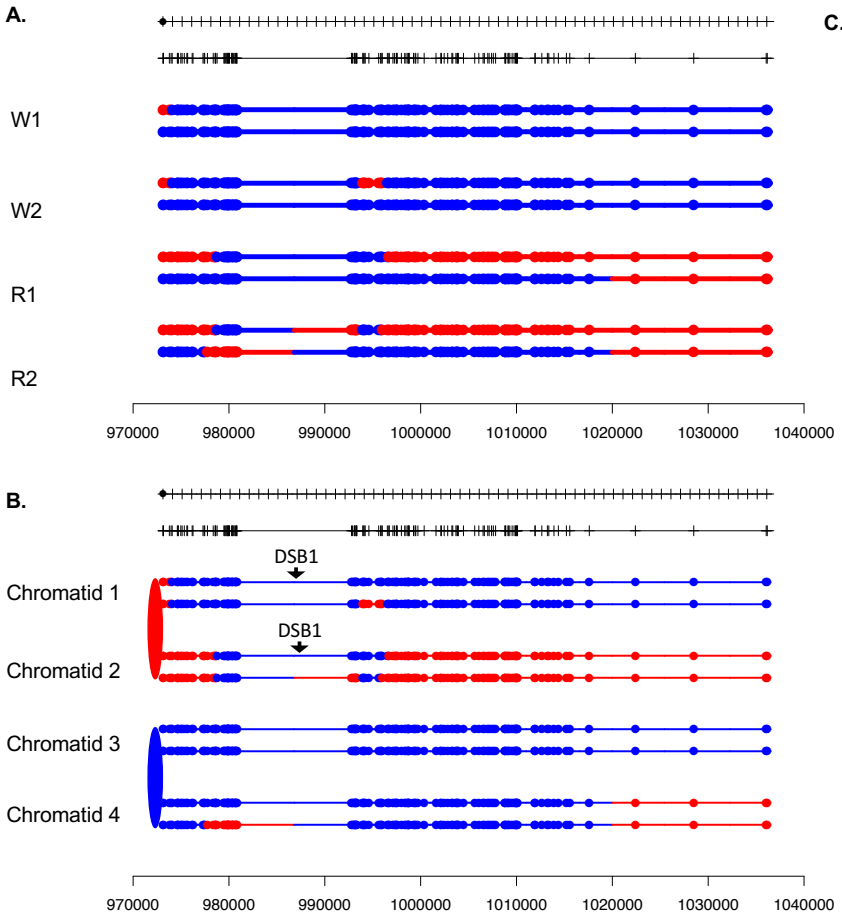

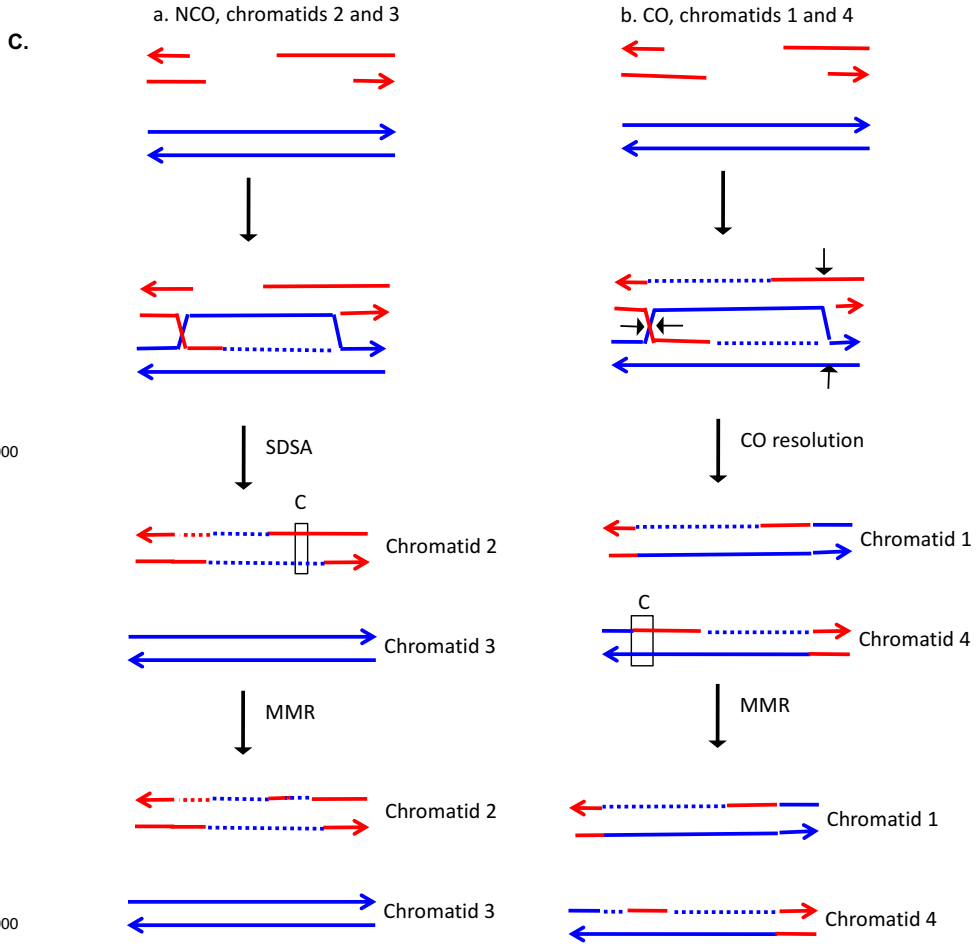

S87	CO	Large region of conversion spanning putative DSB site; uni-directional heteroduplexes on chromatids 1 and 4 propagated in opposite directions;; conversion tract distal to heterodupex tract on chromatid 4	Repair of large gap associated with HS4 hotspot; processing dHJ in CO mode; Mlh1-independent MMR
	NCO	Region of conversion spanning putative DSB site; conversion tract adjacent to heteroduplex	Repair of large gap; SDSA; Mlh1-independent MMR

Fig.S88

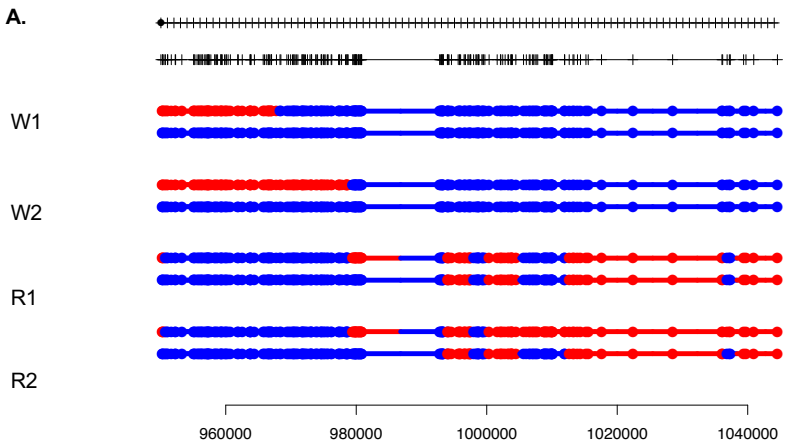

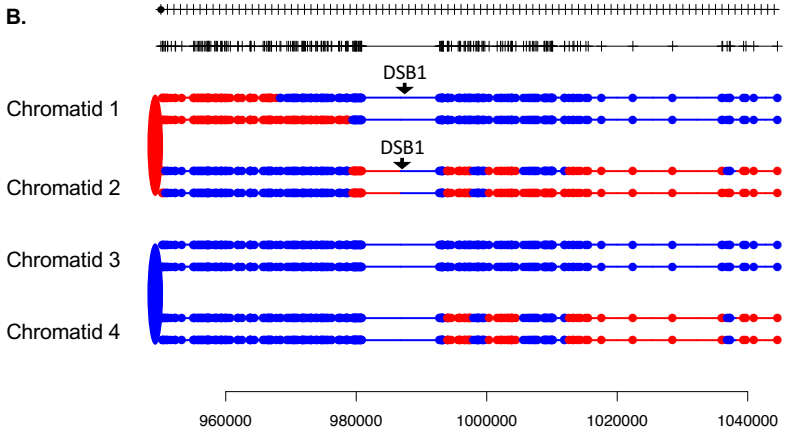

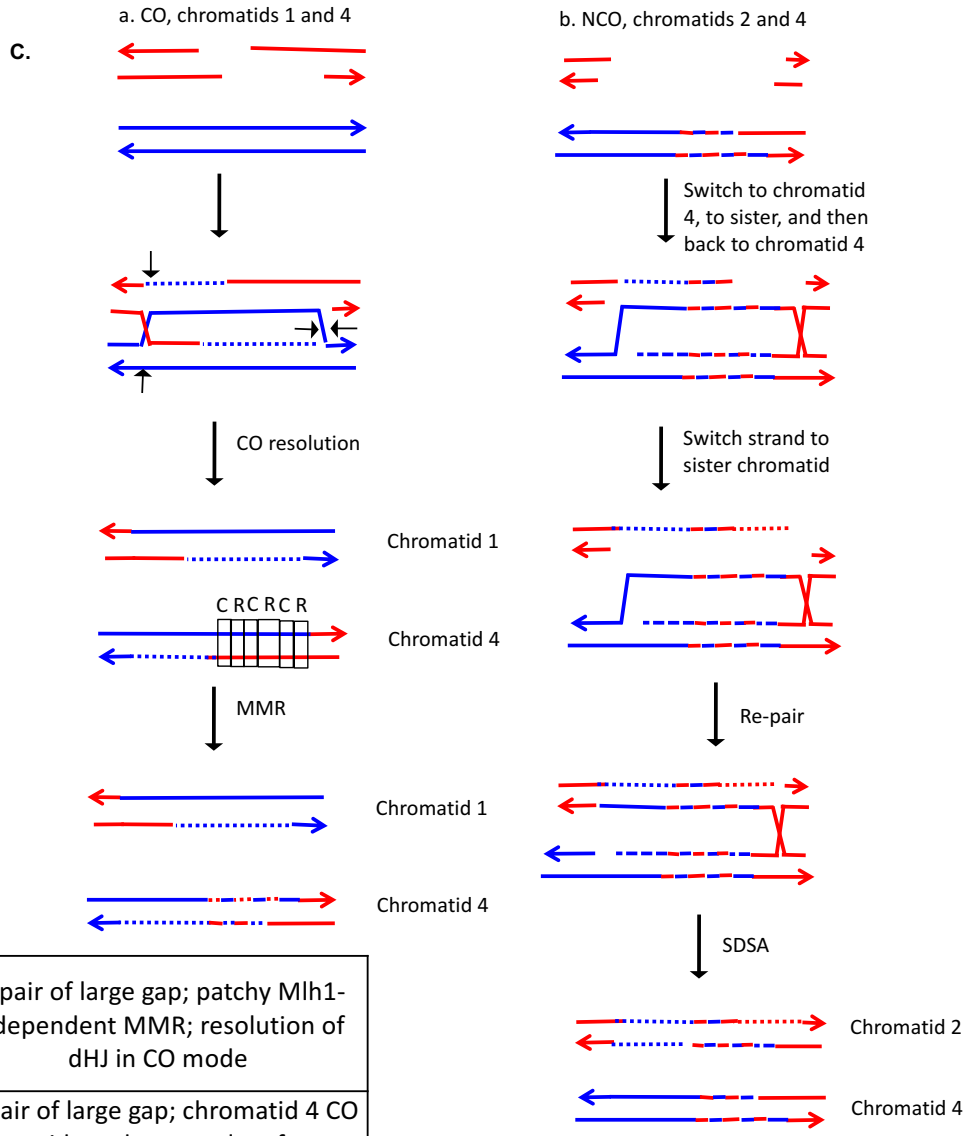

S88	CO	Region of conversion spanning putative DSB site; uni-directional heteroduplex tracts in on chromatids 1 and 4 propagated in different directions; multiple homoduplex tracts within heteroduplex tract on chromatid 4	Repair of large gap; patchy Mlh1-independent MMR; resolution of dHJ in CO mode
	NCO	Large conversion tract spanning putative DSB site; chromatid 3 has a pattern of heteroduplex and homoduplex tracts that is very similar to that of chromatid 4	Repair of large gap; chromatid 4 CO chromatid used as template for part of repair; also, switch of repair templates to sister chromatid

Fig.S89

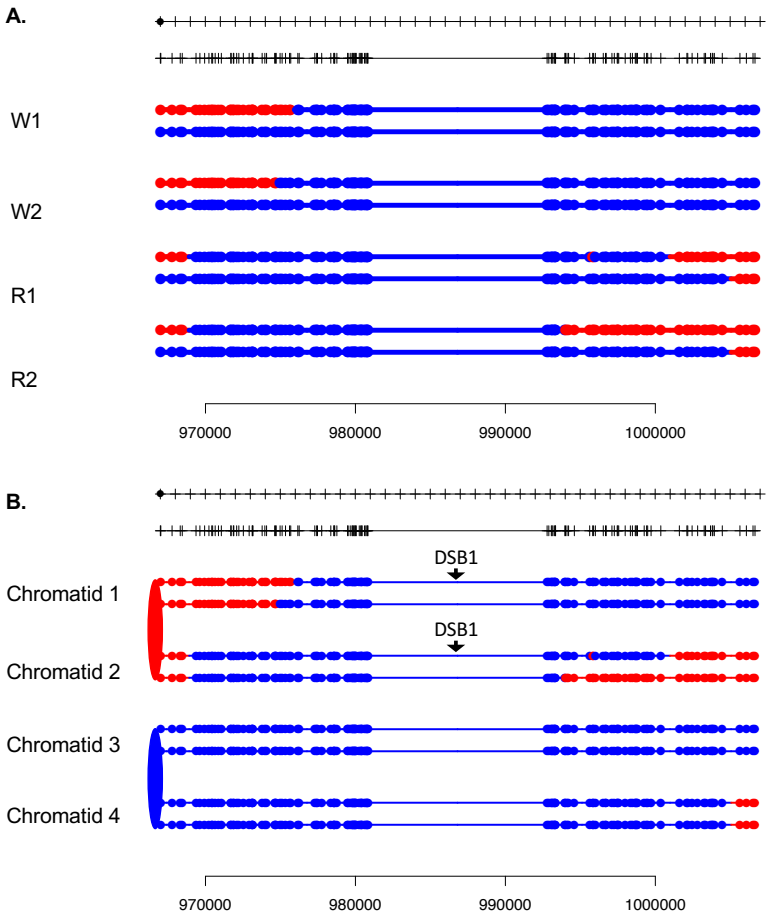

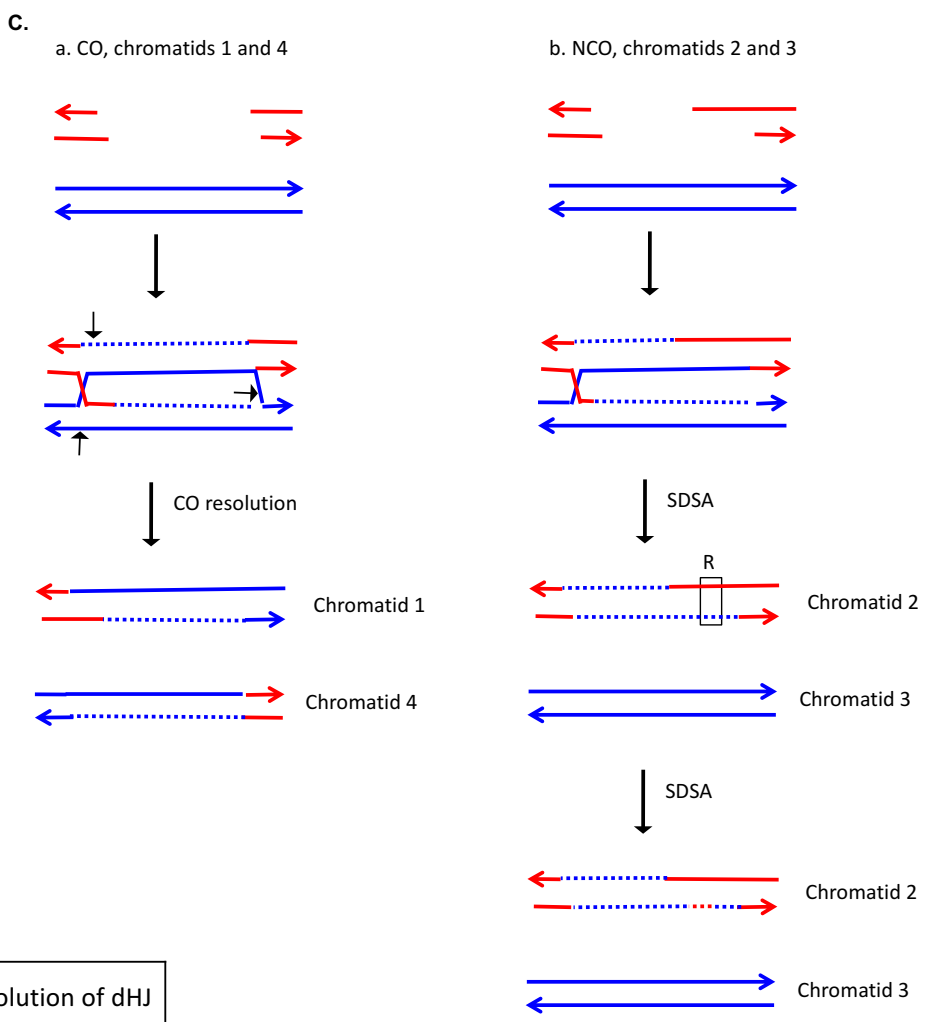

S89	CO	Very large conversion tract spanning putative DSB site; heteroduplex on chromatid 1 but not 4	Repair of large gap; resolution of dHJ in CO mode
	NCO	Very large conversion tract spanning putative DSB site; restoration tract in middle of heteroduplex	Repair of large gap; resolution of dHJ in NCO mode; Mlh1-independent MMR

Fig.S90

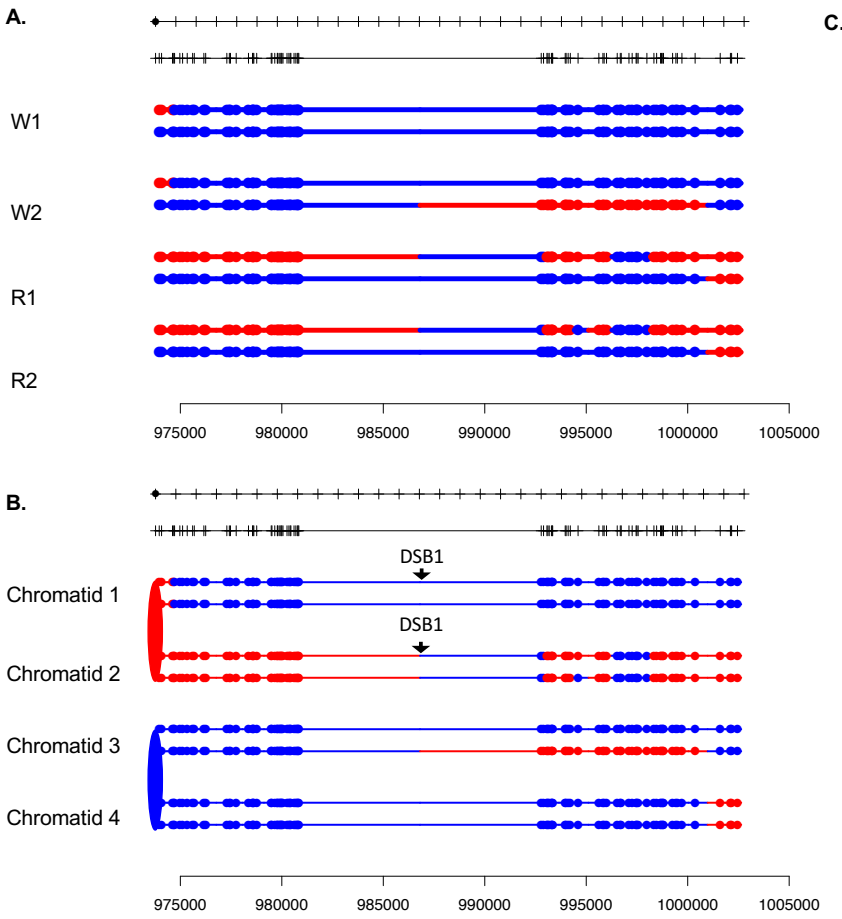

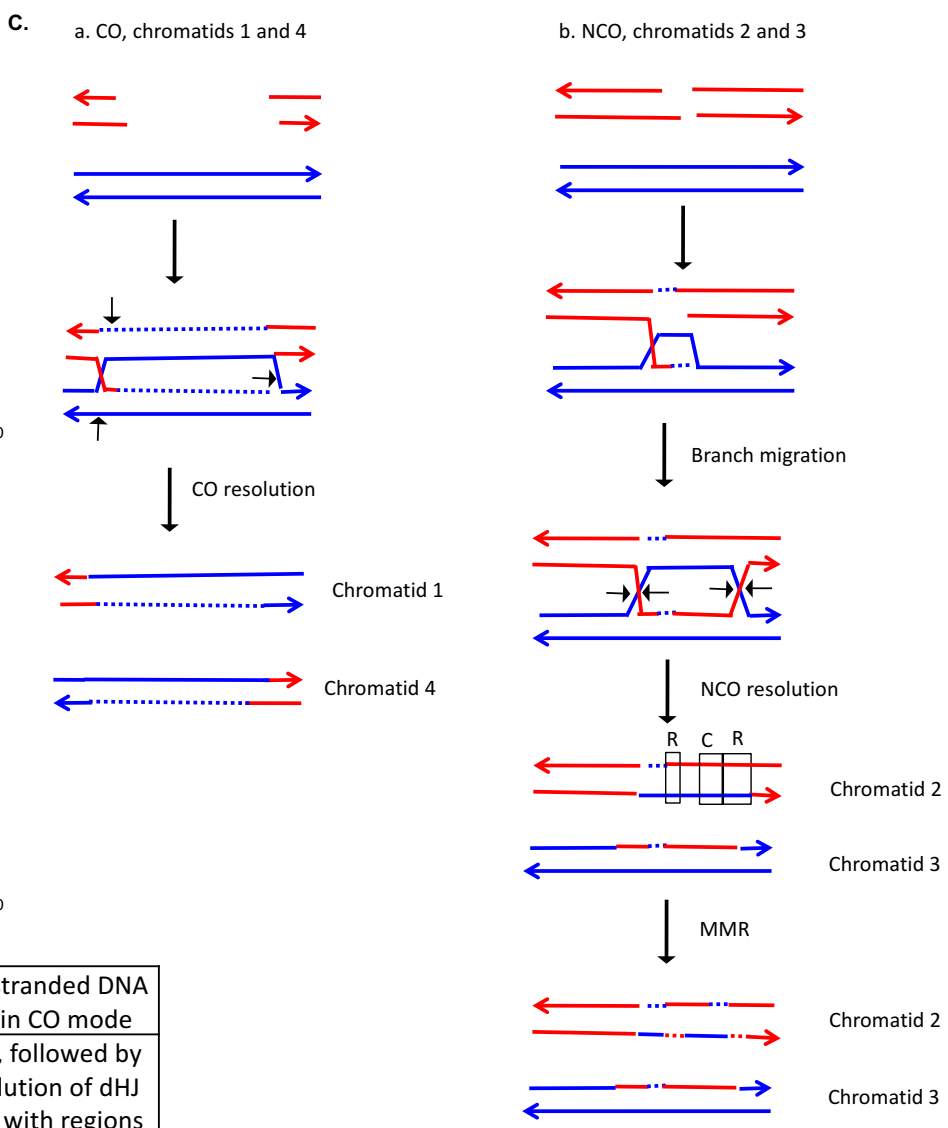

S90	CO	Very large conversion tract spanning DSB site; no heteroduplexes observed	Repair of large double-stranded DNA gap, resolution of dHJ in CO mode
	NCO	Heteroduplexes in both NCO chromatids 2 and 3 on same side of DSB site; homoduplex tracts in heteroduplex	Invasion of broken end, followed by branch migration; resolution of dHJ structure in NCO mode with regions of Mlh1-independent MMR

Fig.S91

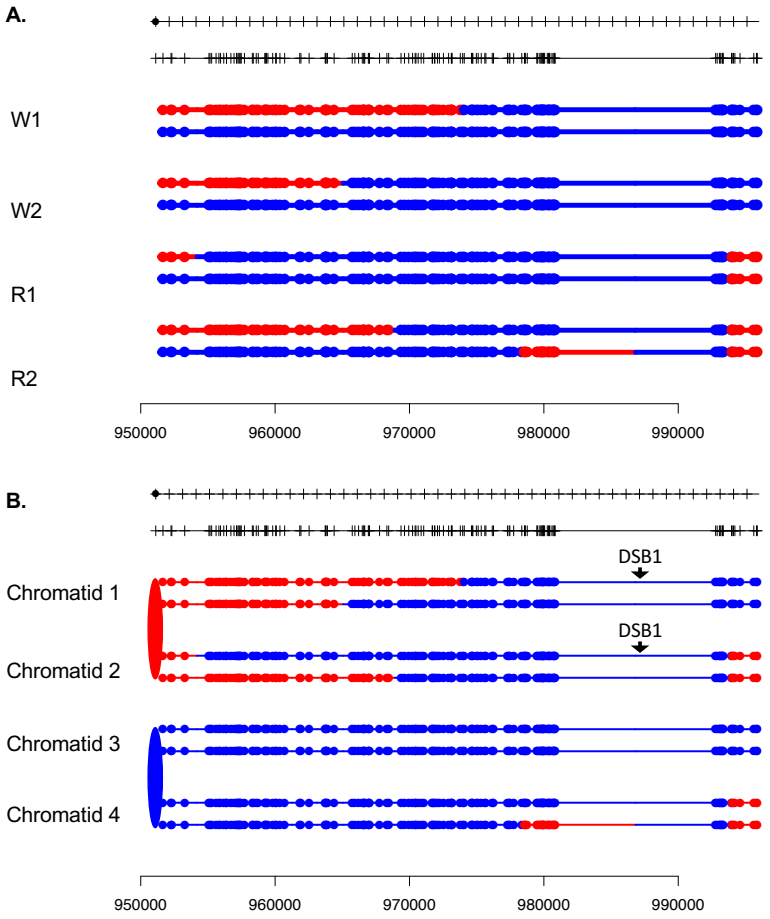

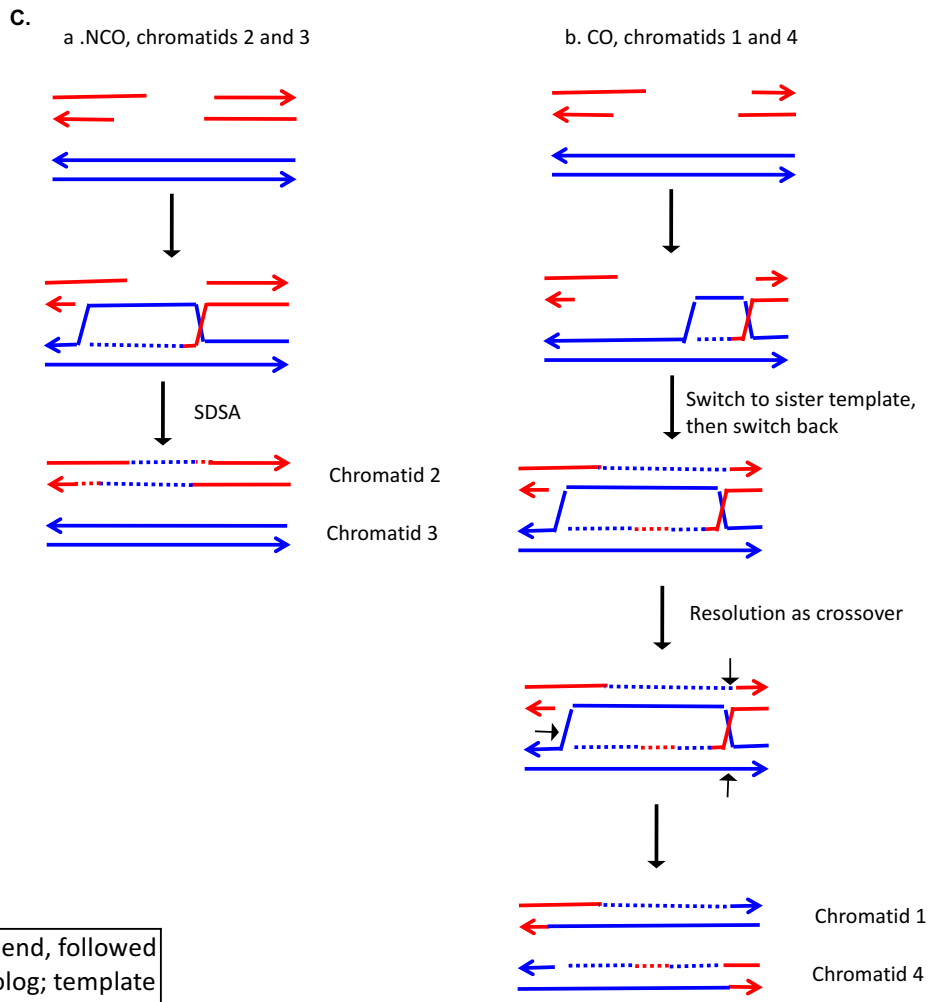

S91	CO	Heteroduplexes on both chromatids 1 and 4 on same side of putative DSB site; large conversion tract flanking DSB site	Invasion of right broken end, followed by synthesis off of homolog; template switch to sister chromatid, and then re-invasion of sister chromatid; resolution of dHJ in CO mode
	NCO	Large conversion tract spanning putative DSB site	Repair of large gap; SDSA

Supplemental figure legends

Fig. S1. Mechanisms that generate Classes 1-5 recombination events. For all events, we show the initiating DSB on the blue chromatid. Dotted lines show sequences generated by replication or during mismatch repair. Black arrows indicate the position of the initiating DSB. The mechanisms are discussed in detail in the main text. Red and blue lines represent DNA strands of the W303-1A-derived chromatid and YJM789-derived chromatid, respectively. Arrows on these strands indicate the 3' ends.

A. Class 1. Class 1 events are NCOs formed by one-ended SDSA.

B. Class 2. These NCO events could be generated by one-ended SDSA, followed by Mlh1p-independent MMR.

C. Class 2. An alterative possibility is that Class 2 events reflect repair of a double-stranded DNA gap.

D. Class 3. In this NCO class, the heteroduplex region is adjacent to a conversion tract. Such events could reflect a heteroduplex tract in which mismatches are repaired in one part of the tract and left unrepaired in the other.

E. Class 3. An alternative model for this class is that the conversion tract is the result of repair of a double-stranded DNA gap with a heteroduplex region at one end.

F. Class 4. For this CO class, a heteroduplex is observed on one chromatid but not the other. This class could be explained by the DSBR pathway in which heteroduplex region is short relative to the other; if the short heteroduplex does not contain a mismatch, it would be undetectable.

Fig. S2. Mechanisms that generate Classes 6-8 recombination events. Events are depicted as in Fig. S1.

A. Class 5. In this NCO class, the heteroduplex region is located on the opposite of the DSB site from the conversion region. This pattern is consistent with the repair of a double-stranded DNA gap that was restricted to one of the broken ends.

B. Class 6. This CO class is identical to the pattern expected for the DSBR model.

C. Class 7. In this CO class, no heteroduplexes or conversion tracts are observed adjacent to the crossover, consistent with the formation of a dHJ with short heteroduplex tracts that do not include mismatches.

D. Class 8, mechanism 1. In this NCO class, one chromatid has a conversion tract, and the other chromatid has a heteroduplex involving SNPs at the same position. This event could reflect resolution of a dHJ intermediate in the NCO model in which one region of heteroduplex is undetectable.

E. Class 8, mechanism 2. An alternative mechanism involves branch migration of a HJ, followed by resolution of the intermediate in a NCO mode. Mismatches in one of the two chromatids are repaired to generate a conversion tract.

Fig. S3-S91. In the upper part of the figure (labeled A), we show the patterns of SNPs derived from the W303-1A homolog (red) and YJM789 homolog (blue). Each line represents a chromosome. Each pair of lines is derived from one of the granddaughter cells in the white (W1 or W2) or red (R1 or R2) sectors. The locations of the SNPs, represented by colored circles, are drawn proportionally with a scale showing SGD coordinates at the bottom of A. In the B part of the figures, we show the arrangement of SNPs in double-stranded chromatids in the mother cell before chromosome segregation; in this part of the figure, each line represents a single-strand of DNA of the chromatids. The inferred positions of the initiating DSBs are indicated with arrows. Chromatids 1 and 2 are sisters, and chromatids 3 and 4 are sisters. In part C, for recombination events that are classified as “Complex”, we show possible mechanistic pathways for their formation. Figure S3-S80 show selected and unselected UV-induced events in strain YYy310. Figures S81-S85 show selected spontaneous events on chromosome V in strain YYy310, and Figures 86-91 represent spontaneous HS4-related crossovers on chromosome V in strain YYy311. The coordinates and classifications of the events represented by these supplemental figures are in Tables S2 and S3, respectively.

Lastly, we note that the event depicted in Fig. S71 has the pattern expected for a BIR event in one of the daughter cells. Because of this complication, we did not attempt to infer the locations of the initiating DSBs.